INVESTIGATION OF SMALL MOLECULE SIGNALING

IN THE MODEL ORGANISM *CAENORHABDITIS ELEGANS*

A Dissertation

Presented to the Faculty of the Graduate School

of Cornell University

in Partial Fulfillment of the Requirements for the

Degree of Doctor of Philosophy

By

Yevgeniy Izrayelit

August 2014

INVESTIGATION OF SMALL MOLECULE SIGNALING

IN THE MODEL ORGANISM *CAENORHABDITIS ELEGANS*

Yevgeniy Izrayelit, Ph.D.

Cornell University, 2014

Caenorhabditis elegans is an important model for the study of aging and disease. The worm has traditionally been used to explore gene function. Notably, one of the first genes shown to extend lifespan was discovered in *C. elegans* and was found to be conserved in humans. In the past ten years, though, it has been shown that this nematode utilizes a diverse class of small molecules called ascarosides that affect a variety of biological phenomena including development, aging, and mating. Yet many aspects of ascaroside biosynthesis and function remain incomplete. A second class of steroidal small molecules, the dafachronic acids, has also been recently discovered to be endogenous regulators of *C. elegans* physiology. It is clear that *C. elegans* is becoming established as a model for chemists. The work presented here highlights recent progress in our understanding of small molecule signaling in *C. elegans.*

My Ph.D. research has contributed novel discoveries in the areas of sex-specific ascaroside biosynthesis, ascaroside modulation of lifespan, and ascaroside based immune system activation. My research has also led to discovery of a small molecule detoxification mechanism in *C. elegans* and utilized an established 2D NMR-based

metabolomics method to investigate a host-pathogen interaction. Finally, this thesis presents a novel statistically powerful 2D NMR metabolomics tool to take small molecule research in *C. elegans* and higher organisms into the 21st century.

BIOGRAPHICAL SKETCH

Yevgeniy Izrayelit was born in St. Petersburg, Russia to Yelena Izrayelit and Leonid Izrayelit on June 3rd, 1984. At the age of eight, Yevgeniy moved with his family to America where they resided in the Bronx, a borough of New York City. A generous scholarship allowed Yevgeniy to attend the Ethical Culture Fieldston School, from which he received a high school diploma in 2002. The next four years of his life were spent in Poughkeepsie, NY studying biochemistry at Vassar College. Yevgeniy received his Bachelor of Arts in Biochemistry in 2006 with financial support from the Elbert Lenrow Fund Scholarship and the New York Lottery Leaders of Tomorrow Scholarship. Yevgeniy's undergraduate thesis at Vassar was conducted with Scott Allen, Ph.D. and focused on the synthesis of cyclic tetrapeptides. From 2006-2007 Yevgeniy worked as an Operations Manager and Research Assistant at the Spinal Muscular Atrophy Foundation, a not-for profit grant giving foundation based in New York, NY. The following year, Yevgeniy joined the office of Dr. Derek Enlander, also based in New York City, where he assisted in the care and support of patients primarily suffering with Fibromyalgia and Chronic Fatigue Syndrome. In the fall of 2008 Yevgeniy enrolled in the University at Buffalo School of Medicine and Biomedical Sciences to pursue a medical degree. After four months, Yevgeniy decided to step away from medical studies to pursue a Ph.D. degree.

In the summer of 2009 Yevgeniy moved to Ithaca, NY to enroll in the Ph.D. program in Chemistry and Chemical Biology at Cornell University. Yevgeniy's graduate research was conducted in the laboratory of Professor Frank Schroeder. During his time at Cornell, Yevgeniy was a participant in the Chemistry Biology Interface Training Grant

and served as its Elected Student Representative in 2012-2013. As a training grant requirement, Yevgeniy spent the summer of 2013 in an internship at Pfizer in the Cardiovascular and Metabolic Diseases Research Unit based in Cambridge, MA. Yevgeniy has also been active in student governance during his time at Cornell, and was a member of the Graduate and Professional Student Assembly from 2009-2013, notably serving as the Chair of the Student Advocacy Committee in 2012-2013. He is also very proud to have been a co-founder in 2009 of the Graduate Association of Chemistry. Yevgeniy has had the privilege to mentor two undergraduate students, Sydney Campbell and Margaux Genoff, during his time at Cornell. He received the Bayer Teaching Excellence Award in 2011 in recognition of outstanding teaching as a teaching assistant in organic chemistry and was a two time recipient of the Vassar College Mary Landon Sague Fellowship. In the spring of 2014 Yevgeniy also received the Proctor & Gamble Cornell Graduate Student Best Paper Award given to the fourth and fifth year Ph.D. students with the most significant publications and the Tunis Wentink Prize for outstanding academic and research performance during a Ph.D.

The research described in this thesis is dedicated to my grandparents:

Amma and Aaron Izrayelit

Maya Dranitskaya and Alexander Gintsburg

ACKNOWLEDGEMENTS

Special Committee Chair and Advisor: Professor Frank C. Schroeder

Special Committee: Professor Siu Sylvia Lee and Professor Richard Cerione

Teaching Advisor: Senior Lecturer Thomas R. Ruttledge, Ph.D.

Collaborating Principal Investigators: Professor Arthur Edison (University of Florida, Gainesville, FL), Professor Paul Sternberg (Caltech, Pasadena, CA), Professor Anne Brunet (Stanford University, Stanford, CA), Professor Doug Portman (University of Rochester, Rochester, NY), Professor Daniel Kalman (Emory University, Atlanta, GA), Professor Leon Avery (Virginia Commonwealth University, Richmond, VA), Professor Jake Bundy (Imperial College London, London, UK), and Professor Donald Riddle (The Univeristy of British Columbia, Vancouver, BC Canada)

Collaborating Researchers: Sydney L. Campbell, Margaux Genoff, Hanno Andreas Ludewig, Ph.D., Stephan von Reuss Ph.D., Rabia Malik, Anna Zimmerman, Parag Mahanti, Ph.D., Bennet Fox, Zihan Ye, Axel Bethke, Ph.D., Alexander Aryukhin, Ph.D., Joshua Yim, Neelanjan Bose, Ph.D., Steve Robinette, Ph.D., Florian Geier, Ph.D., Bettina Bommarius, Ph.D., Akwasi Anyanful, Ph.D., Donha Park, Ph.D., Jagan Srinivasan, Ph.D., Travis Maures, Ph.D., Shuo Han, and Gregg Stupp

Facility Mangers: Ivan Keresztes, Ph.D., Maciej Kukula, and Gary Horvath

Organizations: Department of Chemistry and Chemical Biology and The Boyce Thompson Institute for Plant Research, Cornell University

Funding: Department of Chemistry and Chemical Biology Teaching Fellowship, Chemistry Biology Interface Training Program (GM008500), Cornell University, Vassar College Mary Landon Sague Fellowship, Schroeder Laboratory NIH funding (GM008500)

TABLE OF CONTENTS

PREFACE

The era of genomics in multicellular organisms began with the sequencing of the round worm *Caenorhabditis elegans* (*1*). This 1 mm long nematode was popularized as a model organism by the noble laureate Sydney Brenner in the 1960s (*2*). Its impact in genetics and biology is underscored by the awarding of three noble prizes for work utilizing *C. elegans* for fundamental discoveries that include the elucidation of cell lineage and death, the discovery of the green fluorescent protein, and the identification of interference RNA (*3*).

C. elegans utility for genetics and biomedical research stems from its short lifespan of 2-3 weeks at 20°C, and very short reproduction time of 3 days from egg to reproductive adult, complete cell lineage tracing, and genetic tractability. Facile laboratory culturing methods and the worm's transparent and resilient nature have also made this organism attractive to a diverse array of disciplines (*3*). Of great interest to the research community is the unique *C. elegans* life history (*4*). Typically, under favorable environmental conditions *C. elegans* hatches from an egg and goes through four larval stages to become a self-replicating hermaphroditic adult in about 3-5 days (**Figure P.1**). Notably, if the worm encounters unfavorable environmental conditions as an early larval worm (L1 stage), it can enter an alternative long lived stage called dauer (**Figure P.1**). The dauer worm survives several months as compared to the typical 2-3 weeks for an adult, becomes highly stress resistant, and slows its metabolism to compensate for the absence of food intake.

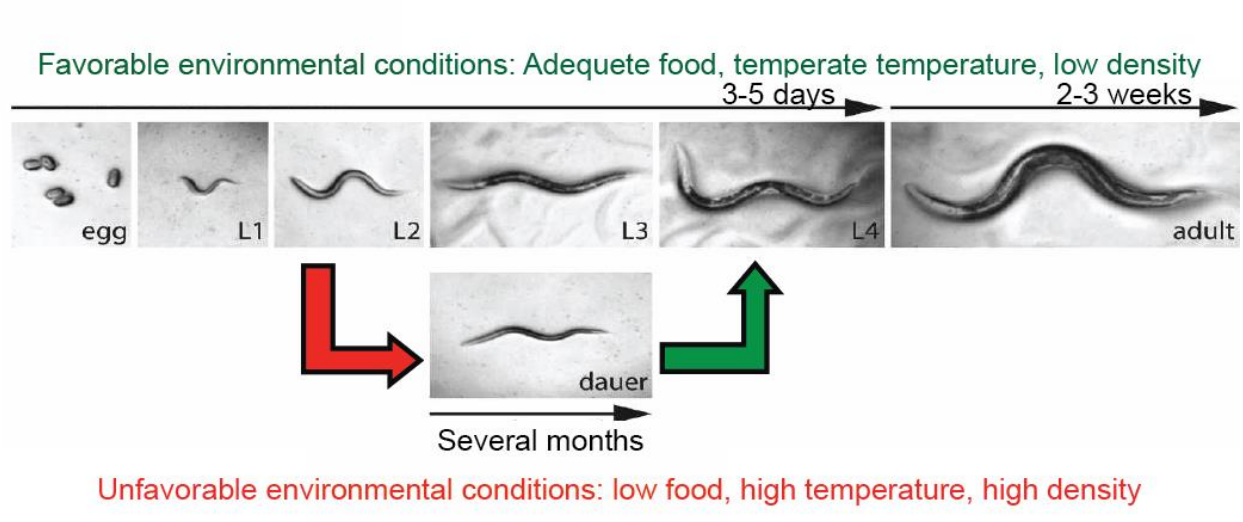

Figure P.1: *C. elegans* life history. Under favorable environmental conditions, the worm hatches from egg to self-replicating hermaphroditic adult in three days and goes on two live for 2-3 weeks. Under unfavorable environmental conditions, *C. elegans* can enter a long lived state called dauer. Notably, the dauer worm can re-enter normal reproductive development when conditions improve. Figure adapted from (*4*).

The genetic study of dauer related pathways led to the discovery one of the first gene shown to regulate aging, the insulin/insulin-like growth factor 1 (IGF) receptor *daf-2* (*5*). Since then, a whole series of genes have been implicated in dauer regulation. These have been termed abnormal **DA**uer **F**ormation or ***daf*** genes. Most of the identified genes in the *daf* family have high homology to genes found in higher organisms such as humans, suggesting that protective aspects of a dauer like state may be achievable in higher organisms. In fact, many dauer related pathways seem to regulate aspects of aging not only in invertebrate model organisms but also in mammals. (*6*).

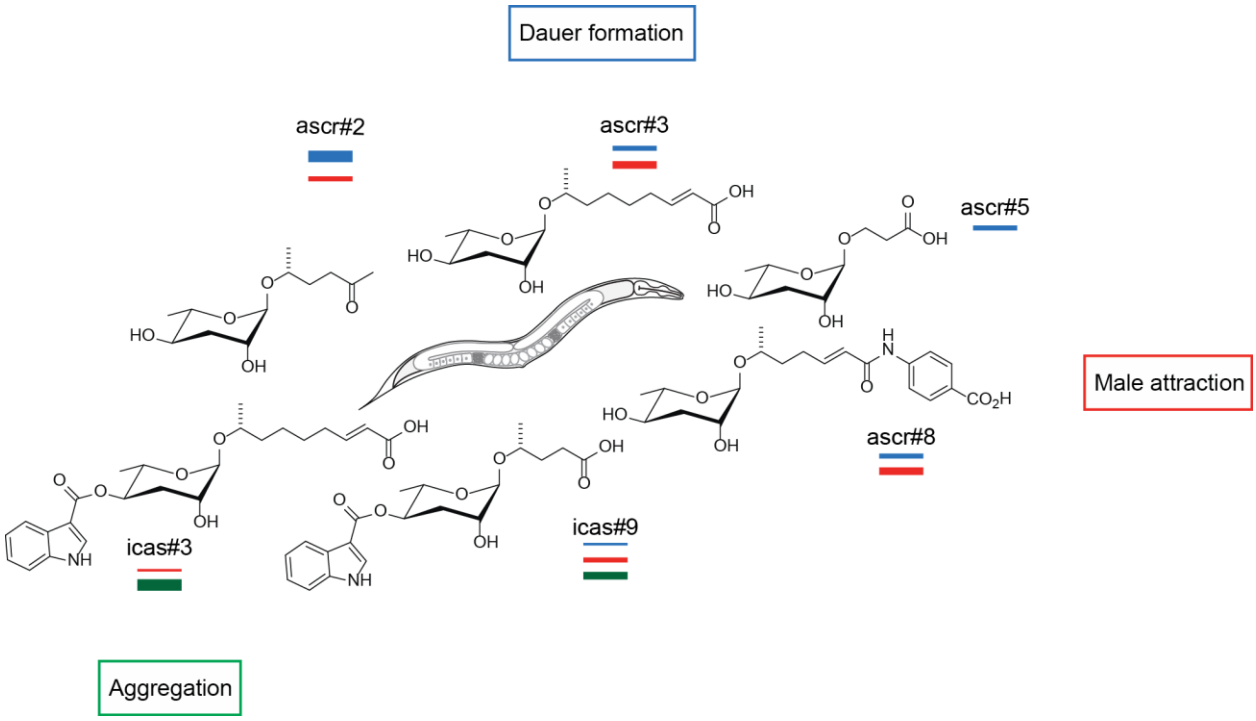

Figure P.2: Figure adapted from (*7*). Six most abundant ascarosides highlighted. Width of bar correlates with general concentration needed to achieve function, and color matches with function.

The discovery of the dauer pheromone as a key component of dauer entry (*8*), highlighted the important role of small molecule signaling in *C. elegans* and higher organism, but also underscored the lack of chemists working in the field. Some 20 years later the discovery of the chemical structures of the ascarosides (*9, 10*) unleashed a wave of research in this area and helped catapult *C. elegans* to the status as a chemist friendly model organism (*3*). Ascarosides all share the dideoxy sugar ascarylose and have variety of lipid side chains as well as modification on the 4' or 2' position on the ring. Since the first ascaroside was identified, our understanding of ascaroside function has grown significantly. **Figure P.2** summarizes ascaroside mediated biological functions of the more abundantly produced ascarosides. Different concentrations and

different combinations of ascarosides regulate a variety of biological functions that include dauer induction, male attraction and hermaphrodite repulsion (*7*).

C. elegans is very well suited for the study of small molecules. The worm can be grown on agar plates or in liquid culture, where both the pellet and media can be analyzed separately (**Figure P.3a**). The *C. elegans* genome has a surprisingly high number of predicted G-protein coupled receptors (GPCR) (*11*). Out of the approximately 19,000 *C. elegans* genes over 1,000 are predicted to function in some ligand binding/signal transduction role as GPCRs. It is therefore not surprising that over 100 ascarosides have been identified to date using a liquid chromatography mass spectrometry (LC/MS) approach (*12*). Connecting small molecule signals to function, though, remains a critical challenge. Traditional activity guided fractionation often loses activity as the fractionation process leads to compound destruction and loss of synergy. To address this, the Schroeder Laboratory developed a method termed differential analysis by 2D NMR spectroscopy (*13*) that overcomes this barrier by comparatively analyzing crude metabolome mixtures between wild type and mutant samples (**Figure P.3b**) (*14*). Using DANS it was possible to identify novel signal molecules and reconstitute function that was absent in the mutant strain through identification of multiple differential metabolites that signal synergistically. Chapter 4 of this thesis also highlights the utility of DANS in identifying signaling molecules (*15*). Chapter 5 presents work integrating multivariate statistics into the DANS method to increase the power of this comparative metabolomics technique.

The work in the thesis hones in on the ability to explore small molecule signaling in *C. elegans* using analytical tools. The work probes sex-specific signaling and

biosynthesis. Small molecule regulation of life and death as well as immune system activation is explored. A novel small molecule detoxification strategy is revealed. And consequently related small molecule toxins are identified in a host-pathogen model. In the last chapter, a new method is presented for small molecule metabolomics that take *C. elegans* research, and that of higher organisms, even further.

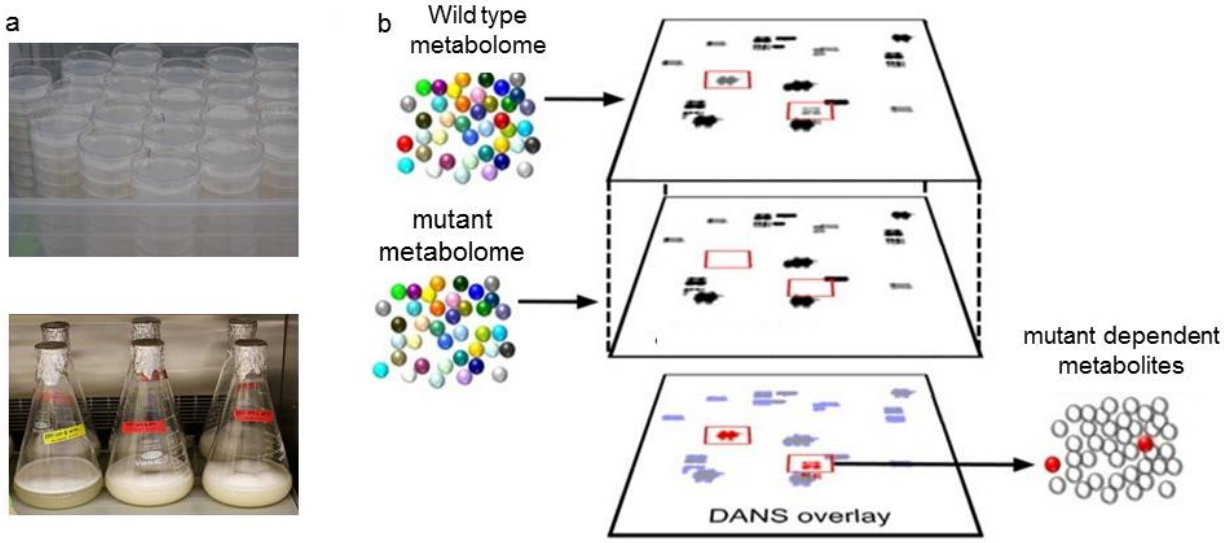

Figure P.3. *C. elegans* is well suited for differential analysis by 2D NMR. (a) *C. elegans* can be grown on both plates and liquid culture. High numbers of worms in liquid can be analyzed for secreted compounds in media or compounds maintained in the worm body. (b) Scheme for DANS adapted from (*14*). 2D NMR spectra of wild type and mutant metaoblome are overlaid revealing mutant dependent metabolites.

Preview of Chapters

In **chapter 1** we present the first look at ascarosides produced by male *C. elegans* (*16*). Enzymes involved in ascaroside biosynthesis reflect a sex-specific biosynthetic pattern further supporting a model of sex-specific small molecule signaling in *C. elegans* and higher organisms. **Chapter 2** explores the beneficial effects of dauer inducing ascarosides, ascr#2 and ascr#3 (*17*). Notably, Ascaroside mediated increase in lifespan and stress resistance (AMILS) requires the conserved NAD+ dependent

deacetylase SIR-2.1. Ascr#2 specific AMILS requires the recently identified ascr#2 receptor daf-37, highlighting the amazing plasticity in small molecule signaling. *daf-37* expression in the ASK neurons is required for AMILS, while *daf-37* expression in the ASI neurons is required for dauer induction (*18*). **Chapter 3** shows that pre-exposure to a pair of ascarosides, ascr#5 and ascr#8, was shown to activate a protective strategy in *C. elegans* against a lethal exposure to the pathogenic bacteria EPEC. This ascr mix conditioned *C. elegans* in a manner dependent on SIR-2.1 as well as components of the unfolded protein response and G-protein coupled signaling. To our knowledge, this ascr mix represents the first endogenous small molecules shown to regulate immunity in *C. elegans* and it also may have strong overlap with the protective strategies seen with AMILS.

Chapter 4 expands on the importance of small molecules in immunity and host-pathogen interaction. In the first portion of the chapter, the discovery of a *C. elegans* detoxification strategy that glycosylates two unrelated toxins, phenazine and indole, to the non-toxic versions is presented (*19*). This has broad implications for anthelmintic drug development for both human and agricultural parasitic nematodes as well establishes *C. elegans* as model for the study of detoxification systems in metazoans. The second portion of **chapter 4** presents work utilizing untargeted NMR-based metabolomics to reveal that enteropathogenic *E. coli* utilizes a family of indoles to kill *C. elegans* in a recently developed system for studying host-pathogen interactions (*15*). Further, discovery of ICA revealed that this molecule is a regulator of general virulence in EPEC and other related attaching and effacing (A/V) bacteria and can actually be protective to the host during pathogen infection. ICA is now being further evaluated as a

potential drug candidate for human infection with EPEC and EHEC. Finally, **chapter 5** presents our efforts to add statistical rigor to comparative metabolomics using 2D NMR spectroscopy. Using a novel MATLAB based platform for 2D NMR analysis an interaction between two conserved biochemical pathways in the model organism *C. elegans* is uncovered (*20*). The thesis concludes with **chapter 6** which highlights recent work and future outlook.

The contributions of collaborators and the author are acknowledged at the beginning of each chapter. Further, work in chapter 1, 2 and 5 resulted in 1st or co-1st author publications and the chapters are presented as published with slight modifications. Material in chapter 3 is in preparation for publication and is fully original writing, just as is the concluding chapter 6. Finally, chapter 4 is a combination of two 3rd author publications from the author, and therefore language and figures from both publications with major modifications are used.

REFERENCES

1. *C. elegans* Sequencing Consortium (1998) Genome sequence of the nematode *C. elegans:* a platform for investigating biology, *Science 282*, 2012-2018.
2. Brenner, S. (1974) The genetics of *Caenorhabditis elegans*, *Genetics 77*, 71-94.
3. Hulme, S. E., and Whitesides, G. M. (2011) Chemistry and the worm: *Caenorhabditis elegans* as a platform for integrating chemical and biological research, *Angew. Chem. Int. Edit. 50*, 4774-4807.
4. Fielenbach, N., and Antebi, A. (2008) *C. elegans* dauer formation and the molecular basis of plasticity, *Genes Dev. 22*, 2149-2165.
5. Kenyon, C., Chang, J., Gensch, E., Rudner, A., and Tabtiang, R. (1993) A *C. elegans* mutant that lives twice as long as wild type, *Nature 366*, 461-464.
6. Fontana, L., Partridge, L., and Longo, V. D. (2010) Extending healthy life span-from yeast to humans, *Science 328*, 321-326.
7. Srinivasan, J., von Reuss, S. H., Bose, N., Zaslaver, A., Mahanti, P., Ho, M. C., O'Doherty, O. G., Edison, A. S., Sternberg, P. W., and Schroeder, F. C. (2012) A *modular library of small molecule signals regulates social behaviors in Caenorhabditis elegans*, *PLoS Biol. 10*, e1001237.
8. Golden, J. W., and Riddle, D. L. (1984) The *Caenorhabditis elegans* dauer larva - developmental effects of pheromone, food, and temperature, *Dev. Biol. 102*, 368-378.
9. Jeong, P. Y., Jung, M., Yim, Y. H., Kim, H., Park, M., Hong, E., Lee, W., Kim, Y. H., Kim, K., and Paik, Y. K. (2005) Chemical structure and biological activity of the *Caenorhabditis elegans* dauer-inducing pheromone, *Nature 433*, 541-545.
10. Butcher, R. A., Fujita, M., Schroeder, F. C., and Clardy, J. (2007) Small-molecule pheromones that control dauer development in *Caenorhabditis elegans*, *Nat. Chem. Biol. 3*, 420-422.
11. Nagarathnam, B., Kalaimathy, S., Balakrishnan, V., and Sowdhamini, R. (2012) Cross-genome clustering of human and *C. elegans* G-protein coupled receptors, *Evol. Bioinform. Online 8*, 229-259.
12. von Reuss, S. H., Bose, N., Srinivasan, J., Yim, J. J., Judkins, J. C., Sternberg, P. W., and Schroeder, F. C. (2012) Comparative metabolomics reveals biogenesis of ascarosides, a modular library of small molecule signals in *C. elegans*, *J. Am. Chem. Soc. 134*, 1817–1824.
13. Anokye-Danso, F., Anyanful, A., Sakube, Y., and Kagawa, H. (2008) Transcription factors GATA/ELT-2 and forkhead/HNF-3/PHA-4 regulate the tropomyosin gene expression in the pharynx and intestine of *Caenorhabditis elegans*, *J. Mol. Biol. 379*, 201-211.
14. Pungaliya, C., Srinivasan, J., Fox, B. W., Malik, R. U., Ludewig, A. H., Sternberg, P. W., and Schroeder, F. C. (2009) A shortcut to identifying small molecule signals that regulate behavior and development in *Caenorhabditis elegans*, *Proc. Natl Acad. Sci. USA 106*, 7708-7713.
15. Bommarius, B., Anyanful, A., Izrayelit, Y., Bhatt, S., Cartwright, E., Wang, W., Swimm, A. I., Benian, G. M., Schroeder, F. C., and Kalman, D. (2013) A family of indoles regulate virulence and Shiga toxin production in pathogenic *E. coli*, *PLoS One 8*, e54456.

16. Izrayelit, Y., Srinivasan, J., Campbell, S. L., Jo, Y., von Reuss, S. H., Genoff, M. C., Sternberg, P. W., and Schroeder, F. C. (2012) Targeted metabolomics reveals a male pheromone and sex-specific ascaroside biosynthesis in *Caenorhabditis elegans*, *ACS Chem. Biol. 7,* 1321-1325.
17. Ludewig, A. H., Izrayelit, Y., Park, D., Malik, R. U., Zimmermann, A., Mahanti, P., Fox, B. W., Bethke, A., Doering, F., Riddle, D. L., and Schroeder, F. C. (2013) Pheromone sensing regulates *Caenorhabditis elegans* lifespan and stress resistance via the deacetylase SIR-2.1, *Proc. Natl Acad. Sci. USA 110*, 5522-5527.
18. Park, D., O'Doherty, I., Somvanshi, R. K., Bethke, A., Schroeder, F. C., Kumar, U., and Riddle, D. L. (2012) Interaction of structure-specific and promiscuous G-protein-coupled receptors mediates small-molecule signaling in *Caenorhabditis elegans*, *Proc. Natl Acad. Sci. USA 109*, 9917-9922.
19. Stupp, G. S., von Reuss, S. H., Izrayelit, Y., Ajredini, R., Schroeder, F. C., and Edison, A. S. (2013) Chemical detoxification of small molecules by *Caenorhabditis elegans*, *ACS Chem. Biol. 8*, 309-313.
20. Izrayelit, Y., Robinette, S. L., Bose, N., von Reuss, S. H., and Schroeder, F. C. (2013) 2D NMR-based metabolomics uncovers interactions between conserved biochemical pathways in the model organism *Caenorhabditis elegans*, *ACS Chem. Biol. 8*, 314-319.

CHAPTER 1

TARGETED METABOLOMICS REVEALS A MALE PHEROMONE AND SEX-SPECIFIC ASCAROSIDE BIOSYNTHESIS IN CAENORHABDITIS ELEGANS

Abstract

In the model organism *Caenorhabditis elegans*, a class of small molecule signals called ascarosides regulate development, mating, and social behaviors. Ascaroside production has been studied in the predominant sex, the hermaphrodite, but not in males, which account for less than 1% of wild-type worms grown under typical laboratory conditions. Using HPLC-MS-based targeted metabolomics, we show that males also produce ascarosides and that their ascaroside profile differs markedly from that of hermaphrodites. Whereas hermaphrodite ascaroside profiles are dominated by ascr#3, containing an α,β-unsaturated fatty acid, males predominantly produce the corresponding dihydro-derivative ascr#10. This small structural modification profoundly affects signaling properties: hermaphrodites are retained by attomole-amounts of male-produced ascr#10, whereas hermaphrodite-produced ascr#3 repels hermaphrodites and attracts males. Male production of ascr#10 is population density-dependent, indicating sensory regulation of ascaroside biosynthesis. Analysis of gene expression data supports a model in which sex-specific regulation of peroxisomal β-oxidation produces functionally different ascaroside profiles.

Contributions

The work in this chapter was conducted by a team of scientists in the Schroeder Lab (Cornell University, Ithaca, NY) and the Sternberg Lab (California Institute of Technology, Pasadena, CA). The data and writing, with minor modifications, in this chapter has been published in ACS Chemical Biology (*1*). ***Yevgeniy Izrayelit (YI) is a first author on this publication. YI designed and performed the metabolomics studies, wrote the manuscript, analyzed results as well as previously published genetic microarray data, and synthesized ascr#10 for LC/MS quantification from previously prepared ascr#3. YI's primary data contribution was HPLC/MS profiling of the male metabolome and the design of a screening method to look at ascarosides on a small scale****.* Jagan Srinivisan (JS) assisted with data analysis and manuscript preparation and conducted all bioassays as a scientist in the Sternberg Lab with the assistance of Yeara Jo (YJ). Sydney Campbell (SLC) and Margaux Genoff (MCG) both assisted YI with preparation of male samples and LC/MS experimentation. Stephan von Reuss assisted with ascaroside identification. Professor Paul Sternberg assisted in manuscript preparation. Professor Frank Schroeder (FCS) supervised the project and also wrote the manuscript.

Introduction

C. elegans is rapidly being developed as a model organism for the study of endogenous small molecule signals that regulate diverse aspects of animal life history, including development, lifespan, and social behaviors (*2-4*). Recently, the Schroeder Lab used targeted comparative metabolomics to investigate the biosynthesis of the ascarosides in *C. elegans*, a family of small molecule signals based on the dideoxy sugar ascarylose and additional building blocks from lipid and amino acid metabolism (**Figure 1.1**) (*4*). Ascarosides were originally identified as the main components of the dauer pheromone (*5, 6*) and have since been shown to mediate other biological activities especially social behaviors such as mating, aggregation, and dispersal (*7, 8*). Of particular interest are sex-specific behaviors as previous studies showed that ascaroside functions are highly sex- and structure-dependent. For example, whereas ascr#3 attracts male *C. elegans* but repeals hermaphrodites, the related icas#3 acts a general aggregation signal, attracting both hermaphrodites and males (*8*). Previous metabolomic analyses have *de facto* profiled ascaroside production of hermaphrodites due to their greater abundance (*8, 9*). Because hermaphrodites and male *C. elegans* markedly differ in their biological responses to ascaroside-derived signaling molecules (*7, 10*), we asked whether male *C. elegans* biosynthesize ascarosides and whether the male ascaroside profile differs from that of hermaphrodites .

Targeted metabolomics of male enriched liquid cultures

C. elegans is androdioecious and laboratory cultures of wild type worms are predominantly composed of selfing hermaphrodites (*11*). Male *C. elegans* in the wild-type strain arise due to spontaneous non-disjunction in 0.1% of the progeny, which

activates a genetic masculinization process (*12, 13*). The incidence of males increases in response to stress, and it is possible that in the wild males are more abundant (*14*). We began with investigating the metabolome of *him-5* worms, a mutant strain that produces a much larger percentage of males (about 30%) than wild-type worms (*12*). Targeted mass spectrometric analyses of the *him-5* exo-metabolome, the entirety of small molecules found in worm conditioned media, revealed the production of the same set of ascarosides found in wild-type controls; however, the relative amounts of some of the most abundant ascarosides in *him-5* and wild-type cultures differed significantly (**Figure 1.1a**). Specifically, relative amounts of the ascaroside ascr#10, which has not previously been studied in detail, and the known hermaphrodite aggregation factor, icas#3 (*8*), were higher in *him-5* exo-metabolome samples than in wild-type. Notably, ascr#3, a male attractant (*7*), was relatively more abundant in the wild-type than in the *him-5* exo-metabolome.

Small scale metabolomics of male *C. elegans*

To determine whether increased production of these ascarosides was due to the larger percentage of males in *him-5* cultures, we developed a protocol for the analysis of the exo-metabolome of small numbers of worms based on selective-ion monitoring (SIM) of ascaroside-associated ions. The identity of peaks whose specific retention times and molecular ions suggested ascarosides was confirmed further by additionally scanning in HPLC-MS/MS mode for precursor ions of *m/z 73*, a fragment ion characteristic for ascarosides (*4*). Using this strategy, attomolar amounts of ascarosides could be detected. We were able to detect ascr#1, ascr#3, and ascr#10 as the major secreted ascarosides in samples derived from as few as 100 wild-type hermaphrodite

worms staged as L4 through young adults (**Figure 1.1b**). Next we analyzed samples of similarly staged 200 *him-5* males, and subsequently wild-type males, which we obtained by increasing male frequency by crossing males and hermaphrodites. These male-only samples revealed the same three ascarosides, ascr#1, ascr#3, and ascr#10, we found in hermaphrodites, but in markedly different proportions (**Figures 1.1b,c**). Whereas hermaphrodites excrete the unsaturated ascr#3 as the major component, the corresponding dihydro derivative, ascr#10, represents the most abundant ascaroside in male samples. Relative production of the saturated ascr#1 did not differ dramatically in males and hermaphrodites. Higher secretion of ascr#10, relative to ascr#3, by males was observed consistently using different growth media (S-media and water) and incubation durations; however, we were unable to detect and reliably quantify the abundance of other ascarosides on this small scale. To check whether increased production of ascr#10 is a general characteristic of male *C. elegans* and not a specific characteristic of the laboratory wild-type strain N2 Bristol, we also investigated the ascaroside profile of a second *C. elegans* wild-type strain, Hawaii CB4846 (*15*). We found that, as in N2 Bristol, ascr#3 is the most abundant ascaroside excreted by hermaphrodites, whereas males excrete predominantly ascr#10 (**Figure A.1**).

Quantitative LC-MS analyses confirmed that males produce and release much larger amounts of ascr#10 than hermaphrodites (**Figures 1.2a,b, and Figure A.2**). However, whereas relative ascaroside abundances were highly reproducible for both males and hermaphrodites (**Figure 1.2a**), we found that ascaroside excretion rates of males, but not hermaphrodites, were highly variable (**Figure 1.2b**). We then asked whether ascaroside release rates are dependent on worm population density. Strikingly,

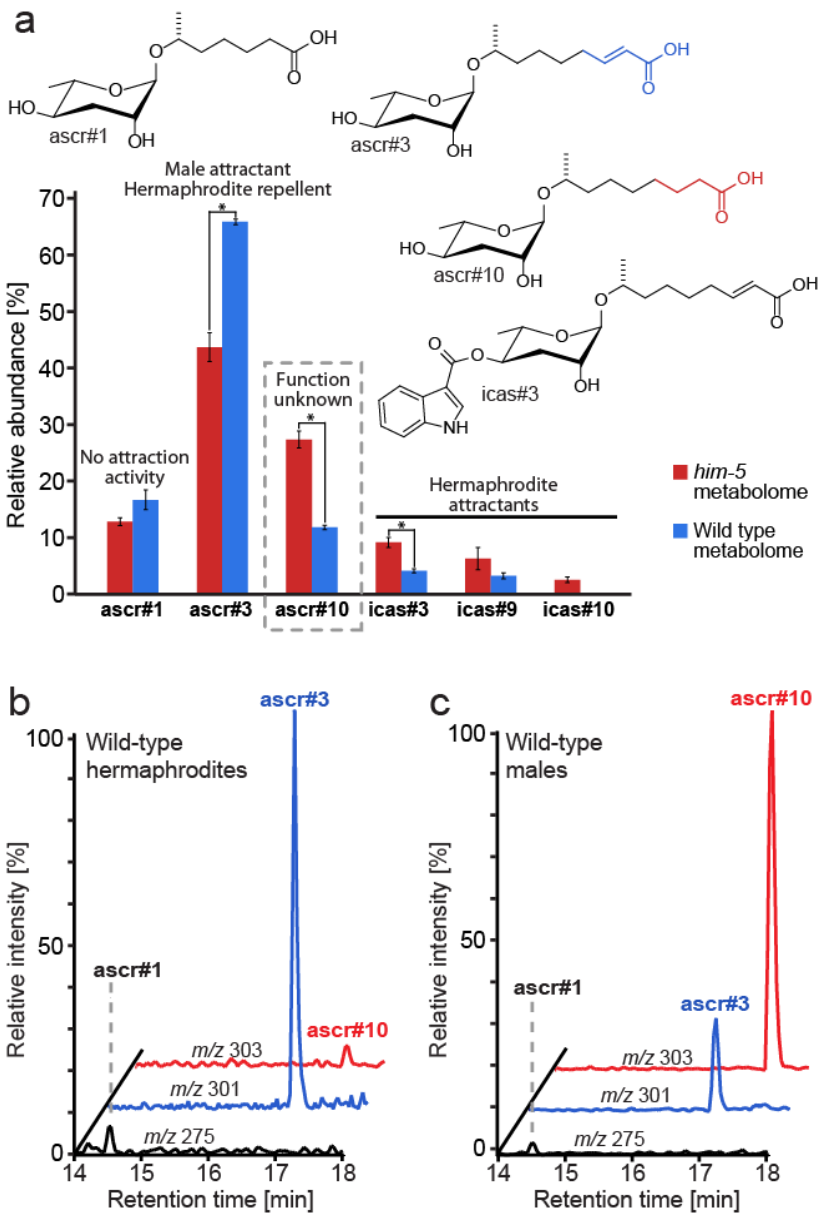

Figure 1.1: Identification of male-specific ascarosides in *C. elegans*. (a) Relative abundances of ascarosides ascr#3, ascr#10, and several indole ascarosides markedly differs between wild-type (N2) and *him-5* metabolomes, whereas abundances of many other ascarosides, for example the dauer pheromone component ascr#1, remains unchanged. Relative abundances were calculated in % of the total amount of the six ascarosides in this Figure (*P<0.05 unpaired *t*-test with Welch's correction; error bars: SD). (b) Ion chromatograms for ascr#1, ascr#3, and ascr#10 from negative-ion ESI-LC/MS analysis of exo-metabolome samples obtained from 200 hermaphrodite *C. elegans*. c) Ion chromatogram for LC/MS analysis of exo-metabolome samples derived from 200 male *C. elegans. LC/MS profiling experiments were conducted by YI with support from SLC and MCG.*

we found that a doubling of the density of wild-type males led to an almost 4-fold increase in the excretion rate of ascr#10, as well as a smaller increase in ascr#3 excretion rate (**Figure 1.2c**). In contrast, ascaroside production by hermaphrodites did not appear to be density dependent, and the presence of hermaphrodites did not increase male production of ascr#10 and ascr#3 (**Figures 1.2c and Figure A.2c**). Furthermore, male ascaroside production dominates in mixtures of wild-type males and hermaphrodites (**Figure 1.2d**). These results show that *C. elegans* males produce a sex-specific blend of ascarosides with ascr#10 as the major component and that ascaroside release in wild-type males is promoted by the presence of other worms.

Exploration of ascr#10 biological function

Ascr#3 has previously been shown to attract males at low concentrations and repel hermaphrodites at higher concentrations (*7*), whereas the biological roles of ascr#10 have not been investigated in detail. Given that ascr#10 production is strongly upregulated in males, we asked whether ascr#10 plays a specific role in hermaphrodite-male interactions. Using synthetic samples we tested ascr#10 on both sexes in a behavioral assay that measures holding time (retention) in response to compound exposure (**Figure 1.3a**). Ascr#10 did not affect male behavior at any of the wide range of sample amounts tested, but elicited a very strong response in hermaphrodites at sample amounts as low as 1 attomole, exceeding the potency of previously identified hermaphrodite attractants such as icas#3 by more than 100-fold in this assay (Figure 3b).(*8*) Next we investigated the effect of ascr#10 on hermaphrodite chemotaxis and aggregation, which revealed significant activity at concentrations of 1 nM (**Figures 1.3b,c, and Figure A.3**). These results show that, compared to icas#3, ascr#10 is much

more potent in the spot retention assay but less active in the chemotaxis and aggregation assays.(*8*) Therefore it appears that ascr#10 serves a specific function as a holding signal, which is also supported by the very long retention times observed with ascr#10 in the spot retention assay (Figure 3b). Given that only 1 attomole of ascr#10 is required to elicit hermaphrodite holding behavior, the amounts of ascr#10 excreted by a single male (about 300 attomole/worm/hour) appear sufficient to induce hermaphrodite retention. We propose that ascr#10, likely in combination with other, less abundant components, is an important part of the male sex pheromone blend in *C. elegans* (*16*).

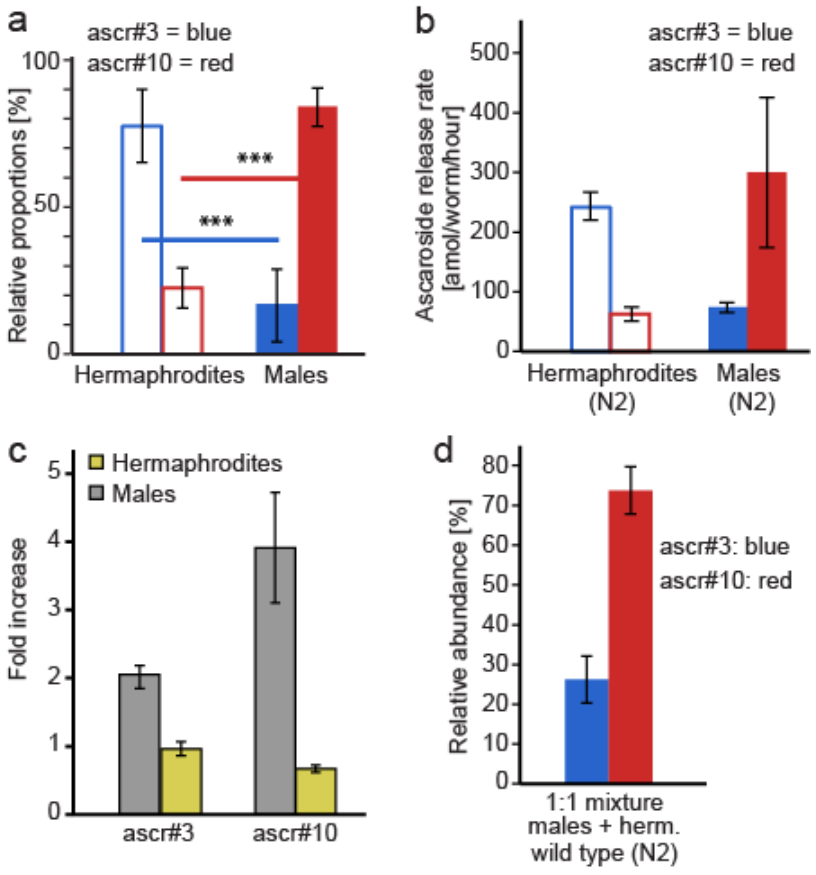

Figure 1.2: Males produce large amounts of ascr#10 (error bars: SD). (a) Relative abundances of ascr#3 and ascr#10 in wild-type (N2) hermaphrodite and male exo-metabolomes. (***P<0.0001 unpaired *t*-test with Welch's correction). (b) Ascaroside release rates of wild-type males and hermaphrodites. (c) Fold increase of ascr#3 and ascr#10 production per worm in response to doubling of worm density from 100 to 200

wild-type hermaphrodites or males per well. Ascaroside production of wild-type hermaphrodites does not change significantly, whereas ascr#3 and ascr#10 production of wild-type males increases 2 fold and 4 fold, respectively. (d) The ascaroside profile of 1:1 mixtures of wild-type (N2) males and hermaphrodites is dominated by the primarily male-produced ascr#10. *LC/MS profiling experiments were conducted by YI with support from SLC and MCG.*

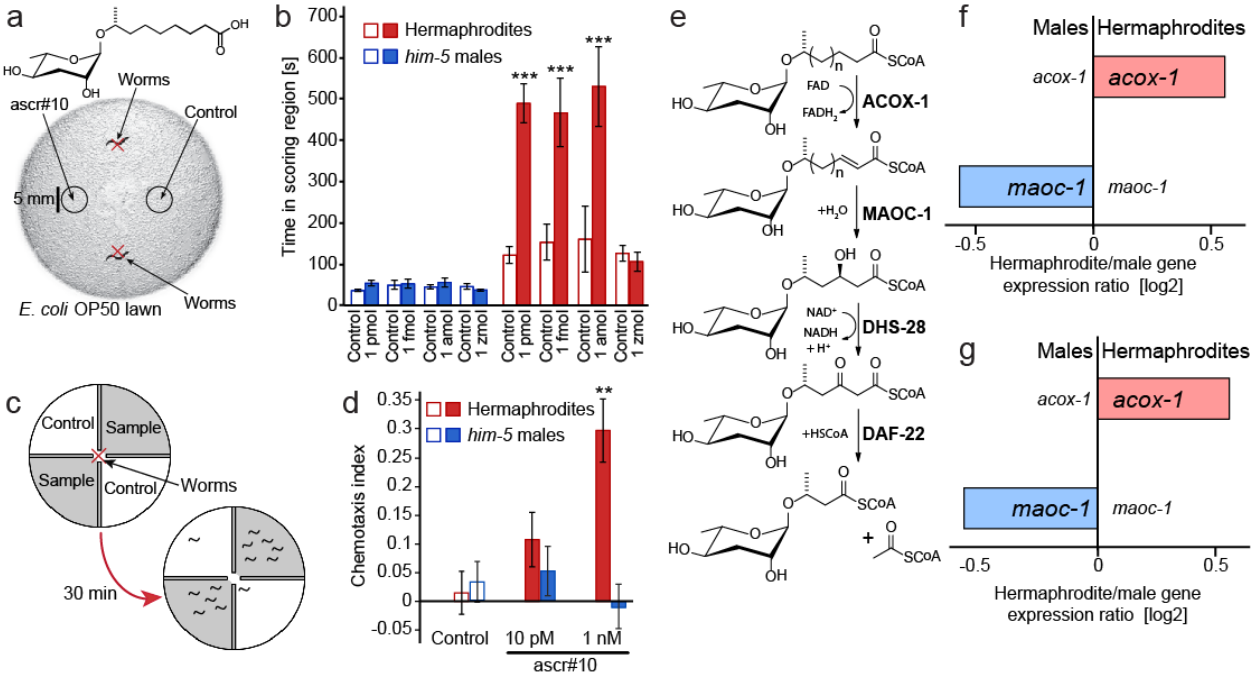

Figure 1.3: Sex-specific behavioral responses to male-produced ascr#10 and regulation of ascaroside biosynthesis. (a) Spot retention assay used to measure the effect of ascr#10 on male and hermaphrodite behavior.(*17*) The red '**X**' denotes the initial position of the assayed worms. (b) Results from spot holding assays reveal that hermaphrodites, but not males, are attracted to ascr#10 sources. *P<0.01, **P< 0.001, ***P<0.0001, unpaired *t*-test followed by Welch's correction; error bars: SD. (c) Schematic representation of quadrant bioassay used to measure chemotaxis to ascr#10. A red "X" marks the spot where worms are placed at the beginning of the assay. (d) Chemotaxis of males and hermaphrodites to ascr#10 as measured by the quadrant assay. **P< 0.01 one-factor ANOVA followed by Dunnett's post-test; error bars: SD. (e) Sex-specific regulation of ascaroside biosynthesis. Shown gene expression ratios are based on DNA microarray experiments of L4-staged worms.*(16)* The expression ratios highlight differential expression of four peroxisomal enzymes involved in biosynthesis of the ascaroside sidechain in hermaphrodites and males. Relatively decreased *acox-1* expression in males is consistent with the observed

increase of saturated ascr#10 in the male exo-metabolome. *Bioassay experiments were conducted by JS with assistance from YJ. DNA microarray data previously published (18) and analyzed by YI.*

Review of DNA microarray data for peroxisomal β-oxidation genes

Next we asked whether sex-specific differences in the regulation of ascaroside biosynthesis enzymes could account for the observed differences between male and hermaphrodite ascaroside profiles. The fatty-acid derived side chains in the ascarosides are derived from peroxisomal β-oxidation of longer-chained precursors (**Figure 1.3d**) (*4*). We found that male worms carrying a mutation in the peroxisomal thiolase *daf-22* do not produce ascarosides, confirming that peroxisomal β-oxidation is required for ascaroside biosynthesis in males (**Figure A.4**). Next we analyzed previously published global DNA microarray data for males and hermaphrodites at the L4 stage, corresponding to the developmental stage we used for our metabolomic analyses. We found significant sex-specific differences in the expression levels of all four enzymes known to participate in peroxisomal β-oxidation in L4 worms (**Figure 1.3d**) (*18*). Relative to the other sex, expression of the acyl-CoA oxidase ACOX-1, which introduces the double bond in the biosynthesis of ascr#3 from ascr#10, is upregulated in hermaphrodites, whereas the next two enzymes in the pathway, MAOC-1 and DHS-28, are upregulated in males. Higher expression levels of ACOX-1 in hermaphrodites are consistent with increased abundance of the α,β-unsaturated ascr#3 in this sex. In addition, relatively higher expression of the downstream enzymes MAOC-1 and DHS-28 may result in further depletion of ascr#3 in males. In conjunction with the results from our metabolomic analyses, these findings indicate sex specific regulation of peroxisomal β-oxidation in *C. elegans*.

Conclusion

In summary, we have demonstrated that ascaroside biosynthesis and functions are sex-specific. We propose a model (**Figure 1.4**) in which male *C. elegans* of reproductive age produce a sex-specific blend of ascarosides, the major component of which, ascr#10, strongly retains and attracts hermaphrodites, whereas *C. elegans* hermaphrodites, also of reproductive age, most abundantly produce the corresponding dehydro-derivative ascr#3, which serves as a male attractant but repels hermaphrodites. A single double bond differentiates ascr#10 and ascr#3, yet dramatically changes the signaling properties of these two molecules. The differences between male and hermaphrodite expression levels of the four genes involved in peroxisomal side chain biosynthesis as well as the results from our worm-body ascaroside analyses suggest that the observed sex-specific differences in ascaroside profiles are not simply the result of relative differences in ascaroside secretion rate, but rather result from sex-specific control of ascaroside biosynthesis. We further show that male *C. elegans* respond to the presence of other worms with increased ascaroside production, a type of response not seen in hermaphrodites. Whether sensing of the male-specific ascarosides plays a role in male population density signaling remains to be determined. Given the large quantities of ascr#10 produced by males and its potent activity, it is likely that ascr#10 constitutes an important component of the male sex pheromone blend in *C. elegans.* Based on our bioassay results it appears that the amounts of ascr#10 excreted by a single male are more than sufficient to affect hermaphrodite behavior. It is likely that other, less abundant ascarosides contribute to hermaphrodite retention and attraction, for example, males may also produce some of

the indole ascarosides we found to be upregulated in the male-rich *him-5* liquid cultures (**Figure 1.1a**). Notably, hermaphrodite worms also release ascr#10, although in much smaller quantities, which could contribute to indole ascaroside-mediated aggregation or counteract dispersal behavior driven by ascr#3 (*8*). Our study shows that minute changes in ascaroside structures can dramatically affect their signaling properties. HPLC-MS-based metabolic profiling of small numbers of worms, as demonstrated here, provides the basis for more detailed exploration of the biological functions and underlying sensory mechanisms of this library of small molecule signals.

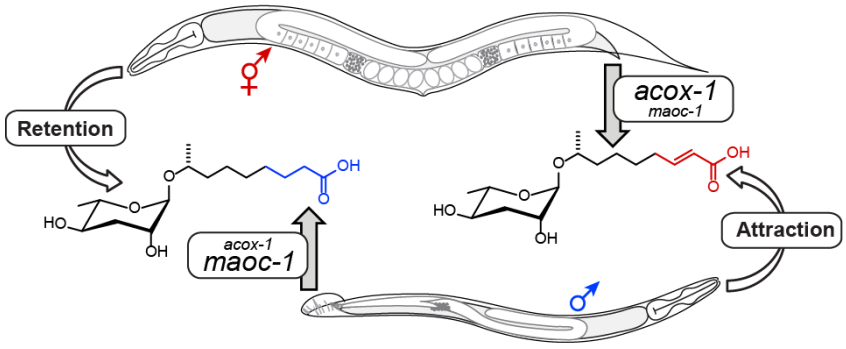

Figure 1.4. Model for sex-specific ascaroside biosynthesis. Male *C. elegans* predominantly produce ascr#10 which is a strong retention signal for hermaphrodites. We also confirmed that hermaphrodites predominantly the dehydro derivative ascr#3, a compound known to act as a male attractant. Published microarray data support sex-specific biosynthesis through regulation of peroxisomal β-oxidation genes. *Model designed by YI and FCS, worm drawings provided by JS.*

REFERENCES

1. Izrayelit, Y., Srinivasan, J., Campbell, S. L., Jo, Y., von Reuss, S. H., Genoff, M. C., Sternberg, P. W., and Schroeder, F. C. (2012) Targeted metabolomics reveals a male pheromone and sex-specific ascaroside biosynthesis in *Caenorhabditis elegans*, *ACS Chem. Biol. 7,* 1321-1325.
2. Fielenbach, N., and Antebi, A. (2008) *C. elegans* dauer formation and the molecular basis of plasticity, *Genes Dev. 22*, 2149-2165.
3. Hulme, S. E., and Whitesides, G. M. (2011) Chemistry and the worm: *Caenorhabditis elegans* as a platform for integrating chemical and biological tesearch, *Angew. Chem. Int. Edit. 50*, 4774-4807.
4. von Reuss, S. H., Bose, N., Srinivasan, J., Yim, J. J., Judkins, J. C., Sternberg, P. W., and Schroeder, F. C. (2012) Comparative metabolomics reveals biogenesis of ascarosides, a modular library of small molecule signals in *C. elegans*, *J. Am. Chem. Soc. 134*, 1817–1824.
5. Jeong, P. Y., Jung, M., Yim, Y. H., Kim, H., Park, M., Hong, E. M., Lee, W., Kim, Y. H., Kim, K., and Paik, Y. K. (2005) Chemical structure and biological activity of the *Caenorhabditis elegans* dauer-inducing pheromone, *Nature 433*, 541-545.
6. Butcher, R. A., Fujita, M., Schroeder, F. C., and Clardy, J. (2007) Small-molecule pheromones that control dauer development in Caenorhabditis elegans, *Nat. Chem. Biol. 3*, 420-422.
7. Srinivasan, J., Kaplan, F., Ajredini, R., Zachariah, C., Alborn, H. T., Teal, P. E. A., Malik, R. U., Edison, A. S., Sternberg, P. W., and Schroeder, F. C. (2008) A blend of small molecules regulates both mating and development in *Caenorhabditis elegans*, *Nature 454*, 1115-1118.
8. Srinivasan, J., von Reuss, S. H., Bose, N., Zaslaver, A., Mahanti, P., Ho, M. C., O'Doherty, O. G., Edison, A. S., Sternberg, P. W., and Schroeder, F. C. (2012) A modular library of small molecule signals regulates social behaviors in Caenorhabditis elegans, *PLoS Biol. 10*, e1001237.
9. Kaplan, F., Srinivasan, J., Mahanti, P., Ajredini, R., Durak, O., Nimalendran, R., Sternberg, P. W., Teal, P. E. A., Schroeder, F. C., Edison, A. S., and Alborn, H. T. (2011) Ascaroside expression in *Caenorhabditis elegans* is strongly dependent on diet and developmental stage, *Plos One 6*, e17804
10. Edison, A. S. (2009) *Caenorhabditis elegans* pheromones regulate multiple complex behaviors, *Curr. Opin. Neurobiol. 19*, 378-388.
11. Chasnov, J. R., and Chow, K. L. (2002) Why are there males in the hermaphroditic species *Caenorhabditis elegans*?, *Genetics 160*, 983-994.
12. Hodgkin, J., Horvitz, H. R., and Brenner, S. (1979) Nondisjunction mutants of the nematode *Caenorhabditis elegans*, *Genetics 91*, 67-94.
13. Schedl, T., Graham, P. L., Barton, M. K., and Kimble, J. (1989) Analysis of the role of tra-1 in germline sex determination in the nematode *Caenorhabditis elegans*, *Genetics 123*, 755-769.
14. Hodgkin, J., and Doniach, T. (1997) Natural variation and copulatory plug formation in *Caenorhabditis elegans*, *Genetics 146*, 149-164.

15. Garcia, L. R., LeBoeuf, B., and Koo, P. (2007) Diversity in mating behavior of hermaphroditic and male-female caenorhabditis nematodes, *Genetics 175*, 1761-1771.
16. Prahlad, V., Pilgrim, D., and Goodwin, E. B. (2003) Roles for mating and environment in *C. elegans* sex determination, *Science 302*, 1046-1049.
17. Srinivasan, J., Kaplan, F., Ajredini, R., Zachariah, C., Alborn, H. T., Teal, P. E., Malik, R. U., Edison, A. S., Sternberg, P. W., and Schroeder, F. C. (2008) A blend of small molecules regulates both mating and development in *Caenorhabditis elegans*, *Nature 454*, 1115-1118.
18. Jiang, M., Ryu, J., Kiraly, M., Duke, K., Reinke, V., and Kim, S. K. (2001) Genome-wide analysis of developmental and sex-regulated gene expression profiles in *Caenorhabditis elegans*, *Proc. Natl Acad. Sci. USA 98*, 218-223.

CHAPTER 2

PHEROMONE SENSING REGULATES *CAENORHABDITIS ELEGANS* LIFESPAN AND STRESS RESISTANCE VIA THE DEACETYLASE SIR-2.1

Abstract

Lifespan in *Caenorhabditis elegans*, *Drosophila*, and mice is regulated by conserved signaling networks, including the insulin/insulin-like growth factor 1 (IGF-1) signaling cascade and pathways depending on sirtuins, a family of NAD^+-dependent deacetylases. Small molecules such as resveratrol are of great interest because they increase lifespan in many species in a sirtuin-dependent manner. However, no endogenous small molecules that regulate lifespan via sirtuins have been identified, and the mechanisms underlying sirtuin-dependent longevity are not well understood. This report shows that in *C. elegans*, two endogenously produced small molecules, the dauer-inducing ascarosides ascr#2 and ascr#3, regulate lifespan and stress resistance through chemosensory pathways and the sirtuin SIR-2.1. Ascarosides extend adult lifespan and stress resistance without reducing fecundity or feeding rate, and these effects are reduced or abolished when nutrients are restricted. We found that ascaroside-mediated longevity is fully abolished by loss of SIR-2.1 and that the effect of ascr#2 requires expression of the G protein-coupled receptor DAF-37 in specific chemosensory neurons. In contrast to many other lifespan-modulating factors, ascaroside-mediated lifespan increases do not require insulin signaling via the FOXO

homolog DAF-16 or the insulin/IGF-1-receptor homolog DAF-2. Our study demonstrates that *C. elegans* produces specific small molecules to control adult lifespan in a sirtuin-dependent manner, supporting the hypothesis that endogenous regulation of metazoan lifespan functions, in part, via sirtuins. These findings strengthen the link between chemosensory inputs and conserved mechanisms of lifespan regulation in metazoans and suggest a model for communal lifespan regulation in *C. elegans*.

Contributions

The work in this chapter was conducted by a team of scientists in the Schroeder Lab (Cornell University, Ithaca, NY), and the Riddle Lab (Michael Smith Laboratories, University of British Columbia, Vancouver, BC, Canada). The data and writing, with minor modifications, in this chapter has been published in Proc. Natl Acad. Sci.(*1*). ***Yevgeniy Izrayelit (YI) is a co-first author on this publication. YI designed and performed the aging studies, wrote the manuscript, analyzed all aging and heat stress results. YI's primary data contribution was design, set up and conduction of aging studies and statistical analysis of lifespan results.*** Hanno Andreas Ludewig (HAL) was a co-first author on this study and performed aging studies, assisted with data analysis and manuscript preparation. Donha Park (DP) performed aging studies with *daf-37* related mutants in the lab of Professor Don Riddle (DLR). Rabia U. Malik (RUM) primarily performed heat stress assays and supported aging experiments as well as assisted with experimental design. Parag Mahanti (PM) and Bennet W. Fox (BWF) synthesized ascarosides for assays. Both Anna Zimmerman (AZ) and Axel Bethke (AB) supported experimental setup. Professor Don Riddle assisted in manuscript preparation. Professor Frank Schroeder (FCS) supervised the project and wrote the manuscript.

Introduction

Caenorhabditis elegans excretes a family of small molecules, the ascarosides, which regulate several different aspects of the life history of this nematode, including developmental timing (*2-4*), mate attraction (*4-6*), aggregation behavior (*7, 8*), and olfactory learning (*9*). These compounds are derived from the dideoxysugar ascarylose, which is linked to fatty acid-like side chains of varying lengths and in some cases features additional substituents derived from amino acid metabolism and other pathways (*8*). Originally, the ascarosides were identified as components of a population density signal, the *C. elegans* dauer pheromone. High population density results in accumulation of the constitutively expressed ascarosides, which in combination with additional environmental stimuli such as limited food availability or temperature stress promote larval arrest at the dauer stage (*2-4*). Dauer larvae are non-feeding, highly stress-resistant, and can survive for up to 6 months before resuming development into adults of a normal lifespan of about 2 weeks (*10*). The signaling cascade from pheromone to dauer induction has been characterized in considerable detail. The dauer-inducing ascarosides are sensed by several different G protein-coupled receptors in specific chemosensory neurons (*11-13*). These are coupled to several downstream signaling cascades, including the conserved insulin/IGF-1, and TGF-β-signalling pathways (*14-16*). Mutations in dauer signaling genes often display long lived lifespan phenotypes in adult *C. elegans* (*17, 18*) and homologs of dauer genes are involved in lifespan regulation of many higher organisms (*14*).

The strong analogies between dauer signaling and conserved aging pathways suggested that dauer pheromone components may also affect *C. elegans* adult lifespan.

Previous studies have yielded conflicting evidence regarding the effects of dauer pheromone on adults (*19-21*); however, these studies tested for the lifespan-extending effects of the entire *C. elegans* exo-metabolome, which in addition to a variety of dauer-inducing ascarosides contains a vast assortment of other metabolites. Therefore, we investigated the effects of pure synthetic samples of dauer-inducing ascarosides on *C. elegans* adult lifespan.

Ascr#2 and ascr#3 extend *C. elegans* lifespan and stress resistance

We tested the effect of ascr#2 and ascr#3 (**Figures 2.1a,b**), the two most consistently produced ascarosides (*2, 4*), on *C. elegans* lifespan. We found that exposure to ascarosides resulted in a concentration-dependent increase of lifespan. Mean lifespan of L4-stage worms transferred onto plates containing ascr#2 or ascr#3 was significantly increased in a concentration-dependent manner (**Figures 2.1c,d, and Table B.1**). Lifespan of worms on plates containing 400 nM of ascr#2 or ascr#3, concentrations typical of high-density *C. elegans* cultures (*8*), was increased by 17% and 21%, respectively. Higher concentrations did not confer significantly higher lifespan gains, and mixtures of ascr#2 and ascr#3 extended lifespan to a similar extent as the individual compounds (**Table B.1 and Figure B.1**).

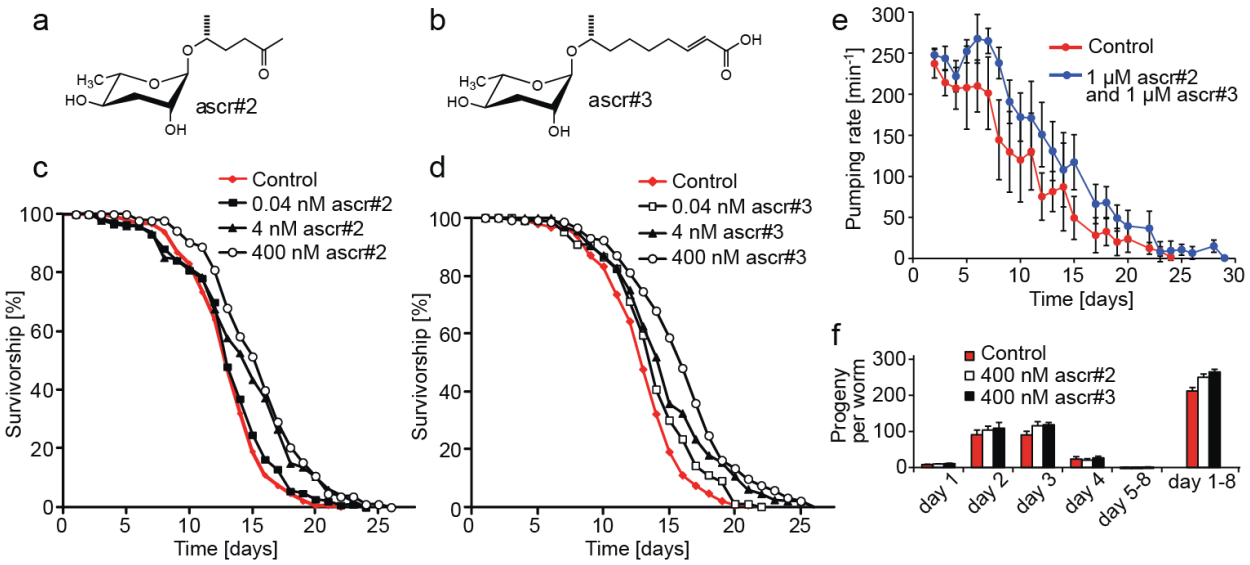

Figure 2.1. Ascarosides increase adult lifespan in wildtype (N2) *C. elegans* in a concentration dependent manner. (a) Chemical structure of ascr#2. (b) Chemical structure of ascr#3. (c) Survivorship of worms at 20 °C exposed to 0.04 nM of ascr#2, number of worms (n) = 147, average lifespan (m) = 13.4 d, p = 0.253; 4 nM ascr#2, n = 137, m = 14.5 d, p < 0.0001; 400 nM of ascr#2, n = 111, m = 15.1 d, p < 0.0001; and mock treated controls n = 155, m = 13.2 d. (d) Survivorship of worms exposed to 0.04 nM of ascr#3, n = 139, m = 14.6 d, p < 0.0001; 4 nM ascr#3, n = 132, m = 14.9 d, p < 0.0001; 400 nM of ascr#3, n = 134, m = 16.0 d, p < 0.0001; and mock treated n = 155, m = 13.2 d. (e) Pharyngeal pumping rate of worms exposed to 1 µM of ascr#2 and ascr#3 compared to mock treated control. Error bars, s.d. (f) Fecundity of worms exposed to 400 nM of ascr#2 or ascr#3 compared to mock treated control. Error bars, s.d. *YI and HAL performed aging studies. HAL measured pumping rate and counted progeny per worm. YI and HAL analyzed data.*

Because in many animals reduced food intake (Dietary Restriction, DR) results in increased lifespan, it seemed possible that ascaroside-mediated lifespan increases were the result of altered feeding behavior. Therefore, we monitored changes in pharyngeal pumping rate, a measure for *C. elegans* food intake, and fecundity upon ascaroside exposure (*22*). Pharyngeal pumping rates of ascaroside-treated worms were similar to control until day 4 of the experiments and significantly higher than control from day 5 until death (**Figure 2.1e**), indicating that reduced food intake is not a likely cause

for the observed lifespan increases. Furthermore, overall fecundity of ascaroside-treated worms was slightly higher than control (**Figure 2.1f**).

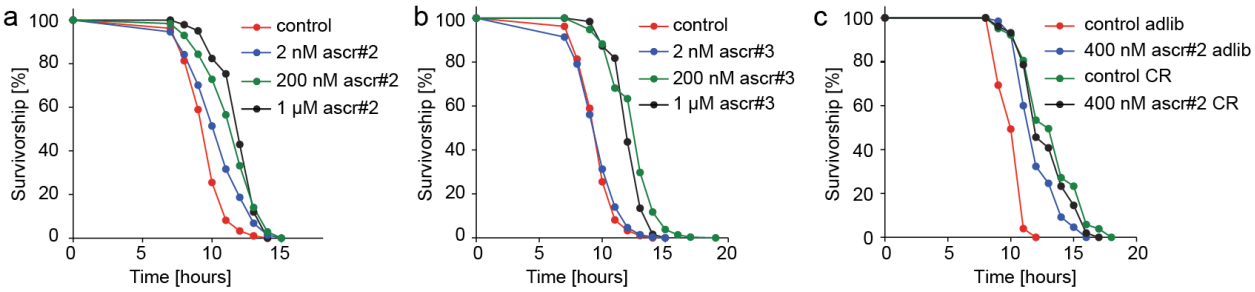

Figure 2.2. Ascarosides increase thermotolerance at 35°C in wildtype (N2) *C. elegans* in a concentration dependent manner. (a) Survivorship of adult worms at 35°C exposed to 2 nM, 200 nM, and 1 µM ascr#2; 2 nM of ascr#2, number of worms (n) = 278, average survival time (m) = 10.6 h, $p < 0.0001$; 200 nM of ascr#2, n = 313, m = 11.6 h, $p < 0.0001$; 1 µM of ascr#2, n = 142, m = 12.1 h, $p < 0.0001$; and mock treated control n = 1062, m = 9.7 h. (b) Survivorship of adult worms at 35°C exposed to 2 nM, 200 nM, and 1 µM ascr#2. 2 nM ascr#3, n = 278, m = 9.8 h, $p = 0.004$; 200 nM ascr#3, n = 289, m = 12.6 h, $p < 0.0001$; 1 µM ascr#3, n = 126, m = 12.6 h, $p < 0.0001$; and mock treated control n = 1062, m = 9.7 h. (c) Survivorship of adult worms at 35°C exposed to 400 nM ascr#2 compared to mock treated controls, using two different nutritional conditions; "adlib" (with bacteria) and "DD" (without bacteria). adlib: ascr#2, n = 65, m = 12.2 h, $p < 0.0001$; control, n = 75, m = 10.2 h. DD: ascr#2, n = 103, m = 12.9 h, $p = 0.145$; control, n = 103, m = 13.3 h. *RUM performed heat stress experiments. RUM and YI analyzed data.*

In *C. elegans* and other organisms, environmental conditions or genetic changes that result in increased lifespan are frequently associated with enhanced resistance to stress, including heat stress and oxidative stress (*23*). We found that ascarosides markedly increased survival under oxidative stress (**Figure B.2a**) and resistance to heat stress in a concentration dependent manner (thermotolerance at 35 ºC, **Figures 2.2a, b, and Table B.2**). We further measured pharyngeal pumping rates under heat stress and found that pumping rates of worms on ascaroside plates were significantly higher than on control plates (**Figure B.2b**). Consequently, we named the observed effect ascaroside-mediated increases of lifespan and stress resistance (AMILS).

AMILS depends on nutritional conditions

Next, we asked whether nutritional conditions influence AMILS. For thermotolerance assays under dietary deprivation (DD) conditions, we used a protocol in which young adult worms are transferred to plates without bacteria before exposure to heat stress (*24*). Mean heat stress survival time under DD conditions was higher than for worms with bacteria, in accordance with previous studies demonstrating increased stress resistance under these conditions (*24*). Notably, addition of ascarosides did not further increase thermotolerance of DD worms (**Figure 2.2c**). Additional lifespan assays using dietary restriction (DR) conditions (*25*) showed a similar pattern (**Figure B.3**). As expected, DR control worms lived longer than non-DR controls; however, ascarosides increased lifespan of DR worms less than of non-DR worms (Fig. S3). These results show that the effect of ascarosides on *C. elegans* thermotolerance and lifespan strongly depends on nutritional conditions.

AMILS requires the histone deacetylase SIR-2.1

To investigate the mechanism of AMILS, we probed conserved genetic pathways known to regulate lifespan in *C. elegans* and other metazoans. The observation that AMILS is reduced or abolished under starvation conditions led us to investigate a possible role of the sirtuin SIR-2.1, a NAD^+-dependent histone deacetylase (*26*). DR, DD, and other forms of caloric restriction (*27*) have been shown to increase lifespan and stress resistance in many organisms, and in several cases, including yeast and mice, this effect has been found to depend on sirtuins (*14, 28-33*). In *C. elegans*, SIR-2.1 has been shown to be required for lifespan increases by resveratrol and other compounds

(*26, 34*), although it is unclear to what extent SIR-2.1 is required for DR-dependent lifespan increases. For example, SIR-2.1 is not required for lifespan extension associated with DD of non-fertile worms (*24*), whereas lifespan increases associated with milder forms of DR appear to require this gene (*14*). The role of sirtuins in *C. elegans* and *Drosophila* lifespan continues to be discussed extensively (*14, 35, 36*).

We found that neither ascr#2 nor ascr#3 extend lifespan or thermotolerance in the null allele *sir-2.1(ok434)* (lifespan: **Figure 2.3a and Table B.1**; thermotolerance: **Figures B.4a,b and Table B.2**). We then investigated the effect of ascr#2 on an outcrossed SIR-2.1-overexpressing strain, NL3909, relative to its control, NL3908 (*35, 37, 38*). ascr#2 increased lifespan of NL3909 worms to a similar extent as for NL3908 control worms (**Figure 2.3b**, **and Table B.1**). These results indicate that SIR-2.1 is required for AMILS, but overexpression of SIR-2.1 does not significantly affect the amount of lifespan extension.

AMILS is largely independent of classical dauer signaling pathways

Because ascarosides induce formation of dauer larvae in *C. elegans*, we asked whether AMILS depends on conserved aging pathways involved in dauer formation, including insulin/IGF-1, TGF-β, and nuclear hormone receptor (DAF-12) signaling (*39*). Testing the effect of ascarosides on the insulin/IGF-1 receptor mutant strain, *daf-2(e1368)* (*14*), we found that both ascr#2 and ascr#3 further increased lifespan and thermotolerance of this long-lived mutant (**Figures 2.3c, B.5, and Table B.1**). DAF-2 negatively regulates the FOXO-like transcription factor DAF-16, which is required for many lifespan or stress resistance-enhancing mutations described for *C. elegans* (*14*). Ascarosides significantly increased lifespan and thermotolerance of the short-lived null

allele *daf-16(mu86)* even at low concentrations (**Figures 2.3c, B.5, and Table B.1**), although the observed lifespan increases were somewhat smaller than for wild type. We confirmed lifespan increase in a second *daf-16* allele, a *daf-16(mgDf50)* mutant in *sir-2.1* overexpressing background (**Figure B.6, and Table B.1**). AMILS, therefore, is largely independent of insulin signaling via DAF-16.

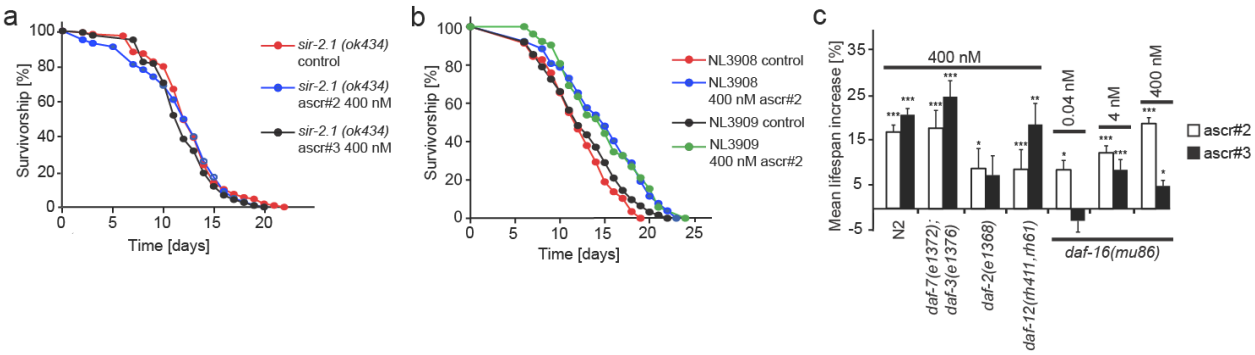

Figure 2.3. AMILS requires SIR-2.1 but not classical dauer pathway genes. (a) Survivorship of *sir-2.1(ok434)* mutant worms exposed to 400 nM of ascr#2 or ascr#3. Ascr#2: number of worms (n) = 100, average lifespan (m) = 11.8 d; ascr#3: n = 119, m = 11.9 d; mock-treated control: n = 109, m = 12.5 d. (b) Survivorship of the *sir-2.1* over expresser NL3909 and its control NL3908 treated with ascr#2 400 nM. NL3909, ascr#2: n = 178, m = 13.7 d, p = 0.002; NL3909, mock-treated control: n = 174, m = 12.4 d. NL3908 ascr#2: n = 111, m = 15.2 d, p < 0.0001; NL30908, mock treated control: n = 125, m = 12.0 d. (c) Mean lifespan extension for mutant strains of genes involved in dauer induction. Error Bars, s. e. m. for highlighted experiments. For full data see Table Table B.1. ***p<0.0001, **p<0.001, *p<0.05. *YI, HAL and RUM performed aging studies.*

AMILS is also maintained in the null allele of another key component of dauer signaling, the nuclear hormone receptor DAF-12 (**Figure 2.3c, and Table B.1**) (*40*). To determine a possible role of TGF-β signaling, we tested the effect of ascarosides on lifespan and thermotolerance of a *daf-7;daf-3* double mutant strain. *daf-7* and *daf-3* encode the TGF-β ligand and a co-SMAD protein that functions as a transcriptional regulator downstream of *daf-7*, respectively (*41*). *daf-7(e1372);daf-3(e1376)* double mutant worms responded to ascarosides similarly to wild type (**Figures 2.3c, B.5, and**

Table B.1). We conclude that AMILS functions largely independently from the main dauer signaling pathways, requiring SIR-2.1 but not insulin/IGF-1 or TGF-β signaling.

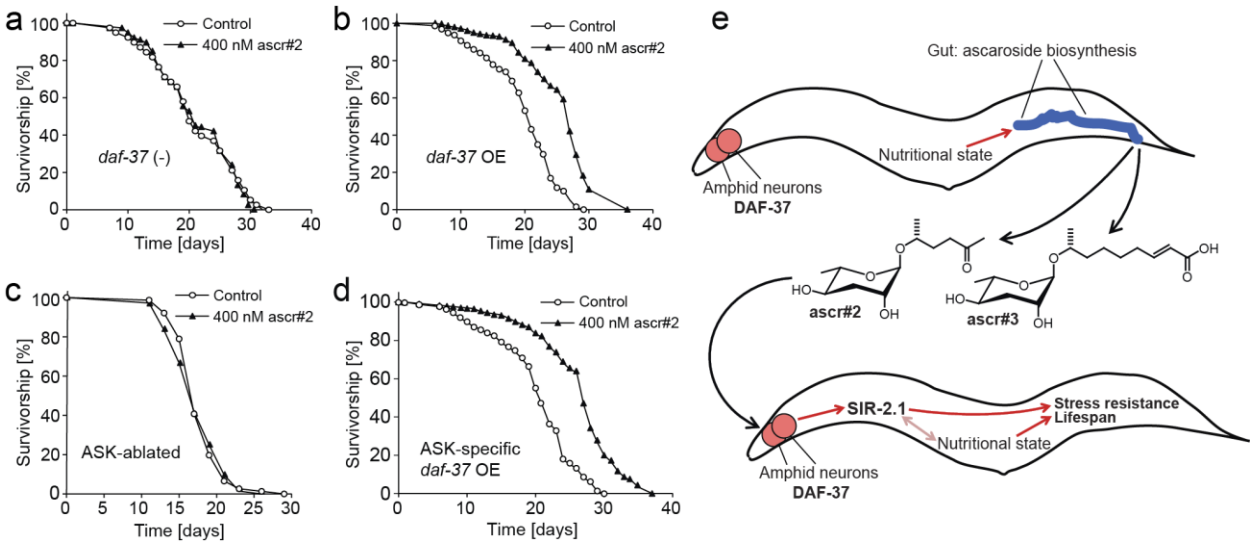

Figure 2.4. ASK neurons and the GPCR DAF-37 are required for lifespan extension via ascr#2. (a) Survivorship of *daf-37 (-)* mutant worms exposed to 400 nM ascr#2, number of worms (n) = 42, average lifespan (m) = 20.9 d, compared to mock-treated controls, n = 38, m = 21.3 d**.** (b) Survivorship of *daf-37;mIs41[daf-37p::cMyc::daf-37]* (*daf-37* OE) worms exposed to 400 nM ascr#2, n = 56, m = 25.5 d, $p < 0.0001$, compared to mock-treated controls, n = 77, m =19.8 d. (c) Survivorship of worms with genetically ablated ASK neurons exposed to 400 nM ascr#2, n = 79, m = 18.8 d, compared to mock treated controls, n = 74, m = 19.0 d. (d) Survivorship of *daf-37; unc-119; mEx188[srbc-64p::daf-37,unc-119(+)]* (ASK neuron-specific *daf-37* OE in *daf-37* null background) worms exposed to 400 nM ascr#2, n = 60, m = 26.2 d, $p < 0.0001$, compared to mock-treated controls n = 85, m = 20.0 d. (e) Model for communal lifespan regulation via pheromone signaling. *C. elegans* constitutively produce ascr#2 and ascr#3, resulting in population density-dependent ascaroside concentrations. Chemosensation of the ascarosides integrated with environmental and nutritional cues results in activation of longevity and/or stress-resistance genes in a SIR-2.1 dependent manner. *DP and YI performed aging studies. Model designed by YI, HAL, and FS.*

Sensory neurons and a GPCR mediate ascr#2-dependent lifespan extension

Next we asked whether AMILS is mediated by chemosensory neurons and receptors that have been shown to participate in ascaroside sensing (*5, 7, 11-13*). For these investigations, we focused on ascr#2 for which we had recently described a highly specific G-protein-coupled receptor, DAF-37 (*13*). DAF-37 expression in the ASI

chemosensory neurons is required for dauer formation in response to ascr#2, whereas the behavioral phenotypes of ascr#2 depend on DAF-37 expression in the ASK neurons. ascr#2 directly binds to DAF-37, and it was further shown that *daf-37* null worms are defective in their dauer and behavioral responses only to ascr#2, but not to other ascarosides (*13*). We found that ascr#2 does not increase lifespan of *daf-37* null worms (**Figure 2.4a**), which could be rescued by *daf-37* cDNA under its own promoter (**Figure 2.4b**). In addition, ascr#2-dependent lifespan increase was fully abolished in worms lacking the ASK neurons (**Figure 2.4c**) due to cell-specific expression of mammalian caspase in the developing neurons. ascr#2-induced lifespan increase was also rescued by *daf-37* cDNA driven by the ASK-selective *srbc-64* promoter (**Figure 2.4d**). In contrast, ascr#2-treatment of worms expressing *daf-37* cDNA under the ASI-specific *gpa-4* promoter resulted in variable results, whereby one experiment showed no change in lifespan compared to control and two subsequent experiments showed a small but significant lifespan decrease (**Figure 2A.7, and Table B.1**). These results indicate that *daf-37* expression in the ASK neurons is sufficient for ascr#2-dependent lifespan increase, in contrast to the dauer inducing effects of ascr#2, which require expression in ASI (*13*).

Conclusion

We here demonstrate that sensing of excreted small molecules regulates *C. elegans* lifespan and stress resistance via pathways that require the sirtuin SIR-2.1. Ascarosides increase adult lifespan at physiological concentrations typical of high-density *C. elegans* cultures, without reducing fecundity or feeding rate. In contrast to many other metazoan examples for life extension, AMILS does not require insulin

signaling *via* DAF-16. Furthermore, AMILS does not depend on DAF-12, which is required for germline-dependent modulation of *C. elegans* lifespan (*42*). These observations starkly differentiate AMILS from dauer formation.

Previous studies suggested a complex role for *sir-2.1* in *C. elegans* lifespan regulation (*14, 21*). There is increasing evidence that sirtuin-overexpression increases lifespan across model systems (*38, 43*), although in some cases this effect may not be as robust as initially reported (*35, 36, 44*). In addition, genetic studies of *sir-2.1* deletion strains suggest that *sir-2.1* influences lifespan in a *daf-16*-independent manner as part of the CR pathway (*45-47*). Recent work connecting sirtuins and longevity in mouse affirmed a conserved role for sirtuins in lifespan regulation (*48*). With regard to sirtuin-dependence, AMILS resembles the lifespan increasing effects of exogenous small molecules such as resveratrol. Comparatively high concentrations of resveratrol (10-100 µM) increase lifespan in *C. elegans* and *Drosophila*, and this effect has been shown to require SIR-2.1 in *C. elegans* and its homolog Sir2 in *Drosophila (26).* Similar to resveratrol-mediated lifespan increases, AMILS does not carry any apparent cost of reproduction, is reduced or abolished when nutrients are restricted, and does not require *daf-16*. It has been suggested that resveratrol increases metazoan lifespan *via* pathways related to CR (*26*); however, the mechanisms of resveratrol-mediated lifespan increases are not well understood (*14*) and it has been suggested that the relatively weak lifespan-increasing effects of resveratrol in *C. elegans* could merely reflect activation of detoxification mechanisms (*36*). Given that AMILS requires much lower (compared to resveratrol) concentrations of compounds that are endogenously

produced and perceived by highly specific membrane receptors, it is unlikely that detoxification plays a role for the lifespan-mediating effects of ascarosides.

In dauer formation, the ascarosides act through several amphid neurons (*5, 49*), and six G-protein-coupled receptors have been associated with ascaroside-mediated dauer induction (*11-13*). We recently showed that DAF-37 is required specifically for sensing of ascr#2, and that DAF-37 expression in the ASK neurons is required for the behavioral phenotypes of ascr#2, whereas DAF-37 expression in the ASI neurons is required for ascr#2-mediated dauer induction (*13*). Here we show that DAF-37 is also required for ascr#2-mediated lifespan extension; and that DAF-37 expression in the ASK neurons is sufficient for this phenotype, further distinguishing AMILS from dauer. Therefore, AMILS provides a direct example for a lifespan regulatory mechanism based on chemosensation of an endogenously produced small-molecule signal.

Genetic and small-molecule screens have previously suggested a connection between GPCR signaling and lifespan in *Drosophila* (*50, 51*). In these studies, GPCR mutation or inhibition of downstream signaling components extended fly lifespan, but it is unclear whether chemosensation played a role. Notably, GPCRs have also been implicated in many age-related diseases (*27*). In Figure 2.4e, we present a simplified model for AMILS in *C. elegans*. As products of peroxisomal β-oxidation and other primary metabolic pathways (*8*), ascarosides integrate input from the nutritional state of the producing animal. Primary site of ascaroside biosynthesis appears to be the worm gut (*52*), and it seems likely that ascarosides are also excreted via the gut. In the perceiving worm, GPCR's in the amphid chemosensory neurons trigger downstream signaling cascades promoting longevity and stress resistance via SIR-2.1, additionally

integrating information about the perceiving animal's nutritional state. In essence, AMILS may represent a model for communal mechanism for lifespan regulation (**Figure 2.4e**).

Our study highlights the significance of sirtuin-dependent signaling pathways for endogenous lifespan regulation, and ascarosides may serve as useful tools to investigate the mechanisms of sirtuin-dependent longevity, which remain poorly understood (*28*). The ascarosides are derived from highly conserved peroxisomal fatty acid β-oxidation, and their biosynthesis is regulated in part by nutritional state (*8*), suggesting a link between nutritional state, fat metabolism, and sirtuin-dependent lifespan regulation. Furthermore, analysis of the adaptive significance of sirtuin-dependent lifespan regulation via ascarosides in *C. elegans* may lead to a better understanding of the evolutionary forces that determine lifespan, and may inspire a search for endogenous small molecules that promote sirtuin-dependent longevity in other metazoans.

REFERENCES

1. Ludewig, A. H., Izrayelit, Y., Park, D., Malik, R. U., Zimmermann, A., Mahanti, P., Fox, B. W., Bethke, A., Doering, F., Riddle, D. L., and Schroeder, F. C. (2013) Pheromone sensing regulates *Caenorhabditis elegans* lifespan and stress resistance via the deacetylase SIR-2.1, *Proc. Natl Acad. Sci. USA 110*, 5522-5527.
2. Butcher, R. A., Fujita, M., Schroeder, F. C., and Clardy, J. (2007) Small-molecule pheromones that control dauer development in *Caenorhabditis elegans*, *Nat. Chem. Biol. 3*, 420-422.
3. Jeong, P. Y., Jung, M., Yim, Y. H., Kim, H., Park, M., Hong, E. M., Lee, W., Kim, Y. H., Kim, K., and Paik, Y. K. (2005) Chemical structure and biological activity of the *Caenorhabditis elegans* dauer-inducing pheromone, *Nature 433*, 541-545.
4. Pungaliya, C., Srinivasan, J., Fox, B. W., Malik, R. U., Ludewig, A. H., Sternberg, P. W., and Schroeder, F. C. (2009) A shortcut to identifying small molecule signals that regulate behavior and development in *Caenorhabditis elegans*, *Proc. Natl Acad. Sci. USA 106*, 7708-7713.
5. Srinivasan, J., Kaplan, F., Ajredini, R., Zachariah, C., Alborn, H. T., Teal, P. E., Malik, R. U., Edison, A. S., Sternberg, P. W., and Schroeder, F. C. (2008) A blend of small molecules regulates both mating and development in *Caenorhabditis elegans*, *Nature 454*, 1115-1118.
6. Izrayelit, Y., Srinivasan, J., Campbell, S. L., Jo, Y., von Reuss, S. H., Genoff, M. C., Sternberg, P. W., and Schroeder, F. C. (2012) Targeted metabolomics reveals a male pheromone and sex-specific ascaroside biosynthesis in *Caenorhabditis elegans*, *ACS Chem. Biol. 7,* 1321-1325.
7. Srinivasan, J., von Reuss, S. H., Bose, N., Zaslaver, A., Mahanti, P., Ho, M. C., O'Doherty, O. G., Edison, A. S., Sternberg, P. W., and Schroeder, F. C. (2012) A modular library of small molecule signals regulates social behaviors in *Caenorhabditis elegans*, *PLoS Biol. 10*, e1001237.
8. von Reuss, S. H., Bose, N., Srinivasan, J., Yim, J. J., Judkins, J. C., Sternberg, P. W., and Schroeder, F. C. (2012) Comparative metabolomics reveals biogenesis of ascarosides, a modular library of small molecule signals in C. elegans, *J. Am. Chem. Soc. 134*, 1817–1824.
9. Yamada, K., Hirotsu, T., Matsuki, M., Butcher, R. A., Tomioka, M., Ishihara, T., Clardy, J., Kunitomo, H., and Iino, Y. (2010) Olfactory plasticity is regulated by pheromonal signaling in *Caenorhabditis elegans*, *Science 329*, 1647-1650.
10. Golden, J. W., and Riddle, D. L. (1984) The *Caenorhabditis elegans* dauer larva - developmental effects of pheromone, food, and temperature, *Dev. Biol. 102*, 368-378.
11. Kim, K., Sato, K., Shibuya, M., Zeiger, D. M., Butcher, R. A., Ragains, J. R., Clardy, J., Touhara, K., and Sengupta, P. (2009) Two chemoreceptors mediate developmental effects of dauer pheromone in *C. elegans*, *Science 326*, 994-998.
12. McGrath, P. T., Xu, Y., Ailion, M., Garrison, J. L., Butcher, R. A., and Bargmann, C. I. (2011) Parallel evolution of domesticated Caenorhabditis species targets pheromone receptor genes, *Nature 477*, 321–325.

13. Park, D., O'Doherty, I., Somvanshi, R. K., Bethke, A., Schroeder, F. C., Kumar, U., and Riddle, D. L. (2012) Interaction of structure-specific and promiscuous G-protein-coupled receptors mediates small-molecule signaling in *Caenorhabditis elegans*, *Proc. Natl Acad. Sci. USA 109*, 9917-9922.
14. Kenyon, C. J. (2010) The genetics of ageing, *Nature 464*, 504-512.
15. Riddle, D. L. (1977) Genetic pathway for dauer larva formation in nematode, *Caenorhabditis elegans*, *Genetics 86*, S51-S52.
16. Shaw, W. M., Luo, S., Landis, J., Ashraf, J., and Murphy, C. T. (2007) The *C. elegans* TGF-beta dauer pathway regulates longevity via insulin signaling, *Curr. Biol. 17*, 1635-1645.
17. Larsen, P. L., Albert, P. S., and Riddle, D. L. (1995) Genes that regulate both development and longevity in *Caenorhabditis elegans*, *Genetics 139*, 1567-1583.
18. Tatar, M., Bartke, A., and Antebi, A. (2003) The endocrine regulation of aging by insulin-like signals, *Science 299*, 1346-1351.
19. Alcedo, J., and Kenyon, C. (2004) Regulation of *C. elegans* longevity by specific gustatory and olfactory neurons, *Neuron 41*, 45-55.
20. Kawano, T., Kataoka, N., Abe, S., Ohtani, M., Honda, Y., Honda, S., and Kimura, Y. (2005) Lifespan extending activity of substances secreted by the nematode *Caenorhabditis elegans* that include the dauer-inducing pheromone, *Biosci. Biotech. Bioch. 69*, 2479-2481.
21. Kenyon, C. (2005) The plasticity of aging: insights from long-lived mutants, *Cell 120*, 449-460.
22. Huang, C., Xiong, C., and Kornfeld, K. (2004) Measurements of age-related changes of physiological processes that predict lifespan of *Caenorhabditis elegans*, *Proc. Natl Acad. Sci. USA 101*, 8084-8089.
23. Lithgow, G. J., White, T. M., Melov, S., and Johnson, T. E. (1995) Thermotolerance and extended life-span conferred by single-gene mutations and induced by thermal stress, *Proc. Natl Acad. Sci USA 92*, 7540-7544.
24. Lee, G. D., Wilson, M. A., Zhu, M., Wolkow, C. A., de Cabo, R., Ingram, D. K., and Zou, S. (2006) Dietary deprivation extends lifespan in *Caenorhabditis elegans*, *Aging Cell 5*, 515-524.
25. Hosono, R., Nishimoto, S., and Kuno, S. (1989) Alterations of life span in the nematode *Caenorhabditis elegans* under monoxenic culture conditions, *Exp, Gerontol. 24*, 251-264.
26. Wood, J. G., Rogina, B., Lavu, S., Howitz, K., Helfand, S. L., Tatar, M., and Sinclair, D. (2004) Sirtuin activators mimic caloric restriction and delay ageing in metazoans, *Nature 431*, 107-107.
27. Alemany, R., Perona, J. S., Sanchez-Dominguez, J. M., Montero, E., Canizares, J., Bressani, R., Escriba, P. V., and Ruiz-Gutierrez, V. (2007) G protein-coupled receptor systems and their lipid environment in health disorders during aging, *Biochim. Biophys. Acta 1768*, 964-975.
28. Finkel, T., Deng, C. X., and Mostoslavsky, R. (2009) Recent progress in the biology and physiology of sirtuins, *Nature 460*, 587-591.
29. Mair, W., and Dillin, A. (2008) Aging and survival: The genetics of life span extension by dietary restriction, *Annu. Rev. Biochem. 77*, 727-754.

30. Bamps, S., Wirtz, J., Savory, F. R., Lake, D., and Hope, I. A. (2009) The *Caenorhabditis elegans* sirtuin gene, *sir-2.1*, is widely expressed and induced upon caloric restriction, *Mech. Ageing Dev. 130*, 762-770.
31. Greer, E. L., and Brunet, A. (2009) Different dietary restriction regimens extend lifespan by both independent and overlapping genetic pathways in *C. elegans*, *Aging Cell 8*, 113-127.
32. Jadiya, P., Chatterjee, M., Sammi, S. R., Kaur, S., Palit, G., and Nazir, A. (2011) Sir-2.1 modulates 'calorie-restriction-mediated' prevention of neurodegeneration in *Caenorhabditis elegans*: Implications for Parkinson's disease, *Biochem. Bioph. Res. Co. 413*, 306-310.
33. Raynes, R., Leckey, B. D., Nguyen, K., and Westerheide, S. D. (2012) Heat shock and caloric restriction have a synergistic effect on the heat shock response in a *sir2.1*-dependent manner in *Caenorhabditis elegans*, *J. Biol. Chem. 287*, 29045-29053.
34. Miller, D. L., and Roth, M. B. (2007) Hydrogen sulfide increases thermotolerance and lifespan in *Caenorhabditis elegans*, *Proc. Natl Acad. Sci. USA 104*, 20618-20622.
35. Burnett, C., Valentini, S., Cabreiro, F., Goss, M., Somogyvari, M., Piper, M. D., Hoddinott, M., Sutphin, G. L., Leko, V., McElwee, J. J., Vazquez-Manrique, R. P., Orfila, A. M., Ackerman, D., Au, C., Vinti, G., Riesen, M., Howard, K., Neri, C., Bedalov, A., Kaeberlein, M., Soti, C., Partridge, L., and Gems, D. (2011) Absence of effects of Sir2 overexpression on lifespan in *C. elegans* and *Drosophila*, *Nature 477*, 482-485.
36. Bass, T. M., Weinkove, D., Houthoofd, K., Gems, D., and Partridge, L. (2007) Effects of resveratrol on lifespan in *Drosophila melanogaster* and *Caenorhabditis elegans*, *Mech. Ageing Dev. 128*, 546-552.
37. Berdichevsky, A., Viswanathan, M., Horvitz, H. R., and Guarente, L. (2006) C. elegans SIR-2.1 interacts with 14-3-3 proteins to activate DAF-16 and extend life span, *Cell 125*, 1165-1177.
38. Rizki, G., Iwata, T. N., Li, J., Riedel, C. G., Picard, C. L., Jan, M., Murphy, C. T., and Lee, S. S. (2011) The evolutionarily conserved longevity determinants HCF-1 and SIR-2.1/SIRT1 collaborate to regulate DAF-16/FOXO, *PLoS Genet. 7*, e1002235.
39. Fielenbach, N., and Antebi, A. (2008) *C. elegans* dauer formation and the molecular basis of plasticity, *Genes Dev. 22*, 2149-2165.
40. Gerisch, B., Rottiers, V., Li, D., Motola, D. L., Cummins, C. L., Lehrach, H., Mangelsdorf, D. J., and Antebi, A. (2007) A bile acid-like steroid modulates *Caenorhabditis elegans* lifespan through nuclear receptor signaling, *Proc. Natl Acad. Sci. USA 104*, 5014-5019.
41. Patterson, G. I., Koweek, A., Wong, A., Liu, Y., and Ruvkun, G. (1997) The DAF-3 Smad protein antagonizes TGF-beta-related receptor signaling in the *Caenorhabditis elegans* dauer pathway, *Genes Dev. 11*, 2679-2690.
42. Yamawaki, T. M., Berman, J. R., Suchanek-Kavipurapu, M., McCormick, M., Gaglia, M. M., Lee, S. J., and Kenyon, C. (2010) The somatic reproductive

tissues of *C. elegans* promote longevity through steroid hormone signaling, *PLoS Biol. 8*, e1000468.
43. Banerjee, K. K., Ayyub, C., Ali, S. Z., Mandot, V., Prasad, N. G., and Kolthur-Seetharam, U. (2012) dSir2 in the adult fat body, but not in muscles, regulates life span in a diet-dependent manner, *Cell Reports 2*, 1485-1491.
44. Viswanathan, M., and Guarente, L. (2011) Regulation of *Caenorhabditis elegans* lifespan by *sir-2.1* transgenes, *Nature 477*, E1-2.
45. Tissenbaum, H. A., and Guarente, L. (2001) Increased dosage of a *sir-2* gene extends lifespan in *Caenorhabditis elegans*, *Nature 410*, 227-230.
46. Wang, Y., Oh, S. W., Deplancke, B., Luo, J., Walhout, A. J., and Tissenbaum, H. A. (2006) *C. elegans* 14-3-3 proteins regulate life span and interact with SIR-2.1 and DAF-16/FOXO, *Mech Ageing Dev 127*, 741-747.
47. Wang, Y., and Tissenbaum, H. A. (2006) Overlapping and distinct functions for a *Caenorhabditis elegans* SIR2 and DAF-16/FOXO, *Mech. Ageing Dev. 127*, 48-56.
48. Kanfi, Y., Naiman, S., Amir, G., Peshti, V., Zinman, G., Nahum, L., Bar-Joseph, Z., and Cohen, H. Y. (2012) The sirtuin SIRT6 regulates lifespan in male mice, *Nature 483*, 218-221.
49. Macosko, E. Z., Pokala, N., Feinberg, E. H., Chalasani, S. H., Butcher, R. A., Clardy, J., and Bargmann, C. I. (2009) A hub-and-spoke circuit drives pheromone attraction and social behaviour in *C. elegans*, *Nature 458*, 1171-1175.
50. Lin, Y. J., Seroude, L., and Benzer, S. (1998) Extended life-span and stress resistance in the *Drosophila* mutant *methuselah*, *Science 282*, 943-946.
51. Spindler, S. R., Li, R., Dhahbi, J. M., Yamakawa, A., and Sauer, F. (2012) Novel protein kinase signaling systems regulating lifespan Identified by small molecule library screening using *Drosophila*, *Plos One 7*.
52. Butcher, R. A., Ragains, J. R., Li, W., Ruvkun, G., Clardy, J., and Mak, H. Y. (2009) Biosynthesis of the *Caenorhabditis elegans* dauer pheromone, *Proc. Natl Acad. Sci. USA 106*, 1875-1879.

CHAPTER 3

PHEROMONE SENSING PROTECTS *C. ELEGANS* FROM ENTEROPATHOGENIC *E.* COLI VIA THE UNFOLDED PROTEIN RESPONSE, THE DEACETYLASE SIR-2.1, AND COMPONENTS OF GPCR SIGNALING

Abstract

C. elegans is an excellent model for studying the nervous system, innate immunity and small molecule signaling. *C. elegans* utilizes GPCR-detected small molecule signals to mediate development, learning, and social interactions. Yet no endogenous small molecule has been associated with immune system modulation in *C. elegans*. Using a host-pathogen model, we show that endogenous *C. elegans* pheromones, the ascarosides, condition *C. elegans* to resist the bacterial pathogen enteropathogenic *E. coli* (EPEC). Exposure to a combination of ascr#5 and ascr#8 increases survival of EPEC-infected *C. elegans* up to two-fold. Non-lethal exposure to EPEC has also been shown to condition C*. elegans*; however, we demonstrate that EPEC and ascaroside conditioning depend on separate molecular pathways. While EPEC conditioning depends the mitogen-activated protein kinase p38 (*1*), we show that ascaroside conditioning requires GPCR signaling, conserved components of the UPR, and the sirtuin SIR-2.1. These results support a model in which chemosensation of endogenous small molecules triggers activation of conserved components of the immune response. Furthermore, results from the first two chapters suggest a model for a general SIR-2.1 protective strategy where AMILS and ascaroside conditioning converge on SIR-2.1, yet

reveal different but complementary aspects of this signaling network, which either promotes life and healthspan or pathogen resistance.

Contributions

The work in this chapter was conducted by a team of scientists in the Schroeder Lab (Cornell University, Ithaca, NY) and the Kalman Lab (Emory University, Atlanta, Georgia). Data in this chapter is in preparation for publication. ***Yevgeniy Izrayelit (YI) will be a co-first author on this publication. YI designed conditioning experiments, prepared ascaroside solutions and worm strains for testing, and analyzed data. YI's primary data contribution is selecting specific ascarosides and mutant strains for testing as data analysis and interpretation.*** Akwasi Anyanful (AF) conducted all conditioning assays. Zihan Ye (ZY) synthesized ascarosides. Professors Daniel Kalman (DK) and Frank Schroeder (FCS) supervised the project.

Introduction

The model organism *C. elegans* is a powerful invertebrate animal for the study of innate immunity (*2*). Although, *C. elegans* lacks an adaptive immune response, in response to a toxic pathogen the worm utilizes three major mechanisms of defense including avoidance, physical barriers and an inducible immune response (*3*). Using a number of chemosensory neurons the worm avoids certain pathogenic bacteria, and can remember noxious odors. Additionally, *C. elegans* has two important physical barriers to pathogen infection, a strong cuticle composed of collagen and chitin that limits permeability to pathogen, and a grinder in the pharyngeal bulb that can kill many pathogens during food ingestion (*4*). While physical barriers are also part of a protective strategy in higher organisms, complex organisms rely on an inducible immune response activated by primary exposure to pathogen. *C. elegans* also relies on an inducible innate immune response, relying on a plethora of signaling pathways conserved in higher organisms (*3*). These include the p38 Mitogen-Activate Protein (MAP) kinase, the insulin/IGF receptor (IGF-1) and the unfolded protein response (*5*, *6*).

Recently, a model for host-pathogen interaction was developed using *C. elegans* and enteropathogenic *E. coli* (EPEC) (*7*). EPEC, a gram negative human gastrointestinal pathogen, causes diarrhea and is a serious public health issue in third world countries (*8*). Exposure to EPEC kills *C. elegans* after a short time, but exposure to non-lethal durations of EPEC or a non-virulent EPEC strain with a mutated bacterial tryptophanase gene (EPEC∆TnaA) activates an innate immune response in *C. elegans*, that is protective to subsequent exposure to EPEC, in essence “conditioning” the worms (*1*). Conditioning depends on the IGF-1 and MAP pathways as well as a neuronal

component. This host-pathogen model presents an excellent system for screening for small molecule immune activators.

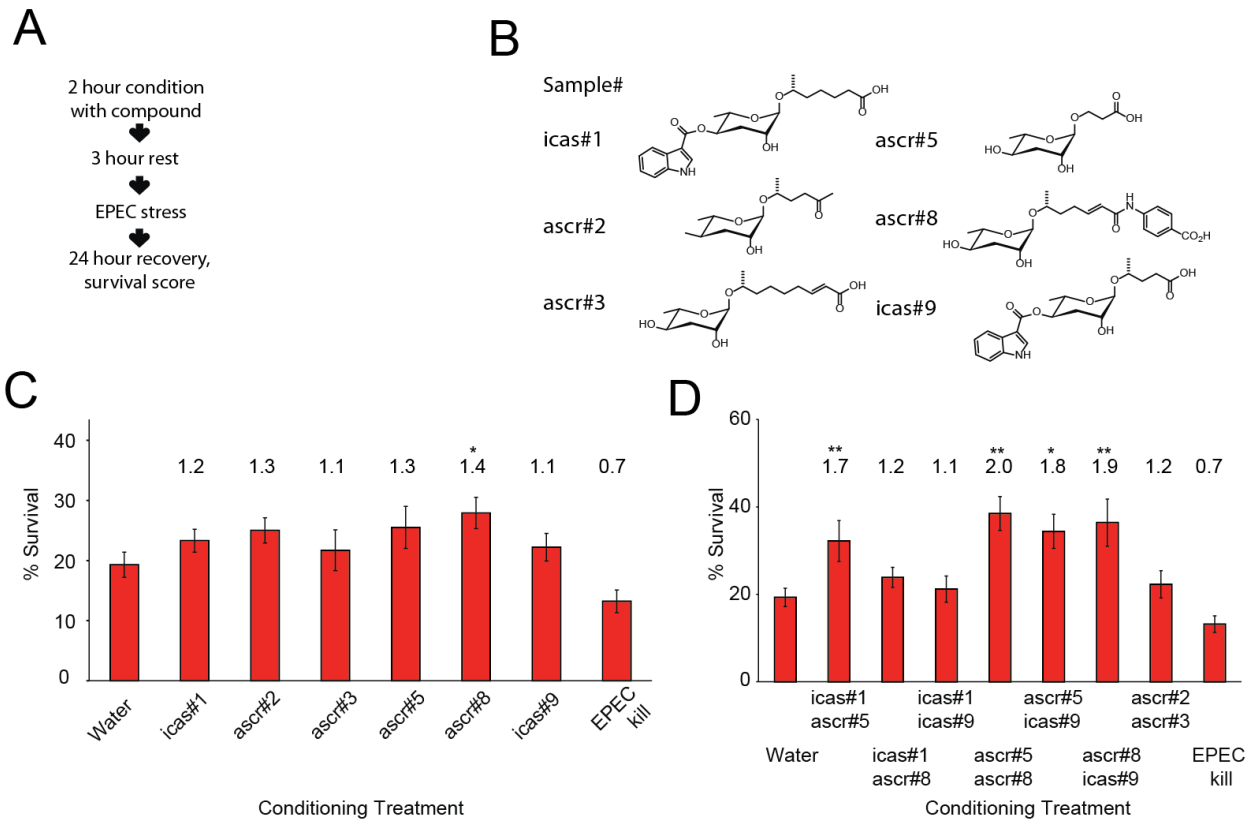

Figure 1. A combination of ascarosides conditions *C. elegans* against EPEC toxicity. (a) Protocol for *C. elegans* treatment for testing ascaroside conditioning properties. (b) Structures of the ascarosides screened in the initial conditioning assay. (c) Survival of *C. elegans* conditioned with either water control or 1 µM of listed ascaroside after 24 hours recovery post EPEC stress. (d) Survival of *C. elegans* conditioned with either water control or a combination of 1 µM of two ascarosides after 24 hours recovery post EPEC stress. . # listed is fold change relative to water. ** $p < 0.01$, * $p < 0.05$, unpaired t-test with Welch's correction. Mean values ± standard deviation presented in all bar graphs. *Ascrs synthesized by ZY, study design YI and AA. Experiments conducted by AA.*

C. elegans utilizes a family of molecules based on the dideoxy sugar ascarylose termed ascarosides for endocrine and exocrine signaling (*9*). Ascarosides have been shown to regulate dauer entry, hermaphrodite and male attraction, as well as hermaphrodite repulsion. Chapter 2 of this thesis highlights that ascr#2 and ascr#3 also extend lifespan in older worms that have bypassed the dauer decision (*10*). In chapter 2

it was found that ascr#2 binds the G protein-coupled receptors (GPCR) *daf-37* in a set of sensory neurons termed ASK to confer lifespan extension (*11*). The striking diversity and high number of GPCR genes in the *C. elegans* genomes (*12*) suggests that many other ascarosides may also have specific GPCR receptors regulating currently known and still undiscovered signaling functions (*13*). Recent work has highlighted that immune system activation in *C. elegans* is carefully regulated by neuronally expressed GPCRs (*14-16*). It is thus surprising that, to date, no endogenous immune system modulators have been discovered in *C. elegans.* We thus set out to use the EPEC - *C. elegans* conditioning model to screen a series of ascarosides for their ability to activate the immune system in the worm.

A combination of ascarosides conditions *C. elegans* against EPEC toxicity

We adapted a previously established conditioning assay for screening ascarosides (*1*). Only 10% of adult *C. elegans* survive 24 hours following a 3 hour exposure to EPEC. Yet a 3 hour exposure to EPEC∆TnaA, a non-toxic mutant (*1*), followed by a 3 hour rest, prior to the same 3 hour exposure to EPEC leads on average to 40% survival. To increase assay speed and also utilize smaller amounts of molecules per assay, the conditioning portion of the assay was adapted for a liquid based screen. In brief, young adult worms were put in 96 well plates with S complete, food, and the compounds in question or water control for 2 hours with slight shaking. The worms were then removed from liquid and allowed to rest for 3 hours on NGM plates with typical food (OP50). EPEC exposure on LBT plates for 3 hours followed by an additional 24 hour rest on NGM/OP50 plates, followed by scoring for life or death (**Figure 3.1a**). Six ascarosides (**Figure 3.1b**) previously shown to have activity in adult *C. elegans* were

screened (*13*). Notably, these six ascarosides had a diversity of structural features such as the indole modification (icas#1 and icas#9), and the aminobenzoic acid modified ascr#8. Further, we included ascr#2 and ascr#3, two ascarosides known to activate a stress resistance pathway in *C. elegans* (*10*) and the ω-substituted ascaroside ascr#5. The six selected ascarosides were screened at concentrations of 1 μM to mimic concentrations necessary for dauer induction and lifespan extension (*10*). Exposure to all ascarosides increased survival relative to no conditioning (**Figure 3.1c, EPEC**), however, only ascr#8 showed significantly increased survival 1.4 fold relative to a water conditioning control, which is known to have a small conditioning effect (**Figure 3.1c**). We then assayed a series of ascarosides in combination (1 μM each) and found that four pairs of ascrs enhanced survival almost 2 fold relative to water control (**Figure 3.1d**). The most robust conditioning occurred with ascr#5 and ascr#8 and this ascaroside mix was used for all further assays. Pre-exposure to EPECΔTnaA conditions the worm to be more resistant to subsequent EPEC exposure (*1*). In each of the conditioning assays, a parallel pre-exposure to EPECΔTnaA was included in order to compare signaling pathways involved in EPECΔTnaA and ascaroside based conditioning. Additionally, all conditioning assays utilizing mutant strains were run in parallel with wild type (N2) worms. While the control for EPECΔTnaA was no conditioning, the control for the ascaroside mix was water conditioning with a similar percentage of ethanol used to make the ascaroside mix.

Genes involved in sirtuin, UPR, and GPCR signaling mediate ascaroside conditioning

Next, we asked whether conditioning with ascr#5 and ascr#8 (ascr mix) requires conserved signaling networks previously associated with ascaroside mediated biology or the innate immune response in *C. elegans* (*9, 14*). Based on recent finding that ascr#2 and ascr#3 require the NAD+ dependent deacetylase SIR-2.1 for lifespan extension and stress resistance (*10*), we tested a *sir-2.1* mutant strain in our conditioning assay. Pre-exposure to EPEC∆TnaA protected the null allele mutant *sir-2.1(ok434)* worms more than 2 fold from subsequent EPEC exposure (**Figure 3.2a)**. In striking contrast, the ascr mix had no conditioning benefit relative to water control to the same *sir-2.1* mutant strain (**Figure 3.2a**). This highlights that EPEC∆TnaA and the ascr mix condition through separate signaling pathways.

Sirtuins have been closely linked with a variety of protective processes including lifespan extension and activation of immunity (*10, 17*). Recently, the unfolded protein response (*5*) has been linked with sirtuin mediated signaling (*18, 19*). The UPR is a conserved cellular stress response that regulates endoplasmic reticulum (ER) chaperone proteins, ER protein synthesis, as well as other aspects of a cellular response to improperly folded proteins (*20*). Separately, the UPR has been implicated in innate immunity regulation in *C. elegans (6, 19)*. We asked whether components of the UPR are necessary for ascr mediated conditioning.

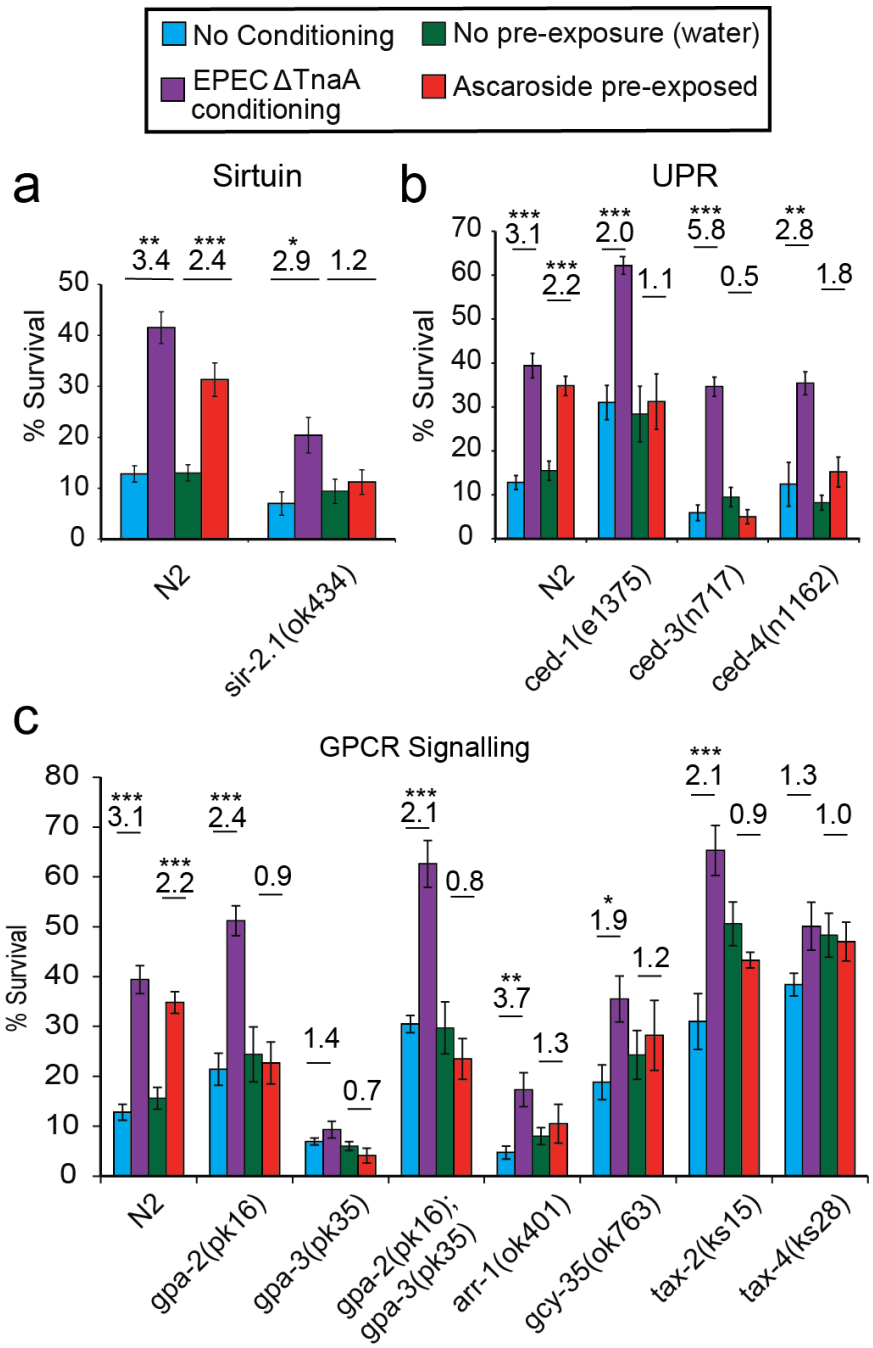

Figure 3.2. Genes involved in UPR, GPCR and Sirtuin signaling mediate ascaroside conditioning. In all experiments ascaroside pre-exposure utilized 1 µM ascr#5 and 1 µM of ascr#8. (A) The *sir-2.1* mutant strain was not conditioned by ascarosides, but conditioned by EPECΔTnaA. (B) Survival of wild type or mutant strains related to UPR signaling. (C) Survival of wild type or mutant strains related to GPCR signaling. ***<0.001, ** p <0.01, * p < 0.05, unpaired t-test with Welch's correction. Mean values ± standard deviation presented in all bar graphs.# listed is fold change relative to control. *Ascrs synthesized by ZY, study design YI and AA, mutant selected and acquired by YI. Experiments conducted by AA.*

We tested three components of the UPR for their requirement in ascr mediated conditioning. *ced-1* is an apoptotic receptor required for engulfment of cells undergoing apoptosis that has been implicated in immunity (*6, 21*). The *ced-3* gene encodes a cysteine-aspartate protease involved in cell death (*22*). Finally, we also tested *ced-4,* a novel-protein, considered a proapoptic factor that facilitates autocatalytic activation of *ced-3 (23-26).* We found that pre-exposure to the ascr mix did not condition *ced-1(e1375)* and *ced-3(n717)* strains (**Figure 3.2b**). These worms were protected when pre-exposed to EPEC∆TnaA. The mutants strain *ced-4(n1162)* was slightly conditioned by ascarosides; however, this was not significant. This suggests that *ced-3* is required and likely *ced-4* is also required for ascr mediated conditioning, supporting the established dogma of UPR activation (*25*). Notably; these UPR related genes were not required for conditioning by EPEC∆TnaA.

In chapter 2 we showed that AMILS signals through an ascr#2 specific GPCR receptor, *daf-37* (*10*). Only a few additional ascr binding GPCRs have been identified (*27*). Unfortunately, we were unable to obtain a mutant strain lacking the putative ascr#5 binding partners *srg-36 and srg-37.* We did screen other mutants lacking components of downstream GPCR signaling. We first tested the G-protein alpha subunits *gpa-2* and *gpa-3,* previously shown to be required for dauer signaling (*28*), followed by *arr-1* which encodes the only known β–arrestin in *C. elegans* and is required for GPCR signaling in a variety of chemosensory neurons involved in UPR (*29*). We also tested a mutant strain deficient in the guanylyl cyclase *gcy*-35 and the α and β subunits of the cyclic nucleotide gated ion channels *tax-4 and tax-2 (15, 30).* **Figure 3.2c** shows that ascr mediated conditioning was deficient in every GPCR related mutant tested. *tax-4* and

tax-2 were conditioned by ethanol control relative to no conditioning, however, no additional conditioning was achieved by pre-exposure to ascr mix. In stark contrast, EPECΔTna successfully conditioned all strains accept for the generally less resilient *gpa-3(pk35)*. This data highlights that pre-exposure to the ascr-mix activates an immune response through conserved portions of GPCR signaling, reinforcing the critical role of the neuronal system in immune system activation (*14*).

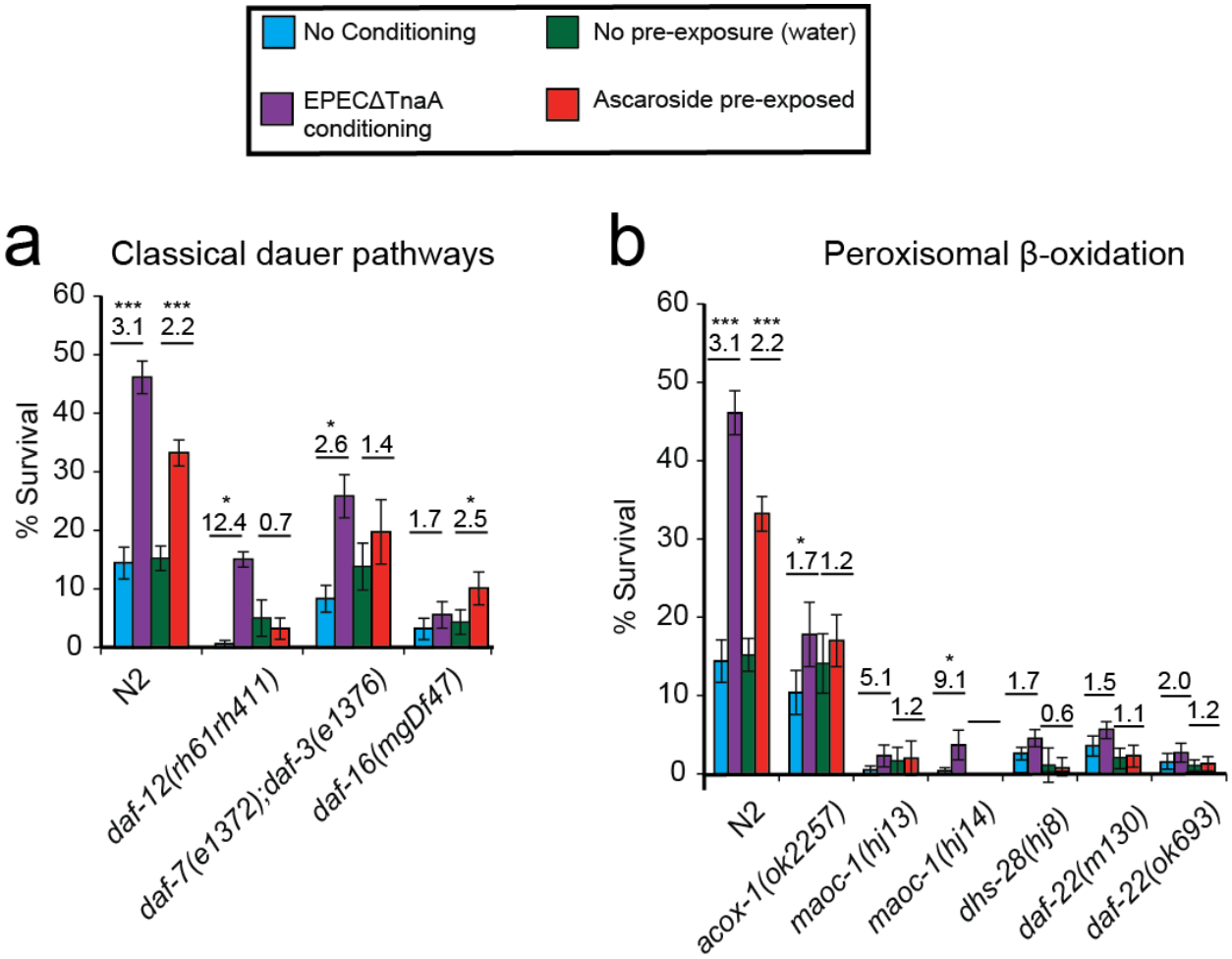

Figure 3.3. Other notable signaling pathways associated with ascaroside conditioning. ***<0.001, ** p <0.01, * p < 0.05, unpaired t-test with Welch's correction. Mean values ± Standard Deviation presented in all bar graphs. # listed is fold change relative to control. *Ascrs provided by FS, study design YI and AA, mutant selected and acquired by YI. Experiments conducted by AA.*

Screening dauer related pathways produced quiet interesting results (**Figure 2.3a**). The nuclear hormone receptor *daf-12* was required for ascaroside induced conditioning but not EPECΔTnaA conditioning. This is in line with recent findings that *daf-12* is involved with microRNA mediated innate immunity control (*31*). TGF-β and the FOXO transcription factor *daf-16* were not clearly required for ascaroside conditioning. Mutants deficient in peroxisomal β-oxidation were generally less resilient to EPEC stress (**Figure 2.3b**). Notably, none of the peroxisomal β-oxidation mutant strains showed any benefit of ascaroside conditioning, suggesting functional peroxisomal β-oxidation may be necessary for this beneficial process. Ascaroside biosynthesis is necessary for olfactory plasticity (*32*). Considering components of olfactory signaling are required for ascaroside conditioning, functional pheromone biosynthesis may be a pre-requisite for the conditioning phenomena described here.

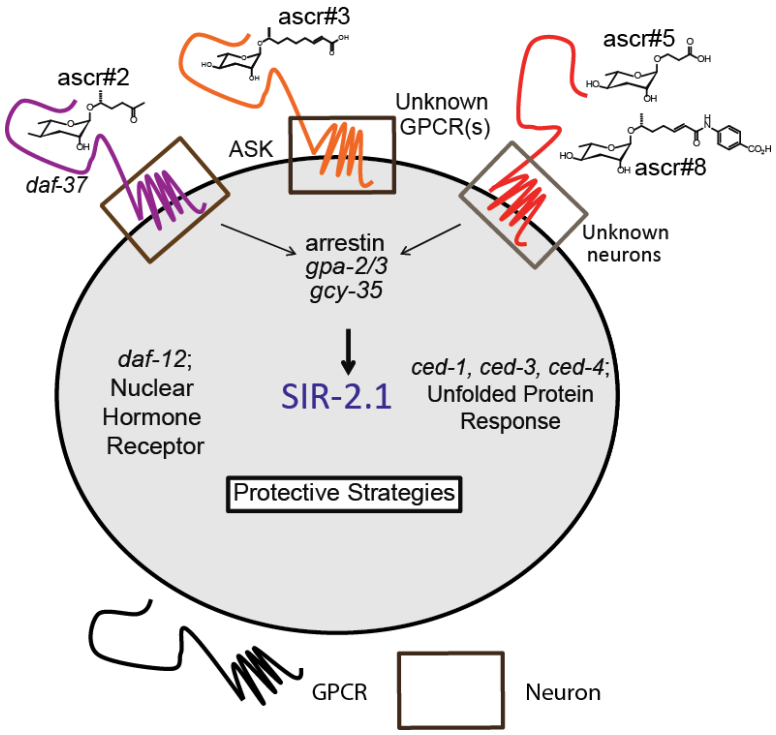

Figure 3.4. Model for protective strategies mediated by ascarosides.

Conclusion

The “conditioning” assay allowed for screening of a series of mutants with genes involved in various aspects of immunity. Pre-exposure of ascarosides, ascr#5 and ascr#8, mediate immune system activation and protection against subsequent EPEC exposure through distinct molecular pathways from that of the previously established EPECΔTnaA conditioning (*1*). The discovery that ascr conditioning but not EPECΔTnaA conditioning requires the sirtuin *sir-2.*1, suggests that this may be a similar protective strategy to AMILS (chapter 2). This presented a great opportunity to tease out unique signaling pathways relevant to ascaroside mediated conditioning, and more generally ascaroside protective strategies.

Previous work has shown that mutations of GPCR signaling components such as *arr-1*, *gcy-35*, *tax-2*, and *tax-4* increase resistance to the gram negative bacterium *Pseudomonas aeruginosa* (*15, 29*). In the case of *gcy-35*, *tax-2* and *tax-4* this was specifically through activation of immune suppressing neurons. This supports the hypothesis that inhibition of certain GPCR signaling machinery may be beneficial for activation of the immune response. It would then seem that in this system ascr#5 and ascr#8 in combination inhibit GPCR signaling. The *arr-1* mutants were also resistant to *P. aeruginosa* in a manner dependent on the UPR (*29*). This further suggests that pre-exposure to the ascr mix inhibits components of the GPCR, inhibiting certain neurons leading to UPR activation. Incorporation of the requirement of SIR-2.1 and the NHR DAF-12 makes this a very exciting, highly conserved immune regulating network.

Figure 3.4 summarizes our current understanding of AMILS and ascr mediated conditioning. Ascr#2 and ascr#3 increase life span and stress resistance through a set of chemosensory neurons converging on SIR-2.1. Ascr#5 and ascr#8, and perhaps

other ascr pairs, were shown to utilize other aspects of chemosensory signaling, specifically components of GPCR mediated signal transduction. The protective strategy activated by ascr#5 and ascr#8 also converged on SIR-2.1, but was shown to require the UPR, as well as the nuclear hormone *daf-12,* but not the FOXO transcription factor *daf-16.* Notably, ascaroside mediated increase in lifespan and stress resistance did not seem to require *daf-12* (chapter 2) while ascr conditioning did, highlighting a divergence in these two ascaroside induced protective strategies. It will be necessary to explore the overlap between these two protective strategies. This chapter presents, to our knowledge, the first endogenous small molecule activator of immunity in *C. elegans* that connects neuronal signaling, with the UPR, and sirtuin signaling.

REFERENCES

1. Anyanful, A., Easley, K. A., Benian, G. M., and Kalman, D. (2009) Conditioning protects *C. elegans* from lethal effects of enteropathogenic *E. coli* by activating genes that regulate lifespan and innate immunity, *Cell Host Microbe 5*, 450-462.
2. Kurz, C. L., and Ewbank, J. J. (2003) *Caenorhabditis elegans*: an emerging genetic model for the study of innate immunity, *Nat. Rev.. Gen. 4*, 380-390.
3. Engelmann, I., and Pujol, N. (2010) Innate immunity in *C. elegans*, *Adv. Exp. Med. Biol. 708*, 105-121.
4. Palaima, E., Leymarie, N., Stroud, D., Mizanur, R. M., Hodgkin, J., Gravato-Nobre, M. J., Costello, C. E., and Cipollo, J. F. (2010) The *Caenorhabditis elegans bus-2* mutant reveals a new class of O-glycans affecting bacterial resistance, *J. Biol. Chem. 285*, 17662-17672.
5. Couprie, B., Claudot, Y., Same-Ekobo, A., Issoufa, H., Leger-Debruyne, M., Tribouley, J., and Ripert, C. (1985) Epidemiologic study of malaria in the rice-growing regions of Yagoua and Maga (North Cameroon), *Bull. Soc. Pathol. Exot. Filiales 78*, 191-204.
6. Haskins, K. A., Russell, J. F., Gaddis, N., Dressman, H. K., and Aballay, A. (2008) Unfolded protein response genes regulated by CED-1 are required for *Caenorhabditis elegan*s innate immunity, *Dev. Cell 15*, 87-97.
7. Anyanful, A., Dolan-Livengood, J. M., Lewis, T., Sheth, S., Dezalia, M. N., Sherman, M. A., Kalman, L. V., Benian, G. M., and Kalman, D. (2005) Paralysis and killing of *Caenorhabditis elegans* by enteropathogenic *Escherichia coli* requires the bacterial tryptophanase gene, *Mol. Microbiol. 57*, 988-1007.
8. Clarke, S. C., Haigh, R. D., Freestone, P. P., and Williams, P. H. (2002) Enteropathogenic *Escherichia coli* infection: history and clinical aspects, *Brit. J. Biomed. Sci. 59*, 123-127.
9. Ludewig, A. H., and Schroeder, F. C. (2013) Ascaroside signaling in *C. elegans*, *WormBook*, 1-22.
10. Ludewig, A. H., Izrayelit, Y., Park, D., Malik, R. U., Zimmermann, A., Mahanti, P., Fox, B. W., Bethke, A., Doering, F., Riddle, D. L., and Schroeder, F. C. (2013) Pheromone sensing regulates *Caenorhabditis elegans* lifespan and stress resistance via the deacetylase SIR-2.1, *Proc. Natl Acad. Sci. USA 110*, 5522-5527.
11. Park, D., O'Doherty, I., Somvanshi, R. K., Bethke, A., Schroeder, F. C., Kumar, U., and Riddle, D. L. (2012) Interaction of structure-specific and promiscuous G-protein-coupled receptors mediates small-molecule signaling in C*aenorhabditis elegans*, *Proc. Natl Acad. Sci. USA 109*, 9917-9922.
12. Nagarathnam, B., Kalaimathy, S., Balakrishnan, V., and Sowdhamini, R. (2012) Cross-genome clustering of human and *C. elegans* G-Protein coupled receptors, *Evol. Bioinform. Online 8*, 229-259.
13. Srinivasan, J., von Reuss, S. H., Bose, N., Zaslaver, A., Mahanti, P., Ho, M. C., O'Doherty, O. G., Edison, A. S., Sternberg, P. W., and Schroeder, F. C. (2012) A modular library of small molecule signals regulates social behaviors in *Caenorhabditis elegans*, *PLoS Biol. 10*, e1001237.

14. Aballay, A. (2013) Role of the nervous system in the control of proteostasis during innate immune activation: insights from *C. elegans*, *PLoS Pathog. 9*, e1003433.
15. Styer, K. L., Singh, V., Macosko, E., Steele, S. E., Bargmann, C. I., and Aballay, A. (2008) Innate immunity in *Caenorhabditis elegans* is regulated by neurons expressing NPR-1/GPCR, *Science 322*, 460-464.
16. Sun, J., Singh, V., Kajino-Sakamoto, R., and Aballay, A. (2011) Neuronal GPCR controls innate immunity by regulating noncanonical unfolded protein response genes, *Science 332*, 729-732.
17. Haigis, M. C., and Sinclair, D. A. (2010) Mammalian sirtuins: biological insights and disease relevance, *Annu. Rev. Pathol. 5*, 253-295.
18. Mouchiroud, L., Houtkooper, R. H., Moullan, N., Katsyuba, E., Ryu, D., Canto, C., Mottis, A., Jo, Y. S., Viswanathan, M., Schoonjans, K., Guarente, L., and Auwerx, J. (2013) The NAD(+)/sirtuin pathway modulates longevity through activation of mitochondrial UPR and FOXO signaling, *Cell 154*, 430-441.
19. Viswanathan, M., Kim, S. K., Berdichevsky, A., and Guarente, L. (2005) A role for SIR-2.1 regulation of ER stress response genes in determining *C. elegans* life span, *Dev. Cell 9*, 605-615.
20. Chakrabarti, A., Chen, A. W., and Varner, J. D. (2011) A review of the mammalian unfolded protein response, *Biotechnol. Bioeng. 108*, 2777-2793.
21. Zhou, Z., Hartwieg, E., and Horvitz, H. R. (2001) CED-1 is a transmembrane receptor that mediates cell corpse engulfment in C-elegans, *Cell 104*, 43-56.
22. Shaham, S., Reddien, P. W., Davies, B., and Horvitz, H. R. (1999) Mutational analysis of the *Caenorhabditis elegans* cell-death gene *ced-3*, *Genetics 153*, 1655-1671.
23. Chinnaiyan, A. M., ORourke, K., Lane, B. R., and Dixit, V. M. (1997) Interaction of CED-4 with CED-3 and CED-9: a molecular framework for cell death, *Science 275*, 1122-1126.
24. Huang, W. J., Jiang, T. Y., Choi, W. Y., Qi, S. Q., Pang, Y. X., Hu, Q., Xu, Y. H., Gong, X. Q., Jeffrey, P. D., Wang, J. W., and Shi, Y. G. (2013) Mechanistic insights into CED-4-mediated activation of CED-3, *Gene Dev. 27*, 2039-2048.
25. Pinan-Lucarre, B., Gabel, C. V., Reina, C. P., Hulme, S. E., Shevkoplyas, S. S., Slone, R. D., Xue, J., Qiao, Y., Weisberg, S., Roodhouse, K., Sun, L., Whitesides, G. M., Samuel, A., and Driscoll, M. (2012) The core apoptotic executioner proteins CED-3 and CED-4 promote initiation of neuronal regeneration in *Caenorhabditis elegans*, *PLoS Biol. 10*, e1001331.
26. Yuan, J. Y., and Horvitz, H. R. (1990) The *Caenorhabditis elegans* genes *ced-3* and *ced-4* act cell autonomously to cause programmed cell death, *Dev. Biol. 138*, 33-41.
27. McGrath, P. T., Xu, Y., Ailion, M., Garrison, J. L., Butcher, R. A., and Bargmann, C. I. (2011) Parallel evolution of domesticated *Caenorhabditis* species targets pheromone receptor genes, *Nature 477*, 321-325.
28. Zwaal, R. R., Mendel, J. E., Sternberg, P. W., and Plasterk, R. H. (1997) Two neuronal G proteins are involved in chemosensation of the *Caenorhabditis elegans* dauer-inducing pheromone, *Genetics 145*, 715-727.

29. Singh, V., and Aballay, A. (2012) Endoplasmic reticulum stress pathway required for immune homeostasis is neurally controlled by arrestin-1, *J. Biol. Chem. 287*, 33191-33197.
30. Ailion, M., and Thomas, J. H. (2000) Dauer formation induced by high temperatures in *Caenorhabditis elegans*, *Genetics 156*, 1047-1067.
31. Liu, F., He, C. X., Luo, L. J., Zou, Q. L., Zhao, Y. X., Saini, R., Han, S. F., Knolker, H. J., Wang, L. S., and Ge, B. X. (2013) Nuclear hormone receptor regulation of microRNAs controls innate immune responses in *C. elegans*, *PLoS Pathog. 9*, e1003545.
32. Yamada, K., Hirotsu, T., Matsuki, M., Butcher, R. A., Tomioka, M., Ishihara, T., Clardy, J., Kunitomo, H., and Iino, Y. (2010) Olfactory plasticity Is regulated by pheromonal signaling in *Caenorhabditis elegans*, *Science 329*, 1647-1650.

CHAPTER 4

NMR-BASED METABOLOMICS REVEALS A FAMILY OF TOXINS AND THEIR DETOXIFACTION MECHANISM IN *CAENORHABDITIS ELEGANS*

Abstract

C. elegans lives in compost and decaying fruit, eats bacteria and is exposed to pathogenic microbes and many indole-based compounds. We show that *C. elegans* is able to modify diverse microbial small-molecule toxins via both O- and N-glucosylation as well as unusual 3'-O-phosphorylation of the resulting glucosides. The resulting glucosylated derivatives have significantly reduced toxicity to *C. elegans*, suggesting that these chemical modifications represent a general mechanism for worms to detoxify their environments. Considering the dedicated detoxification machinery from *E. coli* derived indoles, it is not surprising that pathogenic indole producing bacteria such as enteropathogenic *Escherichia coli* (EPEC), enterohemorrhagic *E. coli* (EHEC) and enteroaggregative *E. coli* (EAEC), intestinal pathogens that cause food and water-borne disease in humans, are also toxic to *C. elegans.* Using biochemical methods and NMR-based comparative metabolomics in conjunction with the nematode *Caenorhabditis elegans*, we developed a bioassay to identify secreted small molecules produced by these pathogens. We identified indole, indole-3-carboxaldehyde (ICA), and indole-3-acetic acid (IAA), as factors that only in combination are sufficient to kill *C. elegans*. The *C. elegans* model in conjunction with metabolomics has facilitated identification of a family of indole derivatives that broadly regulate physiology in *E. coli* and virulence in pathogenic strains.

Contributions

The work in this chapter was conducted by a team of scientists across three Universities, specifically by members of the Schroeder Lab (Cornell University, Ithaca, NY), the Kalman Lab (Emory University, Atlanta, GA), and the Edison Lab (University of Florida, Gainesville, FL). The data and writing, with minor modifications, in this section have been published in two works (*1, 2*). Discoveries reflecting the efforts of Yevgeniy Izrayelit (YI) are presented with additional research points included as needed. ***YI is a third author on each of the two publications that are summarized in this section*** Gregory S. Stupp (GSS) and Stephan H. von Reus (SVR) are co-1st authors in the work presented in the first portion of the chapter (*1*). ***YI's primary contribution was performing indole related toxicity assays using the model organism C. elegans and measuring indole N-glucosylation rate using LC/MS.*** GSS performed all phenazine related assays and metabolomics. SVR synthesized glycosylated phenazine and indole derivatives. FS and Art Edison (AS) supervised the study. In the second portion of the chapter, Bettina Bommarius (BB) and Akawasi Anyanful (AA) are co-1st authors on the work identifying a family of indoles produced by EPEC (*2*). BB and AA conducted all assays. ***YI's primary contribution to this work was using 2D NMR metabolomics and LC/MS to characterize and quantify the series of indole metabolites secreted by EPEC. Notably, YI identified indole-3-carboxaldehyde as a previously unknown EPEC derived toxin.*** Frank C. Schroeder (FS) and Daniel Kalman (DK) supervised the studies.

Introduction

Nematodes live in complex microbial environments that present many potential challenges to their health and viability. *Caenorhabditis elegans*, a commonly used model nematode, has an innate immune system that shares many characteristics with mammalian defenses (*3, 4*) and is susceptible to many mammalian pathogens (*5*). Its immune system is highly specific: worms can distinguish and mount distinct responses to different pathogens (*6*). *C. elegans* possesses an array of immune effectors and detoxification enzymes known to be involved in microbial defense and xenobiotic detoxification. Distinct sets of immune effectors, including lysozymes, lipases, and antibacterial peptides, as well as detoxification enzymes such as UDP-glucuronosyl/UDP-glucosyltransferases (UDPGT), cytochrome P450s (CYP), and glutathione S-transferases (*7*) are modulated during these responses (*6, 8-11*). Having a large arsenal of detoxification and defense genes is not surprising for an organism that lives in environments rich in decomposing organic material, areas in which potential pathogens are also likely to thrive. In this chapter we first present work examining two unrelated bacterial toxins, 1-hydroxyphenazine (1-HP, **1**) and indole (**6**), released by *Pseudomonas aeruginosa* and *Escherichia coli*, respectively (*12*). Both toxins can kill *C. elegans*, and we found that worms glycosylate both toxins, a modification that significantly lowers their toxicity.

Considering *C. elegans* employ such a general detoxification mechanism, it was not surprising to find that pathogenic bacteria utilize diverse small molecule toxins to overcome this defense. In the second portion of this section, work exploring the interaction between pathogenic *E.coli* and *C. elegans* is highlighted.

Enteropathogenic *Escherichia coli* (EPEC) and enterohemorrhagic *E. coli* (EHEC) are gastrointestinal pathogens transmitted via contaminated food and water (*13*). EPEC is a significant public health concern, especially in developing countries where it is a leading cause of infantile diarrhea, leading to dehydration and death (*14*). EHEC and related strains produce two Shiga toxins (STX) that cause bloody diarrhea, hemolytic uremic syndrome, kidney failure, and often death (*15*). There is a strong mandate to develop drugs to treat pathogenic *E. coli* infections.

Whereas considerable information is available on the regulators of virulence determinants, much less is known about the role of secreted small molecules in these regulatory pathways. To identify such factors, we used a model of EPEC pathogenesis in which the bacteria kills the nematode *C. elegans*. Exposure to EPEC or EHEC kills *C. elegans* within hours (*16*). By contrast, brief pre-exposure to these pathogens, a process termed conditioning, induces a long-lasting protective response that allows *C. elegans* to survive a subsequent exposure to EPEC that would otherwise prove lethal (*17*).

To kill or condition *C. elegans*, EPEC use a secreted factor or factors, production of which requires both tryptophan in the media and the bacterial tryptophanase gene *tnaA* (*16*). Tryptophanase converts tryptophan into indole, ammonia, and pyruvate. While indole does kill *C. elegans*, physiologically determined indole levels produced by EPEC were not sufficient to kill *C. elegans*. However, indole is only one of many products of typtophanase, raising the possibility that a variety of indole derivatives also mediate toxicity in *C. elegans.* Using biochemical methods coupled with two-dimensional NMR-based comparative metabolomics, we report in the second portion of

this chapter that indole and the chemically related compounds indole-3-carboxaldehyde (ICA) and indole-3-acetic acid (IAA) are produced by EPEC, EHEC, and by commensal *E. coli*. These molecules act in synergy with indole to kill and condition *C. elegans*. In addition, these molecules regulate biofilm formation, virulence, and production of Shiga toxins in pathogenic *E. coli* strains.

Small molecule toxins are glycosylated by *C. elegans*

We asked whether *C. elegans* employs specific metabolic transformations to eliminate bacterial toxins such as phenazines and indole. After challenging young adult worms in large-scale liquid culture for 24 h with 200 µM of 1-HP (**1**), HPLC-UV analysis of worm media samples revealed at least three new compounds (**2,4,5**) present in samples from worms exposed to 1-HP but not present in control samples (**Figure E.1a**). In addition, we analyzed whole-body extracts of 1-HP-challenged worms and found at least one novel UV peak (*18*) that was absent in control extracts (**Figure E.1b**). These putative 1-HP metabolites were isolated via preparative HPLC and subsequently identified using MS and NMR spectroscopy **(Figure 4.1**, **Figure E.2-5**, **and Table E.1**). We identified 1-*O*-(β-D-glucopyranosyl)-phenazine (**2**) and 1-*O*-(β-D-gentiobiosyl)-phenazine (**4**) as the two most abundant metabolites in the worm media samples, which were accompanied by two compounds (**5**) whose mass and NMR spectra suggested phenazine trisaccharides; however, strong overlap in the NMR spectra of these two compounds prevented their full characterization. In addition, we identified the major phenazine derivative detected in the worm body extracts as 1-*O*-(3'-*O*-phospho-β-D-glucopyranosyl)-phenazine (*18*).

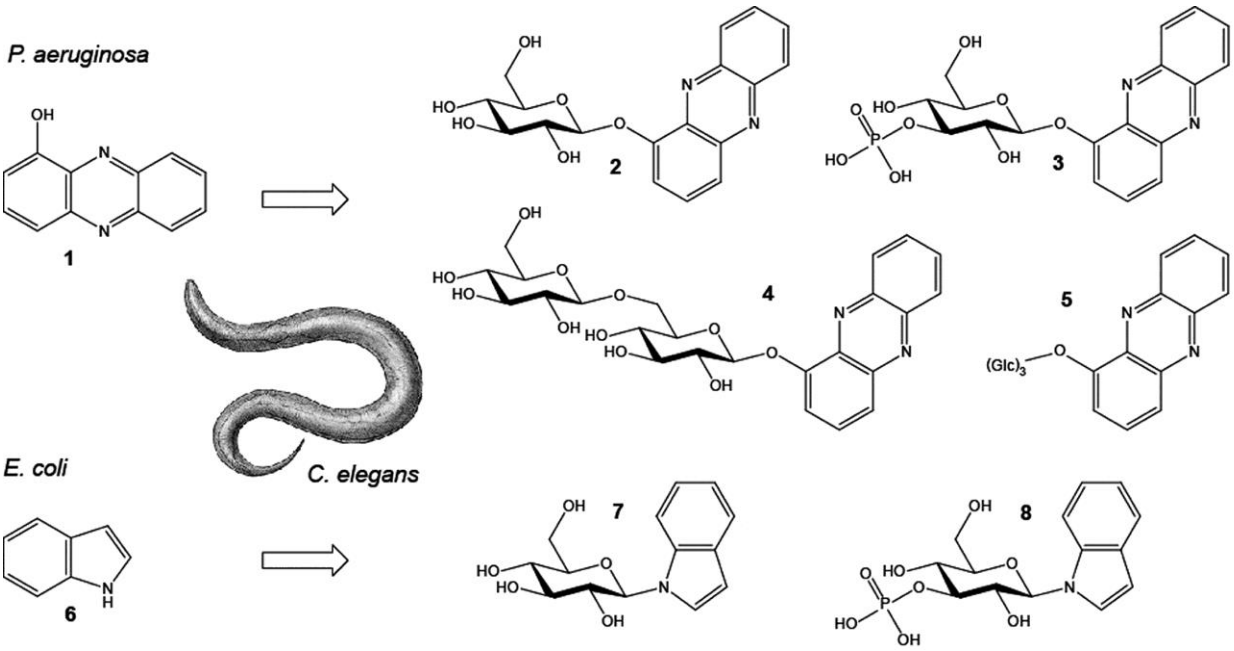

Figure 4.1. Chemical conversion of 1-hydroxyphenazine (1-HP) (**1**) and indole (**6**) by *C. elegans*. 1-HP is converted into 1-*O*-(β-D-glucopyranosyl)-phenazine (**2**), 1-*O*-(β-D-gentiobiosyl)-phenazine (**4**), and two phenazine-trisaccharides (**5**) which are found in the media and worm pellet. 1-*O*-(3'-*O*-phospho-β-D-glucopyranosyl)-phenazine (*18*) is found only in the worm pellet. Indole (**6**) is converted into *N*-(β-D-glucopyranosyl)-indole (**7**) and *N*-(3'-*O*-phospho-β-D-glucopyranosyl)-indole (**8**) which are found in the media and pellet.

These results show that *C. elegans* converts 1-HP into a series of glycosylated derivatives, including a compound featuring an unusual phosphate substitution. Next we asked whether *C. elegans* also modifies *E. coli*-derived indole (**6**). Notably, HPLC-analysis of *C. elegans* large-scale liquid culture extracts revealed only trace amounts of indole 24 h after feeding with indole-rich *E. coli* bacteria. Instead, HPLC-analysis revealed two prominent peaks with UV and mass spectra indicative of highly polar indole derivatives. NMR-spectroscopic analysis (**Figures 4.1, Figure E.6, Table E.1, and Table E.2**), of extract fractions containing these compounds revealed *N*-(β-D-glucopyranosyl)-indole (**7**), of which we prepared an authentic sample via synthesis. In addition, we identified *N*-(3'-*O*-phospho-β-D-glucopyranosyl)-indole (**8**), in direct analogy

to the phosphorylated 1-HP derivative (*18*). We quantified the indole glucoside by HPLC-UV and found that more than 80% of indole provided with the OP50 diet appears to be converted into **7** (**Figure 4.7a**). Analysis of worm body and supernatant extracts further revealed that indole glucoside is predominantly released by *C. elegans* and accumulates in the media (**Figure E.7b**). We also studied the time course of the *N*-glucosylation reaction by feeding of [U-D_7]-indole to *C. elegans* liquid cultures and found that the majority of exogenous indole is converted into the glucosides within 6 h (**Figure 4.2c**).

Glycosylated small molecules are not toxic to *C. elegans*

Our results demonstrate that *C. elegans* modifies two chemically distinct bacterial toxins, 1-HP and indole, by glycosylation and additional 3'-*O*-phosphorylation, suggesting that these modifications may be part of a general detoxification pathway in the nematode. Therefore, we tested the modified glycosides for their toxicity to *C. elegans*. For this purpose we used synthetic *N*-(β-D-glucopyranosyl)-indole (**6**) and isolated samples of the 1-HP glucosides (**2-5**). Using a plate-based assay, we found that whereas 1-HP at concentrations of 200 µM kills about 80% of L4 worms after 6 h, exposure to the same concentrations of 1-HP glycosides results in less than 5% mortality (**Figure 4.2a,b**). Next we compared the toxicity of indole and *N*-(β-D-glucopyranosyl)-indole in plate and liquid-culture assays. We found that indole is more toxic in liquid media assays in comparison to plate-based assays (not shown). In liquid

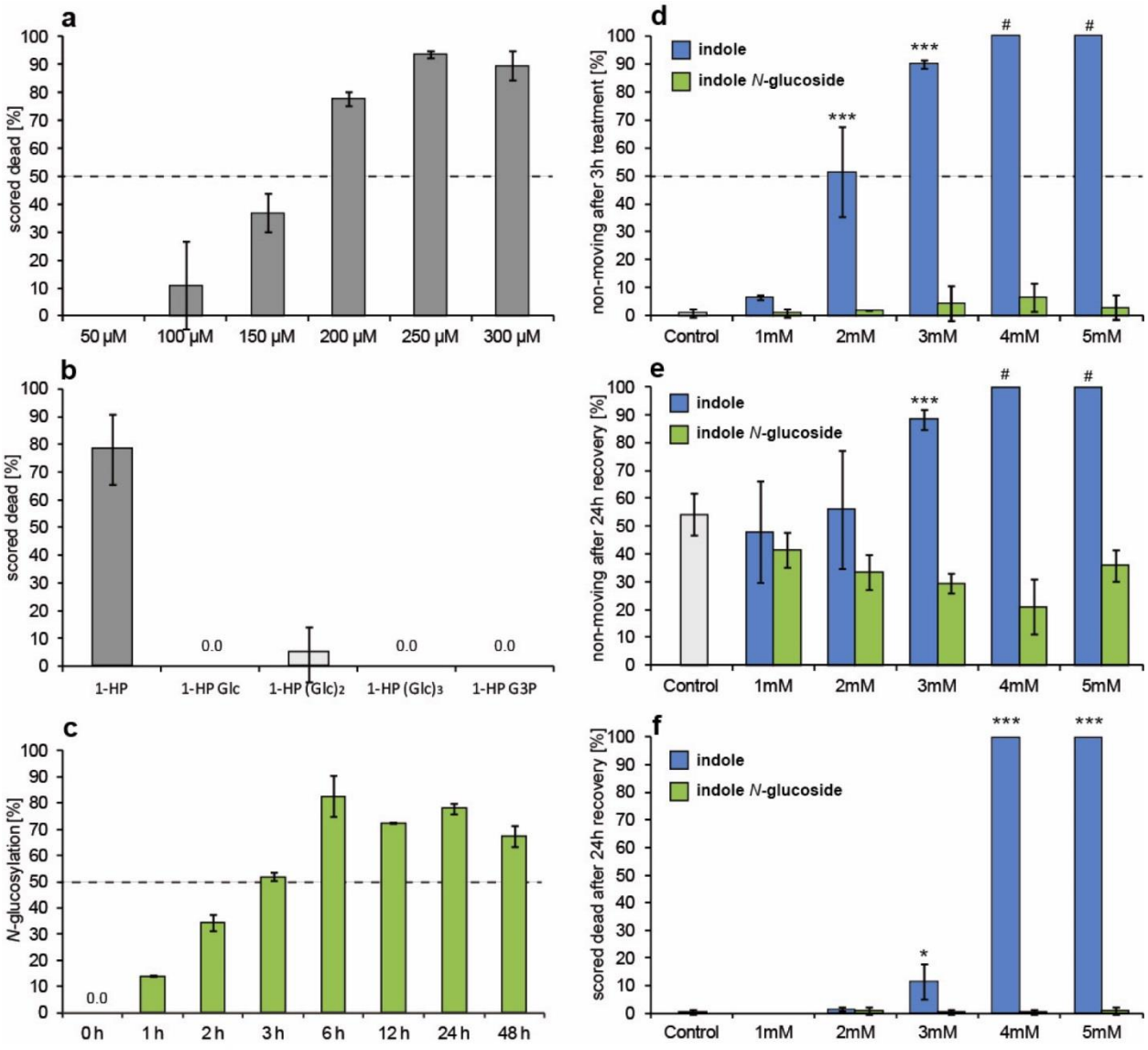

Figure 4.2. Toxicity Assays. Error bars represent mean ± s.d. (a) Killing of L4 stage worms on M9 agar plates containing increasing concentrations of 1-HP after 6 hours (N = 2 or 3 with 20-40 worms per trial). (b) Killing of L4 stage worms on M9 agar plates containing 200 µM of each phenazine glucoside after 6 hours (N = 3 with 40-50 worms). (c) Time course for *N*-glucosylation of indole by *C. elegans* determined by application of 0.5 mg/100 ml [U-D_6]-indole. (d) Paralysis of L4 worms after treatment with increasing amounts of indole or indole-*N*-glucoside in M9 media for 3 h (# worms scored dead after recovery: see f). (e) Paralysis of L4 worms after treatment with indole or indole-*N*-glucoside for 3 h and 24 h recovery in M9 (# worms scored dead after recovery: see f). (f) Killing of L4 worms after treatment with indole or indole-*N*-glucoside for 3 h and 24 h recovery in M9 (N = 4 with 50 worms per trial*. YI conducted all indole and indole N-glucoside assays. GS conducted all phenazine assays.*

media indole kills *C. elegans* at concentrations of 4 mM, whereas lower concentrations of 2 and 3 mM result in reversible paralysis. In contrast, indole glucoside did not kill or elicit paralysis at concentrations as high as 5 mM (**Figure 4.2d-f**). Although our toxicity assays differ significantly from the large-scale liquid culture conditions employed for isolation of glucosylation products, our results demonstrate that the bacterial toxins, 1-HP and indole, kill *C. elegans*, whereas their glucosylation products are much less toxic.

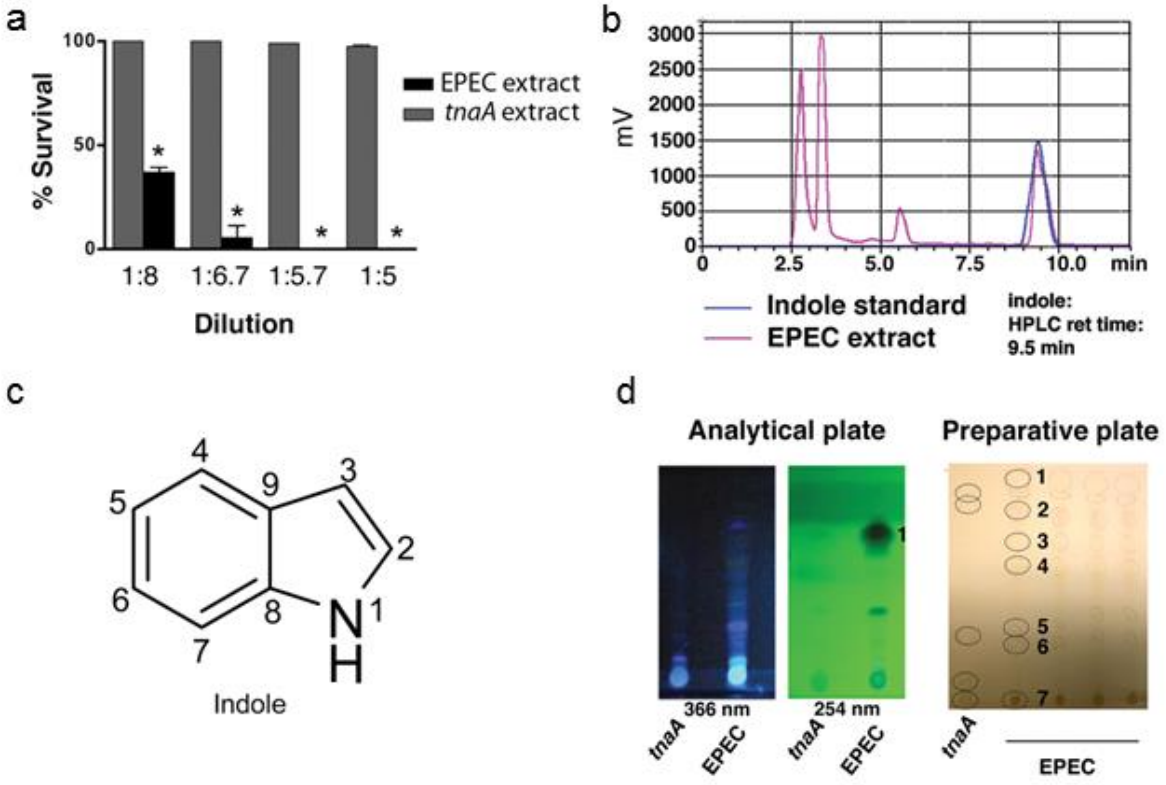

Figure 4.3 Identification of extract components that kill *C. elegans*. (a) Effect on C. elegans survival of dilutions of extracts derived from agar plates on which EPEC or EPECΔtnaA were grown. Extracts comprise only secreted bacterial factors because bacteria were grown on 0.2 mm nitrocellulose filters and then discarded prior to extraction of small molecules from the agar. EPEC, but not EPECΔtnaA, extracts kill C. elegans. Mean +/2 SEM are shown; * corresponds to p, 0.001 with respect to control at each dilution. (b) HPLC profile of EPEC extracts or a synthetic indole standard. Note that the extract peak on the right overlaps with one seen with synthetic indole. The second peak from the left corresponds to tryptophan, and the third to ICA. (c) Structure of indole. (d) Images of analytical and preparative TLC plates used for separation of EPEC and EPECΔtnaA extracts. The preparative plate was imaged under visible light,

and numbers and circles indicate spots, evident under UV illumination, onto which agar filled cylinders were placed and to which *C. elegans* were added. Only spot #1 killed *C. elegans*. *BB and AA performed all experiments for this figure.*

Despite detoxification strategy, indole-like molecules are EPEC derived killing factors

To identify bacterial factors responsible for killing *C. elegans*, EPEC was cultured overnight on nitrocellulose filters atop LB agar plates with added tryptophan (LBT), and then discarded with the filters. After extraction of the agar with organic solvents, a crude extract was generated. As shown in (**Figure 4.3a**), the extract at dilutions up to 1:6 killed all animals within 2 hours. By contrast, an extract from cultured EPECΔ*tnaA* was without effect even at dilutions as high as 1:2. HPLC analysis of the extract yielded several peaks (pink line, **Figure 4.3b**), one of which had the same retention time as commercially available indole (blue line, **Figure 4.2b**). This peak was confirmed as indole (**Figure 4.3c**; **Figure 4.1,** compound **6**) by HPLC-MS (not shown), with the most abundant peak at 118 Da. Because of the requirement for tryptophanase activity in killing by EPEC, the extract was fractionated using a TLC separation method optimized for indole-like compounds. Spots containing indole-like compounds were recognized by their fluorescence upon illumination with UV_{366} or UV_{254} (**Figure 4.3d**). To assess killing activity of the indole-like molecules, conical cylinders were placed over each spot and partially filled with LB agar. After the agar had solidified, *C. elegans* were added to the agar. Cessation of movement was evident within minutes for the spot with the highest Rf (Spot #1,**Figure 4.3d**), and removal of animals one hour later to NGM/OP50 for twenty-four hours confirmed that all animals had died. No other spots proved toxic. Notably, extracts from EPECΔ*tnaA* did not show a spot with the Rf value of spot #1.

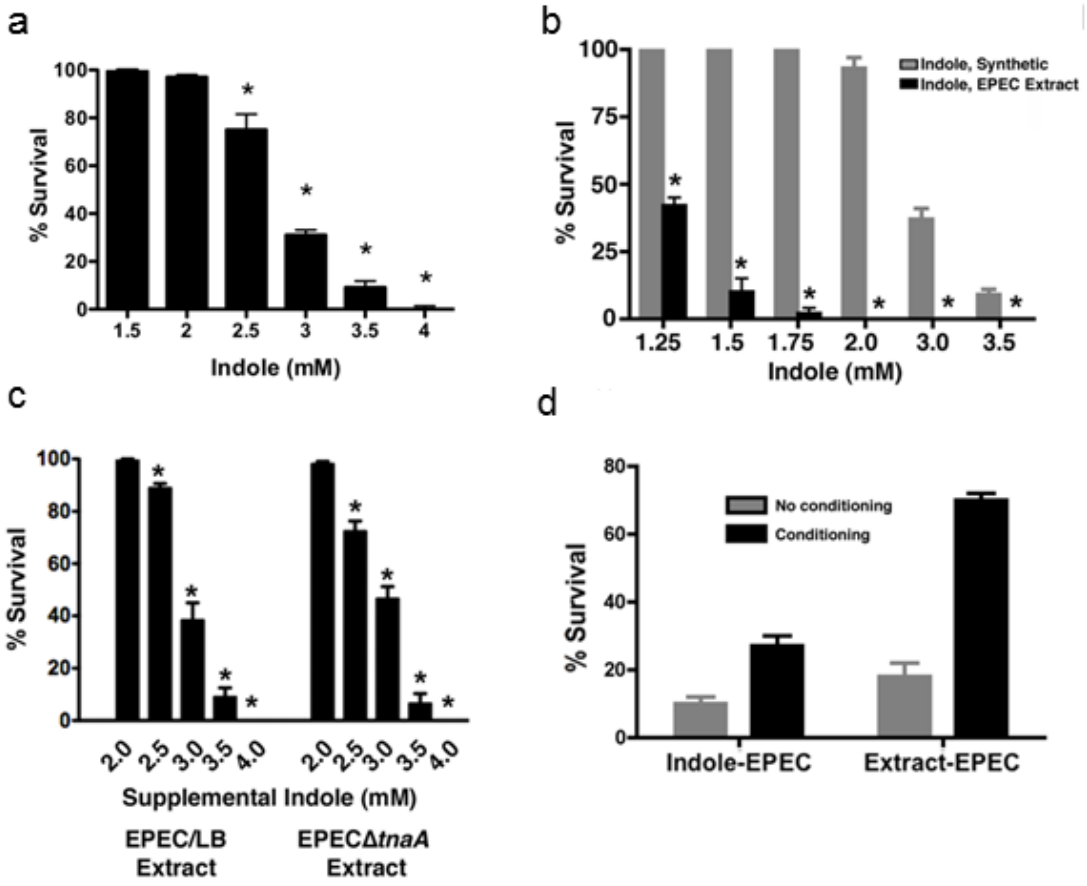

Figure 4.4 Effects of synthetic indole or extract on killing and conditioning of *C. elegans*. (a) Effects on survival of C. elegans N2 upon exposure to various concentrations of synthetic indole in LB broth for 3 hours. (b) Comparison of the effect of synthetic indole or of EPEC agar extracts in which the indole concentration has been estimated based on HPLC measurements of the indole concentration in identically prepared samples. Note that the LD90 for synthetic indole is 3.5 mM, but that the extract kills even at indole concentrations of 1.5 mM, suggesting that additional factors in the extract contribute to killing. Mean +/2 SEM are shown; * corresponds to p,0.001 with respect to control at each dilution.(c) Tryptophan and tryptophanase are required for production of additional killing factors. N2 worms were exposed either to EPEC extracts from LB plates lacking tryptophan or to EPECΔtnaA extracts. Significant killing was evident in either condition only when synthetic indole was added at concentrations greater than 3 mM. Mean +/2 SEM are shown; * corresponds to p, 0.01 with respect to control at each dilution. (d) Comparison of the effects of conditioning C. elegans with either 3.5 mM indole or with extract derived from EPEC/LBT plates, and challenging with EPEC. Note that extract conditions 2-fold better than indole. Mean +/295% confidence intervals are shown. Lack of overlapping error bars indicates significance at the 5% level. *BB and AA performed all experiments for this figure.*

Moreover, HPLC analysis indicated that Spot #1 eluted with the same retention time as commercially available indole (not shown). These data suggest that indole in the extract is toxic to *C. elegans*.

We had previously shown that indole is toxic at 3 mM (**Figure 4.2**). To reconfirm whether synthetic indole affected survival of *C. elegans* and to test smaller concentration increments, we exposed N2 worms to LB broth containing indole at concentrations ranging from 1.5 mM to 4 mM for 3 hours. More than 95% of the animals survived exposure to indole concentrations 2 mM or lower, whereas less than 10% survived exposure to concentrations greater than 3.5 mM (**Figure 4.4a**). Methanol, the solvent used to dissolve indole, was without effect (not shown). These data re-confirm that indole is sufficient to kill *C. elegans*, in accordance with the requirement for tryptophanase activity for EPEC pathogenicity (*16*).

Additional Factor(s) in the Extract Facilitate Killing by Indole

We next determined whether the extract from EPEC plates contained indole concentrations that corresponded to those required to kill or condition *C. elegans*. We first measured the yield of indole in the extraction protocol by using EPECΔ*tnaA* plates spiked with known amounts of indole. On average, the protocol yielded a 13% recovery (n = 4). We next calculated the concentration of indole in the extract dilutions. As shown in **Figure 4.4b**, the extract killed *C. elegans* at lower apparent concentrations of indole than were achieved with synthetic indole. Comparison of the LD_{90} for synthetic indole (~3.50 mM; **Figure 4.4a**) with the LD_{90} for the indole in the extract (~1.5 mM) revealed a 2.3-fold difference (**Figure 4.4b**). Thus, the apparent concentration of indole in the extract alone did not appear sufficient to kill *C. elegans*, raising the possibility that

additional factors in the extract might have killing activity or, alternatively, potentiate the effects of indole.

The additional factor(s) was not capable of killing on its own because no killing was evident with EPEC extracts in which the indole was removed upon fractionation by HPLC (data not shown). Thus, the additional factors appeared to enhance the killing capacity of indole, thereby lowering its critical killing concentration when administered together with lower concentrations of indole.

We next assessed whether tryptophan or tryptophanase were required for production of the additional factor(s). To do this, EPEC was grown on LB agar plates without tryptophan, and an extract lacking indole was prepared. Synthetic indole was then added to the extract at different concentrations. The supplemented extract was only capable of killing *C. elegans* when the concentration of supplemental indole exceeded 3.0 mM, indicating that production of the additional factor likely depended upon tryptophan (**Figure 4.4c**). Moreover, extracts from EPECΔ*tnaA* mutant only killed when supplemented with indole at concentrations greater than 3.0 mM, suggesting that production of sufficient levels of the additional factor also depended upon tryptophanase activity (**Figure 4.4c**). In chapter 3, EPEC based conditioning of *C. elegans* was discussed (chapter 3). We found that EPEC extract conditioned better than indole alone (**Figure 4.4d**). These data suggest that tryptophan and tryptophanase are required for production of additional tryptophan-derived small molecule(s) that contribute(s) to EPEC pathogenicity.

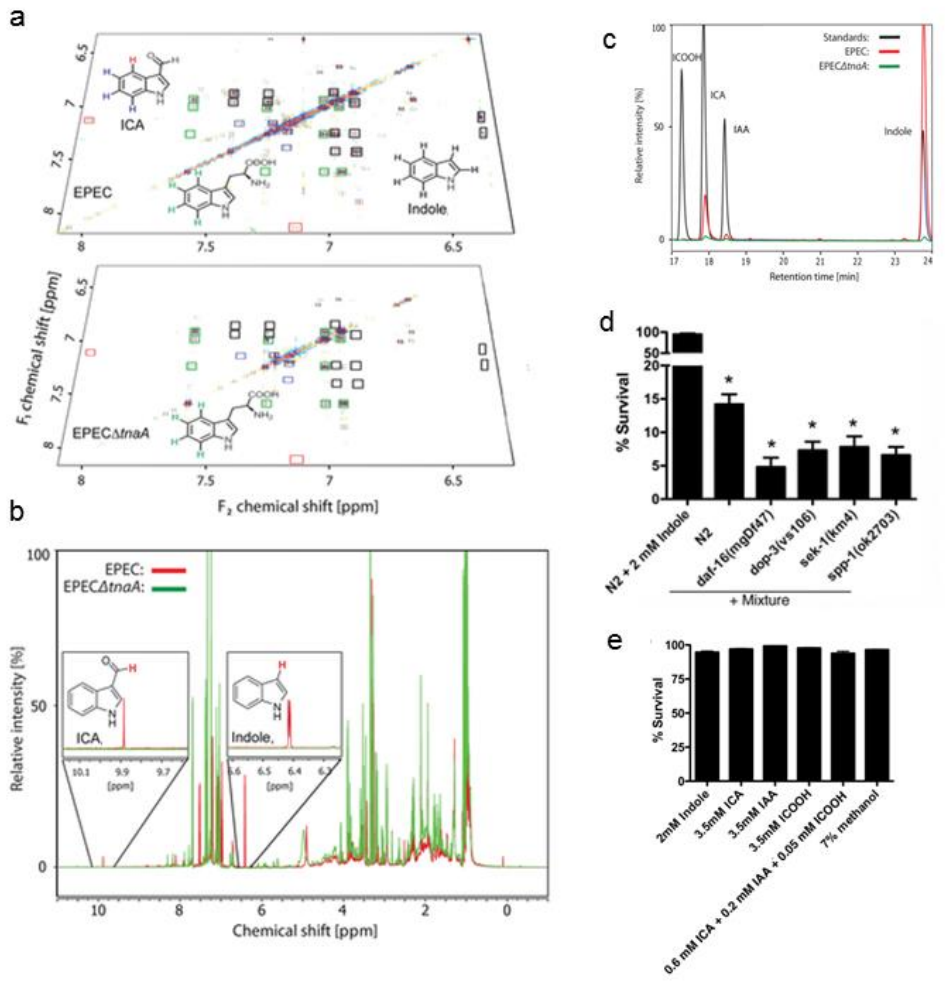

Figure 4.5 Identification of indole derivatives by two-dimensional NMR-based comparative metabolomics. (a) DANS overlay of the aromatic region of a dqfCOSY spectra obtained for the EPEC and EPECΔtnaA extracts highlights differentially present compounds in the EPEC extract. Crosspeaks representing colored protons in the shown indole structures are highlighted by correspondingly colored boxes. For example, the crosspeaks marked with a red box corresponds to a de-shielded protons of ICA, which is present in the EPEC spectrum but absent in the EPECΔtnaA spectrum. (b) Overlay of 1H-NMR spectra from the EPEC extract (red) and the EPECΔtnaA (green). Signals representing indole (zoom of 6.4 ppm) and the aldehyde proton in ICA (at 9.9 ppm) are present in the EPEC spectrum but absent in the EPECΔtnaA spectrum. **(c)** Overlay of UV-HPLC chromatograms (absorption at 260 nm) of the EPEC and EPECΔ*tnaA* extracts as well as of synthetic standards of ICOOH, ICA, IAA, and indole, obtained using a reverse phase HPLC column. (d) (c) Reconstitution of killing with 2 mM indole in combination with 0.6 mM ICA and 0.2 mM IAA. Mean +/2 SEM are shown; * corresponds to p,0.01 with respect to N2. (e) Neither ICA, nor IAA, nor ICOOH alone at the indicated concentrations nor in combination killed *C. elegans*. *YI acquired all NMR and LC/MS spectra and performed analysis with supervision from FS. BB conducted survival assays.*

Identification of Additional Factors in the EPEC Extract

To identify the additional factor(s), we compared extracts from EPEC or EPEC*ΔtnaA* via differential analysis by 2D NMR spectroscopy (*19*) and HPLC-mass spectroscopy-based comparative metabolomics (**Figure 4.5a**) (*20, 21*). EPEC and EPEC*ΔtnaA* extracts were used to acquire double quantum filtered correlation spectroscopy (dqf-COSY) spectra. These spectra were analyzed using the DANS method, which highlights cross peaks stemming from metabolites differentially present in one sample and absent in another (**Figure 4.5a**). DANS revealed a series of strong NMR signals representing indole in the EPEC spectra (**Figure 4.5b**), and as expected indole was absent in the EPEC*ΔtnaA* spectrum. As expected, cross peaks representing tryptophan were more prominent in the EPEC*ΔtnaA* sample. In addition we detected another strong set of indole-like signals in the EPEC spectrum that was absent from EPEC*ΔtnaA* spectrum, and therefore represented an additional tryptophanase-dependent indole derivative. Detailed spectral analysis indicated that this metabolite was either indole-3-carboxaldehyde (**ICA**;**9**, **Figure 4.5a,b**) or indole-3-carboxylic acid, based on the characteristically high chemical shift of a crosspeak representing the proton in position 4 of the indole ring system (**Figure 4.5a)**. Additional analysis of the ^{1}H NMR spectra of EPEC and EPEC*ΔtnaA* extracts revealed an aldehyde proton in the EPEC spectrum that was absent from the EPEC*ΔtnaA* spectrum (**Figure 4.5b**), providing further evidence that extracts from EPEC, but not EPEC*ΔtnaA*, contain ICA. Considering the possibility that indole-3-carboxylic acid (ICOOH) crosspeaks could have been obscured by the more abundant ICA, we further compared the EPEC and EPEC*ΔtnaA* extracts via HPLC-MS, which confirmed the presence of ICA in addition to

smaller amounts of ICOOH and indole-3-acetic acid in EPEC extracts. Indole, ICA and ICOOH were absent in EPEC*ΔtnaA* extracts, whereas IAA was also present in EPEC*ΔtnaA* extracts, although in smaller amounts than in EPEC. Using synthetic standards of known concentrations, UV absorbance at 260 nM was used to calculate the relative concentration of indole:ICA:IAA:ICOOH: in the EPEC extracts as 7:1:0.3:0.1 (**Figure 4.5c**).

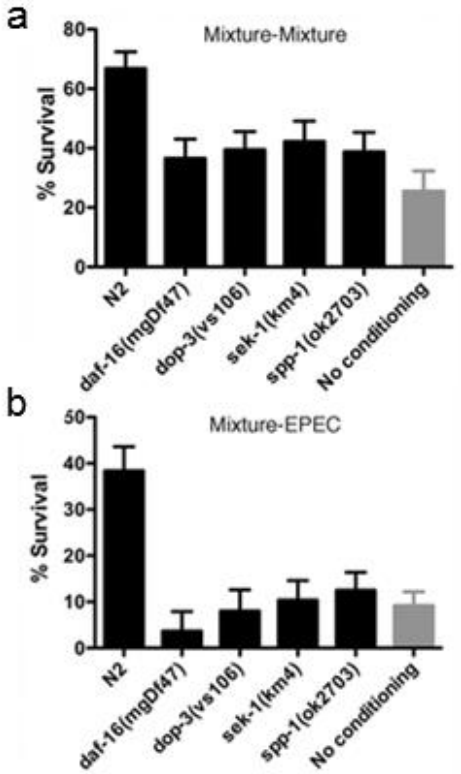

Figure 4.6 Pre-exposure of N2 or various mutants to the indole/ICA/IAA mixture for 30 minutes followed by a 3 hour waiting period on OP50, and then a 3 hour challenge with either the mixture (d) or EPEC (e). Note that killing and conditioning with the mixture closely resembles that seen with EPEC, and utilizes the same gene products in *C. elegans*. In d-e, mean +/295% confidence intervals are shown. Lack of overlapping error bars indicates significance at the 5% level. *BB and AA performed all experiments for this figure.*

Indole Derivatives Facilitate Killing and Conditioning of *C. elegans*

We next assessed the effects of the identified indole derivatives on killing and conditioning. Like indole at 2 mM, neither ICA, nor IAA, nor ICOOH killed *C. elegans*, even when administered at 3.5 mM, the highest concentration tested (**Figure 4.5b**). However, killing was evident with 2 mM indole in combination with ICA and IAA, the latter at concentrations similar to those found in the extract (0.6 mM and 0.2 mM, respectively; **Figure 4.5d**), though over a slightly longer time course (4 hours) than with EPEC or extract. Other ratios proved less optimal, and addition of ICOOH to the mixture was without effect (data not shown). Likewise, the mixture without indole was also without effect (**Figure 4.5e**). Exposure of N2 animals to the indole carrier, methanol, was also without effect (**Figure 4.5e**). Mutants in the dopamine, innate immunity and longevity pathways were more sensitive to the mixture compared to the wild type (**Figure 4.5c**).

In conditioning experiments, pre-exposure to the mixture increased survival of N2 worms upon challenge with either the mixture (**Figure 4.6a**) or EPEC (**Figure 4.6b**). Individual components of the mixture induced only marginal conditioning upon challenge with EPEC. As with EPEC, mutants in the dopamine, innate immunity or longevity pathways were not conditionable with the mixture (**Figure 4.6a and b**). Together, these data suggest that the mixture of indole and its derivatives generally recapitulates the effects of EPEC on both killing and conditioning.

Indole derivatives are critical regulators of virulence

The discovery of these indole derivatives led to the finding that both indole and ICA regulate virulence in EPEC, EHEC and a related attachment and effacing (A/E)

bacteria *Citrobacter rodentium* (*22*). Notably, these molecules did not affect bacterial growth but modulated expression of the well-studied pathogenicity island locus of enterocyte effacement (LEE)-transcriptional regulator Ler (*2*). Consequently, indole and ICA also inhibited pedestal formation induced by EPEC, EHEC and *C. rodentium* (data not shown). These data nevertheless suggest that the regulatory mechanisms modulated by these molecules are conserved amongst A/E pathogens, and that these molecules can affect virulence in bacteria that do not produce them. The next section will describe *in vivo* experiments motivated by and highlighting the impact of these discoveries.

ICA protects against A/E pathogen infections *in vivo*

We assessed whether indole or its derivatives affected morbidity and mortality of A/E pathogens *in vivo*. We tested this possibility in MyD88$^{-/-}$ mice, which unlike wild type animals, succumb to infection with *C. rodentium* (*22*). As shown in Figure 4.7a, ICA delivered orally at 100 mg/kg/day reduced CFU in the colon by 50 fold, and reduced dissemination of the bacteria to other organs including spleen and liver, where CFUs were also reduced by ~10 fold (**Figure 4.7a**). Moreover, histological examination of animals treated with ICA showed no indication of isolated intramural colonic bleeding, colonic distension, or hemorrhagic colitis, effects evident in all untreated or carrier-treated animals (**Figure 4.7b**). Likewise, H&E staining of colon sections from carrier and untreated animals infected with *C. rodentium*, but not ICA-treated animals, revealed gangrenous mucosal necrosis characterized by visible bacterial colonies, neutrophil infiltration, mucosal injury, edema, apoptosis, intramural bleeding, and epithelial injury (**Figure 4.7c)**. Finally, administration of ICA reduced mortality rates in a dose

dependent manner. Thus, 100% of animals treated with ICA survived without detectable signs of disease at a time when all the control animals had succumbed (7d post infection;**Figure 4.7d**). Furthermore, the probability of dying was reduced by 1.7 fold. These data were statistically significant using a Kaplan Meyer test ($p<0.0001$). Collectively, these data suggest that ICA reduces morbidity and mortality of A/E pathogens *in vivo.*

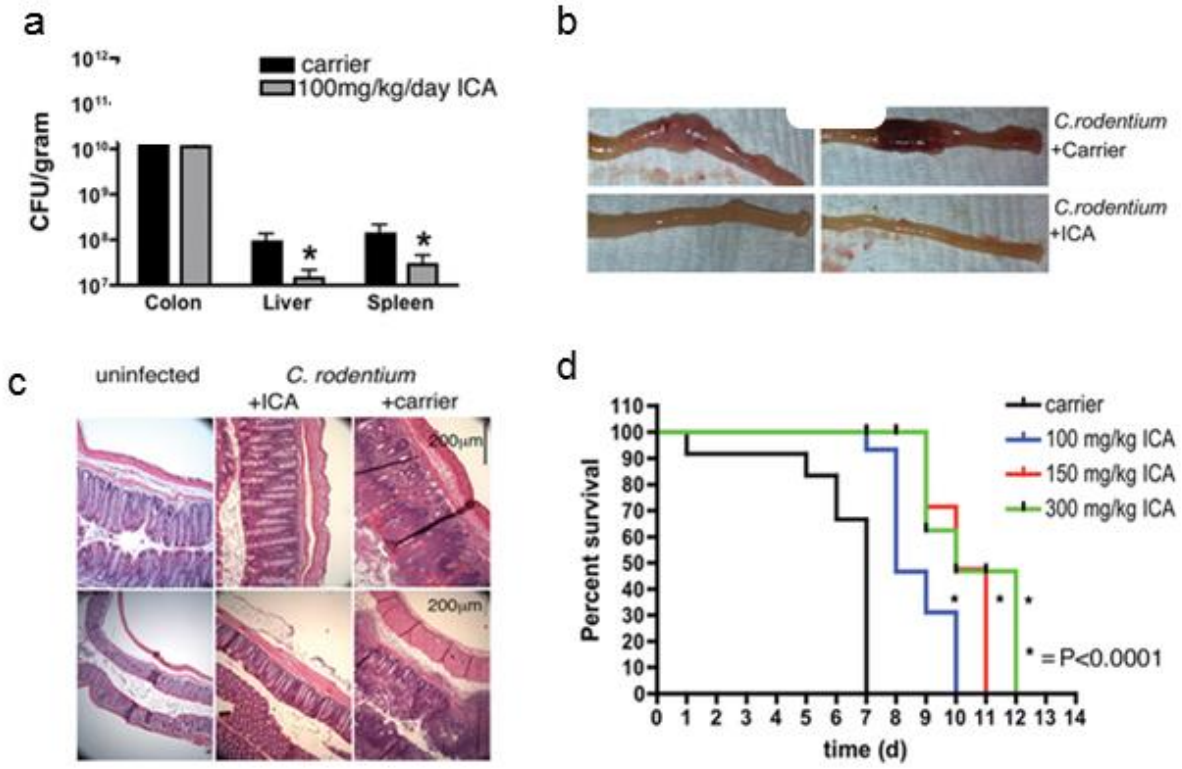

Figure 4.7 ICA reduces virulence of *C. rodentium* in vivo. (c) CFU from colon, liver, and spleen of MyD882/2 mice infected for 7 days with C. rodentium and administered carrier (DMSO/5%Citric acid/PEG400, (30:35:35%)) or ICA (100 mg/kg/day) by oral gavage. Mean +/2 SEM are shown; * corresponds to p, 0.01 with respect to untreated control. 8 mice were used for the control and 9 for the treatment with 100 mg/kg ICA. (d) Images of colons from animals left uninfected and treated with ICA (100 mg/kg/day) for 7 days, or infected with C. rodentium together with carrier or ICA. (e) H&E staining of colon sections from mice left uninfected, or infected with C. rodentium for 7d and administered either ICA (100 mg/kg/day) or carrier. (f) Survival curves of animals treated with carrier or 100 to 300 mg/kg/day ICA. Each curve is from a representative experiment (n = 3

animals per condition), and each experiment was repeated 3 times. Statistical significance was determined by the Kaplan Meyer test. *BB and AA performed all experiments for this figure.*

Conclusion

The discovery of a dedicated small molecule detoxification strategy highlights the utility of *C. elegans* in the study of host-pathogen interactions. *C. elegans* genetics has already been used to determine nematode genes that confer host susceptibility or immunity to various pathogens (*5*). Critically, bacterial virulence and host susceptibility mechanisms identified in *C. elegans* are often highly conserved. Moreover, the same innate immune genes that are deployed against a variety of pathogens in *C. elegans*, are likewise important components of mammalian immune pathways (*23*). This chapter summarizes two separate projects that reveal small molecule signaling involved in host-pathogen interaction and regulation of pathogenicity in various bacteria.

The glycosylation and release of a common anthelminthic drug, albendazole (*24*), and of several small molecules from a synthetic library (*25*) have been described, but the function of glycosylation in *C. elegans* has not previously been explored. In this chapter, we demonstrate that *N*- and *O*-glycosylation serve to detoxify two chemically very different xenobiotics, indole and 1-HP, indicating that glycosylation and subsequent phosphorylation represent general mechanisms to convert and remove environmental toxins. This pathway may involve specific glycosylation enzymes and transporter proteins, whose identification will enable comparing the detoxification systems of nematodes with those of other metazoans. Furthermore, existing treatments of parasitic nematode infections in humans, livestock, and plants could be augmented by inhibiting

small molecule glycosyltransferases and/or transporters to increase drug efficacy by slowing down or preventing release into the environment (*24, 26*).

The discovery of the indole detoxification strategy in *C. elegans* suggested that pathogenic *E. coli* utilize a diverse set of molecules for virulence. Using *C. elegans* as a bioassay system in conjunction with NMR-based metabolomics, we have identified a family of bioactive small molecules related to indole, that are produced by pathogenic *E. coli* strains. These molecules, when presented together, reconstitute the toxicity apparent when *C. elegans* is incubated with EPEC. Thus, indoles join a growing class of small molecules produced by bacteria that act as toxins or immunoregulators in *C. elegans*. Other examples include quinolone signal and pyocyanin in *Pseudomonas aeruginosa* (*23, 27*).

We identified indoles based on their toxicity in *C. elegans*. However, unlike pyocyanins, indoles are protective in mammals likely because they suppress expression of bacterial virulence genes and shigatoxin, at least at high concentrations. Moreover, our findings suggest that whereas indole is itself is toxic to *C. elegans*, indole-like molecules have no evident toxicity in *C. elegans* nor in mice. These results highlight the utility of *C. elegans*-pathogen systems in conjunction with metabolomics for identifying novel signaling molecules. Indeed, these methodologies may be broadly applicable to identifying small signaling molecules in many organisms.

The data in this chapter showing decreased virulence and reduced mortality upon oral administration of ICA in MyD88$^{-/-}$ mice infected with *C. rodentium* raises the possibility that administration of exogenous indoles may represent a novel means to prevent or mollify infections caused by pathogenic *E. coli*. Considering indoles do not

affect bacterial growth, they may not easily engender resistance compared to conventional antibiotics. In summary, by using *C. elegans* in combination with NMR- and MS-based comparative metabolomics, we have obtained data that provide an important advance in the identification of small molecules that regulate multiple aspects of bacterial physiology and pathogenicity.

REFERENCES

1. Stupp, G. S., von Reuss, S. H., Izrayelit, Y., Ajredini, R., Schroeder, F. C., and Edison, A. S. (2013) Chemical detoxification of small molecules by Caenorhabditis elegans, *ACS Chem. Biol. 8*, 309-313.
2. Bommarius, B., Anyanful, A., Izrayelit, Y., Bhatt, S., Cartwright, E., Wang, W., Swimm, A. I., Benian, G. M., Schroeder, F. C., and Kalman, D. (2013) A family of indoles regulate virulence and Shiga toxin production in pathogenic *E. coli*, *PLoS One 8*, e54456.
3. Irazoqui, J. E., Urbach, J. M., and Ausubel, F. M. (2010) Evolution of host innate defence: insights from *Caenorhabditis elegan*s and primitive invertebrates, *Nat. Rev. Immun. 10*, 47-58.
4. Kurz, C. L., and Ewbank, J. J. (2003) *Caenorhabditis elegans*: an emerging genetic model for the study of innate immunity, *Nat. Rev. Genet. 4*, 380-390.
5. Sifri, C. D., Begun, J., and Ausubel, F. M. (2005) The worm has turned - microbial virulence modeled in *Caenorhabditis elegans*, *Trends Microbiol. 13*, 119-127.
6. Irazoqui, J. E., Troemel, E. R., Feinbaum, R. L., Luhachack, L. G., Cezairliyan, B. O., and Ausubel, F. M. (2010) Distinct pathogenesis and host responses during infection of *C. elegans* by *P. aeruginosa* and *S. aureus*, *PLoS Pathog. 6*, e1000982.
7. Alkema, M. J., Hunter-Ensor, M., Ringstad, N., and Horvitz, H. R. (2005) Tyramine functions independently of octopamine in the *Caenorhabditis elegans* nervous system, *Neuron 46*, 247-260.
8. Alper, S., McBride, S. J., Lackford, B., Freedman, J. H., and Schwartz, D. A. (2007) Specificity and complexity of the *Caenorhabditis elegans* innate immune response, *Mol Cell. Biol. 27*, 5544-5553.
9. Lindblom, T. H., and Dodd, A. K. (2006) Xenobiotic detoxification in the nematode *Caenorhabditis elegans*, *J. Exp. Zool. Part A 305*, 720-730.
10. Shivers, R. P., Youngman, M. J., and Kim, D. H. (2008) Transcriptional responses to pathogens in *Caenorhabditis elegans*, *Curr. Opin. Microbiol. 11*, 251-256.
11. Troemel, E. R., Chu, S. W., Reinke, V., Lee, S. S., Ausubel, F. M., and Kim, D. H. (2006) p38 MAPK regulates expression of immune response genes and contributes to longevity in *C. elegans*, *PLoS Genet. 2*, e183.
12. Mavrodi, D. V., Bonsall, R. F., Delaney, S. M., Soule, M. J., Phillips, G., and Thomashow, L. S. (2001) Functional analysis of genes for biosynthesis of pyocyanin and phenazine-1-carboxamide from *Pseudomonas aeruginosa* PAO1, *J. Bacteriol. 183*, 6454-6465.
13. Nataro, J. P., and Kaper, J. B. (1998) Diarrheagenic *Escherichia coli*, *Clin. Microbiol. Rev. 11*, 142-201.
14. Clarke, S. C., Haigh, R. D., Freestone, P. P., and Williams, P. H. (2002) Enteropathogenic *Escherichia coli* infection: history and clinical aspects, *Brit. J. Biomed. Sci. 59*, 123-127.

15. Denamur, E. (2011) The 2011 Shiga toxin-producing *Escherichia coli* O104:H4 German outbreak: a lesson in genomic plasticity, *Clin. Microbiol. Infec. 17*, 1124-1125.
16. Anyanful, A., Dolan-Livengood, J. M., Lewis, T., Sheth, S., Dezalia, M. N., Sherman, M. A., Kalman, L. V., Benian, G. M., and Kalman, D. (2005) Paralysis and killing of *Caenorhabditis elegans* by enteropathogenic *Escherichia coli* requires the bacterial tryptophanase gene, *Mol. Microbiol. 57*, 988-1007.
17. Anyanful, A., Easley, K. A., Benian, G. M., and Kalman, D. (2009) Conditioning protects *C. elegans* from lethal effects of enteropathogenic *E. coli* by activating genes that regulate lifespan and innate immunity, *Cell Host Microbe 5*, 450-462.
18. Perna, N. T., Plunkett, G., 3rd, Burland, V., Mau, B., Glasner, J. D., Rose, D. J., Mayhew, G. F., Evans, P. S., Gregor, J., Kirkpatrick, H. A., Posfai, G., Hackett, J., Klink, S., Boutin, A., Shao, Y., Miller, L., Grotbeck, E. J., Davis, N. W., Lim, A., Dimalanta, E. T., Potamousis, K. D., Apodaca, J., Anantharaman, T. S., Lin, J., Yen, G., Schwartz, D. C., Welch, R. A., and Blattner, F. R. (2001) Genome sequence of enterohaemorrhagic *Escherichia coli* O157:H7, *Nature 409*, 529-533.
19. Anokye-Danso, F., Anyanful, A., Sakube, Y., and Kagawa, H. (2008) Transcription factors GATA/ELT-2 and forkhead/HNF-3/PHA-4 regulate the tropomyosin gene expression in the pharynx and intestine of *Caenorhabditis elegans*, *J. Mol. Biol. 379*, 201-211.
20. Forseth, R. R., and Schroeder, F. C. (2011) NMR-spectroscopic analysis of mixtures: from structure to function, *Curr. Opin. Chem.Biol. 15*, 38-47.
21. Pungaliya, C., Srinivasan, J., Fox, B. W., Malik, R. U., Ludewig, A. H., Sternberg, P. W., and Schroeder, F. C. (2009) A shortcut to identifying small molecule signals that regulate behavior and development in *Caenorhabditis elegans*, *Proc. Natl Acad. Sci. USA 106*, 7708-7713.
22. Lebeis, S. L., Bommarius, B., Parkos, C. A., Sherman, M. A., and Kalman, D. (2007) TLR signaling mediated by MyD88 is required for a protective innate immune response by Neutrophils to *Citrobacter rodentium*, *J. Immunol. 179*, 566-577.
23. Partridge, F. A., Gravato-Nobre, M. J., and Hodgkin, J. (2010) Signal transduction pathways that function in both development and innate immunity, *Dev. Dynam. 239*, 1330-1336.
24. Sheps, J. A., Ralph, S., Zhao, Z. Y., Baillie, D. L., and Ling, V. (2004) The ABC transporter gene family of *Caenorhabditis elegans* has implications for the evolutionary dynamics of multidrug resistance in eukaryotes, *Genome Biol. 5*.
25. Laing, S. T., Ivens, A., Laing, R., Ravikumar, S., Butler, V., Woods, D. J., and Gilleard, J. S. (2010) Characterization of the xenobiotic response of *Caenorhabditis elegans* to the anthelmintic drug albendazole and the identification of novel drug glucoside metabolites, *Biochem. J. 432*, 505-514.
26. Burns, A. R., Wallace, I. M., Wildenhain, J., Tyers, M., Giaever, G., Bader, G. D., Nislow, C., Cutler, S. R., and Roy, P. J. (2010) A predictive model for drug bioaccumulation and bioactivity in *Caenorhabditis elegans*, *Nat. Chem. Biol. 6*, 549-557.

27. Denning, G. M., Wollenweber, L. A., Railsback, M. A., Cox, C. D., Stoll, L. L., and Britigan, B. E. (1998) Pseudomonas pyocyanin increases interleukin-8 expression by human airway epithelial cells, *Infect. Immun. 66*, 5777-5784.

CHAPTER 5

2D NMR-BASED METABOLOMICS UNCOVERS INTERACTIONS BETWEEN CONSERVED BIOCHEMICAL PATHWAYS IN THE MODEL ORGANISM *CAENORHABDITIS ELEGANS*

Abstract

Ascarosides are small-molecule signals that play a central role in *C. elegans* biology, but many aspects of their biosynthesis remain unknown. Using automated 2D NMR-based comparative metabolomics, we identified ascaroside ethanolamides as shunt metabolites in *C. elegans* mutants of *daf-22*, a gene with homology to mammalian 3-ketoacyl-CoA thiolases predicted to function in conserved peroxisomal lipid β-oxidation. Two groups of ethanolamides feature β-keto functionalization confirming the predicted role of *daf-22* in ascaroside biosynthesis, whereas α-methyl substitution points to unexpected inclusion of methylmalonte at a late stage in the biosynthesis of long-chain fatty acids in *C. elegans*. We show that ascaroside ethanolamide formation in response to defects in *daf-22* and other peroxisomal genes is associated with severe depletion of endocannabinoid pools. These results indicate unexpected interaction between peroxisomal lipid β-oxidation and the biosynthesis of endocannabinoids, which are major regulators of lifespan in *C. elegans*. Our study demonstrates the utility of unbiased comparative metabolomics for investigating biochemical networks in metazoans.

Contributions

The work in this chapter was conducted by a team of scientists in the Schroeder Lab (Cornell University, Ithaca, NY), as well as a colleague, Steven L. Robinette (Department of Surgery and Cancer, Imperial College London, London, UK). The data and writing, with minor modifications, in this chapter has been published in ACS Chem. Biol. (*1*). ***Yevgeniy Izrayelit (YI) is a co-first author on this publication. YI designed the experiments, analyzed extracts, ran NMR experiments, applied MATLAB based metabolomics methods, isolated and characterized natural products, and wrote the manuscript. YI's primary data contribution was preparation of extracts, acquisition of NMR data and analysis of metabolomics experiments.*** Steven Robinette (SLR) is a co-first author on this study and designed the MATLAB based algorithm for mvaDANS as well as assisted with data analysis and manuscript preparation. Additionally, Neelanjan Bose (NB) and Stephan H. von Reuss (SVR) assisted in characterization of novel mutant dependent metabolites. Professor Frank Schroeder (FCS) supervised the project and wrote the manuscript.

Introduction

The free-living nematode *Caenorhabditis elegans* is used extensively as a model system for the study of aging and metabolism (*2-4*). Recent analyses of the *C. elegans* metabolome revealed a family of structurally diverse small molecules, the ascarosides, as products of conserved peroxisomal β-oxidation (**Figure 5.1**) (*5-7*). The ascarosides form a modular compound library, integrating building blocks from lipid, carbohydrate and amino acid metabolism into small molecule signals that regulate key aspects of *C. elegans* biology (*8-11*). Previous work used mass spectrometry-based comparative metabolomics to characterize the functions of three enzymes in ascaroside biosynthesis, the acyl-CoA oxidase ACOX-1, the enoyl-CoA hydratase MAOC-1, and the 3-hydroxyacyl-CoA dehydrogenase DHS-28 (**Figure 5.1b**) (*5*). However, the predicted role of the fourth enzyme in the peroxisomal β-oxidation cascade, which is encoded by the gene *daf-22*, a close homolog of mammalian 3-keto-acyl-CoA thiolases, could not be confirmed because no characteristic shunt metabolites were found. Given the central role of *daf-22* in the proposed peroxisomal β-oxidation pathway, we hypothesized that other, yet unidentified metabolites accumulate in *daf-22* mutants, which may help confirm the biochemical function of this enzyme and provide insight into interactions with other biochemical pathways.

Therefore, we reinvestigated the *daf-22* metabolome using unbiased NMR spectroscopy-based metabolomics. Previously, we had employed manual comparisons of 2D NMR spectra of wild-type and *daf-22* metabolomes to identify additional members of the ascaroside family of signaling molecules (*7, 10, 12*). These studies highlighted the utility of 2D NMR spectra for comparative metabolomics, but also demonstrated the

need for computational tools that would enable statistical analysis of series of spectra from different mutants. For this purpose, we developed multivariate Differential Analysis by 2D NMR Spectroscopy (mvaDANS), which enables automated processing and comparative computational analysis for sets of 2D NMR spectra.

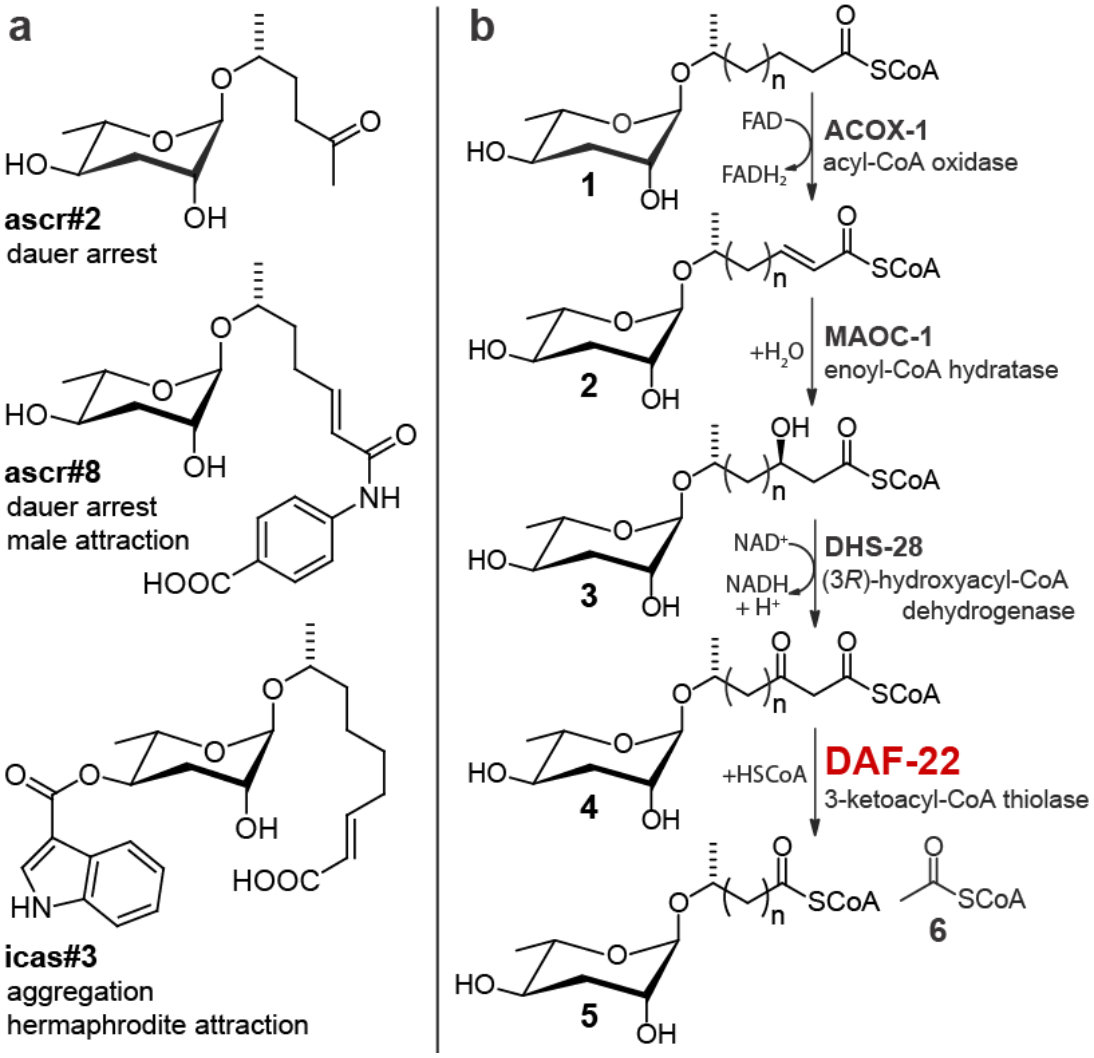

Figure 5.1. Ascarosides are signaling molecules in *C. elegans*. (a) Example structures and biological functions of ascaroside-based signaling molecules in *C. elegans*. (b) Model for peroxisomal biosynthesis of ascaroside side chains and roles of peroxisomal β-oxidation enzymes ACOX-1, MAOC-1, DHS-28, and the putative 3-ketoacyl-CoA thiolase DAF-22.

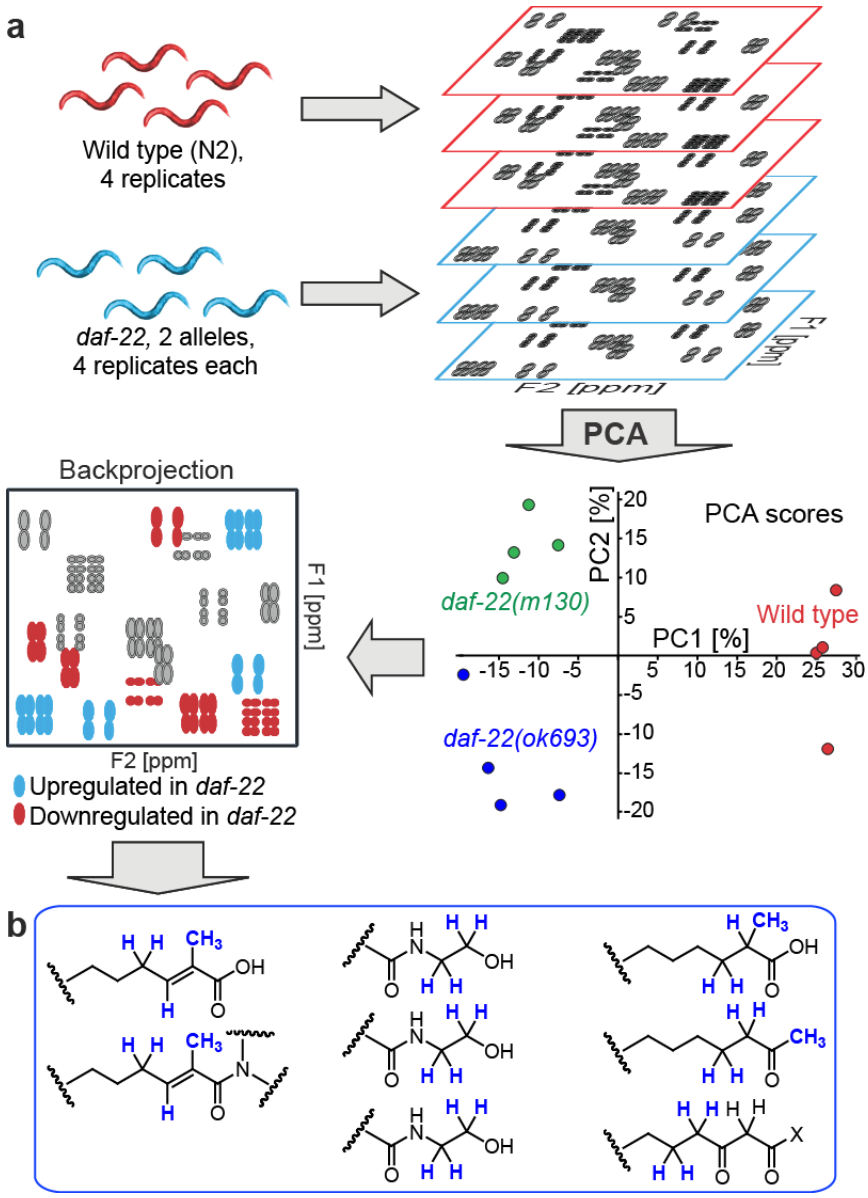

Figure 5.2. mvaDANS reveals structural motifs upregulated in *daf-22* mutants. (a) Schematic overview of mvaDANS for identification of up- and downregulated metabolites in *daf-22* mutants. In the Principal Component Analysis (PCA), PC 1 separates the four wild-type data sets (blue dots) from both *daf-22* mutant data sets (red and brown dots), whereas PC2 separates the two *daf-22* alleles. In the back projection (lower left), the coloring of cross speaks corresponds to the PC 1 loading coefficients; blue peaks represent signals downregulated and red peaks signals upregulated in the two *daf-22* mutant strains. See Figure S4 for actual spectra. (b) Partial structures inferred from manual analysis of *daf-22*-specific crosspeaks suggesting α-methyl branched fatty acids, methyl ketones, and β-keto fatty acid derivatives. *SLR designed mvaDANS, YI prepared samples, ran NMR and characterized metabolites. SVR and NB assisted with partial structure identification.*

mvaDANS reveals novel *daf-22* dependent shunt metabolites

mvaDANS builds on previous efforts to use 2D NMR for metabolomic analysis by incorporating dynamic signal detection and pattern recognition (see Methods) (*13-19*). **Figure 5.2** summarizes the use of this approach for identifying compounds that are upregulated in *daf-22* mutants and thus may represent shunt metabolites or biosynthetic intermediates. We acquired dqfCOSY spectra for metabolome extracts obtained from two different *daf-22* alleles (*m130*, *ok693*) and wild-type *C. elegans*, including four independent biological replicates (**Figures 5.2a, and E.1,2**). Automatic crosspeak identification and binning (**Figure E 3**) prepared the dqfCOSY spectra for statistical analysis via Principal Component Analysis (PCA, see Methods) (*20*), which clustered the data by genotype (**Figure 5.2a**). Coefficients from the PCA loadings were back-projected onto the dqfCOSY spectra, which revealed a large number of crosspeaks that are up- or downregulated in *daf-22* mutants relative to wild-type (**Figures 5.2a, E.4, and E.5**).

For this study, we restricted analysis to crosspeaks that were strongly featured in spectra from both *daf-22* alleles but were very weak or undetectable in wild-type. Furthermore, we excluded crosspeaks also present in the *E. coli* food source. Manual analysis of the remaining strongly *daf-22*-upregulated crosspeaks and inputs from additional HMBC spectra suggested a series of partial structures, including methyl ketones, α-methyl branched fatty acids and corresponding ethanolamides as well as β-keto fatty acid derivatives (**Figure 5.2b**). Considering the proposed role of *daf-22* in ascaroside biosynthesis (**Figure 5.1b**), we hypothesized that these structural features belong to accumulated shunt metabolites. Subsequent fractionation of the *daf-22*

metabolome guided by the *daf-22*-specific NMR signals led to isolation of six different very long-chain ascarosides (VLCA) that account for all of the predicted structural features (**Figure 5.3**, see Supporting Information for full spectroscopic data). None of these *daf-22* mutant-specific compounds had previously been reported. Most prominent are a series of (ω-1)-*O*-ascarosyl 2-ketones (**12**) as well as (ω-1)-*O*-ascarosyl 3-keto fatty acid ethanolamides, which include the 2-methyl pentacosanoic acid derivative **7** and the straight-chain heptacosanoic acid derivative **8**. Compounds **7** and **8** are accompanied by smaller amounts of the corresponding *bis*-norhomologues. Similarly, the 2-methyl pentacos-2-enoic acid ethanolamide **9** and the two fatty acids **10** and **11** are accompanied by *bis*-norhomologues. In contrast, chain lengths of the (ω-1)-*O*-ascarosyl 2-ketones (**12**) vary more broadly and are not preferentially odd-numbered (**Figure 5.3c**). HPLC-MS analysis confirmed the absence of these components in wild-type samples (**Figure 5.3a**).

Ethanolamides link two conserved nutrient regulating signaling pathways

The incorporation of ethanolamine in the *daf-22* specific VLCAs was unexpected and suggested the possibility of interactions between peroxisomal β-oxidation and ethanolamide-based signaling pathways. Recently, N-acyl-ethanolamines (NAEs) were identified as endocannabinoid-like signaling molecules in *C. elegans* and linked to dietary restriction-dependent lifespan regulation (*21*). We asked whether the upregulation of VLCAs in *daf-22* mutants affects NAE levels. We found that NAE production, including the most active endocannabinoid in *C. elegans* (*21*), eicosapentaenoyl ethanolamide (**13**, EPEA), and the ligand of mammalian cannabinoid receptors, arachidonoyl ethanolamide (AEA, or anandamide), was dramatically

downregulated in both *daf-22* alleles (**Figures 5.3d and E.6**), suggesting a shift of ethanolamine utilization from the NAEs to VLCAs. Similarly, we found greatly reduced EPEA and AEA production in mutants of *maoc-1* and *dhs-28* (**Figures 5.3d and E.6**) which act directly upstream of *daf-22* (**Figure 5.1b**). EPEA-levels in *acox-1* mutant worms were not significantly affected and AEA levels only slightly decreased, corresponding to the much weaker effect of the *acox-1* mutation on peroxisomal β-oxidation (*5*). EPEA and AEA production was not rescued by growing *daf-22* worms with addition of synthetic ascarosides (**Figures 5.3d and E.6**), suggesting that the observed reduction of NAE levels in peroxisomal β-oxidation mutants is not an indirect effect of the lack of ascaroside pheromone. These findings indicate that in *C. elegans* specific defects in peroxisomal β-oxidation result in depletion of endocannabinoid pools (**Figure 5.3e**). It is unknown whether conditions that reduce expression of peroxisomal β-oxidation genes in healthy animals trigger down-regulation of endocannabinoids, which could serve as a regulatory mechanism tying fat metabolism and ascaroside signaling to dietary restriction pathways. Ethanolamides of short-chain ascarosides serve as pheromones in a parasitic nematode species (*22*), suggesting that interactions of peroxisomal β-oxidation and ethanolamide metabolism also exist in other nematode genera.

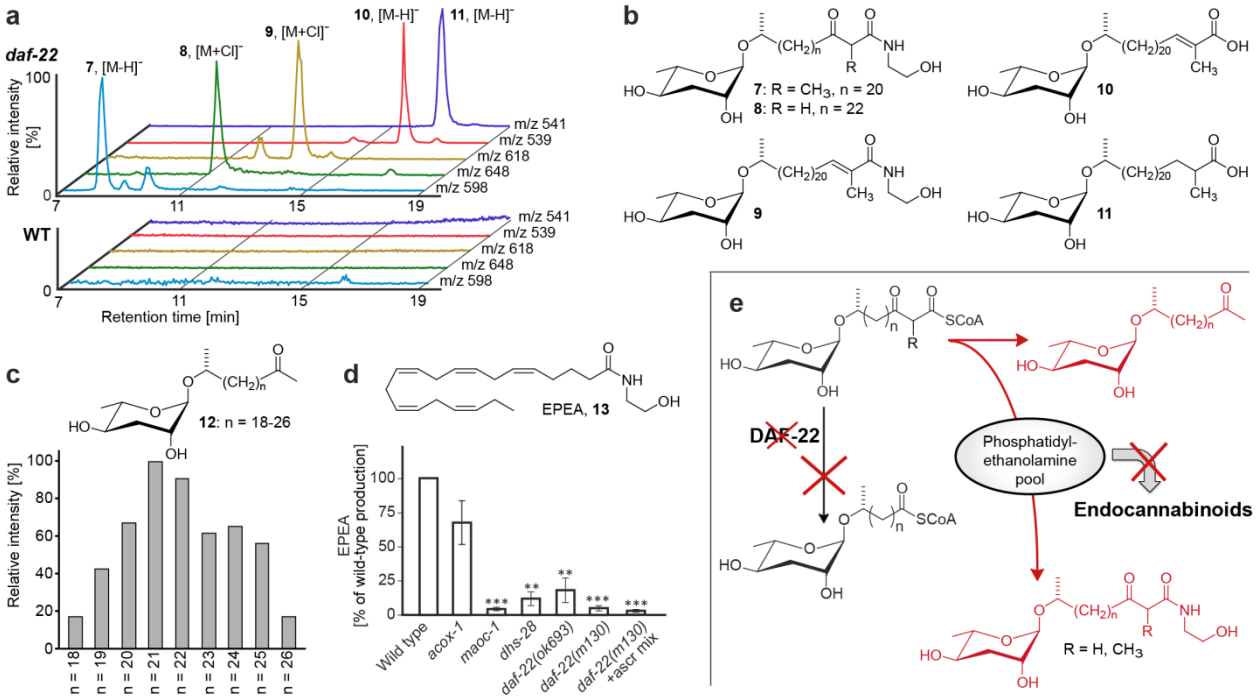

Figure 5.3. Long-chain ascarosides identified in the *daf-22*-mutant metabolome and interaction with NEA biosynthesis. (a) HPLC-MS analysis confirms long-chain ascarosides and ethanolamides in the *daf-22* metabolome that are absent in wild-type. (b) *daf-22* mutant-specific VLCAs identified *via* mvaDANS and subsequent HPLC-MS analysis. (c) Quantitative distribution of *daf-22*-upregulated ascarosyl methylketones. (d) Mutation of *maoc-1*, *dhs-28*, and *daf-22* greatly reduces EPEA production and addition of ascarosides (2.5 µM ascr#3 and ascr#9) to *daf-22(m130)* cultures does not rescue EPEA production.* P<0.05, ** P<0.01, *** P<0.001. (e) Interactions of peroxisomal β-oxidation and endocannabinoid biosynthesis. Mutation of *daf-22* abolishes processing of long-chain ascaroside CoA esters, whose conversion into ethanolamides is associated with reduced endocannabinoid production (13), likely due to depletion of phosphatidylethanolamine pools. *YI performed VLCA profiling and characterized VLCAs. NB and SVR provided assistance with profiling of VLCA and structural characterization. NB conducted ascaroside feeding experiments.*

Conclusion

Mammalian homologs of *daf-22* are thought to be specifically required for chain shortening of branched-chain fatty acids such as phytanic acid (*23, 24*). However, the co-occurrence of straight-chain and methyl-branched derivatives among the *daf-22*

mutant-specific VLCAs suggests that *daf-22* is involved in processing of both branched and straight-chain fatty acids. The chain lengths of the *daf-22* mutant-specific VLCAs indicate that 23- to 27-carbon fatty acids may represent endpoints of *C. elegans* fatty acid biogenesis, in which the last chain-extension step incorporates either malonate or methylmalonate. Notably, our metabolomic analyses provided no evidence for incorporation of methylmalonate at earlier stages in the biosynthesis of these fatty acid derivatives. The chain lengths of the *daf-22*-mutant upregulated VLCAs in *C. elegans* are similar to those of very long-chain fatty acids that accumulate in human disorders involving defects in peroxisomal β-oxidation such as Zellweger syndrome (*23, 24*). However, human fatty acid biosynthesis is not known to selectively incorporate propionate or methylmalonate in the last chain-extension step to form α-methyl-branched variants.

In a biosynthetic model (**Figures 5.1b, 5.3e**), the identified *daf-22* mutant-specific compounds plausibly represent shunt metabolites derived from fatty-acid and β-keto-acid CoA esters, in which the α,β-unsaturation and β-keto functionalities result from upstream action of ACOX-1, MAOC-1, and DHS-28. The *daf-22*-upregulated long-chain methyl ketones may derive from corresponding β-keto fatty acids, which are highly prone to decarboxylation. Although described in an earlier study (*6*), we could not find any evidence for β-keto fatty acids in our metabolite extracts by either NMR spectroscopy or HPLC-MS. The odd-numbered side-chain lengths of the *daf-22*-upregulated ascarosyl-fatty acids are consistent with the structures of the known end products of peroxisomal β-oxidation, the short-chain ascaroside pheromones, most of which include side chains with 3, 5, 7, or 9 carbons (**Figure 5.1a**) (*5*). These odd-

numbered side chains further suggest that ascaroside side-chain biosynthesis starts with a three-carbon (methylmalonate-derived) template or that *C. elegans* elongates odd-numbered fatty acids obtained from food.

In conclusion, mvaDANS-based comparison of *daf-22* and wild-type metabolomes revealed long-chain ascarosyl ethanolamides as an unexpected class of shunt metabolites in *daf-22* mutant worms. The abundance of β-keto derivatives and methyl ketones among the identified long-chain ascarosides supports that *daf-22* acts as a thiolase in ascaroside pheromone biosynthesis, as had been suspected based on homology to mammalian peroxisomal thiolases. Our results will motivate more detailed inspection of similarities of nematode and mammalian fatty-acid metabolism, especially with regard to possible interactions between endocannabinoid signaling, phosphatidylethanolamine utilization, and peroxisomal β-oxidation. In *C. elegans*, reduced NAE levels promote dietary-restriction-induced lifespan extension (*21*), suggesting that defects in peroxisomal β-oxidation may affect lifespan via changes in NAE levels.

Untargeted comparative metabolomics will form an important tool for reinvestigating metazoan biochemistry. mvaDANS extends the scope of 2D NMR-based metabolomic analysis (*25-27*) by introducing automated cross-peak identification and integration. Whereas pattern recognition techniques have been applied previously to 2D NMR spectra, these approaches have either relied on manual peak selection,(*28*) parametric approaches,(*29*) or used spectral unfolding/refolding techniques *(10, 11).* We expect that advances in statistical spectroscopy will continue to accelerate the structural and functional characterization of biogenic small molecules.

REFERENCES

1. Izrayelit, Y., Robinette, S. L., Bose, N., von Reuss, S. H., and Schroeder, F. C. (2013) 2D NMR-based metabolomics uncovers interactions between conserved biochemical pathways in the model organism *Caenorhabditis elegans*, *ACS Chem. Biol. 8*, 314-319.
2. Fielenbach, N., and Antebi, A. (2008) *C. elegans* dauer formation and the molecular basis of plasticity, *Genes Dev. 22*, 2149-2165.
3. Kenyon, C. J. (2010) The genetics of ageing, *Nature 464*, 504-512.
4. Jones, K. T., and Ashrafi, K. (2009) *Caenorhabditis elegans* as an emerging model for studying the basic biology of obesity, *Dis. Mod. Mech. 2*, 224-229.
5. von Reuss, S. H., Bose, N., Srinivasan, J., Yim, J. J., Judkins, J. C., Sternberg, P. W., and Schroeder, F. C. (2012) Comparative metabolomics reveals biogenesis of ascarosides, a modular library of small molecule signals in *C. elegans*, *J. Am. Chem. Soc. 134*, 1817–1824.
6. Butcher, R. A., Ragains, J. R., Li, W., Ruvkun, G., Clardy, J., and Mak, H. Y. (2009) Biosynthesis of the *Caenorhabditis elegans* dauer pheromone, *Proc. Natl Acad. Sci. USA 106*, 1875-1879.
7. Pungaliya, C., Srinivasan, J., Fox, B. W., Malik, R. U., Ludewig, A. H., Sternberg, P. W., and Schroeder, F. C. (2009) A shortcut to identifying small molecule signals that regulate behavior and development in *Caenorhabditis elegans*, *Proc. Natl Acad. Sci. USA 106*, 7708-7713.
8. Butcher, R. A., Fujita, M., Schroeder, F. C., and Clardy, J. (2007) Small-molecule pheromones that control dauer development in *Caenorhabditis elegans*, *Nat. Chem. Biol. 3*, 420-422.
9. Srinivasan, J., Kaplan, F., Ajredini, R., Zachariah, C., Alborn, H. T., Teal, P. E., Malik, R. U., Edison, A. S., Sternberg, P. W., and Schroeder, F. C. (2008) A blend of small molecules regulates both mating and development in *Caenorhabditis elegans*, *Nature 454*, 1115-1118.
10. Srinivasan, J., von Reuss, S. H., Bose, N., Zaslaver, A., Mahanti, P., Ho, M. C., O'Doherty, O. G., Edison, A. S., Sternberg, P. W., and Schroeder, F. C. (2012) A modular library of small molecule signals regulates social behaviors in *Caenorhabditis elegans*, *PLoS Biol. 10*, e1001237.
11. Macosko, E. Z., Pokala, N., Feinberg, E. H., Chalasani, S. H., Butcher, R. A., Clardy, J., and Bargmann, C. I. (2009) A hub-and-spoke circuit drives pheromone attraction and social behaviour in *C. elegans*, *Nature 458*, 1171-1175.
12. Robinette, S. L., Bruschweiler, R., Schroeder, F. C., and Edison, A. S. (2011) NMR in metabolomics and natural products research: two sides of the same coin, *Acc. Chem. Res*. *45*, 288-297.
13. Hedenström, M., Wiklund-Lindstrom, S., Oman, T., Lu, F., Gerber, L., Schatz, P., Sundberg, B., and Ralph, J. (2009) Identification of lignin and polysaccharide modifications in *Populus* wood by chemometric analysis of 2D NMR spectra from dissolved cell walls, *Mol. Plant 2*, 933-942.
14. Hedenström, M., Wiklund, S., Sundberg, B. r., and Edlund, U. (2008) Visualization and interpretation of OPLS models based on 2D NMR data, *Chemometr. Intell. Lab. 92*, 110-117.

15. Robinette, S. L., Ajredini, R., Rasheed, H., Zeinomar, A., Schroeder, F. C., Dossey, A. T., and Edison, A. S. (2011) Hierarchical alignment and full resolution pattern recognition of 2D NMR spectra: application to nematode chemical ecology, *Anal. Chem. 83*, 1649.
16. Robinette, S. L., Zhang, F., Bruschweiler-Li, L., and Bruschweiler, R. (2008) Web server based complex mixture analysis by NMR, *Anal. Chem. 80*, 3606-3611.
17. Zhang, F., Dossey, A. T., Zachariah, C., Edison, A. S., and Bruschweiler, R. (2007) Strategy for automated analysis of dynamic metabolic mixtures by NMR. application to an insect venom, *Anal. Chem. 79*, 7748-7752.
18. Zhang, F., and Bruschweiler, R. (2007) Robust deconvolution of complex mixtures by covariance TOCSY spectroscopy, *Angew. Chem. Int. Ed. 46*, 2639-2642.
19. Zhang, F., Bruschweiler-Li, L., Robinette, S. L., and BruÌˆschweiler, R. (2008) Self-consistent metabolic mixture analysis by heteronuclear NMR. Application to a human cancer cell line, *Anal. Chem. 80*, 7549-7553.
20. Wold, S., Esbensen, K., and Geladi, P. (1987) Principal component analysis, *Chemometr. Intell. Lab. 2*, 37-52.
21. Lucanic, M., Held, J. M., Vantipalli, M. C., Klang, I. M., Graham, J. B., Gibson, B. W., Lithgow, G. J., and Gill, M. S. (2011) N-acylethanolamine signalling mediates the effect of diet on lifespan in *Caenorhabditis elegans*, *Nature 473*, 226-229.
22. Noguez, J. H., Conner, E. S., Zhou, Y., Ciche, T. A., Ragains, J. R., and Butcher, R. A. (2012) A novel ascaroside controls the parasitic life cycle of the entomopathogenic nematode *Heterorhabditis bacteriophora*, *ACS Chem. Biol*.
23. Wanders, R. J. A., and Waterham, H. R. (2006) Biochemistry of mammalian peroxisomes revisited, *Annu. Rev. Biochem. 75*, 295-332.
24. Wanders, R. J. A. (2004) Peroxisomes, lipid metabolism, and peroxisomal disorders, *Mol. Genet. Metab. 83*, 16-27.
25. Wishart, D. S. (2007) Current progress in computational metabolomics, *Brief. Bioinform. 8*, 279-293.
26. Nicholson, J. K., Connelly, J., Lindon, J. C., and Holmes, E. (2002) Metabonomics: a platform for studying drug toxicity and gene function, *Nat. Rev. Drug Discov. 1*, 153-161.
27. Gartland, K. P., Beddell, C. R., Lindon, J. C., and Nicholson, J. K. (1991) Application of pattern recognition methods to the analysis and classification of toxicological data derived from proton nuclear magnetic resonance spectroscopy of urine, *Mol. Pharmacol. 39*, 629-642.
28. Van, Q. N., Issaq, H. J., Jiang, Q., Li, Q., Muschik, G. M., Waybright, T. J., Lou, H., Dean, M., Uitto, J., and Veenstra, T. D. (2008) Comparison of 1D and 2D NMR spectroscopy for metabolic profiling, *J. Proteome Res. 7*, 630-639.
29. Chylla, R. A., Hu, K., Ellinger, J. J., and Markley, J. L. (2011) Deconvolution of two-dimensional NMR spectra by fast maximum likelihood reconstruction: application to quantitative metabolomics, *Anal. Chem. 83*, 4871-4880.

CHAPTER 6

CONCLUSIONS AND OUTLOOK

The discovery of ascarosides as components of the dauer pheromone started a new era in *C. elegans* research that focused on the small molecule components of biology (*1, 2*). Since that time, our understanding of ascaroside signaling and function has increased dramatically (*3*). The identification of N-acylethanolamines as key signaling components of dietary restriction further cemented *C. elegans* at the forefront of chemical biology focused research (*4, 5*).

The work presented here takes another step to a more complete understanding of small molecule signaling in *C. elegans.* We reveal how small molecules regulate a plethora of biological phenomena including lifespan, sex-specific interaction, immunity activation, toxin detoxification, and host-pathogen interactions. We started by profiling small molecules in a targeted manner using LC/MS (chapters 1-3) and transition into an untargeted approach using 2D NMR (chapter 4 and 5), culminating with a new method in untargeted metabolomics using 2D NMR spectroscopy. As such, this work both provides insight into current understanding of *C. elegans* biology and also sets the stage for future discovery in higher organisms utilizing novel analytical tools.

Current and future work

There are a number of findings presented in this thesis that have already motivated new and exciting research efforts. The discovery of sex-specific ascaroside biosynthesis suggests that the sex-determination pathway in *C. elegans* regulates

peroxisomal β–oxidation and ascaroside biosynthesis (*6, 7, 8*). The two sexes in *C. elegans* arise based on the status of the sex-chromosomes. Hermaphrodites are XX, while spontaneous nondisjunction of the sex chromosome in males leads to XO. The number of X chromosomes activates a series of regulatory genes that either promote feminization or masculinization. Molecular biology advances have allowed for cooption of this system for tissue specific control of sex determination (*9*). *daf-22,* the thiolase required for the terminal step of peroxisiomal β–oxidation of ascarosides (*10*), is localized to intestine, hypodermis and body wall in *C. elegans* (*11*). Considering ascarosides are regulated by environmental and dietary status (*12*) the intestine is a likely tissue for ascaroside biosynthesis (*13*). Therefore, we asked whether masculinization or feminization of the intestine affects ascaroside biosynthesis.

We used an LC/MS targeted metabolomic approach to look at ascaroside release on a small scale, profiling the two most abundant ascarosides, ascr#3 and ascr#10 (*14*). Chapter 1 presents data showing that wild type adult hermaphrodites predominantly release ascr#3 followed by ascr#10. While wild type males predominantly release ascr#10 followed by ascr#3 (**Figure 6.1**). Intestine masculinization by overexpression of *fem-3* with an intestine specific promoter had no effect on ascaroside production in masculinized hermaphrodites or masculinized males (**Figure 6.1**).We found that the relative distribution of ascr#3 and ascr#10, presented as a pie graph, matched the profile of the wild type like *him-5* males and hermaphrodites. *Him*-5 males have a higher incidence of males but behave as wild type worms, specifically in their ascaroside signaling (*14*). Strikingly, feminizing the intestine of males, by overexpression of the transmembrane receptor *tra-2* with an intestine specific promoter*,*

reversed the ascaroside profile (**Figure 6.1)**. Feminized males produced similar or more ascr#3 than ascr#10, a profile typically seen in adult hermaphrodites. This was observed in only two biological replicates, however ascaroside profiles are very robust (*14*). Feminized hermaphrodites had a wild type like ascaroside profile. Finally, we looked at males and hermaphrodites of a *mab-3* mutant. *mab-3* is a Doublesex and MAB-3 (DM) domain containing protein involved in many aspects of sex determination downstream of the global regulatory gene *tra-1* (*15*). The mutant *mab-3(e1240)* is therefore also considered feminized in all somatic tissues. Surprisingly, *mab-3* males had a typical male-like ascaroside profile (**Figure 6.1**). This suggests that *tra-2* feminization of male intestine leads to a change in ascaroside profile through a non *tra-1-mab-3* gene axis.

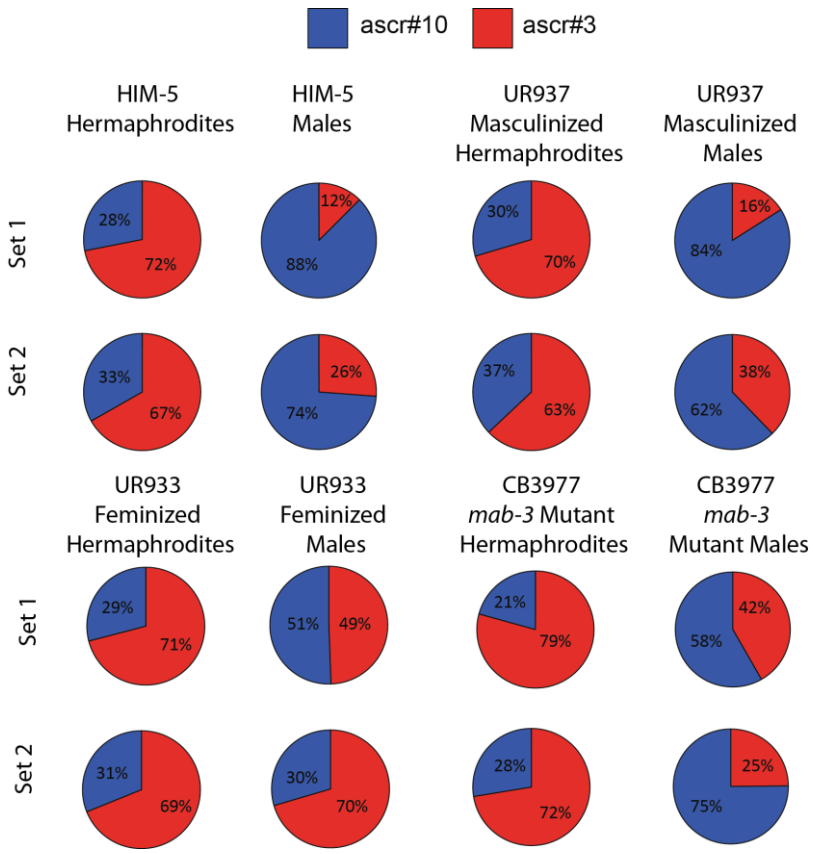

Figure 6.1. Male feminization reverses ascr profile. Pie graph representations of the relative abundance of ascr#10 (*16*) and ascr#3 (red) released by 100 young adult worms (either pure hermaphrodites or males) overnight in 96 well plates. The UR937 strain overexpresses the feminizing gene *fem-3* in an intestine specific promoter. The UR933 strain overexpresses the masculinizing gene *tra-2* in an intestine specific promoter. The CB3977 strain has a mutation in *mab-3,* a DM containing protein necessary for male development*, and* are also considered feminized. All three strains have a *him-5(e1490)* mutation in the background. Profiling conducted in replicate. *LC/MS profiling experiments were conducted by YI with support from SLC.*

These findings motivate further exploration of sex-specific ascaroside biosynthesis. The development of a liquid based ascaroside profiling method (*14*), allows fpr a higher throughput profiling of mutant strains. Specifically, it will be important to profile a variety of MAB-3 family proteins to identify the DM containing proteins that may signal downstream of *tra-1* in male ascaroside biosynthesis. The lack of reversal in masculinized hermaphrodites suggests that other tissues with *daf-22* expression such as the hypodermis and body wall may be important (*11*). This highlights that *C. elegans* is an excellent model for sex-specific biosynthesis of pheromones. An ongoing collaboration will explore the influence on ascaroside biosynthesis of other feminized and masculinized tissues.

We recently helped show that the presence of male *C. elegans* decreases the lifespan of hermaphrodites by more than 20% (*17*). This finding was termed male induced demise (MID). While aspects of lifespan shortening between sexes had been explored (*18, 19*), this work showed that MID required a series of conserved genes to for hermaphrodite life span decrease, including an insulin peptide (*ins-11*), a histone H3 demethylase *utx-1*, and a gene predicted to be a conserved small guanosine triphosphatase (GTPase) of the Rab family. Notably, male *C. elegans* required functional ascaroside biosynthesis to induce full MID. Plates conditioned with wild type

males induced MID in hermaphrodites subsequently grown on those plates. The plates conditioned by *daf-22* mutant males, unable to biosynthesize short chain ascarosides, did not induce full MID (*17*).

In chapter 2 we found that ascr#2 and ascr#3 extend lifespan, showing that ascarosides play an important role in regulation of lifespan. In chapter 1, we highlighted that males predominantly release ascr#10 and so we recently asked whether ascr#10 is responsible for the pheromone portion of the MID phenotype.

We found that in three replicates, two run in parallel and pooled (**Figure 6.2a**), and one run separately (**Figure 6.2b**), hermaphrodites grown on 400 nM of ascr#10, as young adults had a decreased lifespan of 11% and 15%, respectively, both with high significance ($P<0.0001$). In both cases, ascr#3 extended lifespan (**Figure 6.2**) as seen previously (chapter 2). Worms exposed to a mixture of 400 nM of both ascr#3 and ascr#10 showed an intermediary response (increase of +5%). As described in previous chapters, ascaroside#3 and #10 only differ by one double bond, ascr#10 is the dihydro version of ascr#3 (**Figure 6.2c**). It is striking that one double bond can come between life and death (**Figure 6.2**).

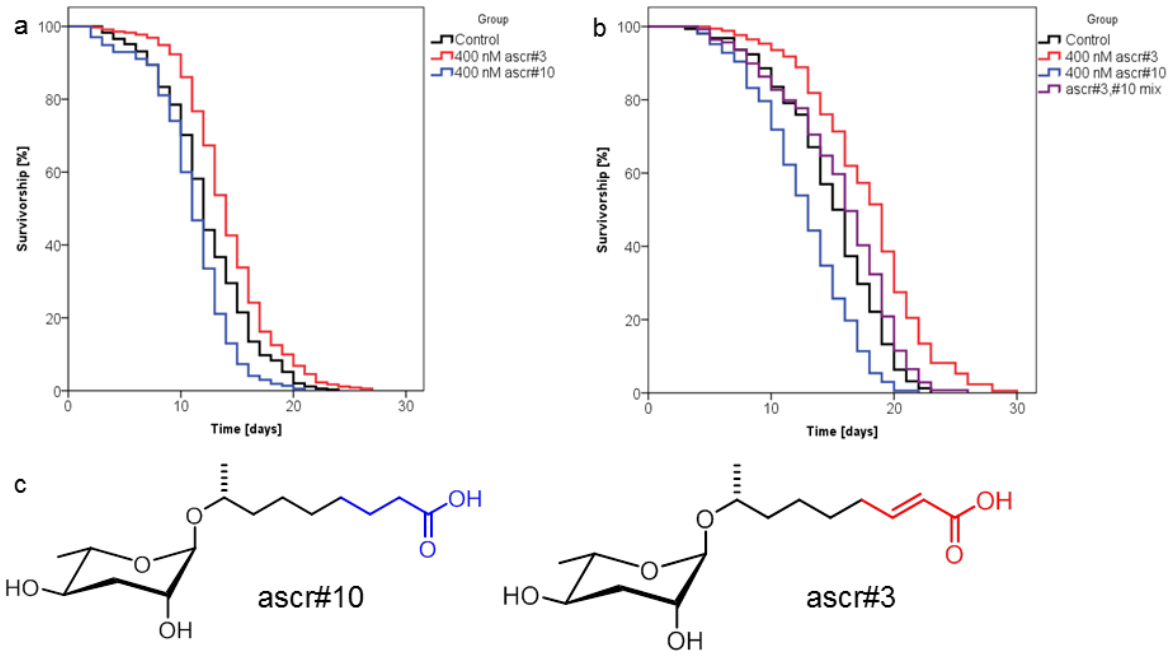

Figure 6.2. Ascarosides both increase and decrease adult lifespan in wildtype (N2) *C. elegans.* Study in (a) conducted with wildtype strain from Schroeder Laboratory (Cornell University). Study in (b) conducted with wildtype strain from Brunet Laboratory (Stanford University) (a) Survivorship of worms at 20°C (pooled from two studies run in parallel) exposed to 400 nM ascr#3, number of worms (n) = 352, m = 14.2 d, $p < 0.0001$; 400 nM ascr#10, n = 370, average lifespan (m) = 11.1 d, $p<0.0001$; and mock treated controls n = 349, m = 12.4 d. (b) Survivorship of worms at 20°C exposed to 400 nM ascr#3, n = 186, m = 17.9 d, $p < 0.0001$; 400 nM ascr#10, n = 175, m = 12.7, $p < 0.0001$; 400 nM ascr#3 and 400 nM ascr#10, n = 139, m = 15.7 d; and mock treated controls n = 167, m = 14.9 d. (c) Chemical structure of ascr#10 (*16*) and ascr#3 (red). Note that these molecules differ by one double bond. *YI and HAL performed aging studies. YI and HAL analyzed data.*

Additional experiments were conducted to explore the mechanism of ascr#10 lifespan decrease. We first confirmed that lifespan decrease was due to sensing of ascarosides, as *che-13(e1805)* mutants deficient in pheromones sensing (*20*) did not respond to ascr#10 or ascr#3 (**Figure 6.3a**). Further, we tested the null *sir-2.1(ok434)* mutant motivated by our findings that AMILS required SIR-2.1. We found that lifespan decrease induced by exposure to ascr#10 also requires functional SIR-2.1 (**Figure 6.3b**). ascr#3 did not extend lifespan in this mutant as expected. Ascr#10 lifespan

decrease also required the insulin peptide *ins-11* (**Figure 6.3c**). ascr#3 also did not affect this mutant suggesting that *ins-11* may have a previously unknown role in AMILS. Finally, we tested the insulin/IGF-1 receptor mutant *daf-2(1370)* and found that ascr#10 does decrease lifespan in this mutant (**Figure 6.3d**, study in progress). As previously reported, ascr#3 also extends lifespan in this strain. MID also occurs with the long lived mutant strain (*17*), supporting a model where MID is mediated by ascr#10. Notably, *ins-11* mutant hermaphrodites were only partially resistant to MID, and similarly, male conditioned plates only recapitulated partial lifespan decrease of MID (~10-15% decrease). Our findings suggest that ascr#10 requires *ins-11* and that it recapitulates the partial decrease of MID further supports ascr#10's role in MID and integrates the role of insulin peptides in signaling downstream of ascaroside signaling but independent of the insulin/IGF-1 receptor *daf-2.*

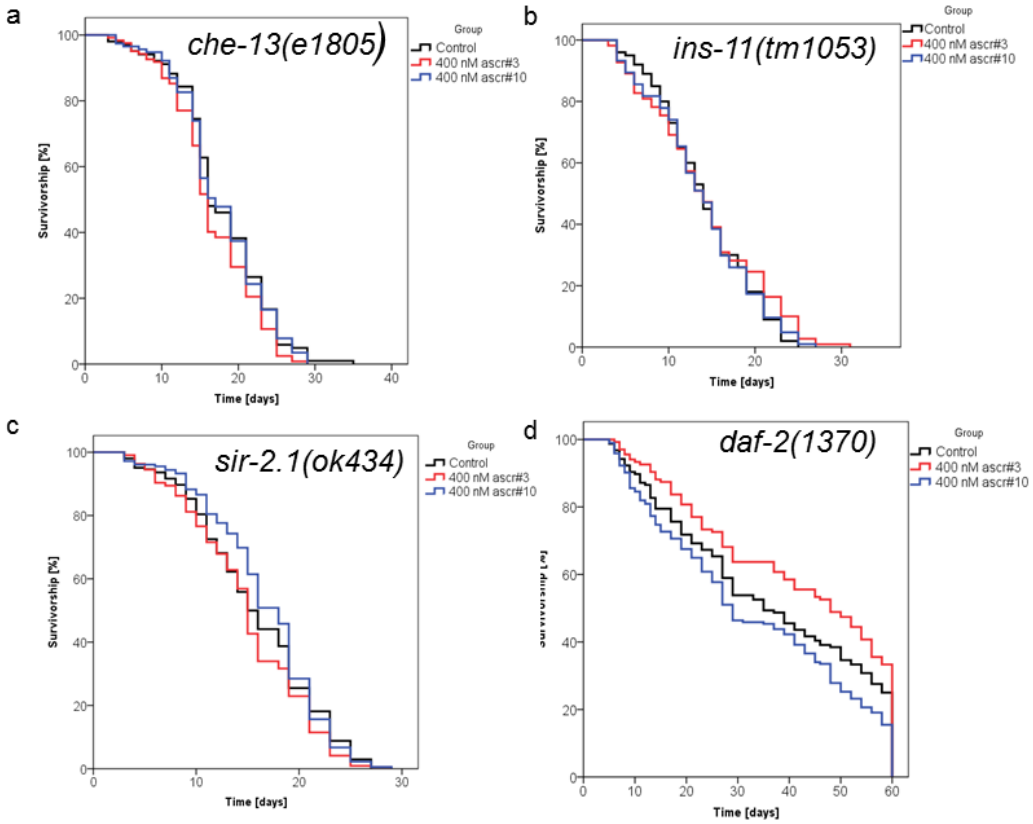

Figure 6.3. Ascaroside lifespan modulation requires pheromone sensing (*che-13),* an insulin peptide (*ins-11*) and a sirtuin (*sir-2.1*) but is independent on the insulin/IGF-1 receptor (*daf-2).* (a) Survivorship of *che-13(e1805)* worms treated with 400 nM, number of worms (n) = 122, average lifespan (m) = 16.6 d, p = 0.057; 400 nM ascr#10, n = 115, m = 17.8 d, p = 0.773; and mock treated control n = 102, m = 17.8 d. (b) Survivorship of *ins-11(tm1053)* worms treated with 400 nM, n = 110, m = 14.2 d, p = 0.227; 400 nM ascr#10, n = 104, m = 13.9 d, p = 0.880; and mock treated control n = 100, m = 14.2 d. (c) Survivorship of *sir-2.1(ok434)* worms treated with 400 nM, n = 218, m = 15.0 d, p = 0.093; 400 nM ascr#10, n = 179, m = 16.7 d, p = 0.389; and mock treated control n = 204, m = 15.8 d. (d) Study ongoing, all worms assumed dead, survivorship of *daf-2(e1370)* worms treated with 400 nM, n = 135, m = 41.6 d, p = 0.043; 400 nM ascr#10, n = 194, m = 33.1 d, p = 0.035; and mock treated control n = 156, m = 36.5 d.*YI and HAL performed aging studies. YI and HAL analyzed data.*

Interestingly, *sir-2.1* expression levels did not change significantly in hermaphrodites in response to MID (*17*). The fact that in this case SIR-2.1 mediates both lifespan increase and decrease suggests that SIR-2.1 levels may dramatically change, however, sirtuin function does. Further exploration using this system may shed

light on the controversial field of sirtuin longevity (*21-25*) and may support recent findings that more subtle control, or previously unexplored functions, of sirtuins are necessary to achieve positive lifespan modulation (*26, 27*).

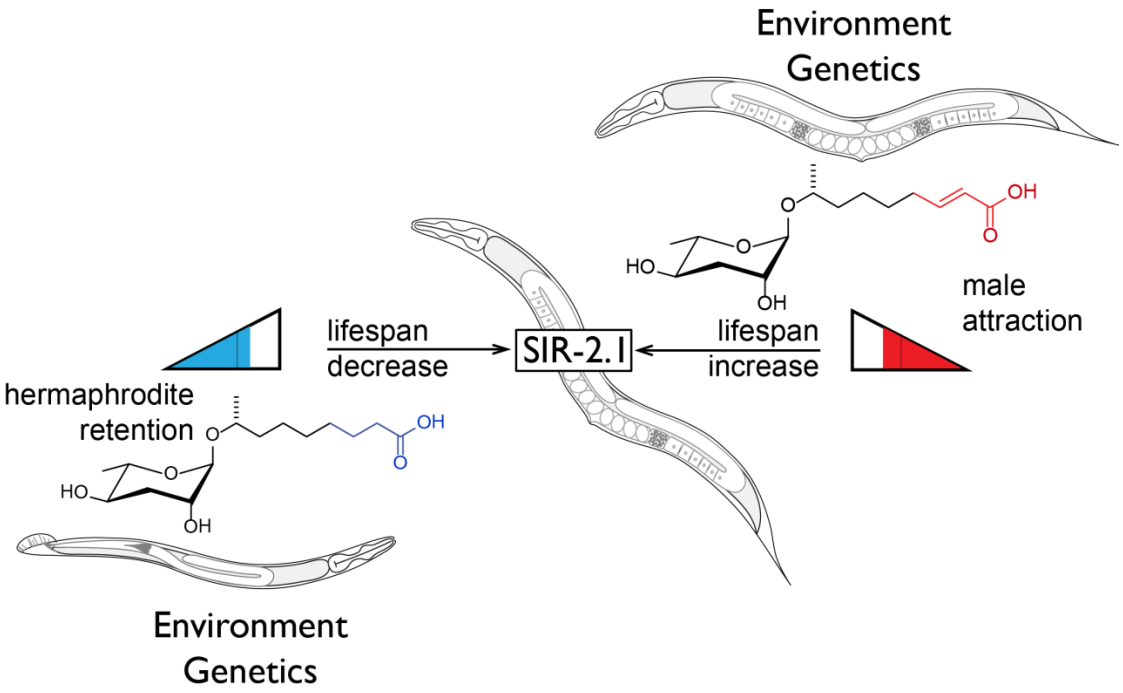

Figure 6.4. Model for lifespan control by ascr#3 and ascr#10. Endogenously released pheromones regulate social interactions such as male attraction and hermaphrodite retention at low concentrations. However at higher concentrations these signals lead to either a lifespan increase or lifespan decrease in adult hermaphrodite worms sensing the signal. The balance between life and death is regulated by the conserved NAD+ dependent deacetylase SIR-2.1. *Model designed by YI.*

Figure 6.4 presents a model for our current understanding of ascr#3/ascr#10 signaling. Notably, most of the ascr#10 related findings summarized in this model were first presented in the enclosed chapters. Male induction in *C. elegans* progeny can be achieved by increasing temperature or alcohol content. The presence of a large number of males is suggestive of an unfavorable environment. It is possible that accumulation of ascr#10 is indicative of low food availability and signals a need to conserve resources

and remove older worms from the population. Alternatively, accumulation of hermaphrodites suggests an abundance of food and temperatures conductive to survival therefore longer survival does not pose a burden on environmental cost.

Despite the intriguing implications for nematode survival, the true impact of this work stems from the conserved nature of the signaling pathways underlying this lifespan modulation. To our knowledge, small molecule mediators of sirtuin dependent lifespan decrease have not been reported in the literature. Further understanding how sensing pheromones regulates sirtuin dependent pathways is a promising avenue for pharmacological intervention in lifespan. Finally, it is striking that the insulin peptide *ins-* is required while the insulin/IGF-1 receptor *daf-2* is not. *Ins-11* is one of 38 insulin-like peptides found in *C. elegans* and is expressed in inner labial neurons (*28*). The ascr#2 specific receptor the GPCR *daf-37* has been shown to be expressed in a set of chemosensory neurons as well as the IL-2 interneurons (*29*). This suggests a possible signaling mechanism from ascaroside sensing by chemosensory neurons, or even interneurons, and subsequent *ins-11* peptide release. Humans have two putative receptors for insulin and IGF-1 (*30*), yet many of the 7 insulin peptides still lack a cognitive receptor (*28*). *daf-2* is the only *C. elegans* gene predicted to be an insulin receptor and it is very probably that other receptors will be identified. These results suggest that *ins-11* signals through a non *daf-2* receptor to mediate lifespan and does so potentially in a sirtuin dependent manner. Future work will focus on understanding how ascr#10 and ascr#3 utilize *ins-11* to regulate lifespan and how SIR-2.1 regulates both lifespan increase and decrease.

Thus far we have focused on upstream signals that regulate many aspects of *C. elegans* development and social interactions. Ascarosides are sensed by chemosensory neurons and propagate biological signals through a variety of conserved signaling pathways such as TGF-β, insulin/IGF and others. We have shown in chapter 1 and above that ascaroside profiles are different in males and hermaphrodites. Similarly, the response to these signals is sex-specific (*31*). In many aspects of ascaroside signaling, the nuclear hormone receptor (NHR) *daf-12* is a downstream signaling component that regulates genes involved in dauer, development, lifespan and metabolism (*3, 32*). Dafachronic acids have been shown to be the small molecule ligands of DAF-12, and by binding the NHR they facilitate dissociation of the co-repressor DIN-1 and subsequent binding of a yet unknown co-activator (*33, 34*). Dafachronic acids are characterized by a steroid core, a carboxylic acid functionalized side group and double bonds named according to their position on the steroid core (**Figure 6.5a**). Just like ascarosides were originally identified as dauer pheromones, the dafachronic acids were also first shown to be required for bypassing dauer (*32*). Since then, dafachronic acids have also been shown to regulate various aspects of adult physiology, including lifespan and mate searching, at times in a sex specific manner (*35, 36*). It is thus important to look for sex-specific dafachronic acid biosynthesis.

daf-9 is a cytochrome P450 involved in oxidation of the dafachronic acid side chain. Worms deficient in this enzyme are dauer constitutive and can only bypass dauer with addition of dafachronic acids (*33*). A sensitive *in vivo* assay for dafachronic acid is the application of metabolome fractions obtained from *C. elegans* grown in liquid cultures to *daf-9(dh6)* mutant worms. If the worms are rescued and continue on to

reproductive development the fraction is considered a hit for dafachronic acid(s) (**Figure 6.5b**). We have also embarked on enriching him-5 cultures from 30% males to greater than 90% males using a filtering scheme (*37, 38*). As an initial profiling attempt, liquid cultures of 76,000 males (>95% purity) were fractionated using an established normal phase chromatography protocol (*33*). A hermaphrodite rich culture was also grown in parallel as control. Fractions were applied to *daf-9(dh6)* mutant worms. **Figure 6.5** highlights that fraction 26 in the male metabolome rescued *daf-9* mutant worms. A synthetic dafachronic acid was used as a positive control. Hermaphrodite metabolome fractions from liquid cultures on the same population scale (72,000 worms) also showed rescue in fraction 27. Using this fractionation protocol, dafa#1 and dafa#2 are expected to elude in this polarity region. Subsequent GC/MS analysis suggested that both males and hermaphrodite fractions in this region have similar amounts of dafa#2 (data not shown, inconclusive due to excessive background). Hermaphrodite fraction 31 also showed rescue. dafa#3 would be expected to elute in this polarity region. To our knowledge, this represents the first identification of dafachronic acid based activity in male *C. elegans.* Future efforts will focus on growing larger liquid cultures enriched for males and more thorough characterization of the male metabolome. Characterization of the sex-specific nature of dafachronic acid will advance understanding of sex-specific NHR signaling in higher organisms.

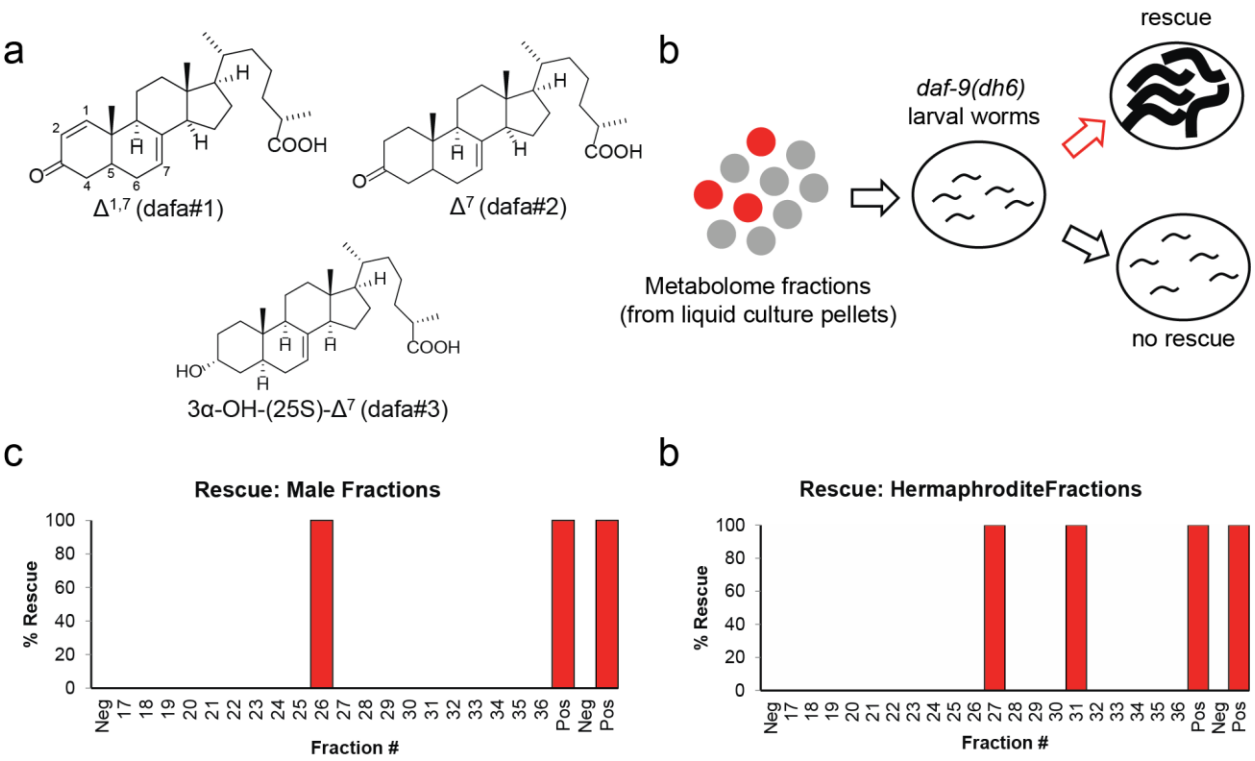

Figure 6.5. Male *C. elegans* produce dafachronic acids. (a) Chemical structure of three dafachronic acids: dafa#1, dafa#2, dafa#3. Note that the steroid core double bond is included in the name. (b) Schematic for daf-9 in vivo dauer rescue assay. Daf-9(dh6) L1 larval worms are given food and metabolome fractions, and growth into adulthood is a marker for rescue. (c) *daf-9(dh6)* dauer rescue assay. Male enriched metabolome fraction 26 rescues. Pos is 20 uM of synthetic Δ4 dafachronic acid. (d) *daf-9(dh6)* dauer rescue assay. Hermaphrodite metabolome fractions 27 and 31 show rescue. Pos is 20 uM of synthetic Δ4 dafachronic acid. *YI prepared metabolome fractions and ran daf-9 dauer assays with assistance from SLC and NB. JJ provided synthetic dafachronic acid.*

Outlook

The field of small molecule signaling in *C. elegans* is at its infant stage. The chemical characterization of ascarosides and dafachronic acids has led to great insight into *C. elegans* and metazoan biology, but this is just the tip of the iceburg. Chapter 5 presents a novel metabolomics method that was used to re-investigate a previously studied biosynthetic mutant, *daf-22*. Identification of novel mutant dependent metabolites revealed an association between two conserved signaling pathways.

Untargeted metabolomics using 2D NMR and LC/MS will continue to reveal unexpected findings. While it took over 20 years to identify the components of the dauer pheromone, analytical chemistry is now outpacing the ability to connect structure to function. Future efforts should focus on incorporating tools for prioritization for metabolomic discoveries. To that end, coupling of different analytical methodologies using statistics will allow for a more integrative approach that will highlight key small molecule signals.

Until then, discoveries presented in this work will motivate future studies to expand functional annotation of currently known small molecule signals. The fact that a double bond between ascr#3 and ascr#10 regulates lifespan in a sirtuin dependent manner is just one of many amazing discoveries to come from small molecule based research in *C. elegans.*

REFERENCES

1. Butcher, R. A., Fujita, M., Schroeder, F. C., and Clardy, J. (2007) Small-molecule pheromones that control dauer development in *Caenorhabditis elegans*, *Nat. Chem. Biol. 3*, 420-422.
2. Jeong, P. Y., Jung, M., Yim, Y. H., Kim, H., Park, M., Hong, E., Lee, W., Kim, Y. H., Kim, K., and Paik, Y. K. (2005) Chemical structure and biological activity of the *Caenorhabditis elegans* dauer-inducing pheromone, *Nature 433*, 541-545.
3. Ludewig, A. H., and Schroeder, F. C. (2013) Ascaroside signaling in *C. elegans*, *WormBook*, 1-22.
4. Hulme, S. E., and Whitesides, G. M. (2011) Chemistry and the worm: *Caenorhabditis elegans* as a platform for integrating chemical and biological research, *Angew. Chem. Int. Edit. 50*, 4774-4807.
5. Lucanic, M., Held, J. M., Vantipalli, M. C., Klang, I. M., Graham, J. B., Gibson, B. W., Lithgow, G. J., and Gill, M. S. (2011) N-acylethanolamine signalling mediates the effect of diet on lifespan in *Caenorhabditis elegans*, *Nature 473*, 226-229.
6. Brenner, S. (1974) The genetics of *Caenorhabditis elegans*, *Genetics 77*, 71-94.
7. Villeneuve, A. M., and Meyer, B. J. (1990) The regulatory hierarchy controlling sex determination and dosage compensation in *Caenorhabditis elegans*, *Adv. Genet. 27*, 117-188.
8. Zarkower, D. (2006) Somatic sex determination, *WormBook*, 1-12.
9. Portman, D. S. (2007) Genetic control of sex differences in *C. elegans* neurobiology and behavior, *Adv. Genet. 59*, 1-37.
10. Izrayelit, Y., Robinette, S. L., Bose, N., von Reuss, S. H., and Schroeder, F. C. (2013) 2D NMR-based metabolomics uncovers interactions between conserved biochemical pathways in the model organism *Caenorhabditis elegans, ACS Chem. Biol. 8*, 314-319.
11. Butcher, R. A., Ragains, J. R., Li, W., Ruvkun, G., Clardy, J., and Mak, H. Y. (2009) Biosynthesis of the *Caenorhabditis elegans* dauer pheromone, *Proc. Natl Acad. Sci. USA 106*, 1875-1879.
12. Kaplan, F., Srinivasan, J., Mahanti, P., Ajredini, R., Durak, O., Nimalendran, R., Sternberg, P. W., Teal, P. E., Schroeder, F. C., Edison, A. S., and Alborn, H. T. (2011) Ascaroside expression in *Caenorhabditis elegans* is strongly dependent on diet and developmental stage, *Plos One 6*, e17804.
13. Edison, A. S. (2009) *Caenorhabditis elegans* pheromones regulate multiple complex behaviors, *Curr. Opin. Neurobiol. 19*, 378-388.
14. Izrayelit, Y., Srinivasan, J., Campbell, S. L., Jo, Y., von Reuss, S. H., Genoff, M. C., Sternberg, P. W., and Schroeder, F. C. (2012) Targeted metabolomics reveals a male pheromone and sex-specific ascaroside biosynthesis in *Caenorhabditis elegans*, *ACS Chem. Biol. 7,* 1321-1325.
15. Yi, W., Ross, J. M., and Zarkower, D. (2000) *mab-3* is a direct *tra-1* target gene regulating diverse aspects of *C. elegans* male sexual development and behavior, *Development 127*, 4469-4480.
16. Hoss, S., Ahlf, W., Bergtold, M., Bluebaum-Gronau, E., Brinke, M., Donnevert, G., Menzel, R., Mohlenkamp, C., Ratte, H. T., Traunspurger, W., von Danwitz, B., and Pluta, H. J. (2012) Interlaboratory comparison of a standardized toxicity

test using the nematode *Caenorhabditis elegans* (ISO 10872), *Environ. Toxicol. Chem. 31*, 1525-1535.
17. Maures, T. J., Booth, L. N., Benayoun, B. A., Izrayelit, Y., Schroeder, F. C., and Brunet, A. (2014) Males shorten the life span of *C. elegans* hermaphrodites via secreted compounds, *Science 343*, 541-544.
18. Gems, D., and Riddle, D. L. (2000) Genetic, behavioral and environmental determinants of male longevity in *Caenorhabditis elegans*, *Genetics 154*, 1597-1610.
19. Gems, D., and Riddle, D. L. (2000) Defining wild-type life span in *Caenorhabditis elegans*, *J. Gerontol. A Biol. Sci. Med. Sci. 55*, B215-219.
20. Perkins, L. A., Hedgecock, E. M., Thomson, J. N., and Culotti, J. G. (1986) Mutant sensory cilia in the nematode *Caenorhabditis elegans*, *Dev. Biol. 117*, 456-487.
21. Baur, J. A., Ungvari, Z., Minor, R. K., Le Couteur, D. G., and de Cabo, R. (2012) Are sirtuins viable targets for improving healthspan and lifespan?, *Nat. Rev. Drug. Discov. 11*, 443-461.
22. Burnett, C., Valentini, S., Cabreiro, F., Goss, M., Somogyvari, M., Piper, M. D., Hoddinott, M., Sutphin, G. L., Leko, V., McElwee, J. J., Vazquez-Manrique, R. P., Orfila, A. M., Ackerman, D., Au, C., Vinti, G., Riesen, M., Howard, K., Neri, C., Bedalov, A., Kaeberlein, M., Soti, C., Partridge, L., and Gems, D. (2011) Absence of effects of Sir2 overexpression on lifespan in *C. elegans* and *Drosophila*, *Nature 477*, 482-485.
23. Guarente, L. (2013) Calorie restriction and sirtuins revisited, *Genes Dev. 27*, 2072-2085.
24. Mair, W., and Dillin, A. (2008) Aging and survival: The genetics of life span extension by dietary restriction, *Annu. Rev. Biochem. 77*, 727-754.
25. Wood, J. G., Rogina, B., Lavu, S., Howitz, K., Helfand, S. L., Tatar, M., and Sinclair, D. (2004) Sirtuin activators mimic caloric restriction and delay ageing in metazoans, *Nature 430*, 686-689.
26. Schmeisser, K., Mansfeld, J., Kuhlow, D., Weimer, S., Priebe, S., Heiland, I., Birringer, M., Groth, M., Segref, A., Kanfi, Y., Price, N. L., Schmeisser, S., Schuster, S., Pfeiffer, A. F. H., Guthke, R., Platzer, M., Hoppe, T., Cohen, H. Y., Zarse, K., Sinclair, D. A., and Ristow, M. (2013) Role of sirtuins in lifespan regulation is linked to methylation of nicotinamide, *Nat. Chem. Biol. 9*, 693-+.
27. Whitaker, R., Faulkner, S., Miyokawa, R., Burhenn, L., Henriksen, M., Wood, J. G., and Helfand, S. L. (2013) Increased expression of *Drosophila* Sir2 extends life span in a dose-dependent manner, *Aging 5*, 682-691.
28. Pierce, S. B., Costa, M., Wisotzkey, R., Devadhar, S., Homburger, S. A., Buchman, A. R., Ferguson, K. C., Heller, J., Platt, D. M., Pasquinelli, A. A., Liu, L. X., Doberstein, S. K., and Ruvkun, G. (2001) Regulation of DAF-2 receptor signaling by human insulin and ins-1, a member of the unusually large and diverse *C. elegans* insulin gene family, *Genes Dev. 15*, 672-686.
29. Park, D., O'Doherty, I., Somvanshi, R. K., Bethke, A., Schroeder, F. C., Kumar, U., and Riddle, D. L. (2012) Interaction of structure-specific and promiscuous G-protein-coupled receptors mediates small-molecule signaling in *Caenorhabditis elegans*, *Proc. Natl Acad. Sci. USA 109*, 9917-9922.

30. Kjeldsen, T., Andersen, A. S., Wiberg, F. C., Rasmussen, J. S., Schaffer, L., Balschmidt, P., Moller, K. B., and Moller, N. P. (1991) The ligand specificities of the insulin receptor and the insulin-like growth factor I receptor reside in different regions of a common binding site, *Proc. Natl Acad. Sci. USA 88*, 4404-4408.
31. Srinivasan, J., Kaplan, F., Ajredini, R., Zachariah, C., Alborn, H. T., Teal, P. E. A., Malik, R. U., Edison, A. S., Sternberg, P. W., and Schroeder, F. C. (2008) A blend of small molecules regulates both mating and development in *Caenorhabditis elegans*, *Nature 454*, 1115-U1146.
32. Fielenbach, N., and Antebi, A. (2008) *C. elegans* dauer formation and the molecular basis of plasticity, *Genes Dev. 22*, 2149-2165.
33. Mahanti, P., Bose, N., Bethke, A., Judkins, J. C., Wollam, J., Dumas, K. J., Zimmerman, A. M., Campbell, S. L., Hu, P. J., Antebi, A., and Schroeder, F. C. (2014) Comparative metabolomics reveals endogenous ligands of DAF-12, a nuclear hormone receptor, regulating *C. elegans* development and lifespan, *Cell Met. 19*, 73-83.
34. Motola, D. L., Cummins, C. L., Rottiers, V., Sharma, K. K., Li, T. T., Li, Y., Suino-Powell, K., Xu, H. E., Auchus, R. J., Antebi, A., and Mangelsdorf, D. J. (2006) Identification of ligands for DAF-12 that govern Dauer formation and reproduction in *C. elegans*, *Cell 124*, 1209-1223.
35. Kleemann, G., Jia, L., and Emmons, S. W. (2008) Regulation of *Caenorhabditis elegans* male mate searching behavior by the nuclear receptor DAF-12, *Genetics 180*, 2111-2122.
36. Shi, C., and Murphy, C. T. (2014) Mating induces shrinking and death in *Caenorhabditis* mothers, *Science 343*, 536-540.
37. Meyer, B. J., and Casson, L. P. (1986) *Caenorhabditis elegans* compensates for the difference in X-chromosome dosage between the sexes by regulating transcript levels, *Cell 47*, 871-881.
38. Reinke, V., Gil, I. S., Ward, S., and Kazmer, K. (2004) Genome-wide germline-enriched and sex-biased expression profiles in *Caenorhabditis elegans*, *Development 131*, 311-323.

Appendix A

TARGETED METABOLOMICS REVEALS A MALE PHEROMONE AND SEX-SPECIFIC ASCAROSIDE BIOSYNTHESIS IN CAENORHABDITIS ELEGANS

Preparation of metabolite extracts. Large liquid culture exo-metabolome samples of wild-type and *him-5* mutant worms were prepared as described previously.(*1*) Briefly, wild-type or *him-5* mutant worms were grown for two generations on 6 cm NGM plates seeded with *E. coli* OP50 bacteria. Worms from three NGM plates were washed into 100 mL of S-media into a 500 mL Erlenmeyer flask and grown at 22 °C and 220 pm. Concentrated bacteria from 1 L cultures, grown overnight, were added on day 1 and day 3. On day 5, the liquid culture was split into two 500-mL Erlenmeyer flasks and S-media was added to maintain a volume of 100 ml per flask. Additional concentrated bacteria derived from 1-L OP50 culture was added as food upon splitting. The cultures were harvested on day 7 by centrifugation at 4750 rpm. The supernatant was lyophilized and the residue extracted with 95% ethanol (300 mL) at room temperature for 12 h. The resulting suspension was filtered and evaporated *in vacuo* at room temperature.

For preparation of small-scale exo-metabolome samples, wild-type (N2), *him-5*, and *daf-22* worms were grown for at least two generations on NGM plates seeded with OP50. Male production in wild-type (N2) and *daf-22* worms was induced by placing L4 hermaphrodite worms at 30 °C with ethanol for 6 h (WormAtlas, http://www.wormatlas.org/). Wild type and *daf-22* mutant worms were synchronized by timed egg lay from mated parents. *him-5* worms were synchronized by timed egg lay.

For exo-metabolome collection, 100 or 200 L4 male or hermaphrodite worms were picked with an aluminum wire pick and placed into 250 µL of water or S-media in a 96 well plate (BD Biosciences) and incubated for 17 hours at 22 °C and 220 pm. The solution was filtered over cotton to remove worms and evaporated *in vacuo* at room temperature. The extract was taken up in 100 µL methanol for subsequent HPLC-MS analysis. For mixed-gender experiments a mixture of 50 male and 50 hermaphrodite L4 worms (all wild-type) was incubated in 250 µL of water in a 96 well plate for 17 h at 22 °C and 220 pm. Samples were extracted and prepared for analysis as described above.

For density experiments, synchronized wild-type (N2) L4 lavae were used. 100 males, 100 hermaphrodites, 200 males, 200 hermaphrodites, or 100 males and 100 hermaphrodites (all L4 stage) were placed into 250 µL of water in a 96 well plate and incubated for 17 h at 22 °C and 220 pm. Samples were extracted and prepared for analysis as described above.

Small-scale worm pellet extracts (worm body extracts) were prepared similarly to worm exo-metabolome samples except for the following modifications. 200 synchronized L4 male or hermaphrodite worms were picked onto a seeded NGM plate. M9 buffer was used to wash the worms into a 10 mL falcon tube, and the worms were washed twice with M9 buffer. A suspension of the worms in a small amount of M9 buffer (~50 µL) was lyophilized and the residue was extracted with 95% ethanol (2 ml). After filtration, the extract was evaporated to dryness and re-dissolved in 100 µL of methanol for subsequent HPLC-MS analysis. For all worm exo-metabolome analyses at least 2 independent replicates were performed. Figure 2a summarizes data from 11 biological replicates.

Mass spectrometric analysis. HPLC-MS analysis was performed using an Agilent 1100 Series HPLC system equipped with an Agilent Eclipse XDB-C18 column (9.4 x 250 mm, 5 µm particle diameter) connected to a Quattro II spectrometer (Micromass/Waters) using a 10:1 split. Samples of 10-30 µL of metabolite extract dissolved in methanol was injected and run over a water (0.1% acetic acid) – acetonitrile gradient with a flow rate of 3.6 mL/min. The acetonitrile content was held at 5% for the first 5 minutes then increased to 100% over a period of 40 minutes. Samples were analyzed by HPLC-ESI-MS in negative and positive ion modes using a capillary voltage of 3.5 kV and a cone voltage of -40 V and +20 V, respectively. Single Ion Monitoring (SIM) in negative-ion ionization mode was used to detected the molecular ions of ascr#1, ascr#3, and ascr#10 at *m/z* 247.2, 301.2 and 303.2, respectively, for their corresponding $(M-H)^-$. Identification of ascarosides were confirmed by comparison with published retention times (*1*) and injection of authentic synthetic standards.

Quantification of ascarosides. Relative ascaroside content was quantified by integration of LC-MS signals from corresponding ion traces. Absolute quantification of ascarosides was achieved by injection of solutions of known concentration of synthetic ascr#1, ascr#3, and ascr#10. Ascaroside release was calculated in attomoles of ascarosides per hour per worm, and ascaroside content in worm body extracts was calculated in attomoles of ascarosides per worm.

Spot retention assays. Spot retention assays were performed as described previously.(*2, 3*) Briefly, for both *C. elegans* hermaphrodites and males, we harvested 50-60 L4-stage worms daily and stored them segregated by sex at 20 °C overnight to be used as young adults the following day. Aliquot of ascr#10 assay solutions, dissolved

in 10% ethanol, were stored at -20 ^{o}C in 20 µL tubes. 10% ethanol in water was used as control.

Quadrant chemotaxis assays. Chemotaxis to ascr#10 was assessed on 10 cm four-quadrant Petri plates. Each quadrant was separated from adjacent ones by plastic spacers (Figure 3b). Pairs of opposite quadrants were filled with nematode growth medium (*4*) agar containing ascr#10 at different concentrations. Animals were washed gently in a S-basal buffer and placed in the center of a four-quadrant plate with ascarosides in alternating quadrants, and scored after 15 min and 30 min. A chemotaxis index was calculated as (the number of animals on ascaroside quadrants minus the number of animals on buffer quadrants)/(total number of animals).

Aggregation assays. We measured aggregation behavior of worms using a previously described assay.(*5*) Aggregation assays were conducted on standard NGM plates. Assay plates containing ascr#10 were made by adding the ascr#10 stock solution to the NGM media before they were poured onto the plates. These plates were dried at room temperature for 2-3 days. Control plates were treated similarly except that instead of ascr#10 solutions, vehicle (10% ethanol in water) was added to the plates. Final ethanol concentrations of the plates were below 0.1% for all conditions. After drying, both control plates and plates containing ascr#10 were seeded with 150 µl of an overnight culture of *E. coli* OP50 using a micropipette and allowed to dry for 2 days at room temperature. For aggregation assays, we placed 20 worms onto the lawn and left them at 20 ^{o}C for 3 hours. Aggregation behavior was quantified as the number of animals that were in touch with 2 or more animals at >50% of their body length.

Statistical analysis. Figure 1a: we used unpaired student's *t*-tests with Welch's correction for comparing the relative abundance of ascr#1, 3, 10, and icas#1, 3, 10. * P<0.05. Figure 2a: We used unpaired students *t*-tests with Welch's correction for comparing the relative abundance of ascr#3 and ascr#10 in the hermaphrodite and male exo-metabolome ***P<0.0001 Figure 3a: We used unpaired students *t*-tests with Welch's correction for comparing attraction of hermaphrodites and males on ascarosides *P<0.01, **P< 0.001, ***P<0.0001. Figure 3c: For comparing the quadrant chemotaxis indices of the various strains, we used one-factor ANOVA followed by Dunnett's post-test, **P< 0.01. Figure S3: For comparing aggregation of *C. elegans* (N2) worms on ascr#10 plates, we used one-factor ANOVA followed by Dunnett's post-test, *P<0.05, **P< 0.01.

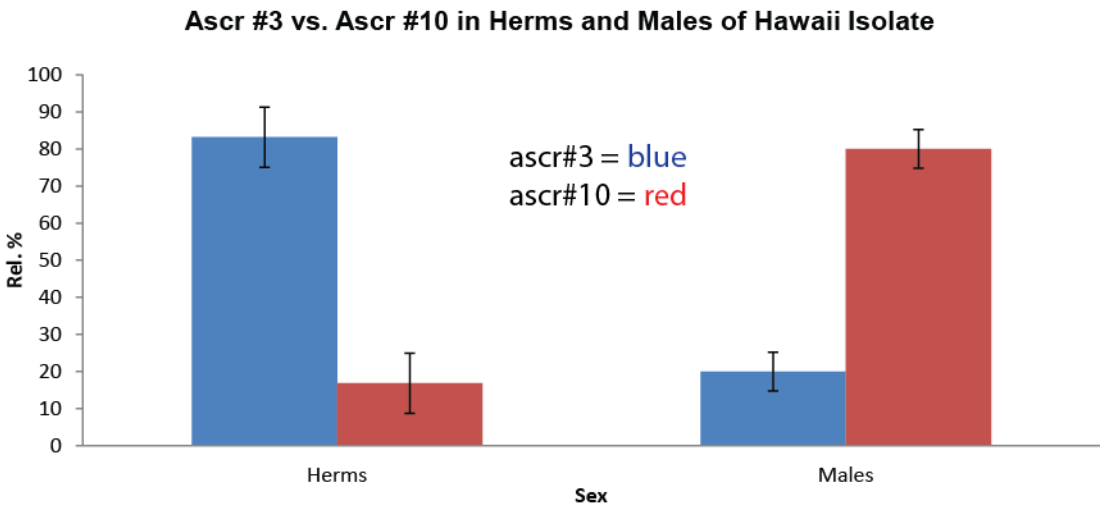

Figure A.1: Relative abundances of ascr#10 and ascr#3 in males and hermaphrodites of *C. elegans* wild-type strain CB4856 (isolated at Hawaii). Error bars: SD. *Profiling experiments were conducted by YI.*

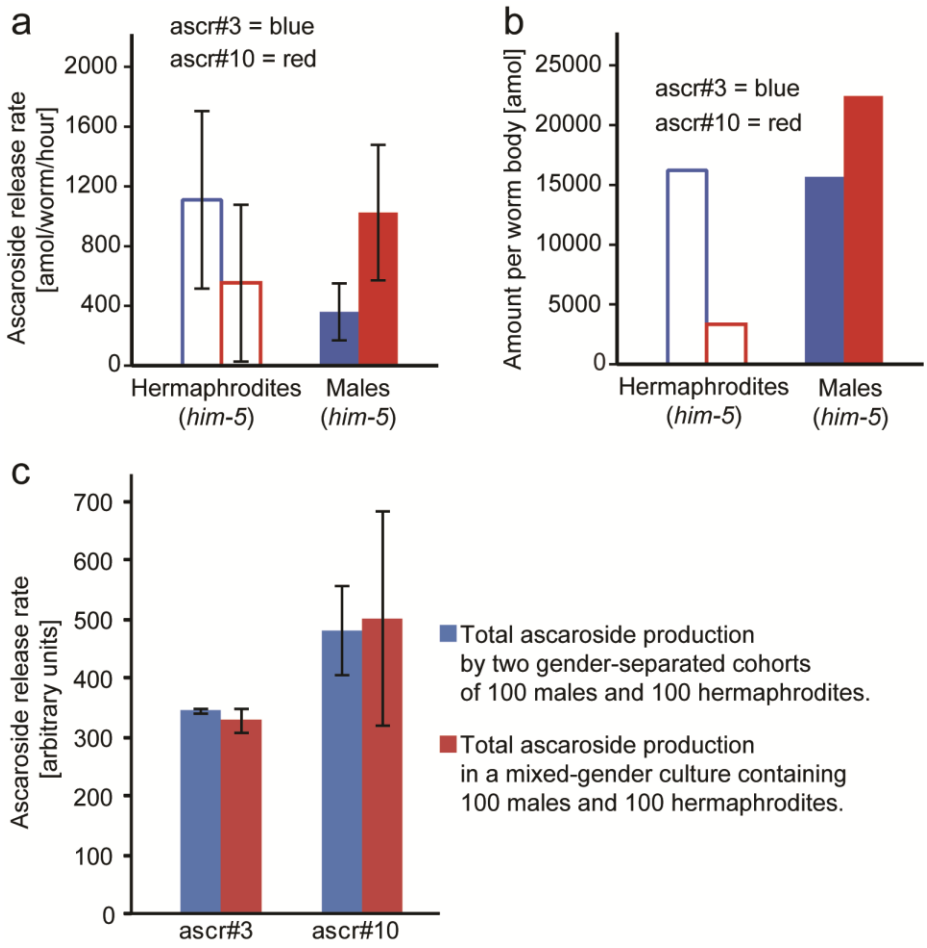

Figure A.2: Ascaroside production in males and hermaphrodites (error bars: SD). (a) Ascaroside release rates of *him-5* males and hermaphrodites. (b) Ascaroside content of worm whole-body extracts (*him-5* males and hermaphrodites). (c) Comparison of ascaroside production by separate and mixed cohorts of wild-type males and hermaphrodites. ascr#3 and ascr#10 production of a mixed cohort of males and hermaphrodites (red) is very similar to gender-averaged ascaroside production in separately incubated males and hermaphrodites (see Methods for details). *Profiling of worm media and worm pellets were conducted by YI with support from SLC and MCG.*

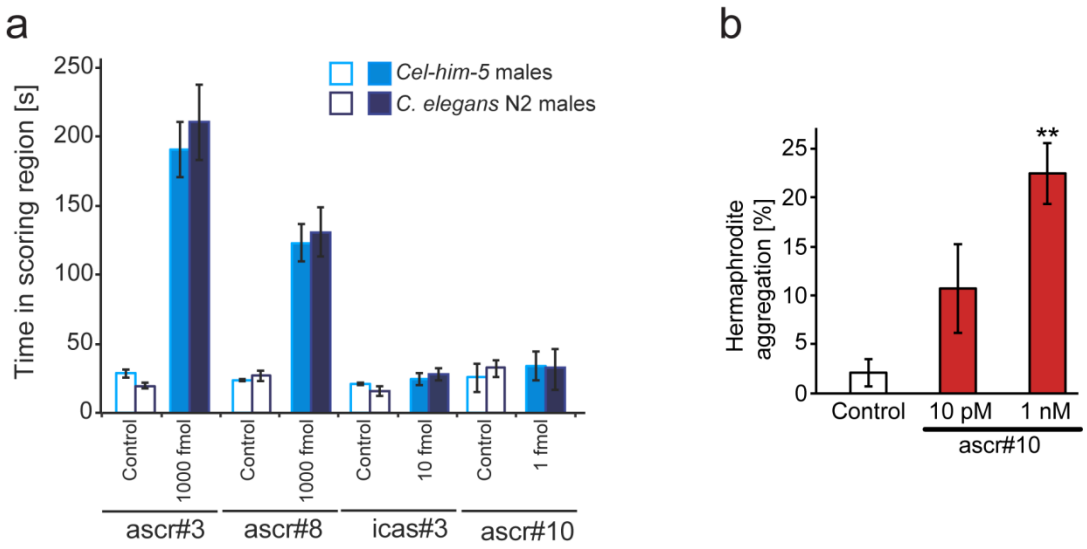

Figure A.3: (a) Comparison of ascaroside responses of *him-5* and wild-type males. Wild-type male responses to previously described male-specific attractants ascr#3 and ascr#8 and to the hermaphrodite-specific attractants icas#3 and ascr#10 are indistinguishable from those of *him-5* males.(*6*) icas#3 and ascr#10 were assayed at concentrations that elicit strong attraction or retention in hermaphrodites. (b) Ascr#10 increases aggregation behavior of normally solitary N2 hermaphrodites;(*6*) one-factor ANOVA followed by Dunnett's post-test, *P < 0.05, **P < 0.01. *Bioassays were conducted by JS with assistance from YJ*

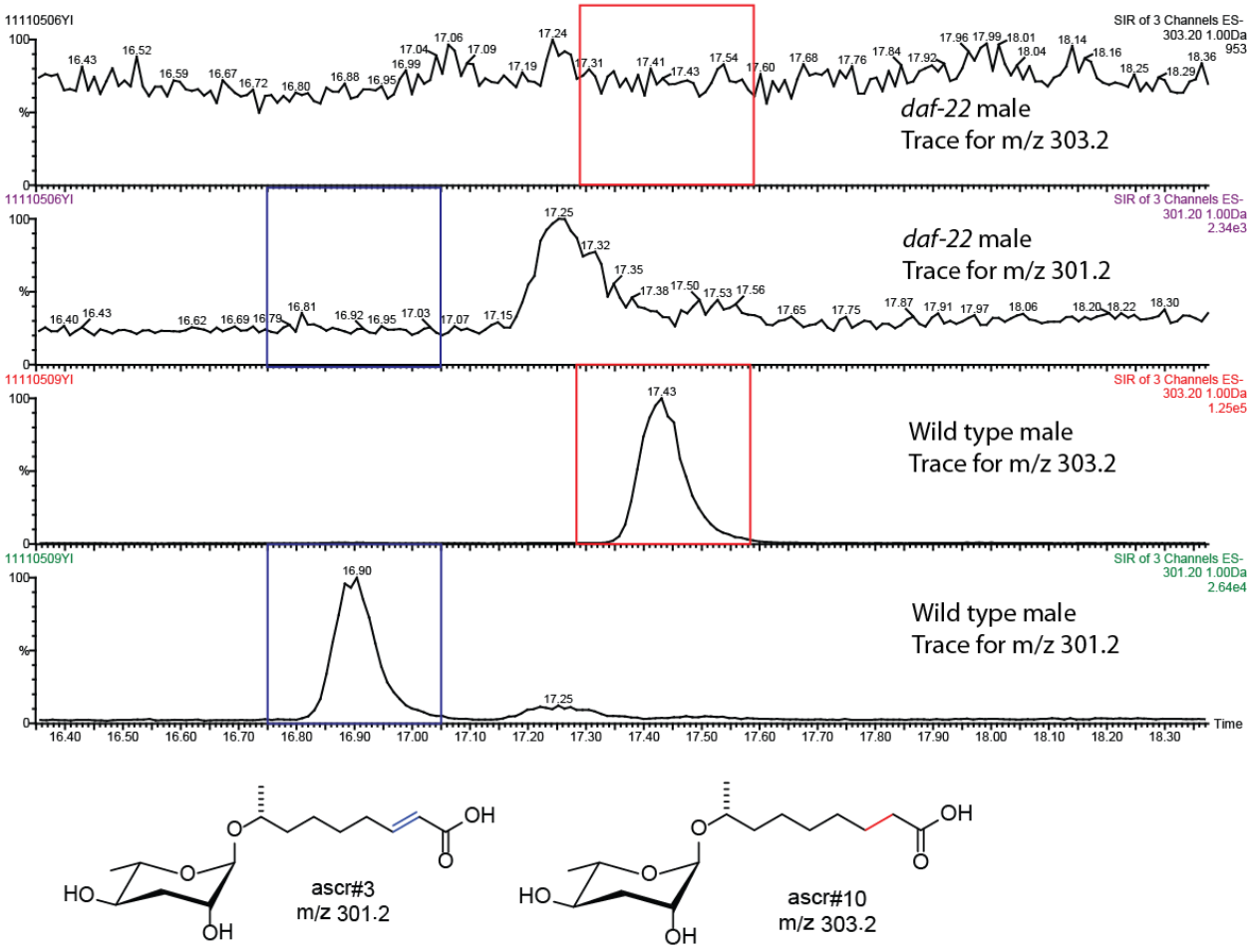

Figure A.4. HPLC-MS analysis of *daf-22* male exometabolome. Shown are ion traces for *m/z* of 303.2 (ascr#10) and m/z of 301.2 (ascr#3) obtained via HPLC-MS analysis (ESI^-) of samples from 100 *daf-22* mutant males and 100 wild-type (N2 Bristol) males. Blue boxes highlight the retention time window for ascr#3 (16.90±0.02 min) and red boxes highlight the retention time window for ascr#10 (17.44±0.02 min) .(*1*). *Profiling experiments were conducted by YI with support from SLC and MCG*

REFERENCES

1. von Reuss, S. H., Bose, N., Srinivasan, J., Yim, J. J., Judkins, J. C., Sternberg, P. W., and Schroeder, F. C. (2012) Comparative metabolomics reveals biogenesis of ascarosides, a modular library of small molecule signals in *C. elegans*, *J. Am. Chem. Soc. 134*, 1817–1824.
2. Srinivasan, J., Kaplan, F., Ajredini, R., Zachariah, C., Alborn, H. T., Teal, P. E., Malik, R. U., Edison, A. S., Sternberg, P. W., and Schroeder, F. C. (2008) A blend of small molecules regulates both mating and development in *Caenorhabditis elegans*, *Nature 454*, 1115-1118.
3. Pungaliya, C., Srinivasan, J., Fox, B. W., Malik, R. U., Ludewig, A. H., Sternberg, P. W., and Schroeder, F. C. (2009) A shortcut to identifying small molecule signals that regulate behavior and development in *Caenorhabditis elegans*, *Proc. Natl Acad. Sci. USA 106*, 7708-7713.
4. Shivers, R. P., Youngman, M. J., and Kim, D. H. (2008) Transcriptional responses to pathogens in *Caenorhabditis elegans*, *Curr. Opin. Microbiol. 11*, 251-256.
5. de Bono, M., and Bargmann, C. I. (1998) Natural variation in a neuropeptide Y receptor homolog modifies social behavior and food response in *C. elegans*, *Cell 94*, 679-689.
6. Srinivasan, J., von Reuss, S. H., Bose, N., Zaslaver, A., Mahanti, P., Ho, M. C., O'Doherty, O. G., Edison, A. S., Sternberg, P. W., and Schroeder, F. C. (2012) A modular library of small molecule signals regulates social behaviors in *Caenorhabditis elegans*, *PLoS Biol. 10*, e1001237.

Appendix B

PHEROMONE SENSING REGULATES *CAENORHABDITIS ELEGANS* LIFESPAN AND STRESS RESISTANCE VIA THE DEACETYLASE SIR-2.1

Worm strains. The following *C. elegans* strains were obtained from the Caenorhabditis Genetics Center: wild type (N2), *daf-2(e1368), daf-16(mu86), sir-2.1(ok434), daf-12(rh61rh411).* The strains *daf-7(e1372);daf-3(e1376),* the low-copy SIR-2.1-overexpressing strain NL3909 *pkIs1642(unc-119[+] sir-2.1[+])* and its control NL3908 *pkIs1641(unc-119[+])*, as well as a *daf-16(mgDf50);NL3909* were kind gifts of Adam Antebi (Baylor College, Houston, Texas), Paul Sternberg (Caltech in Pasadena, California) and Sylvia Lee (Cornell University, New York). The following *daf-37* overexpressor and mutant strains were created as described earlier: *daf-37(DR2585)* (*daf-37* null mutant), *daf-37; mIs41[daf-37p::daf-37,rol-6(su1006)]* (*daf-37* overexpressor in *daf-37* mutant background), *daf-37; unc-119; mEx188[srbc-64p;;daf-37,unc-119(+)]* (ASK-specific *daf-37* overexpressor in *daf-37* mutant background), and *daf-37;unc-119;mEx187[gpa-4p;;daf-37,unc-119(+)]* (ASI-specific *daf-37* overexpressor in *daf-37* mutant background) (*1*). Nematode stocks were maintained on Nematode Growth Medium (*2*) plates with added bacteria (*E. coli* strain OP50) at 20 °C (http:// www.wormbook.org/, Brenner, 1974), unless indicated otherwise.

Plate preparation. Ascarosides ascr#2 and ascr#3 were synthesized as described previously (*3*). For preparation of ascaroside containing NGM plates, ascr#2 and ascr#3 were dissolved in 100% ethanol producing 10.6 mM (ascr#2) and 7.6 mM (ascr#3) stock solutions, which were further diluted with water to yield stock solutions of micromolar and nanomolar concentrations, as needed. Controls for mock treated had

corresponding amounts of ethanol added. Plates were allowed to dry for 24 h. For the heat stress and lifespan assays, 6-cm diameter Petri dish plates were prepared using noble agar-based NGM prepared according to http://www.wormbook.org/. Minimal Growth Medium (MGM) plates ("-peptone plates") were prepared as described for NGM plates but without adding peptone. 200 µL of ascaroside solutions or mock solutions were spread on the surface of NGM plates. After drying overnight, 60 µL bacteria (*E. coli* OP50 pellet), freshly grown at 37 ºC in LB media, were spread onto the plates, and plates were incubated for 24 h at 22 ºC. For thermotolerance assays, plates were exposed to UV-radiation for one hour to kill the bacteria prior to putting worms on the plates.

Lifespan assays. For lifespan assays, worm strains were thawed from frozen stock and grown for two generations on well-fed conditions. 6-cm NGM plates containing ascr#2, ascr#3, 1:1 mixtures of ascr#2 and ascr#3 and mock-treated control plates were used. Late L4-stage worms were picked from synchronized NGM plates and transferred (25-30 worms/plate) to experimental plates at 20°C. Table S1 contains full lifespan data. Survival was monitored by scoring for touch-provoked movement every other day, in some cases every day. Live worms were transferred every other day to remove progeny until day 10. Day 0 corresponds to the time of transfer of the worms at the L4 stage. All experiments, except the experiment using 0.04 nM of either ascr#2 and ascr#3 (Figure 1), were carried out at least twice at two different times, started at least one week apart. For testing the effect of ascarosides on *C. elegans* adult lifespan without peptone supplementation, MGM plates were used. For some lifespan experiments see Table S1), FUdRwas used. SPSS V. 19 (IBM) statistical analysis package was used for all

lifespan and thermotolerance statistics. *P*-values were calculated using the Log-rank (Mantel-Cox) method.

Lifespan assays using FUdR. Late L4-stage worms were picked from synchronized NGM plates and transferred (30 worms/plate) to control plates or plates containing ascarosides. Subsequently, plates were treated with FUdR to induce sterility by adding 100 µL of a 5 mg/mL aqueous FUdR solution around the edges of the bacterial lawn, for a final concentration of 50 µg/mL FUdR. Worms were scored and transferred as described above.

Thermotolerance assays. 6 cm NGM plates containing ascr#2, ascr#3, 1:1 mixtures of ascr#2 and ascr#3 and mock-treated control plates were used. Experimental plates were prepared using noble agar-based nematode growth medium (*2*). *E. coli* OP50 was UV-killed prior to placing worms on plates. Late L4-stage worms were picked from synchronized NGM plates and transferred (15-25 worms/plate) to experimental plates. After completion of development to adults at 20°C (14-20 h, depending on strain), plates were incubated at 35 ºC. Survival was scored hourly, beginning after 5-8 h of heat exposure, by checking for touch-provoked movement until all worms had died. At least 4 plates (usually 5) for each ascaroside concentration were used, in addition to 6 control plates, and all experiments were carried out at least twice at two different times. SPSS V. 19 (IBM) statistical analysis package was used for all thermotolerance statistics. *P*-values were calculated using the Log-rank (Mantel-Cox) method.

Thermotolerance assays with caloric restriction (*4*). Late stage L4 worms were picked from synchronized NGM plates and placed on experimental plates. After completion of development to adults at 20°C (16 h), worms were transferred to “adlib” or

“CR” plates; “adlib” plates: NGM plates with bacteria containing 400 nM ascr#2 or control; “CR” plates: NGM plates without bacteria containing 400 nM ascr#2 or control, additionally treated with 200 µL of 5 mg/ml streptomycin sulfate and penicillin solution. Immediately following worm transfer, “adlib” or “CR” plates were exposed to 35 ºC. Survival was monitored as described above. SPSS V. 19 (IBM) statistical analysis package was used for all thermotolerance statistics. *P*-values were calculated using the Log-rank (Mantel-Cox) method.

Oxidative stress (H_2O_2) resistance assay. Synchronized L4-stage worms were placed on NGM plates (mock-treated control or containing various concentrations ascr#2 and ascr#3) with bacteria (OP50) at 20 ºC. After reaching young adult stage (12-16 h), worms were transferred to NGM plates (mock-treated control or containing various concentrations ascr#2 or ascr#3) with bacteria and containing 0.6 mM H_2O_2. Survival was scored after 6 hours at 20 ºC.

Brood size measurement. To determine average brood size per worm, living eggs and L1 progeny were counted on the plates used for the lifespan experiments described above. Worms were transferred 8-10 times over the course of the experiments. The number of progeny per worm was determined by dividing the total number of eggs and L1 worms counted per plate by the number of live worms transferred. 5-6 plates per condition (ascaroside treated and control) with 20-30 worms per plate, were counted.

Measurement of pharyngeal pumping rates. Pumping of worms was counted over 1 minute intervals by eye. 10 worms per condition and time point in the lifespan assays were scored, beginning at day one of the experiment and continued daily until all worms

had died. In the thermotolerance assays, pharyngeal pumping rates of at least 5 worms were scored every 30 min starting 8 h after placing the worms in the incubator.

Statistical Analysis. SPSS V. 19 (IBM) statistical analysis package was used for all lifespan and thermotolerance statistics. *P*-values were calculated using the Log-rank (Mantel-Cox) method.

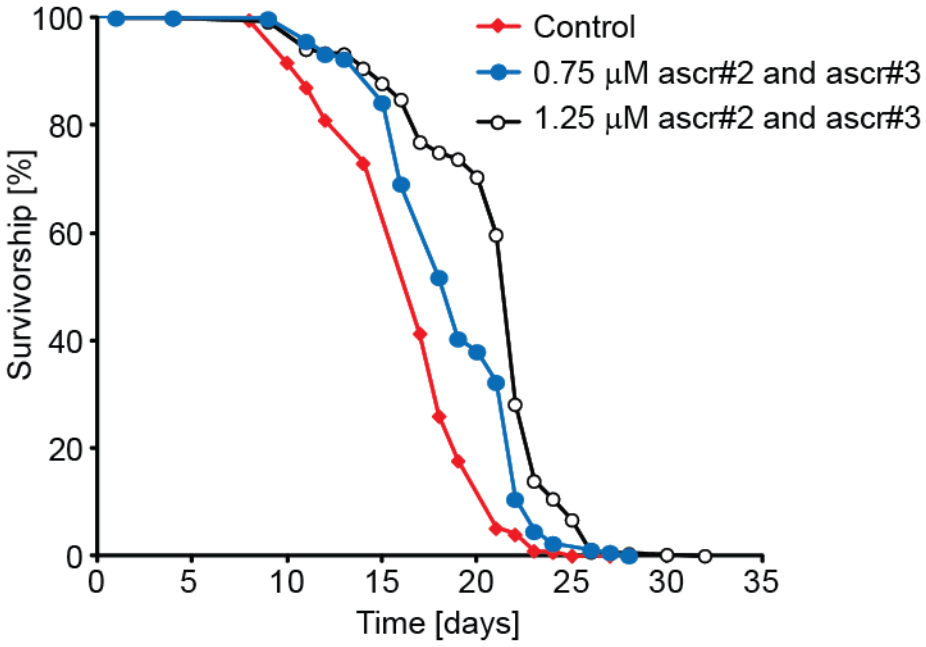

Figure B.1. Mixtures of ascarosides increase *C. elegans* lifespan. Survivorship at 20°C of wildtype (N2) worms exposed to a mixture of 0.75 µM of each ascr#2 and ascr#3, 1.25 µM of each ascr#2 and ascr#3, or mock treated control. *Aging experiments performed by HAL, analyzed by YI and HAL.*

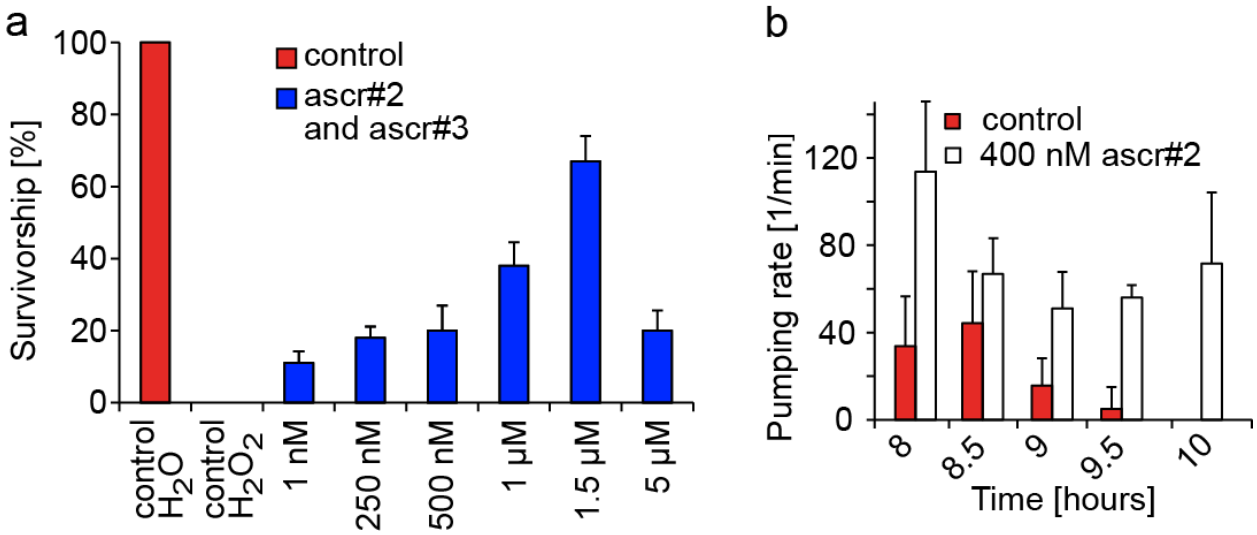

Figure B.2. Ascarosides increase survival under oxidative stress. (a) Survivorship of wildtype (N2) worms exposed to mock solution or 0.6 mM H_2O_2 for 6 hours. Worms were raised either on mock-treated control plates or on plates containing the indicated concentrations ofascr#2 and ascr#3. Error bars, s.d. (b) Pharyngeal pumping rate under heat stress of wildtype (N2) worms exposed to 400 nM of ascr#2 compared to untreated controls. Error bars, s. d. *Experiments performed by RUM and HAL.*

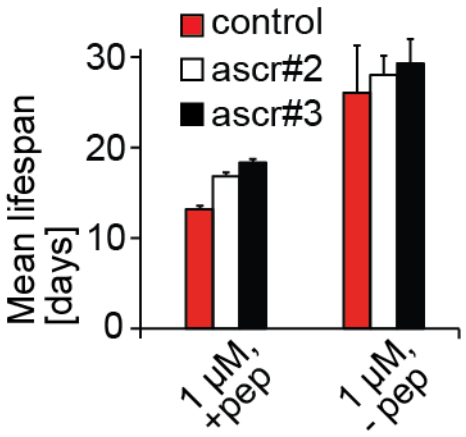

Figure B.3. Nutritional conditions affect lifespan extension by ascr#2 and ascr#3. Mean lifespan of wild type (N2) worms on NGM (with peptone, "+pep") and MGM (without peptone, "-pep") plates containing 1 µM of ascr#2 or 1 µM of ascr#3. *Experiment performed by HAL*.

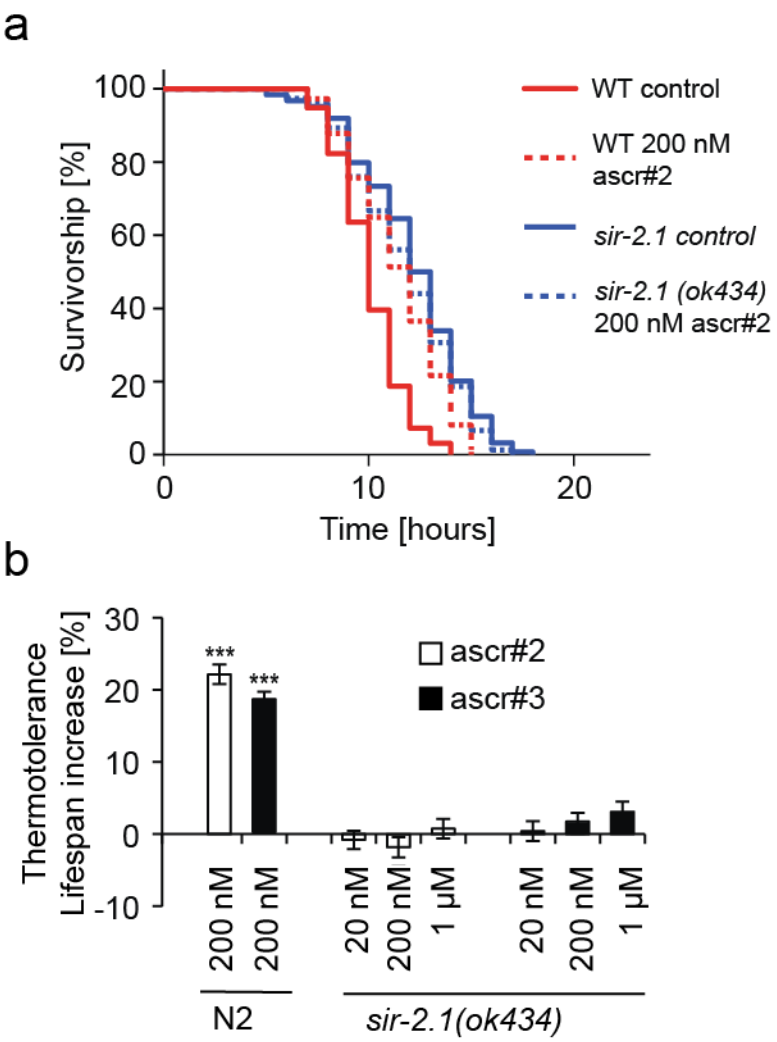

Figure B.4. Ascaroside-induced thermotolerance requires SIR-2.1. (a) Survivorship at 35°C of wild type (N2) worms and *sir-2.1(ok434)* strain exposed to 200 nM ascr#2 or mock treated control. (b) Mean survival time under heat stress of *sir-2.1(ok434)* mutant worms exposed to 20 nM, 200 nM and 1 µM of ascr#2 or ascr#3, normalized to mock-treated *sir-2.1(ok434)* control worms. Mean survival time increases under heat stress for wildtype worms (N2) exposed to 200 nM of ascr#2 or ascr#3 are shown for comparison. *Aging experiments performed by YI and HAL. Thermotolerance experiments performed by RUM.*

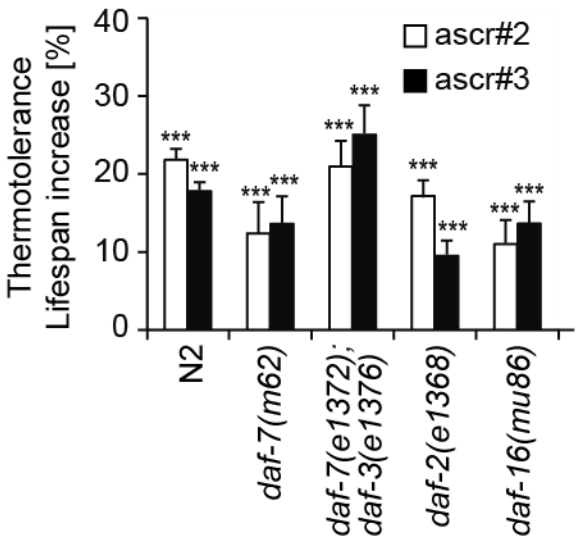

Figure B.5. Ascaroside-induced thermotolerance is largely independent of classical dauer signaling genes. Mean survival time increase of wildtype (N2) and mutant worms exposed to 200 nM ascr#2 or ascr#3 at 35°C relative to untreated controls. ***p<0.0001. Error bars, s.e.m. *Experiments performed by RUM.*

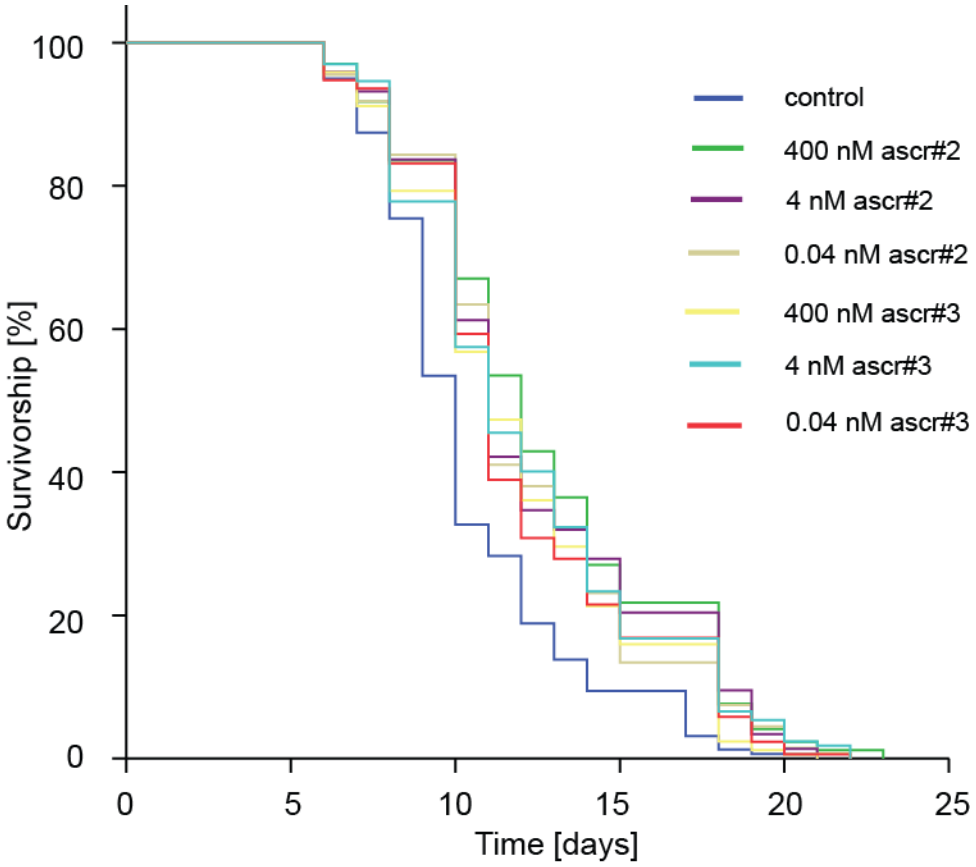

Figure B.6. ascr#2 extends lifespan of a *daf-16(mgDf50)* mutant worms in a sirtuin over expression background. Survivorship of *sir-2.1* OE (NL3909); *daf-16 (mgDf50)* mutant worms treated with 400 nM, 4 nM and 0.04 nM ascr#2, 400 nM, 4 nM and 0.04 nM ascr#3, as well as mock control. For full data see Table S1. *Experiments performed by YI, RUM, and HAL.*

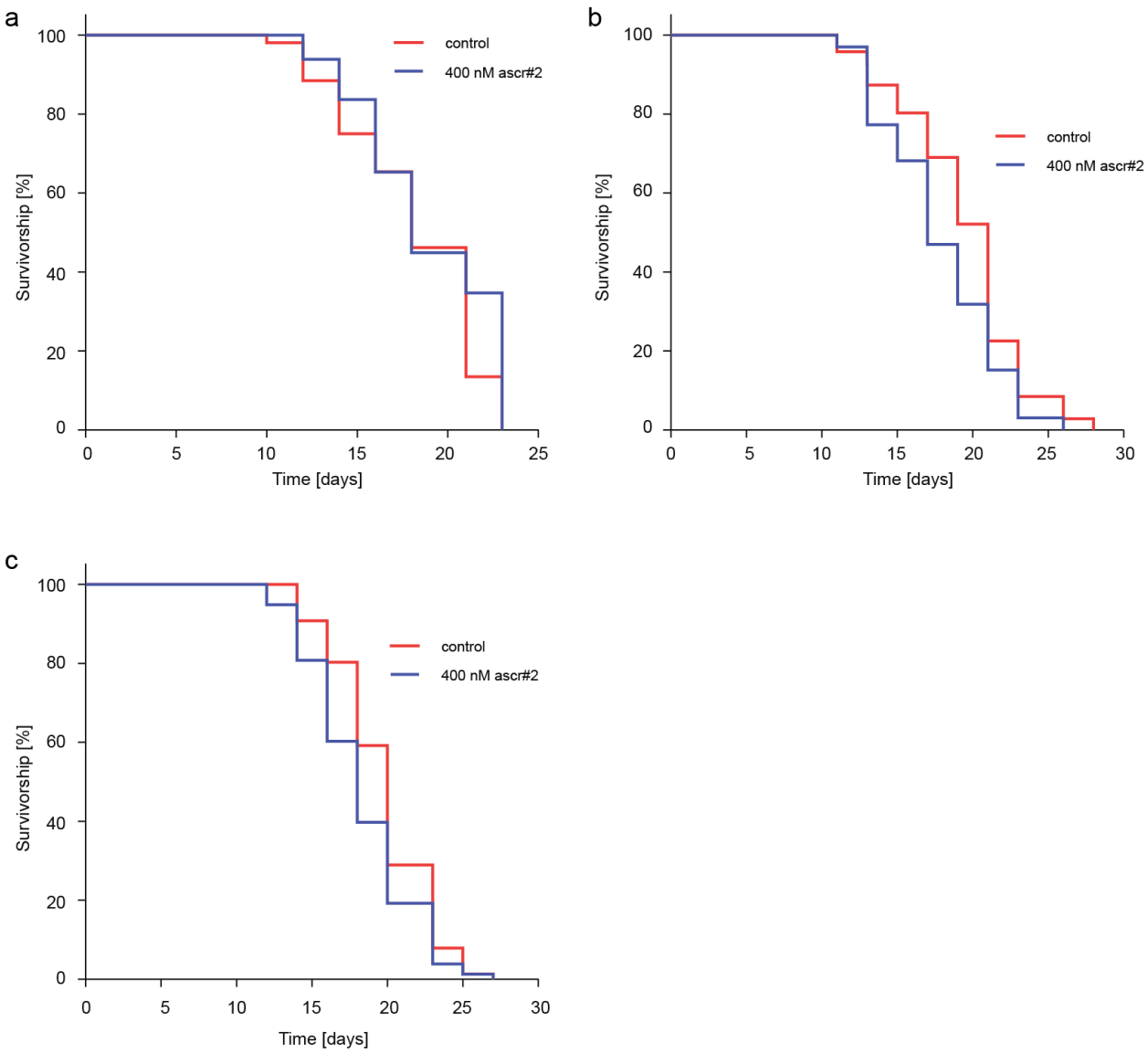

Figure B.7. ascr#2 does not increase lifespan of worms overexpressing *daf-37* in the ASI neurons. Survivorship of *daf-37;unc-119;mEx187[gpa-4p;;daf-37,unc-119(+)],* a strain overexpressing daf-37 in ASI neurons in a *daf-37* mutant background, treated with 400 nM ascr#2 or mock control. Whereas the experiment shown in (a) shows no lifespan extension, experiments (b) and (c) show a modest but significant lifespan decrease. See Table S1 for full data. *Experiments performed by YI and DP.*

Table B.1. Lifespan Data. *Lifespan assays conducted by YI, RUM, HAL, and DP.*

Experiment no.	Strain	Treatment	Mean lifespan, d	No. of worms, *N*	*P* value (log rank) vs. control	Mean lifespan extension, %	N2 study done in parallel
1	N2 (wild type)	Control	13.2	155			
	N2	0.04 nM ascr#2	13.4	147	0.253	1.52	
	N2	4 nM ascr#2	14.5	137	<0.0001	9.85	
	N2	400 nM ascr#2	15.1	111	<0.0001	14.39	
	N2	0.04 nM ascr#3	14.6	139	<0.0001	10.61	
	N2	4 nM ascr#3	14.9	132	<0.0001	12.88	
	N2	400 nM ascr#3	16.0	134	<0.0001	21.21	
2	N2	Control	12.8	141			
	N2	400 nM ascr#2	13.9	129	0.001	8.59	
3	N2	Control	14.0	143			
	N2	400 nM ascr#2	16.4	154	<0.0001	17.14	
4	N2	Control	17.2	217			
	N2	1 μM ascr#3	19.4	99	<0.0001	12.79	
5	N2	Control	13.9	218			
	N2	400 nM ascr#2	15.8	175	<0.0001	13.90	
6	N2	Control	18.8	273			
	N2	1 μM ascr#2 and ascr#3	21.6	334	<0.0001	14.89	
7	N2	Control	16.8	254			
	N2	0.75 μM ascr#2 and ascr#3	18.9	258	<0.0001	12.50	
	N2	1.25 μM ascr#2 and ascr#3	20.6	314	<0.0001	22.62	
	N2	3 μM ascr#2 and ascr#3	18.6	274	<0.0001	10.71	
8	*sir-2.1(ok434)*	Control	12.5	109			3
	sir-2.1(ok434)	0.04 nM ascr#2	12.0	124	0.117	−4.00	
	sir-2.1(ok434)	4 nM ascr#2	11.8	85	0.273	−5.60	
	sir-2.1(ok434)	400 nM ascr#2	11.8	100	0.481	−5.60	
	sir-2.1(ok434)	0.04 nM ascr#3	12.1	109	0.367	−3.20	
	sir-2.1(ok434)	4 nM ascr#3	12.9	120	0.297	3.20	
	sir-2.1(ok434)	400 nM ascr#3	11.9	119	0.076	−4.80	
9	*sir-2.1(ok434)*	Control	18.7	111			3
	sir-2.1(ok434)	400 nM ascr#2	18.1	112	0.253	−3.21	
10	*sir-2.1* wt (NL3908)	Control	12.0	125			3
	sir-2.1 wt (NL3908)	0.04 nM ascr#2	13.0	110	0.056	8.33	
	sir-2.1 wt (NL3908)	4 nM ascr#2	13.3	107	0.001	10.83	
	sir-2.1 wt (NL3908)	400 nM ascr#2	15.2	111	<0.0001	26.67	
11	*sir-2.1* wt (NL3908)	Control	15.9	135			5
	sir-2.1 wt (NL3908)	400 nM ascr#2	17.8	124	<0.001	11.42	
12	*sir-2.1* OE (NL3909)	Control	12.4	172			3
	sir-2.1 OE (NL3909)	4 fM ascr#2	12.2	169	0.754	−1.61	
	sir-2.1 OE (NL3909)	400 fM ascr#2	13.1	159	0.094	5.65	
	sir-2.1 OE (NL3909)	0.04 nM ascr#2	13.2	166	0.032	6.45	
	sir-2.1 OE (NL3909)	4 nM ascr#2	13.5	172	0.003	8.87	
	sir-2.1 OE (NL3909)	400 nM ascr#2	13.7	178	0.002	10.48	
13	*sir-2.1* OE (NL3909)	Control	12.6	104			3
	sir-2.1 OE (NL3909)	0.04 nM ascr#2	15.3	106	<0.0001	21.43	
	sir-2.1 OE (NL3909)	4 nM ascr#2	13.9	106	0.022	10.32	
	sir-2.1 OE (NL3909)	400 nM ascr#2	14.2	92	0.004	12.70	
14	*sir-2.1* OE (NL3909)	Control	18.0	154			5
	sir-2.1 OE (NL3909)	400 nM ascr#2	19.6	154	0.016	8.89	
15	*sir-2.1* OE (NL3909); *daf-16(mgDf50)*	Control	10.4	159			4
	sir-2.1 OE (NL3909); *daf-16(mgDf50)*	0.04 nM ascr#2	12.1	134	<0.0001	16.35	
	sir-2.1 OE (NL3909); *daf-16(mgDf50)*	4 nM ascr#2	12.3	147	<0.0001	18.27	
	sir-2.1 OE (NL3909); *daf-16(mgDf50)*	400 nM ascr#2	12.6	170	<0.0001	21.15	
	sir-2.1 OE (NL3909); *daf-16(mgDf50)*	0.04 nM ascr#3	11.9	172	<0.0001	14.42	
	sir-2.1 OE (NL3909); *daf-16(mgDf50)*	4 nM ascr#3	12.1	167	<0.0001	16.35	
	sir-2.1 OE (NL3909); *daf-16(mgDf50)*	400 nM ascr#3	11.9	169	<0.0001	14.42	
16	*sir-2.1* OE (NL3909); *daf-16(mgDf50)*	Control	9.5	138			4
	sir-2.1 OE (NL3909); *daf-16(mgDf50)*	400 nM ascr#2	10.4	169	0.008	9.47	
17	*daf-16 (mu86)*	Control	10.4	145			1
	daf-16 (mu86)	0.04 nM ascr#2	11.3	184	0.014	8.65	
	daf-16 (mu86)	4 nM ascr#2	11.7	150	<0.0001	12.50	

Experiment no.	Strain	Treatment	Mean lifespan, d	No. of worms, *N*	*P* value (log rank) vs. control	Mean lifespan extension, %	N2 study done in parallel
18	*daf-16 (mu86)*	Control	13.7	152			1
	daf-16 (mu86)	4 nM ascr#2	15.0	146	<0.0001	9.49	
	daf-16 (mu86)	40 nM ascr#2	14.0	125	0.229	2.19	
	daf-16 (mu86)	400 nM ascr#2	15.3	133	<0.0001	11.68	
	daf-16 (mu86)	4 nM ascr#3	14.9	139	<0.0001	8.76	
	daf-16 (mu86)	40 nM ascr#3	14.9	143	<0.0001	8.76	
	daf-16 (mu86)	400 nM ascr#3	14.4	139	0.031	5.11	
19	*daf-16 (mu86)*	Control	10.4	183			1
	daf-16 (mu86)	400 nM ascr#2	12.4	145	<0.0001	19.23	
20	*daf-16 (mu86)*	Control	11.0	178			1
	daf-16 (mu86)	0.04 nM ascr#3	10.7	126	0.05	−2.73	
21	*daf-12 (rh411rh61)*	Control	10.3	153			1
	daf-12 (rh411rh61)	400 nM ascr#2	11.2	153	0.002	8.74	
	daf-12 (rh411rh61)	400 nM ascr#3	11.3	118	0.024	9.71	
22	*daf-12 (rh411rh61)*	Control	10.6	48			1
	daf-12 (rh411rh61)	400 nM ascr#2	11.5	54	<0.0001	8.49	
	daf-12 (rh411rh61)	400 nM ascr#3	12.6	51	0.001	18.87	
23	*daf-2 (e1368)*	Control	18.5	96			1
	daf-2 (e1368)	400 nM ascr#2	19.9	97	0.036	7.80	
24	*daf-2 (e1368)*	Control	18.8	95			1
	daf-2 (e1368)	400 nM ascr#2	20.5	100	0.077	9.04	
	daf-2 (e1368)	400 nM ascr#3	20.2	113	0.002	7.45	
25	*daf-7(e1372);daf-3(e1376)*	Control	15.4	189			1
	daf-7(e1372);daf-3(e1376)	400 nM ascr#2	16.8	165	0.002	9.09	
	daf-7(e1372);daf-3(e1376)	400 nM ascr#3	17.4	154	<0.0001	12.99	
26	*daf-7(e1372);daf-3(e1376)*	Control	14.8	69			1
	daf-7(e1372);daf-3(e1376)	400 nM ascr#2	17.5	76	<0.0001	18.24	
	daf-7(e1372);daf-3(e1376)	400 nM ascr#3	18.5	122	<0.0001	25.00	
27	*ASK ablation*	Control	21.1	49			2
	ASK ablation	400 nM ascr#2	20.3	38	0.443	−3.79	
28	*ASK ablation*	Control	19.0	74			2
	ASK ablation	400 nM ascr#2	18.8	79	0.552	−1.05	
29	*ASK ablation*	Control	17.9	76			2
	ASK ablation	400 nM ascr#2	17.5	72	0.812	−2.23	
30	*daf-37 OE in ASI*	Control	18.2	49			2
	daf-37 OE in ASI	400 nM ascr#2	18.9	52	0.132	3.85	
31	*daf-37 OE in ASI*	Control	19.7	76			2
	daf-37 OE in ASI	400 nM ascr#2	18.2	78	0.018	−7.61	
32	*daf-37 OE in ASI*	Control	19.5	71			2
	daf-37 OE in ASI	400 nM ascr#2	17.8	66	0.015	−8.72	
33	*N2**	Control	20.6	78			
	*N2**	400 nM ascr#2	22.8	76	0.001	10.68	
34	*N2**	Control	20.6	81			
	*N2**	400 nM ascr#2	22.3	75	0.007	8.25	
35	*daf-37 (−)**	Control	21.3	38			33
	*daf-37 (−)**	400 nM ascr#2	20.9	42	0.968	−1.88	
36	*daf-37 (−)**	Control	19.6	81			34
	*daf-37 (−)**	400 nM ascr#2	20.6	80	0.011	5.10	
37	*daf-37 OE in ASK**	Control	21.2	79			33
	*daf-37 OE in ASK**	400 nM ascr#2	23.3	68	0.01	9.91	
38	*daf-37 OE in ASK**	Control	20.0	85			34
	*daf-37 OE in ASK**	400 nM ascr#2	26.2	60	<0.0001	31.00	
39	*daf-37 OE**	Control	21.2	40			33
	*daf-37 OE**	400 nM ascr#2	25.2	41	<0.0001	18.87	
40	*daf-37 OE**	Control	19.8	77			34
	*daf-37 OE**	400 nM ascr#2	25.5	56	<0.0001	28.79	

wt, wild type.

*Studies with an asterisk were conducted in the D.L.R. laboratory (Vancouver, BC, Canada) with 2′-deoxy-5-fluorouridine (FUdR). All other lifespan experiments were conducted in the F.C.S. laboratory (Ithaca, NY) without FUdR.

Table B.2. Additional heat stress data. *Data acquired by RUM.*

Experiment no.	Strain	Treatment	Mean survival, h	No. of worms, *N*	*P* value (log rank) vs. control	Mean survival extension, %
1	N2	Control	7.06	147		
	N2	200 nM ascr#2	8.01	139	<0.0001	13.46
	N2	400 nM ascr#2	8.34	176	<0.0001	18.13
2	*sir-2.1(ok434)*	Control	7.86	193		
	sir-2.1(ok434)	200 nM ascr#2	7.33	172	0.007	−6.74
	sir-2.1(ok434)	400 nM ascr#2	7.42	159	0.034	−5.60

REFERENCES

1. Park, D., O'Doherty, I., Somvanshi, R. K., Bethke, A., Schroeder, F. C., Kumar, U., and Riddle, D. L. (2012) Interaction of structure-specific and promiscuous G-protein-coupled receptors mediates small-molecule signaling in *Caenorhabditis elegans*, *Proc. Natl Acad. Sci. USA 109*, 9917-9922.
2. Shivers, R. P., Youngman, M. J., and Kim, D. H. (2008) Transcriptional responses to pathogens in *Caenorhabditis elegans*, *Curr. Opin. Microbiol. 11*, 251-256.
3. Pungaliya, C., Srinivasan, J., Fox, B. W., Malik, R. U., Ludewig, A. H., Sternberg, P. W., and Schroeder, F. C. (2009) A shortcut to identifying small molecule signals that regulate behavior and development in *Caenorhabditis elegans*, *Proc. Natl Acad. Sci. USA 106*, 7708-7713.
4. Lee, G. D., Wilson, M. A., Zhu, M., Wolkow, C. A., de Cabo, R., Ingram, D. K., and Zou, S. (2006) Dietary deprivation extends lifespan in *Caenorhabditis elegans*, *Aging Cell 5*, 515-524.

Appendix C

PHEROMONE SENSING PROTECTS *C. ELEGANS* FROM ENTEROPATHOGENIC *E.* COLI VIA THE UNFOLDED PROTEIN RESPONSE, THE DEACETYLASE SIR-2.1, AND COMPONENTS OF GPCR SIGNALING

Worm strains. The following *C. elegans* strains were obtained from the Caenorhabditis Genetics Center: wild type (N2), *sir-2.1(ok434), ced-1(e1375), ced-3(n717), ced-4(n1162), gpa-2(pk16), gpa-3(pk35), gpa-2(pk16);gpa-3(pk35), arr-1(ok401), gcy-35(ok763), tax-2(ks15), tax-4(ks28),daf-12(rh61rh411), , daf-16(mu86), acox-1(ok2257), maoc-1(hj13), maoc-1(hj14), dhs-28(hj8), daf-22(m130), daf-22(ok693).* The strain *daf-7(e1372);daf-3(e1376)* was a kind gift of Adam Antebi (Baylor College, Houston, Texas). Nematode stocks were maintained on Nematode Growth Medium (*1*) plates with added bacteria (*E. coli* strain OP50) at 20 °C (http:// www.wormbook.org/, Brenner, 1974), unless indicated otherwise.

Conditioning assays. Enteropathogenic *E. coli* serotype 0127:H6 strain E2348/69 and *E. coli* OP50 were used. Conditioning assays were adapted from (*2*). Briefly, EPEC and EPECΔ*tnaA*, was cultured in LB broth overnight to an OD_{600} of 0.8–1.0 and 170 µl spread on 6 cm LB agar (Fisher; Pittsburgh, PA) plates containing 2 mg/ml tryptophan (LBT plates). After incubation for 20 hr at 37°C, the plates were cooled for 1 hr in 25°C incubators. For the EPECΔ*tnaA* conditioning and control, young adult animals maintained at 20°C were transferred to each plate, young adult worms were exposed to LBT/ EPECΔ*tnaA* for 3 hours (pre-exposure) or kept on NGM/OP50 plates (no

conditioning) then transferred to OP50 on NGM plates for 3 hr (waiting period), and then again to fresh LBT/EPEC for 3 hr (challenge). For the ascaroside conditioning, worms were transferred for 2 hr to an Eppendorf with given concentration of ascarosides (ascaroside pre-exposure) or water (with same etoh as in ascr mix) control. The ependorf tubes were under gentle shaking. The worms were then transferred to OP50 on NGM plates for 3 hr (waiting period), and then again to fresh LBT/EPEC for 3 hr (challenge). After the challenge, worms were transferred to OP50/NGM plates and scored after 24 hr. At least 180 worms per strain were tested for each experiment. Ascarosides were synthesized as previously reported (*3*-*5*). All assays were performed at 25°C

REFERENCES

1. Shivers, R. P., Youngman, M. J., and Kim, D. H. (2008) Transcriptional responses to pathogens in *Caenorhabditis elegans*, *Curr. Opin. Microbiol. 11*, 251-256.
2. Anyanful, A., Easley, K. A., Benian, G. M., and Kalman, D. (2009) Conditioning protects *C. elegans* from lethal effects of enteropathogenic *E. coli* by activating genes that regulate lifespan and innate immunity, *Cell Host Microbe 5*, 450-462.
3. Pungaliya, C., Srinivasan, J., Fox, B. W., Malik, R. U., Ludewig, A. H., Sternberg, P. W., and Schroeder, F. C. (2009) A shortcut to identifying small molecule signals that regulate behavior and development in *Caenorhabditis elegans*, *Proc. Natl Acad. Sci. USA 106*, 7708-7713.
4. Srinivasan, J., Kaplan, F., Ajredini, R., Zachariah, C., Alborn, H. T., Teal, P. E. A., Malik, R. U., Edison, A. S., Sternberg, P. W., and Schroeder, F. C. (2008) A blend of small molecules regulates both mating and development in *Caenorhabditis elegans*, *Nature 454*, 1115-1118.
5. von Reuss, S. H., Bose, N., Srinivasan, J., Yim, J. J., Judkins, J. C., Sternberg, P. W., and Schroeder, F. C. (2012) Comparative metabolomics reveals biogenesis of ascarosides, a modular library of small molecule signals in *C. elegans*, *J. Am. Chem. Soc. 134*, 1817–1824.

Appendix D

NMR-BASED METABOLOMICS REVEALS A FAMILY OF TOXINS AND THEIR DETOXIFACTION MECHANISM IN *CAENORHABDITIS ELEGANS*

Methods for phenazine and indole detoxification portions of the chapter (*1*).

Toxicity Assays (phenazine). *C. elegans* N2 eggs were arrested at the L1 stage for 24 hours in M9 buffer and then grown for 42-48 h at 20 °C on NGM plates to L4 stage as verified by observation with a stereoscope. Worms were washed off plates, allowed to settle, and dispensed onto test plates made with M9 buffer and 2% agar (a small lawn of OP50 was placed on the plate to discourage worms from crawling off). After 6 h, worms that failed to respond to physical touch with a platinum pick were scored as dead.

Toxicity assays (indole). Toxicity was determined in 12 well plates using 50 worms per well, which were placed into 0.5 ml M9 buffer (control), or buffer containing 1, 2, 3, 4, or 5 mM indole or indole glucoside. 0.1% methanol was present in all experiments. Worms were inspected for spontaneous movement after 3 h, the solution removed, and the worms washed 2 times with 2 ml fresh M9 buffer. After 24 h recovery, worms were inspected for spontaneous movement and scored for survival by physical touch with a platinum pick.

Quantification of indole in *E. coli*. *E. coli* OP50 from a 1 L culture was centrifuged at 5251 g for 45 min and the resulting bacterial pellet (3.1 mL) was lyophilized. The

resulting material (637 mg) was sonicated in 5 mL methanol (10 min) and extracted with methanol (3 x 15 mL). The filtered extract was concentrated *in vacuo* and the residue taken up in 3 mL methanol and analyzed by HPLC using a DAD-detector. Indole was quantified by comparison of the UV absorbance at 230 and 260 nm with those of a synthetic standard of known concentration.

Glucoside collection and analysis (phenazine). Adult *C. elegans* were synchronized with a bleach solution. The eggs were hatched overnight into L1s, which were then grown at a worm density of 10,000 worms/mL at 22 °C at 250 rpm in S-complete medium supplemented with 2% *E. coli* (strain HB101) for 43 hours until they reached young adult stage verified by observation with a stereoscope. The worms were concentrated to 30,000 worms/mL, washed once with M9, and fed 1% *E. coli* HB101. 1-HP from a DMSO stock, or the appropriate amount of DMSO was added to the cultures, which were incubated at 22°C at 250 rpm for 24 hours. The supernatant was removed by centrifugation (2,000 rpm, 2 min), filtered through a 0.22 µm nitrocellulose filter, lyophilized, extracted with 5 mL methanol, filtered, and concentrated. The residue was resuspended in 1 mL of methanol and used for HPLC analysis. The worm pellet was washed 4 times in M9 buffer, resuspended in one volume of 80% methanol and homogenized with a BioSpec MiniBeadbeater-8 (3 cycles of 30 sec, with 1 min on ice). The lysate was spun at 14,000 rpm for 10 min, and the supernatant dried under N_2 gas. The residue was resuspended in 1 mL of methanol and used for HPLC analysis.

Worm water was analyzed on an Agilent 1100 Series HPLC system equipped with a diode array detector and an automated fraction collector. Absorbance was monitored at 254 nm. For worm media separation, an aqueous methanol gradient was

used from 5-95% on a Zorbax SB C-18 column (4.6 cm x 150 mm, 5 µm particle diameter). For worm pellet separation, 5% methanol (A) and 95% 5mM Phosphate buffer pH 7.2 (B) was held isocratically for 4 min, increasing to 95% A and 5% B over 30 min and then held for 5 min, followed by reequilibriation of the column, at a flow rate of 2 mL min^{-1} in a Zorbax SB C-18 column (9.4 cm x 250 mm, 5 µm). Fractions were collected automatically by peak detection. Aliquots of each fraction were analyzed by high-resolution mass spectrometry by the University of Florida Spectroscopy Service in the Chemistry Department or in the Biomedical Mass Spectrometry Core at the Clinical and Translational Science Institute at the University of Florida.

Glucoside collection and analysis (indole). *C. elegans* worms from 10 cm NGM plates were washed using M9 medium into a 100 ml S-medium pre-culture where they were grown for four days at 22°C on a rotary shaker at 220 rpm. Concentrated OP50 derived from 1 L of bacterial culture (grown for 16 h in LB media) was added as food at days 1 and 3. Subsequently, the pre-culture was divided equally into four 1 L Erlenmeyer flasks containing 400 mL of S-medium for a combined volume of 425 mL of S-medium, which was then grown for an additional 10 d at 22 °C on a rotary shaker. Concentrated OP50 derived from 1 L of bacterial culture was added as food every day from days 1 to 9. Subsequently, the cultures were centrifuged and the supernatant media and worm pellet were lyophilized separately. The lyophilized materials were extracted with 95% ethanol (250 mL 2 times) at room temperature for 12 h. The resulting yellow suspensions were filtered and the filtrate evaporated *in vacuo* at room temperature, producing media and worm pellet metabolite extracts. The media metabolite extract from two cultures was adsorbed on 6 g of octadecyl-functionalized

silica gel and dry loaded into an empty 25 g RediSep *Rf* sample loading cartridge. The adsorbed material was then fractionated via a reversed-phase RediSep *Rf* GOLD 30 g HP C18 column using a water-methanol solvent system, starting with 100% water for 4 min, followed by a linear increase of methanol content up to 100% methanol at 42 min, which was continued up until 55 min. The fractions generated from this fractionation were evaporated *in vacuo* and the residue was analyzed by HPLC-MS and 2D-NMR spectroscopy.

Nuclear magnetic resonance for phenazine derivatives. Pooled fractions were dried and resuspended in 150 µL of 99.95% methanol-d_4 with 0.111 mM TSP as an internal standard, and transferred into 2.5 mm NMR tubes. 1D-^{1}H and 2D COSY spectra along with ^{1}H-^{13}C HSQC and ^{1}H-^{1}H NOESY where appropriate were collected on a Bruker Avance II 600 MHz spectrometer using a 5 mm TXI cryoprobe or an Agilent 600 MHz spectrometer using a 5 mm cryoprobe in the AMRIS facility at the University of Florida or Varian INOVA 600, INOVA 500, and INOVA 400 spectrometers at Cornell's NMR facility. Spectra were processed and analyzed with MestReNova 7.0 (Mestrelab Research) or Varian VNMR.

Feeding experiment with [U-D_7]-indole. *C. elegans* were cultivated in 100 mL S. complete medium by providing *E. coli* OP50 as a food source. After a worm density of 88,000 worms/mL was reached, 0.6 mg [U-D_7]-indole in 100 µL methanol was added to the culture. Aliquots of 6 mL were taken after 0, 1, 2, 3, 6, 12, and 24 h, centrifuged at 5251 g for 10 min, and 5 mL of supernatant was lyophilized, extracted with 2 mL methanol, filtered and concentrated *in vacuo*. The residues were taken up in 200 µL methanol and analyzed by HPLC with UV and ESI-MS detection.

Synthesis of *N*-(β-D-glucopyranosyl)indole (7). A solution of indoline (1.0 g, 8.4 mmol) in ethanol (60 mL) was treated with β-D-glucose (0.7 g, 3.9 mmol) in water (2 mL) and stirred at 90 °C. Additional water (0.8 mL) was added after 7 and 14 h. After 28 h the solution was concentrated *in vacuo* and the residue fractionated on silica using a gradient of 0 – 10% methanol in dichloromethane to get *N*-(β-D-glucopyranosyl)indoline (1.05 g, 3.7 mmol, 96% yield) as a yellowish solid. A solution of *N*-(β-D-glucopyranosyl)indoline (85 mg, 300 µmol) in 1,4-dioxane (15 mL) was treated with 2,3-dichloro-5,6-dicyano-1,4-benzochinone (82 mg, 360 µmol). After stirring for 14 h the mixture was concentrated. Flash column chromatography on silica gel using 20% methanol in dichloromethane afforded *N*-(β-D-glucopyranosyl)indole (70 mg, 251 µmol, 83% yield). Reverse phase HPLC on a C_{18} column afforded a pure sample for toxicity testing.

Methods for indole dependent virulence regulation in pathogenic E. coli (*2*).

Bacterial strains. The bacteria strains used in our experiments include enteropathogenic *E. coli* (EPEC) serotype O127:H6 strain E2348/69 (from B.B. Finlay;(Levine, 1985 #703), *E. coli* OP50 (*3*), *E. coli* P90C, and *E. coli*MG1665 (from Bernard Weiss, Emory University), and EPECΔ*tnaA* (*4*). EHEC strains used include EDL933 serotype O157:H7, and 8624 serotype O157:H7, and 3023–94 serotype O104:H21. 3023–94 is derived from the outbreak of bloody diarrhea in Montana and is positive for stx2 (stx2a and stx2d variants), negative for *eae*, and positive for *ehxA* (enterohemolysin). It is also negative for *aggR* and *aatA* (pCVD432), two genes on

plasmid pAA in EAEC. Enteroaggregative (EAEC) *E. coli* strains include 2011C-3493, 2009EL-2071 (O104:H4) and (*5*), Strains 3493 and 2071 are both positive for *stx2* (stx2a variant) and for *aggR* and *aatA*. The *C. rodentium* strain used was ATCC 51116. All bacterial strains were cultured in LB broth (Difco) to an OD_{600} of 0.8–1.0 before use.

***C. elegans* strains.** The following *C. elegans* mutants were obtained from the *Caenorhabditis* Genetics Center: wild-type Bristol strain N2, *daf-2(e1370), sek-1(km4), spp-1(ok2703),* and *dop3(vs106)*. *daf-16(mgDf47)* was provided by S. Lee. All *C. elegans* strains were maintained on Nematode Growth Medium (NGM) under standard culturing conditions with *E. coli* OP50 as food source.

***C. elegans* killing assays.** All assays were performed at 25°C essentially as described previously (*4, 6*). Briefly, EPEC was cultured in Luria-Bertani (LB) broth overnight to an OD_{600} of 0.8–1.0 and 170 µL spread on 6 cm LB agar (Fisher) plates containing 2 mg/mL tryptophan (LBT plates). After incubation for 20 hours at 37°C, the LBT/EPEC plates were cooled in 25°C incubators for an hour. Young adult worms, maintained at 20°C, were collected with M9 buffer (3 g KH_2PO_4, 6 g Na_2HPO_4, 5 g NaCl, 1 mL 1 M $MgSO_4$ in 1 L of water) and exposed to EPEC for 3 hours at 25°C before being transferred to OP50 on NGM plates. After 24 hours at room temperature, worms were gently prodded with a platinum wire and considered dead if they failed to respond to touch and showed no indication of pharyngeal pumping. At least 250 worms were tested for each experiment.

Indole killing assays. Synthetic indole (Sigma-Aldrich) was dissolved in methanol (Sigma) to form a 1 M stock solution. Because indole readily oxidizes, solutions were made fresh and a new batch was ordered every three months. To prepare 3.5 mM

indole-LB agar plates, indole was added to 100 mL of autoclaved LB agar prior to dispensing into 6 cm diameter Petri dishes (10 mL per dish). For killing assays, synchronized young adult worms maintained at 20°C were exposed to indole or methanol on the LB agar plates for 3 hours at 25°C before being transferred to OP50 on NGM plates. For experiments with indole or methanol in LB broth, worms were added to 1 ml broth in Eppendorf tubes, and gently shaken for 3 hours at 25°C, after which the worms were transferred to OP50/NGM plates. Twenty-four hours later, the *percent survival was determined*

Indole conditioning assays. Conditioning assays followed the general scheme described previously (*4*) with slight modifications. For indole pre-exposure and challenge assays**,** young adult worms were pre-exposed either to LB agar with 3.5 mM indole or in LB broth for 15 minutes (pre-exposure), washed in M9 buffer solution and transferred to OP50 on NGM plates for 3 hours (wait), and then transferred again to 3.5 mM indole on LB agar or in LB broth for 3 hours (challenge). After challenge, worms were transferred to OP50 on NGM for 24 hours (recovery) and the percent survival determined. For indole pre-exposure and EPEC challenge assays, young adult animals were pre-exposed as described above, and then challenged on LBT/EPEC plates for 3 hours before transfer to NGM/OP50. For EPEC pre-exposure and indole challenge assays, worms were pre-exposed to LBT/EPEC for 30 minutes, allowed to incubate on NGM/OP50 for 3 hours, and then challenged on 3.5 mM indole for 3 hours. For all experiments with indole, methanol controls were performed simultaneously.

Extraction of small molecules from LB agar LBT agar plates, layered with or without 0.22 µm cellulose acetate filters, were incubated with various bacterial strains for 20

hours at 37°C. Cellulose acetate filters were used to distinguish between total amounts of molecules produced by the bacteria and molecules secreted into the agar. The filter was then removed and small molecules were extracted from the agar using a solvent mixture of dichlormethane:methanol:ethylacetate (2:1:3) and incubation for 15 minutes in an ultrasonic water bath. Eight 10 cm plates, each with 25 mL agar, were extracted with 60 mL of solvent and reduced to dryness using a rotary evaporator. The residue was redissolved in 2 mL methanol and analyzed for the presence of indole-like structures by TLC and HPLC. The efficiency of extracting indole was determined by spiking agar plates with known indole concentrations, and extracting as above. The percent recovery based on three independent experiments was 13%.For experiments where indole supplemented extracts, indole in LB broth was added to dried extract to a final concentration of 2 mM. The mixture was warmed for 10 minutes at 40°C, and then cooled to 25°C prior to addition of worms. After 3 hours at 25°C, worms were transferred to NGM/OP50 and the percentage survival determined 24 hours later.

Killing and conditioning assays with indole and indole derivatives. Stock solutions of indole (500 mM), ICA (10 mM), IAA (50 mM) and ICOOH (25 mM; all from Sigma-Aldrich) were made in methanol. To perform killing assays, young adult worms were exposed to LB broth containing 2 mM indole, 0.6 mM ICA, 0.2 mM IAA, and 0.05 mM ICOOH for 4 hours. Worms were then washed once in M9 buffer and transferred to NGM/OP50 and the percentage survival determined after 24 hours. Methanol was used as a control. For conditioning, worms were pre-exposed to the above mixtures for 30 minutes, washed once with M9 buffer and transferred to NGM/OP50 for 3 hours, and then challenged either in the mixture for 4 hours (mixture-mixture) or on LBT/EPEC

plates for 3 hours (mixture-EPEC). We also pre-exposed the worms for 30 minutes to EPEC/LBT, transferred to NGM/OP50 for 3 hours, and then challenged in the mixture for four hours (EPEC-mixture).

Thin-layer chromatography. TLC methods optimized for indole and indole-like structures were used to analyze components of the extracts. The extract was separated on either analytical or preparative TLC plates (analytical: HPTLC plates 10×10 cm, SilicaGel 60 F_{254} (Merck); preparative: fluorescent SilicaGel G, 20×20 cm (Analtech) using toluene:acetone:chloroform (2:1:1) as the mobile phase (*7*). Plates were run in a TLC chamber for 45 min. TLC plates were coated with a fluorescent silicate, enabling detection of compounds upon excitation with UV light. A UV lamp with excitation wavelengths at 254 nm and 366 nm was used for detection. For preparative TLC plates, separated spots were tested for their ability to kill worms. Small plastic cylinders were placed on the identified spots and partially filled with LB agar. After the agar had hardened, worms were placed in the cylinders for 1 hour, after which they were moved to NGM/OP50 plates and the percentage survival determined after twenty-four hours.

HPLC, MS and NMR analysis. The extract was fractionated on a Shimadzu LC solution HPLC system using an Zorbax XD C18 column (Agilent) and an isocratic gradient of 50% methanol for 11 minutes at 0.5 mL/minute. For known components, standards were used to verify the identity and determine the concentration. Peak fractions were collected and analyzed by mass spectrometry (Chemical Core Facility, Emory University) and ^{1}H NMR spectroscopy (Chemistry Department, Emory University) on a Varian Inova 400 (400 MHz) NMR spectrometer using $CDCl_3$ as the solvent.

Two-dimensional NMR-based comparative metabolomics. Extracts from EPEC or EPECΔtnaA were suspended in 1 mL of 99.8% CD_3OD. After 1 hour at 22°C, the samples were evaporated to dryness and subsequently re-suspended in 600 µL of 99.95% CD_3OD (Cambridge Isotope Laboratories). The resulting suspensions were centrifuged at 4,400 rpm for 2 minutes, and the supernatants were transferred to 5 mm NMR tubes. ^{1}H and high-resolution dqfCOSY NMR spectra (acquisition time 0.6 second, sweep width 10 ppm, number of increments 600) were recorded on a Varian INOVA 600 NMR (600 MHz for ^{1}H, 151 MHz for ^{13}C) with a 5 mm inverse-detection HCN probe. dqfCOSY spectra were processed using Topspin (Bruker) and zero filled 8 k and 4 k points in the direct and indirect dimensions, respectively. Differential analysis of dqf-COSY spectra was adapted from previous work (*8, 9*). In short, dqfCOSY spectra were overlaid using Topspin and differentially present peaks were further characterized. HPLC-MS analysis was conducted using an HPLC system with a diode array detector operating at wavelengths of 210, 230, and 260 nm and connected to a Quattro II spectrometer (Micromass/Waters) operated in positive-ion (ESI+) or negative-ion electrospray ionization (ESI-) mode. Data acquisition and processing for the HPLC-MS was controlled by Waters MassLynx software. Reverse phase chromatography using an eclipse XDB-C18 column (Agilent) was performed using a 95% to 0% H_2O (0.1% acetic acid)/acetonitrile gradient. Indole, ICA, ICOOH, indole acetic acid standards (Sigma Aldrich, St. Louis MO) were used for structural confirmation and to determine the concentration of these compounds in the bacterial extracts based on UV absorbance.

In vivo infections and analysis MyD88$^{-/-}$mice on a C57BL/6 background were the generous gift of David Underhill, and were originally generated in the lab of Shizuo Akira

(see also [30]). Animal care was provided in accordance with protocols approved by the Institutional Animal Care and Use Committee of Emory University. *C. rodentium* were prepared by overnight culturing (12 to 16 hours) at 37°C in LB without shaking. Cultures were harvested by centrifugation and resuspended in a 20% sucrose solution. For infections, drinking water was replaced with *C. rodentium* suspension overnight. The volume of suspension was measured before and after administration, and the number of bacteria in the inoculum was calculated following retrospective plating. The average dosage was 2×10^8CFU/mouse. Survival of infected mice and changes in body weight were monitored daily. Mice losing at least 15% of their original weight were euthanized. For histological studies, colons, livers, and spleens were removed from infected mice, fixed in 10% formalin, and embedded in paraffin. Sections (5 µm) were cut and stained with H&E by the Translational Research Lab at Emory University. To measure the CFU of C. rodentium, tissue samples of colon, liver and spleen weighing ~0.1 to 0.3 g were homogenized at low speed with a Tissuemizer (Fisher Scientific) in 1 mL of PBS. The lysate was plated on MacConkey agar plates at various dilutions, and C. rodentium colonies were recognized as pink with a white rim as previously described (*10, 11*). Pink colonies were counted after 20 hours of incubation at 37°C to determine the CFU per gram of tissue. A total of 45 mice were used to conduct the experiments; all mice were age-matched.

Statistical analysis. Methods have been described in detail elsewhere (*4*). Briefly, for *C. elegans* survival experiments, we used an ANOVA and a test for linear trend in survival over time. The comparisons were highly significant. Mean survival +/− SEM is shown for the indicated time point. For conditioning experiments, we used ANCOVA to

remove the effects of pre-existing mutant differences, and ensure that mutants are starting out approximately equal, on average, with respect to all factors that might be pertinent to how well they are likely to respond to the conditioning paradigms. Such a correction is useful because individual differences in conditioning displayed by a particular mutant could potentially be correlated with survival rate. For these experiments, 95% confidence intervals are shown. Thus, significance at the 0.05 level is achieved between conditions or mutants when confidence intervals do not overlap. For mortality curves with mice, a Kaplan Meyer test determined statistical significance. For other experiments in Figures 5–7, a Student's t test assessed statistical significance. Results were considered significant if the p value was less than 0.01. Statistical significance relative to the control is indicated by an *.

Table D.1. High-resolution MS data for 1-HP and indole-derived *C. elegans* metabolites acquired using negative-ion and positive-ion electrospray ionization (*12*). *GS and SVH acquired data.*

Compound	Ion	Ion formula	Calculated *m/z*	Observed *m/z*
2	$[M+H]^+$	$C_{18}H_{19}N_2O_6^+$	359.1238	359.1221
3	$[M-H]^-$	$C_{18}H_{18}N_2O_9P^-$	437.0755	437.0755
4	$[M+H]^+$	$C_{24}H_{29}N_2O_{11}^+$	521.1766	521.1757
5a-b	$[M+H]^+$	$C_{30}H_{39}N_2O_{16}^+$	683.2294	683.2222
7	$[M-H]^-$	$C_{14}H_{16}NO_5^-$	278.1034	278.1071
8	$[M-H]^-$	$C_{14}H_{17}NO_8P^-$	358.0697	358.0701

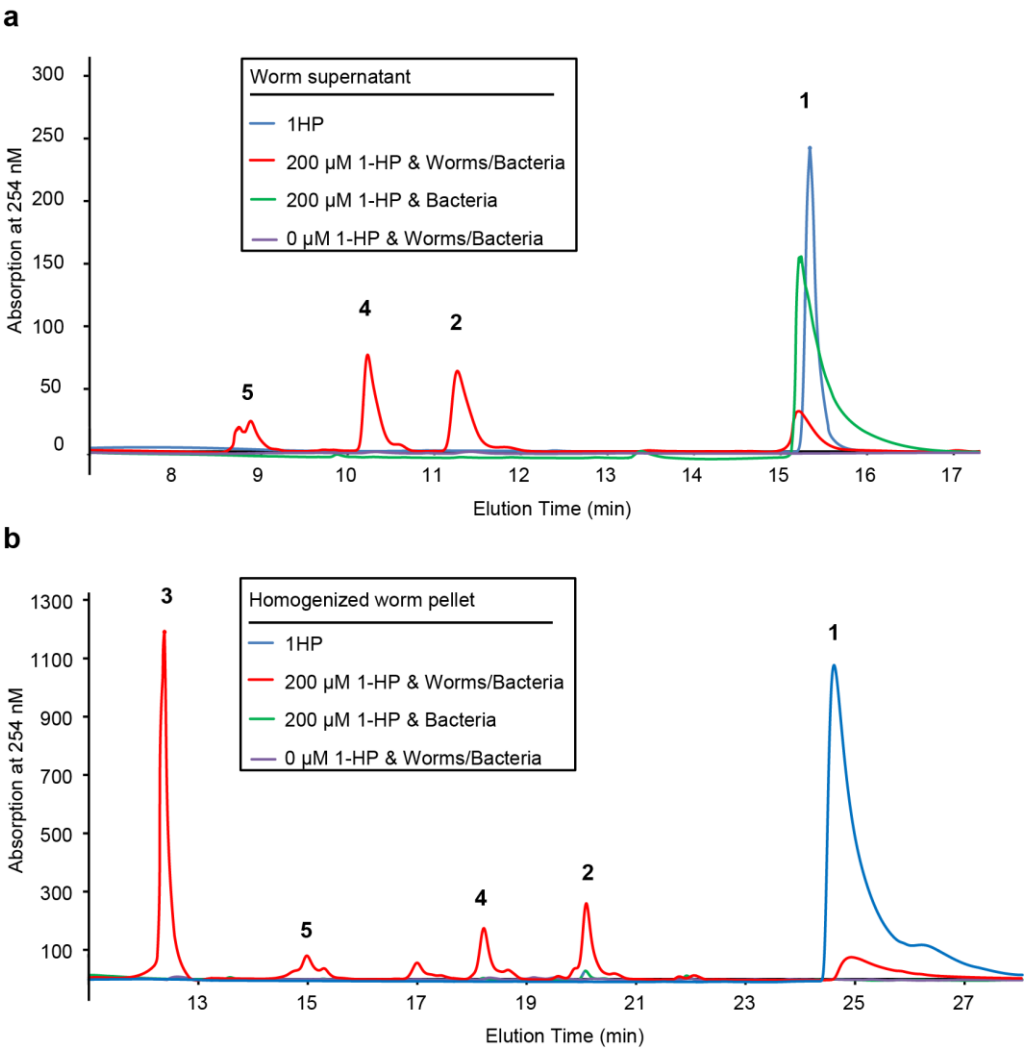

Figure D.1. HPLC-UV-Chromatograms of *C. elegans* supernatants and homogenized worm pellets after treatment with 1-HP. (a) UV Chromatogram of 1-HP (dark blue), worm media from 1 million wild type (N2) young adults exposed to 0 µM 1-HP (purple) or 200 µM 1-HP (red) for 24 hours, and 1% *E. coli* HB101 exposed to 200 µM 1-HP for 24 hours (green). (b) UV chromatogram of 1-HP (blue), the homogenates of 1 million wild type (N2) young adults exposed to 0 µM 1-HP (purple) or 200 µM 1-HP (red) for 24 hours, and 1% *E. coli* HB101 exposed to 200 µM 1-HP for 24 hours (green). The 1-HP curves should be interpreted for elution time only and may not indicate relative amounts of the compound. In both (a) and (b) peaks are labeled to indicate compounds as in Figure 1. *GS acquired data, YI assisted with analysis.*

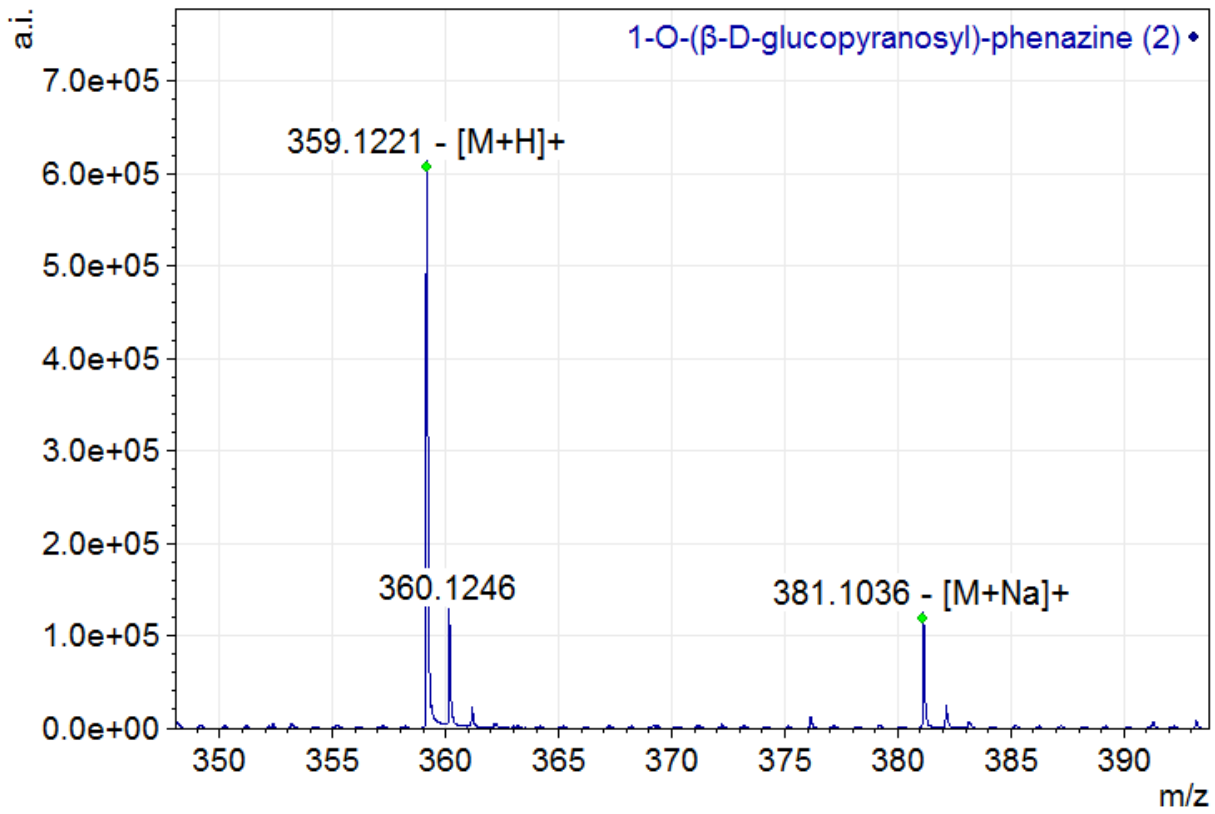

Figure D.2.1. Mass spectrum of purified 1-*O*-(β-D-glucopyranosyl)-phenazine (2) from the supernatants of 1-HP exposed young-adult worms in ESI+ mode with annotation of the $[M+H]^+$ peak at *m/z* 359 and the $[M+Na]^+$ peak at *m/z* 381. *Data acquired by GS.*

a

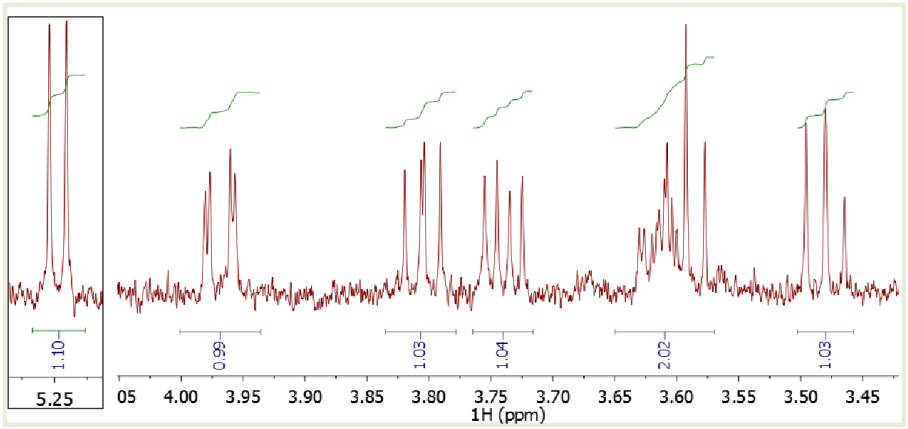

b

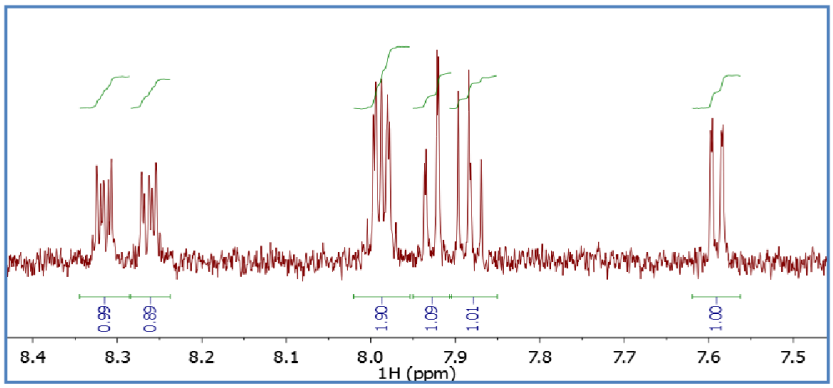

c

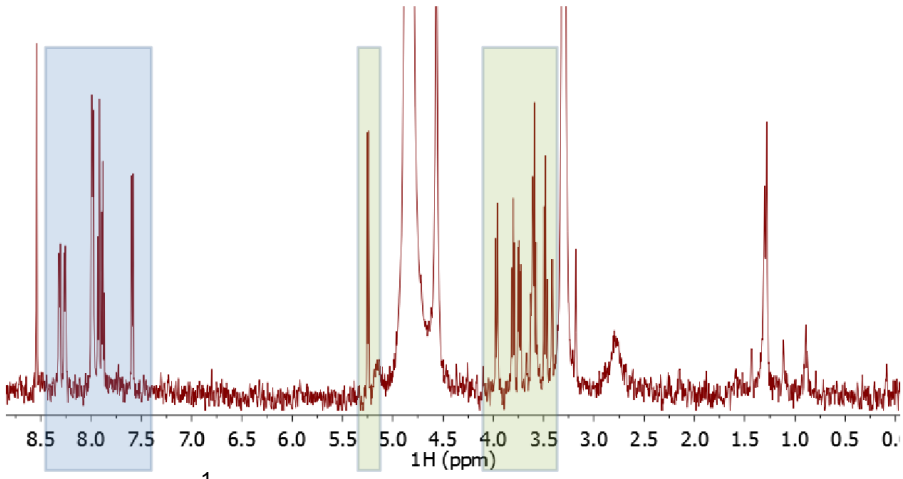

Figure D.2.2. ^{1}H NMR Spectrum (600 MHz, methanol-d_4) of purified 1-*O*-(β-D-glucopyranosyl)-phenazine (2). Expansions of the ^{1}H-NMR spectrum highlighting the carbohydrate (a) and aromatic (b) regions. (c) Full ^{1}H-NMR spectrum with regions shown in (a) and (b) highlighted in blue and green, respectively. *Data acquired by GS.*

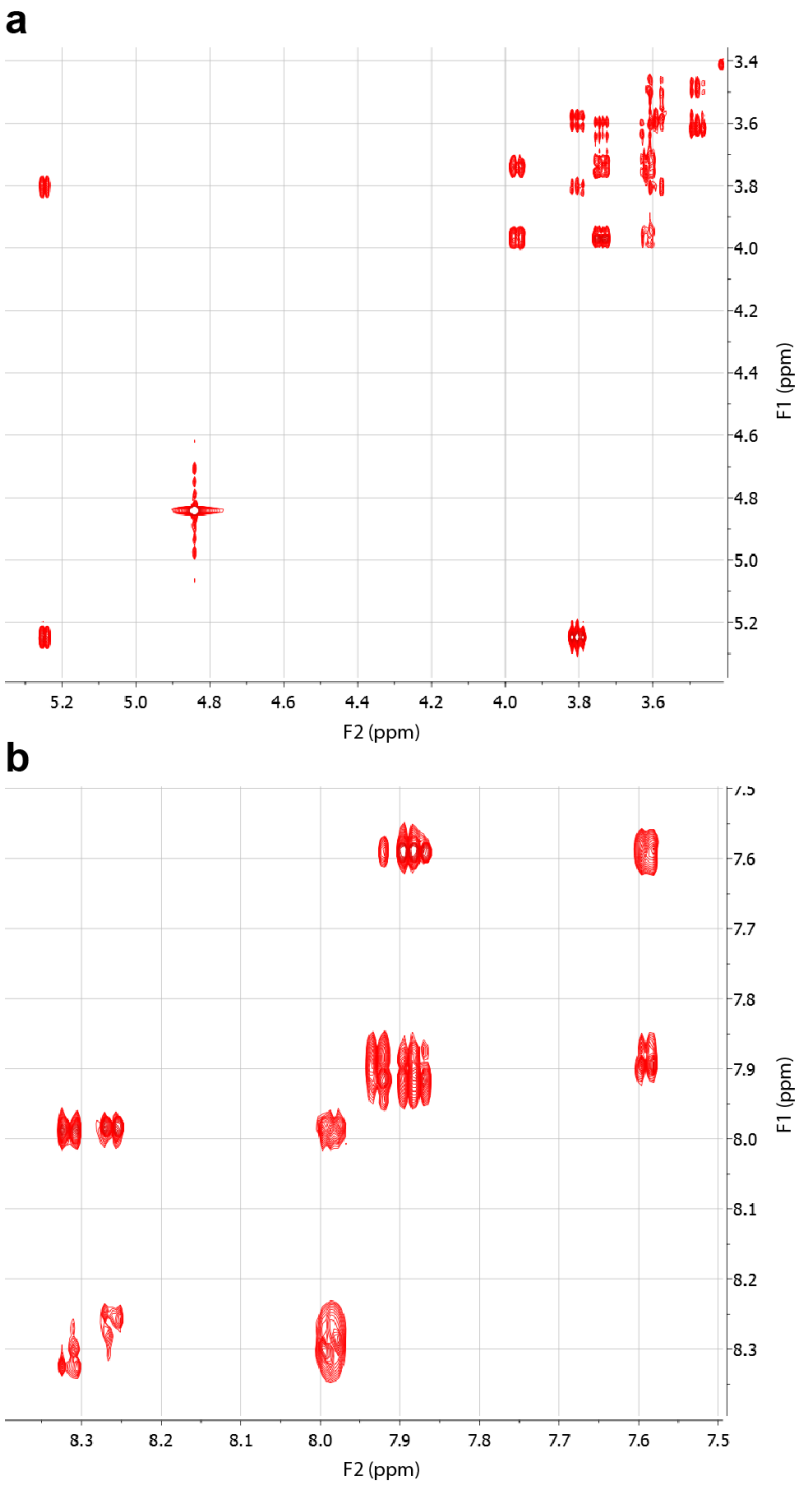

Figure D.2.3. gCOSY Spectrum (600 MHz, methanol-d_4) of purified 1-*O*-(β-D-glucopyranosyl)-phenazine (2). Expansions showing the carbohydrate (a) and aromatic (b) regions. *Data acquired by GS.*

a

#	Type	δ_H [ppm]	J [Hz]
2	dd	7.59	7.5, 1.2
3	dd	7.88	8.9, 7.5
4	dd	7.93	8.8, 1.2
6	ddd	8.32	
7	ddd	7.98	
8	ddd	7.98	
9	ddd	8.26	
1’	d	5.25	7.8
2’	dd	3.81	9.4, 7.8
3’	dd	3.59	9.2, 9.2
4’	dd	3.48	9.3, 9.3
5’	ddd	3.62	9.9, 6.1, 2.4
6’a	dd	3.74	12.1, 6.0
6’b	dd	3.97	12.0, 2.2

b

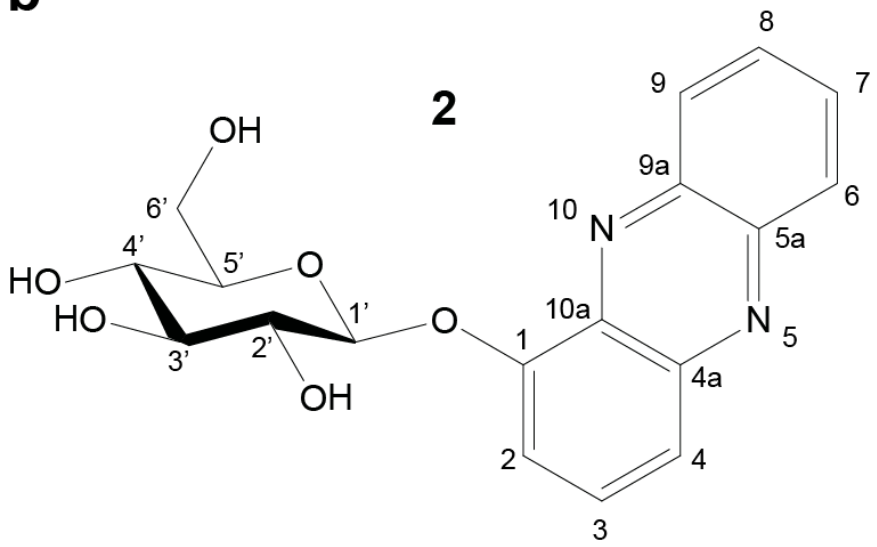

Figure D.2.4. NMR data and structure of purified 1-*O*-(β-D-glucopyranosyl)-phenazine (2) in methanol-d_4. (a) Table showing assignments (b) Structure of 1-*O*-(β-D-glucopyranosyl)-phenazine with atom numbers. *Data acquired by GS.*

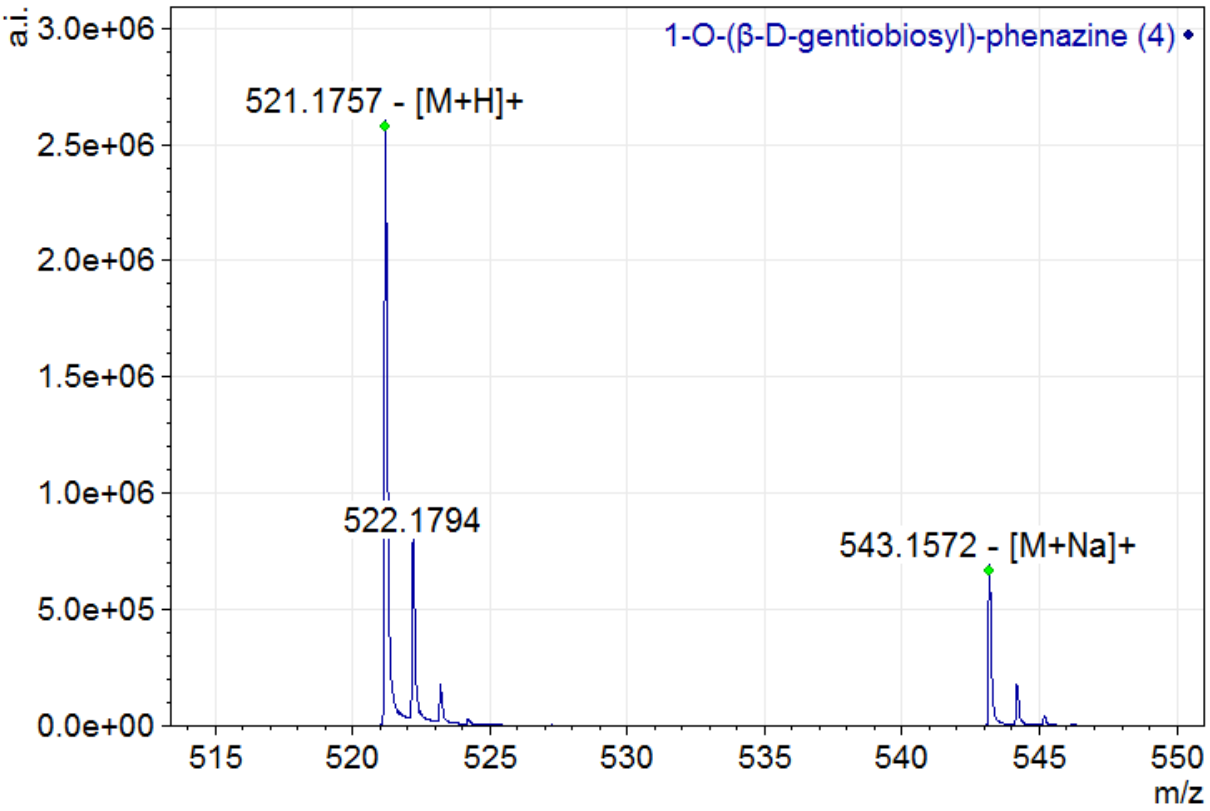

Figure D.3.1. Mass spectrum of purified 1-O-(β-D-gentiobiosyl)-phenazine (4) from the supernatants of 1-HP exposed young-adult worms in ESI+ mode with annotation of the $[M+H]^+$ peak at *m/z* 521 and the $[M+Na]^+$ peak at *m/z* 543. *Data acquired by GS.*

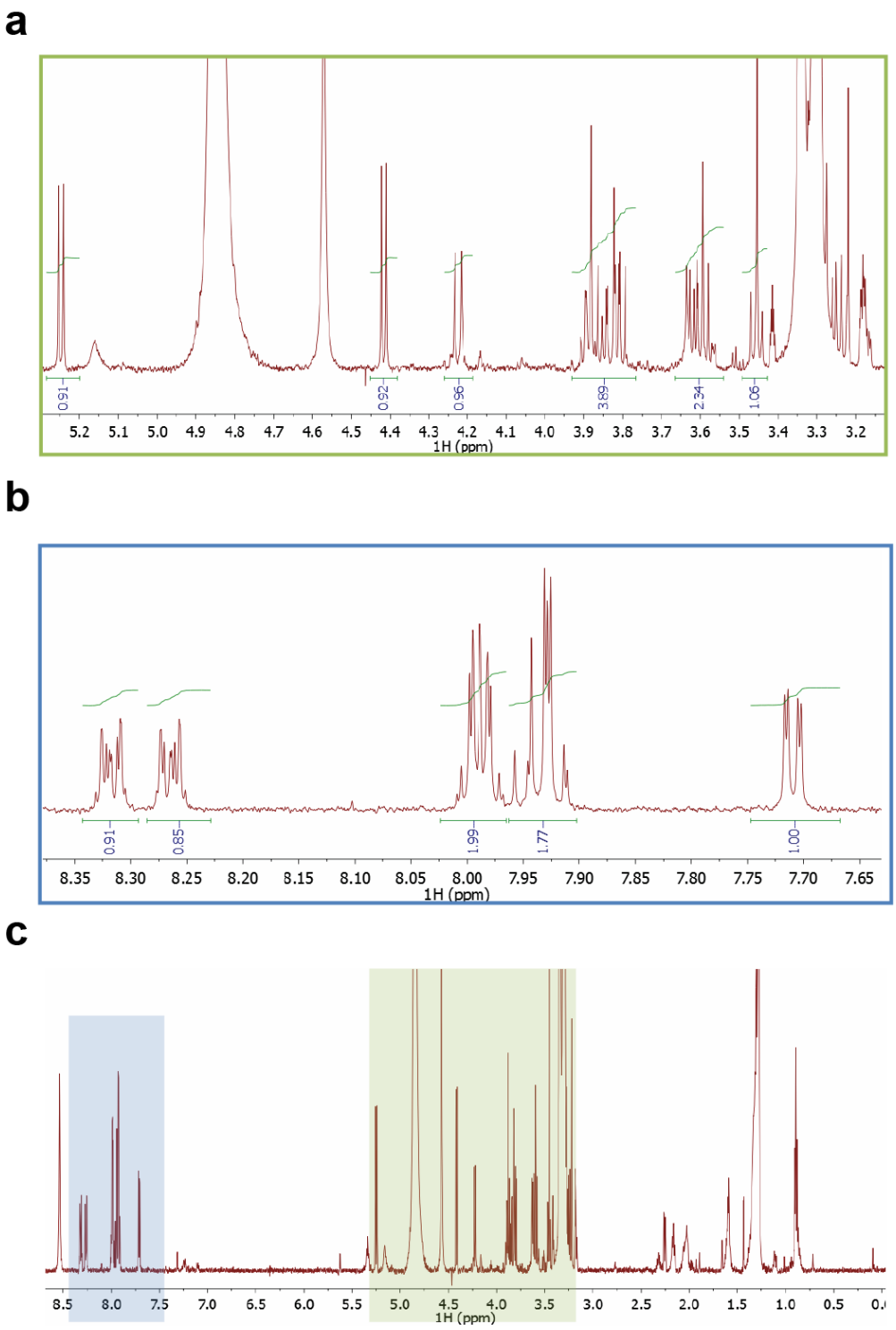

Figure D.3.2. ^{1}H NMR Spectrum (600 MHz, methanol-d_4) of purified 1-O-(β-D-gentiobiosyl)-phenazine (4). Expansions showing the carbohydrate (a) and aromatic (b) regions. (c) Full spectrum. Regions shown in (a) and (b) are highlighted in blue and green, respectively. *Data acquired by GS.*

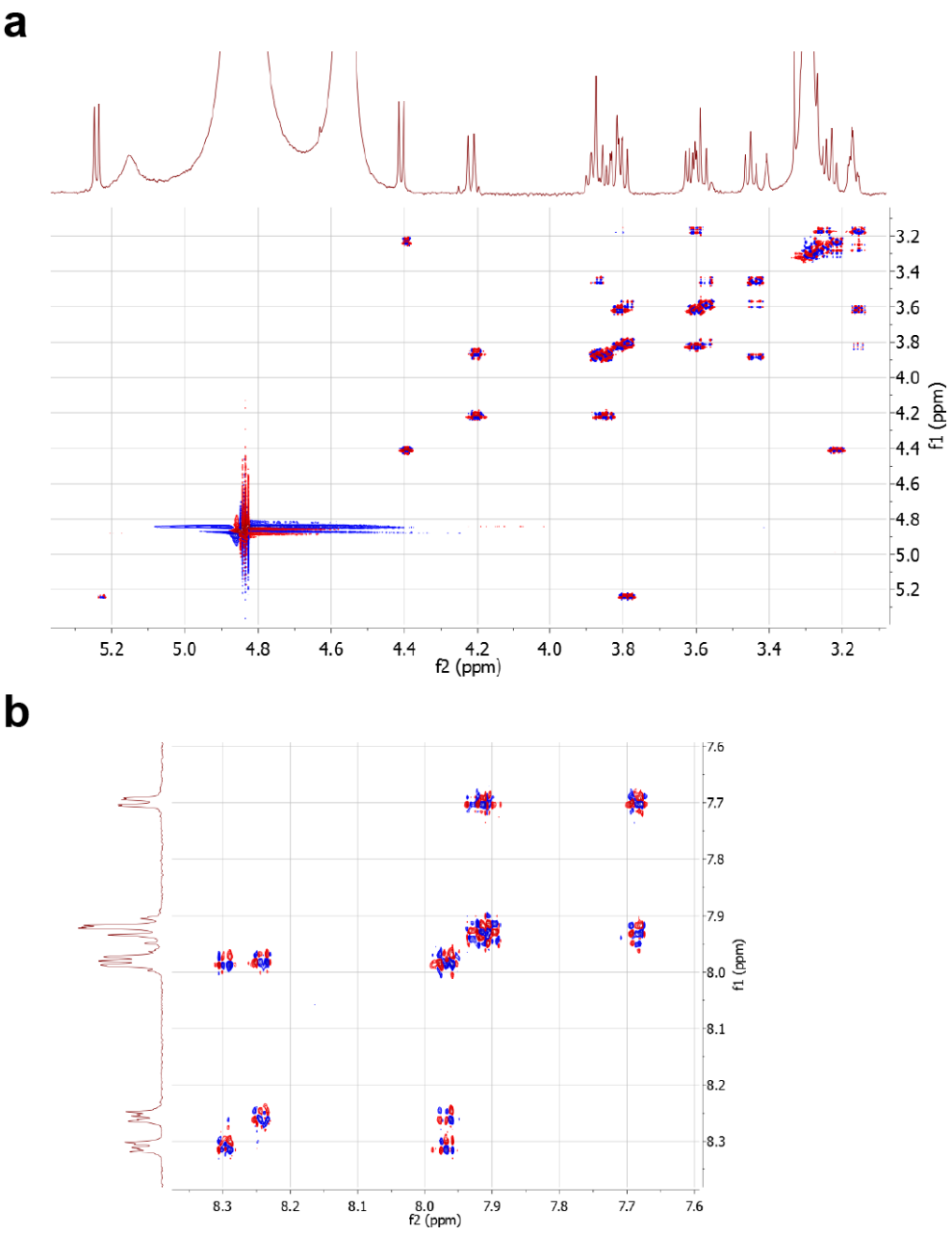

Figure D.3.3. dqfCOSY Spectrum (600 MHz, methanol-d_4) of purified 1-O-(β-D-gentiobiosyl)-phenazine (4). Expansions showing the carbohydrate (a) and aromatic (b) regions. *Data acquired by GS.*

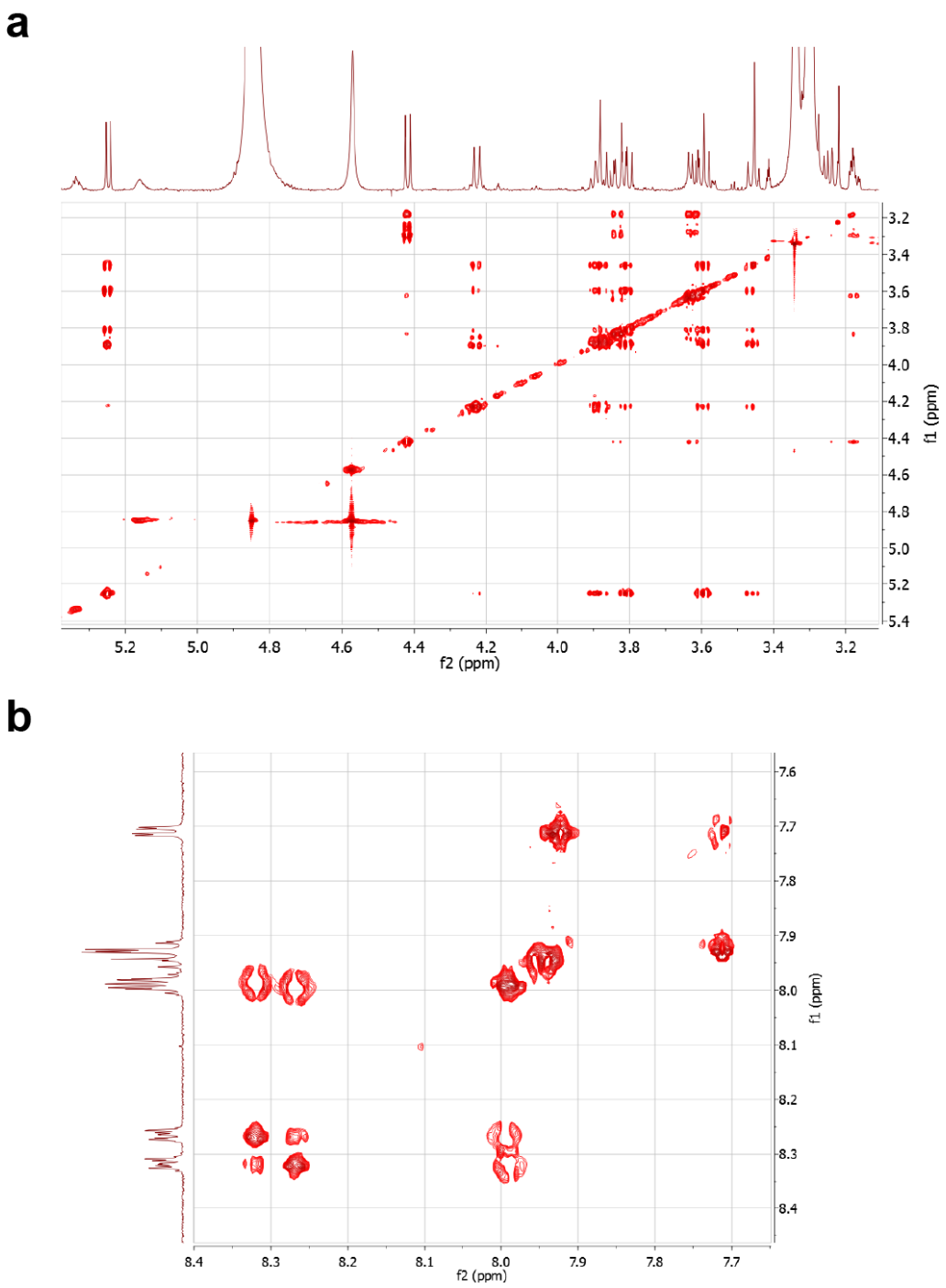

Figure D.3.4. TOCSY Spectrum (600 MHz, methanol-d_4) of purified 1-O-(β-D-gentiobiosyl)-phenazine (4). Expansions showing the carbohydrate (a) and aromatic (b) regions. *Data acquired by GS.*

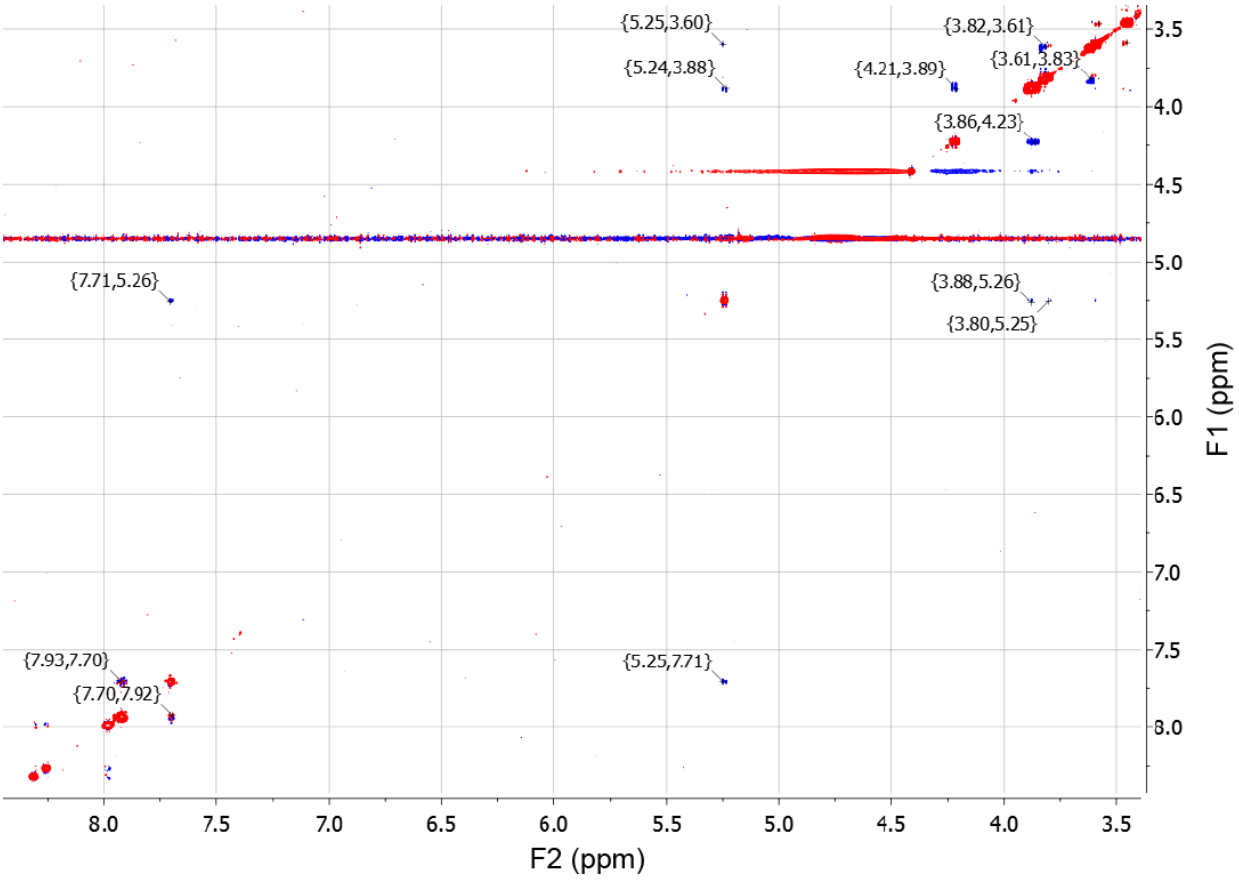

Figure D.3.5. NOESY Spectrum (600 MHz, methanol-d_4) of purified 1-O-(β-D-gentiobiosyl)-phenazine (4). *Data acquired by GS.*

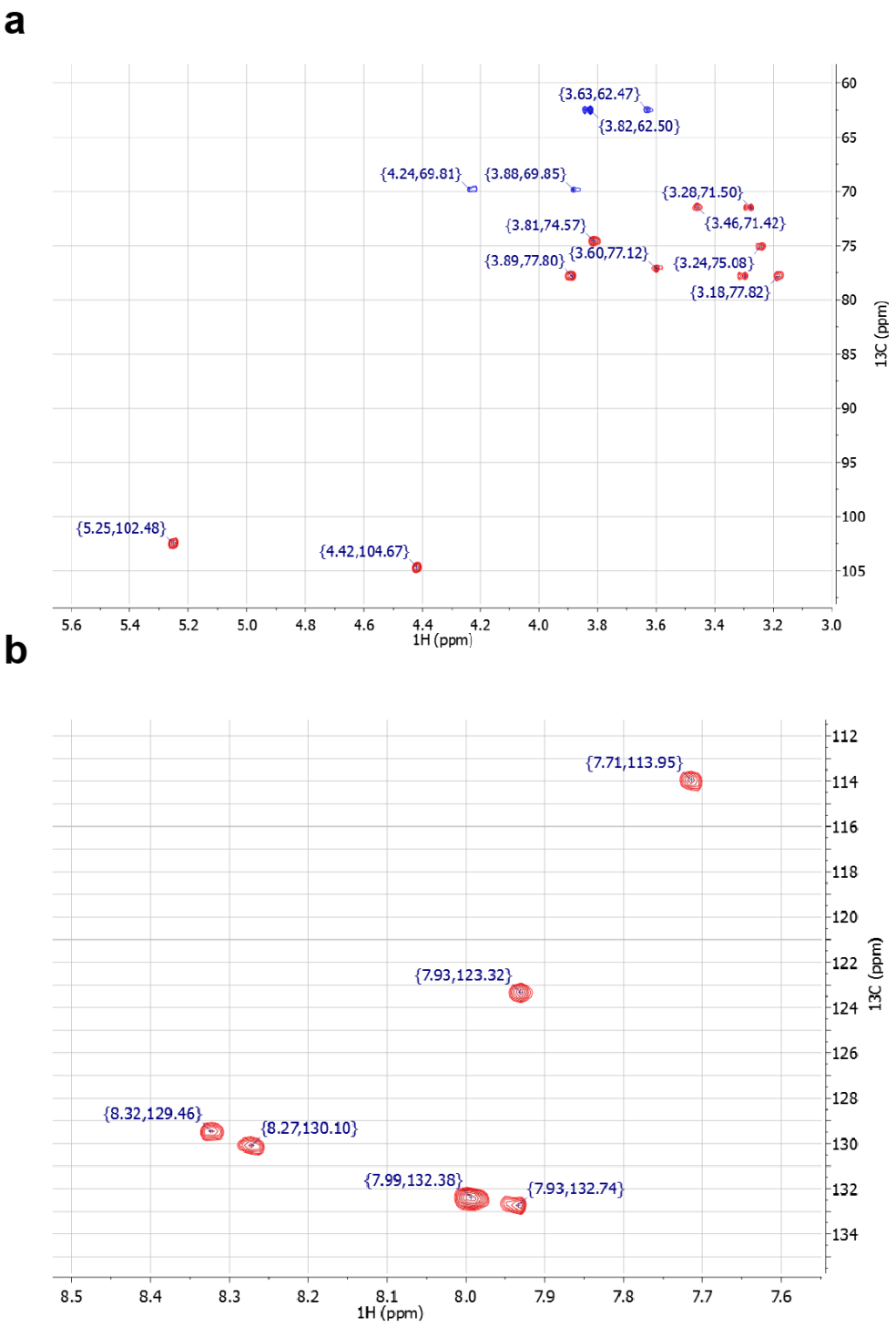

Figure D.3.6. HSQC Spectrum (600 MHz for ^{1}H, 150 MHz for ^{13}C, methanol-d_4) of purified 1-O-(β-D-gentiobiosyl)-phenazine (4). Expansions showing the carbohydrate (a) and aromatic (b) regions. *Data acquired by GS.*

a

#	Type	δ_H [ppm]	J [Hz]	δ_C	NOESY
2	dd	7.7	6.9, 1.8	114	1'
3-4	dd	7.93		132.7, 123.3	
6	ddd	8.31		129.5	
7-8	ddd	7.99		132.4, 132.4	
9	ddd	8.26		130.1	
1'	d	5.24	7.8	102.5	2
2'	dd	3.8	9.3, 7.7	74.6	
3'	dd	3.59	9.2, 9.2	77.1	
4'	dd	3.45	9.2, 9.2	71.4	
5'	ddd	3.89		77.8	
6a'	dd	3.87		69.9	6b'
6b'	dd	4.22	10.2	69.8	6a'
1"	d	4.41	7.6	104.7	
2"	dd	3.24	8.3, 8.3	75.1	
3"	dd	3.3		77.8	
4"	dd	3.27		71.5	
5"	ddd	3.17		77.8	
6a"	dd	3.61	11.9, 6.0	62.5	
6b"	dd	3.82	11.6, 2.6	62.5	

b

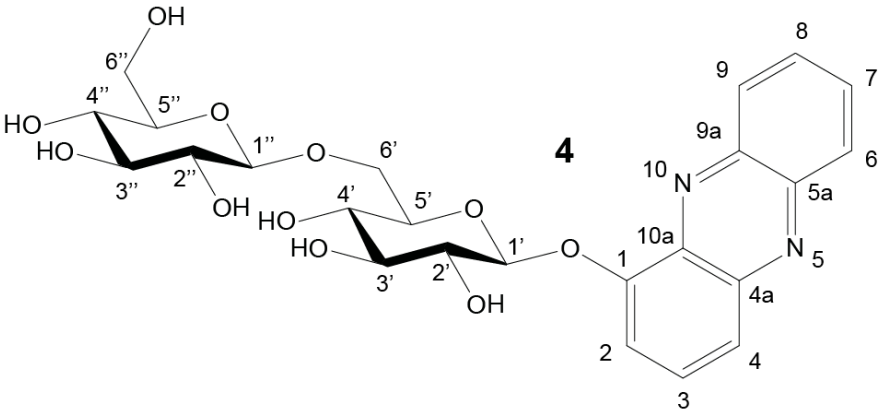

Figure D.3.7. NMR data of purified 1-O-(β-D-gentiobiosyl)-phenazine (4) in methanol-d_4 . (a) Table showing assignments (b) Structure. *Data acquired by GS.*

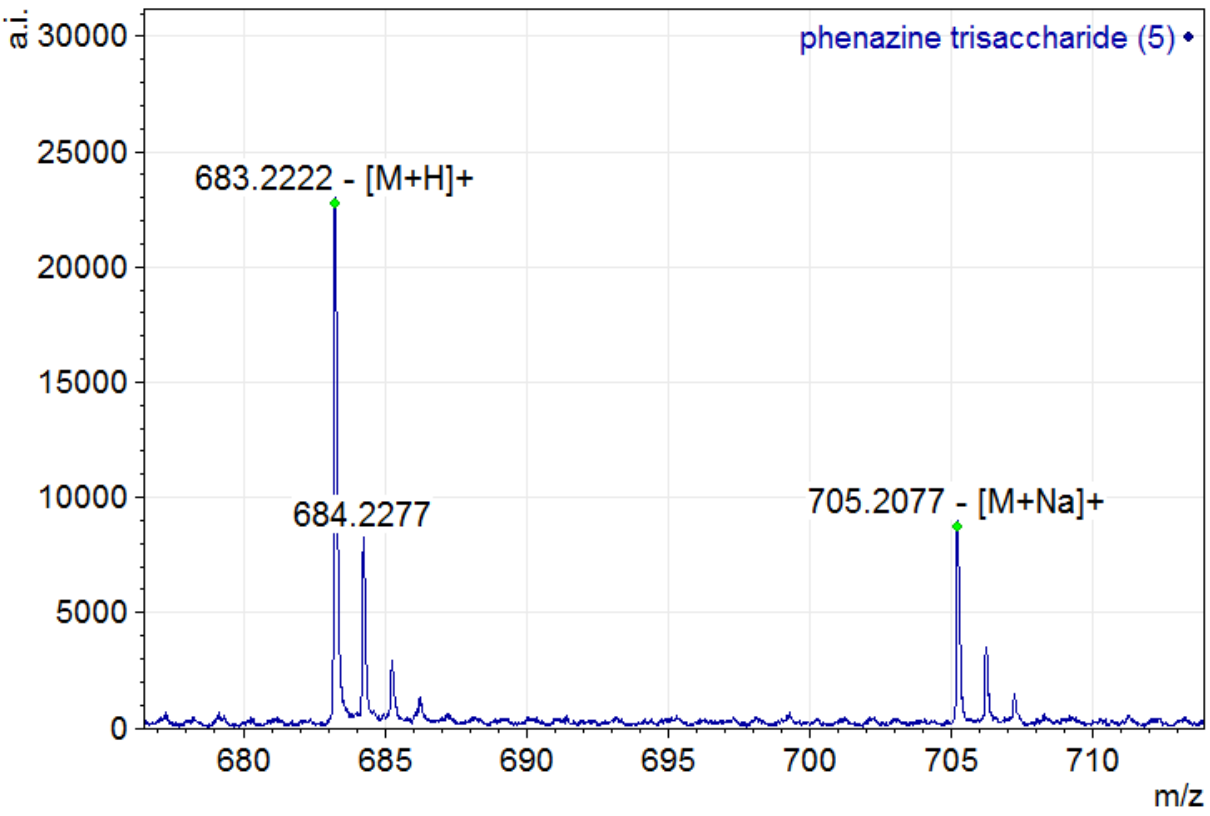

Figure E.4.1. Mass spectrum of purified phenazine trisaccharide (5) from the supernatants of 1-HP exposed young-adult worms in ESI+ mode with annotation of the $[M+H]^+$ peak at *m/z* 683 and the $[M+Na]^+$ peak at *m/z* 705. *Data acquired by GS.*

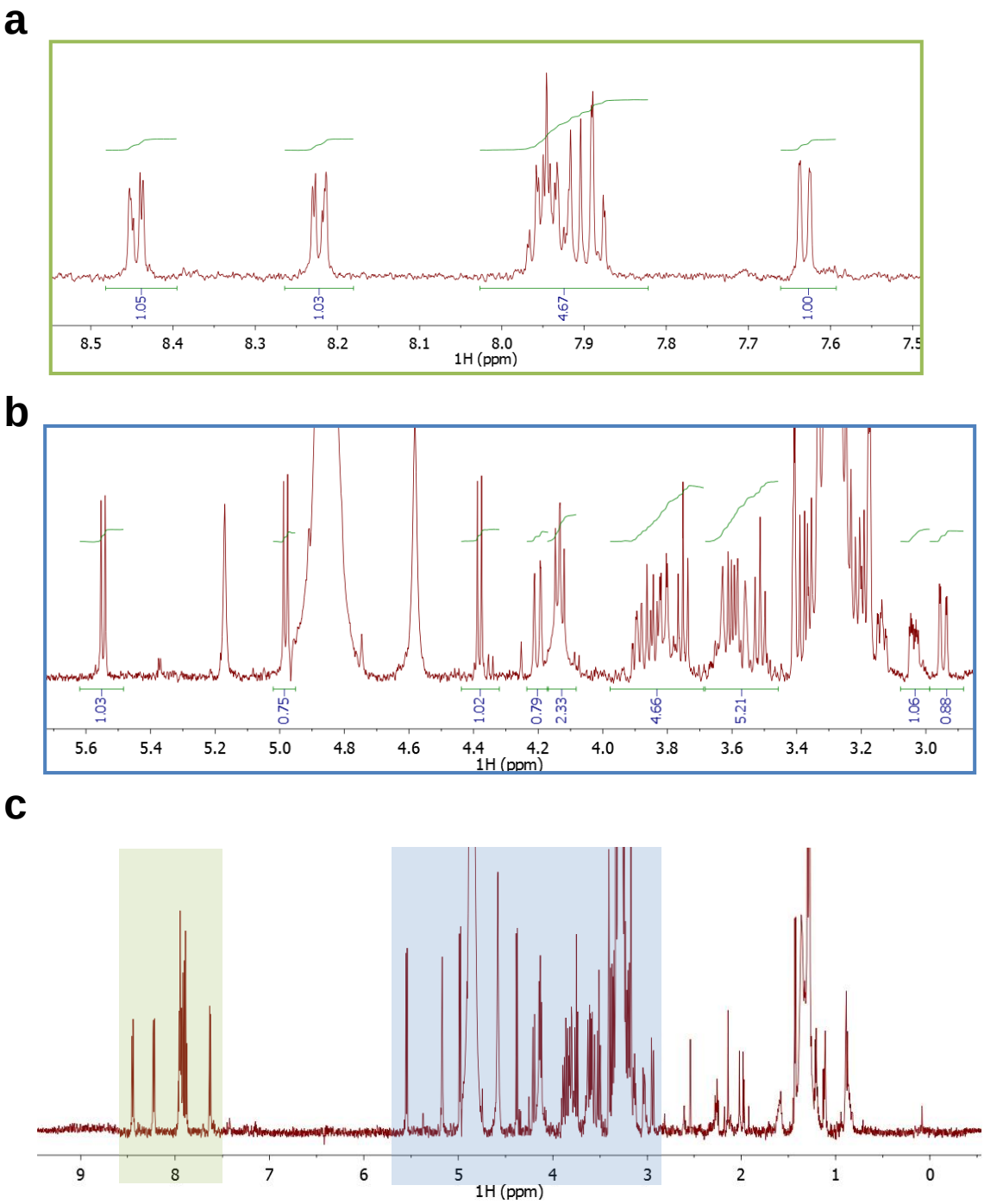

Figure D.4.2. ^{1}H NMR Spectrum (600 MHz, methanol-d_4) of purified phenazine trisaccharide (5). Expansions showing the aromatic (a) and carbohydrate (b) regions. (c) Full spectrum. Regions shown in (a) and (b) are highlighted in blue and green, respectively. *Data acquired by GS.*

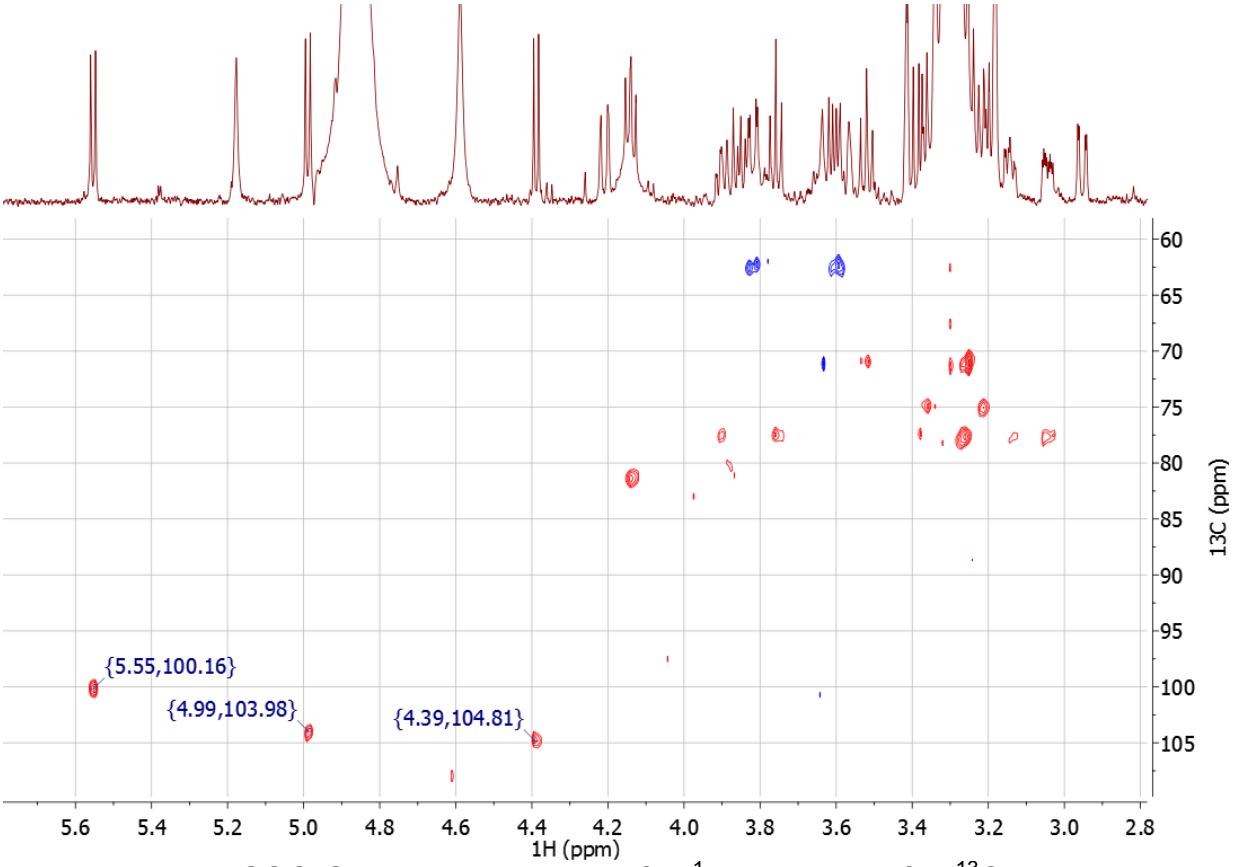

Figure D.4.3. HSQC Spectrum (600 MHz for ^{1}H, 150 MHz for ^{13}C, methanol-d_4) of purified phenazine trisaccharide (5). Expansion showing the carbohydrate region. The three anomeric carbons are labeled. *Data acquired by GS.*

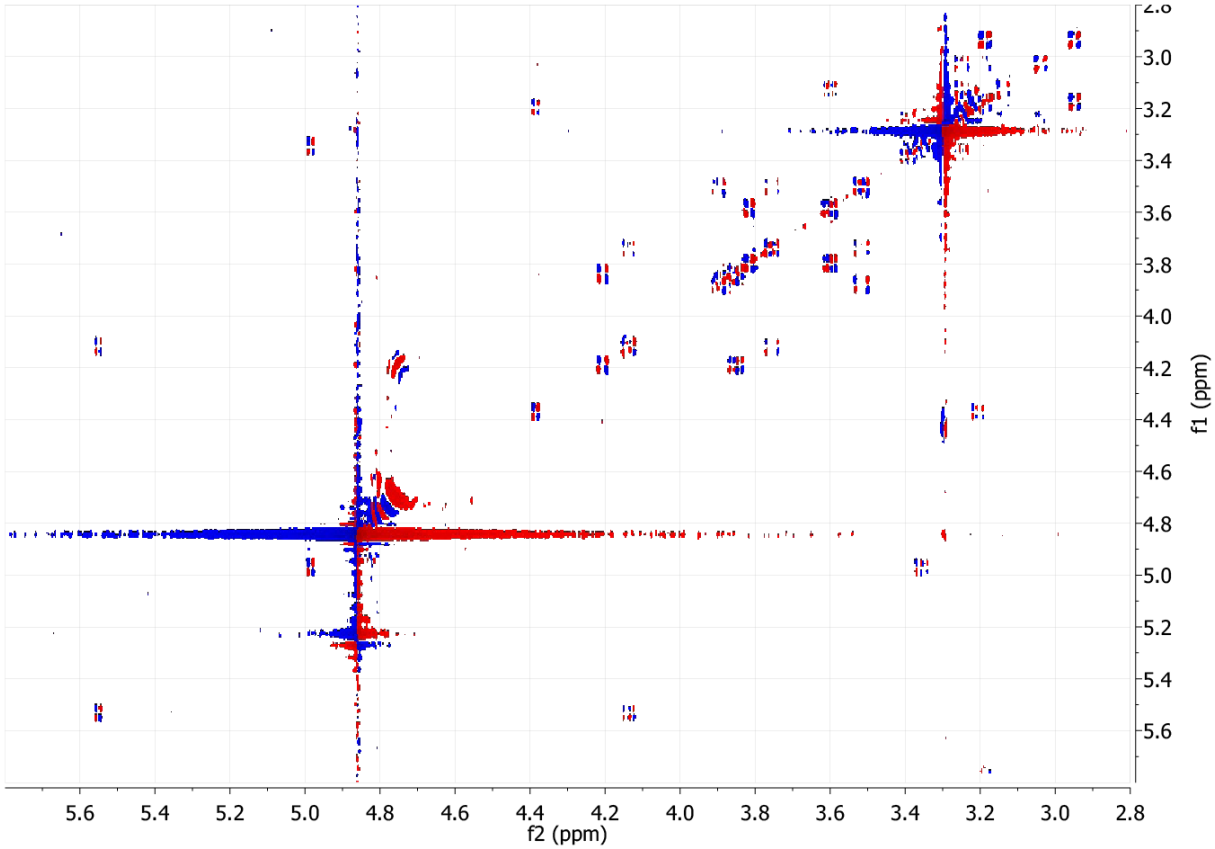

Figure D.4.4. dqfCOSY Spectrum (600 MHz, methanol-d_4) of purified phenazine trisaccharide (5). Expansion showing the carbohydrate region. *Data acquired by GS.*

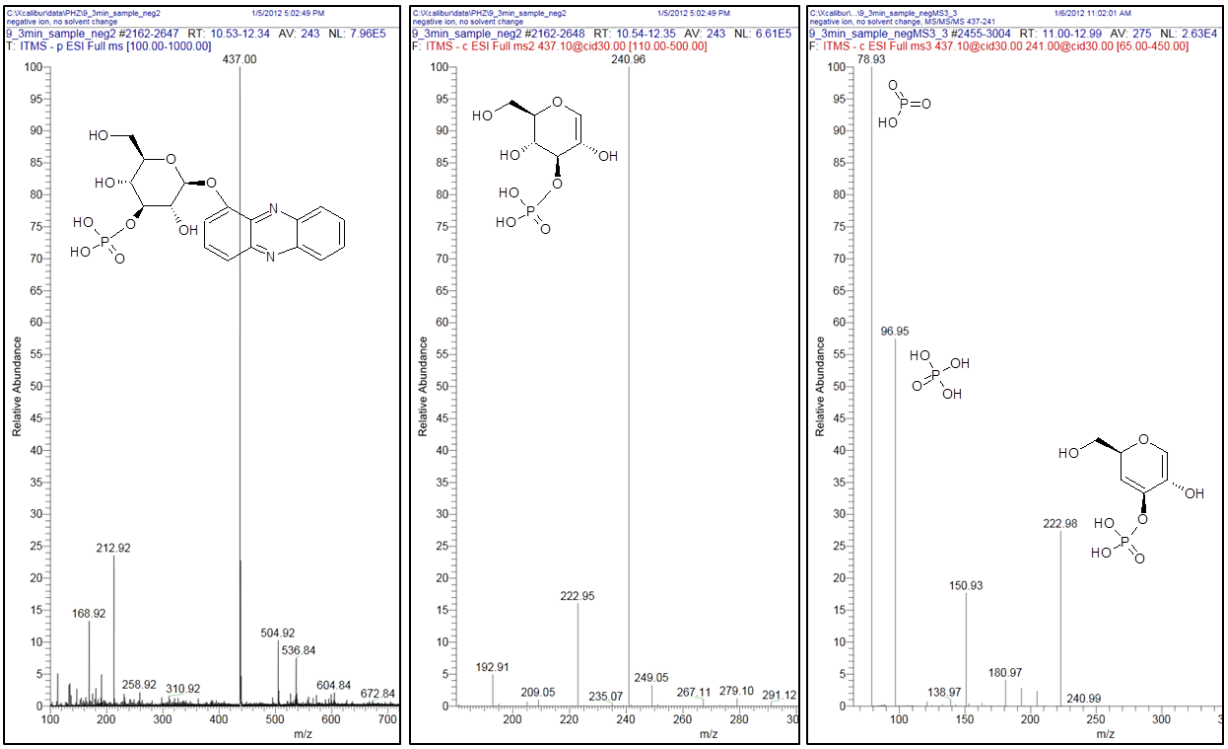

Figure D.5.1. Mass Chromatograms of purified 1-*O*-(3'-*O*-phospho-β-D-glucopyranosyl)-phenazine (*13*) from the homogenates of 1-HP exposed young-adult worms. (left) Total ion scan showing the $[M-H]^-$ peak at *m/z* 437 (center) MS-MS of *m/z* 437 showing the $[M-H]^-$ peak at *m/z* 241 (right) MS^3 of *m/z* 241 showing $[M-H]^-$ peaks at *m/z* 223, 96, and 79. *Data acquired by GS.*

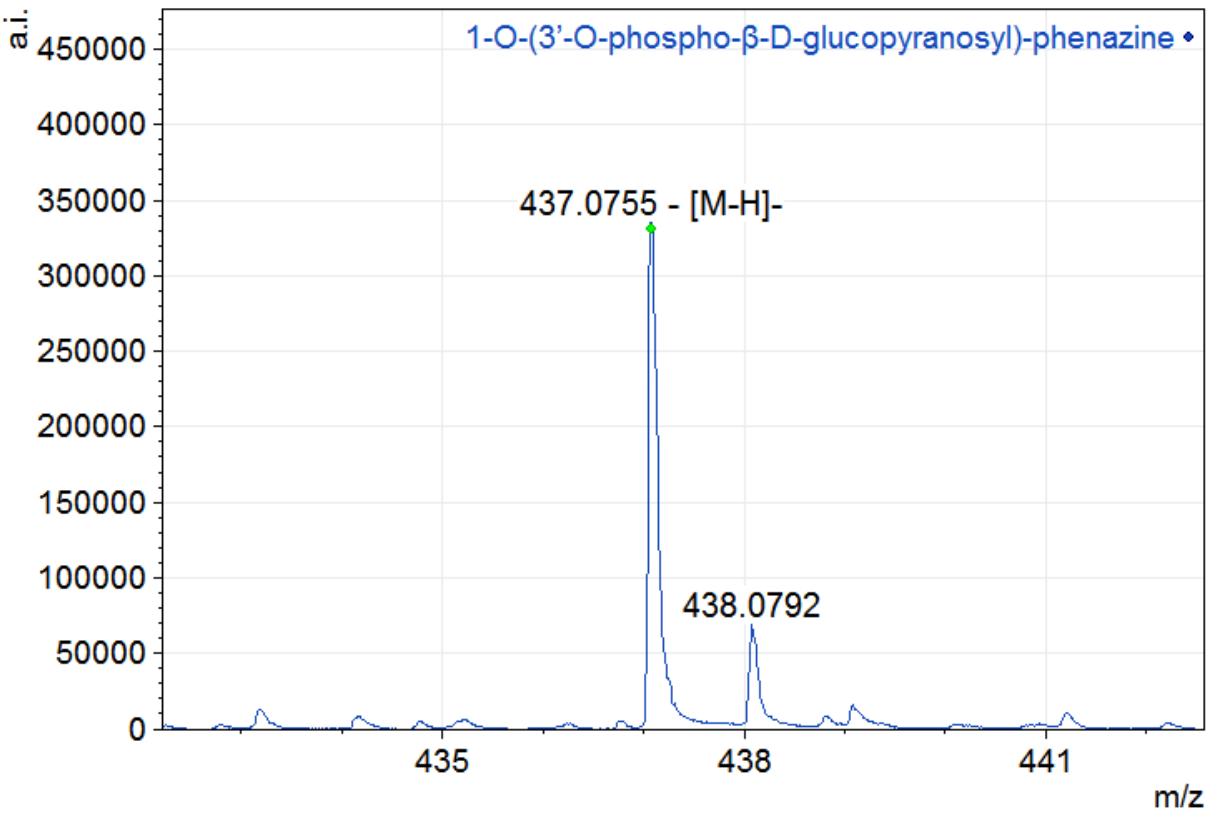

Figure D.5.2. Mass spectrum of purified 1-*O*-(3'-*O*-phospho-β-D-glucopyranosyl)-phenazine (*13*) from the homogenates of 1-HP exposed young-adult worms in ESI- mode with annotation of the $[M-H]^-$ peak at *m/z* 437. *Data acquired by GS.*

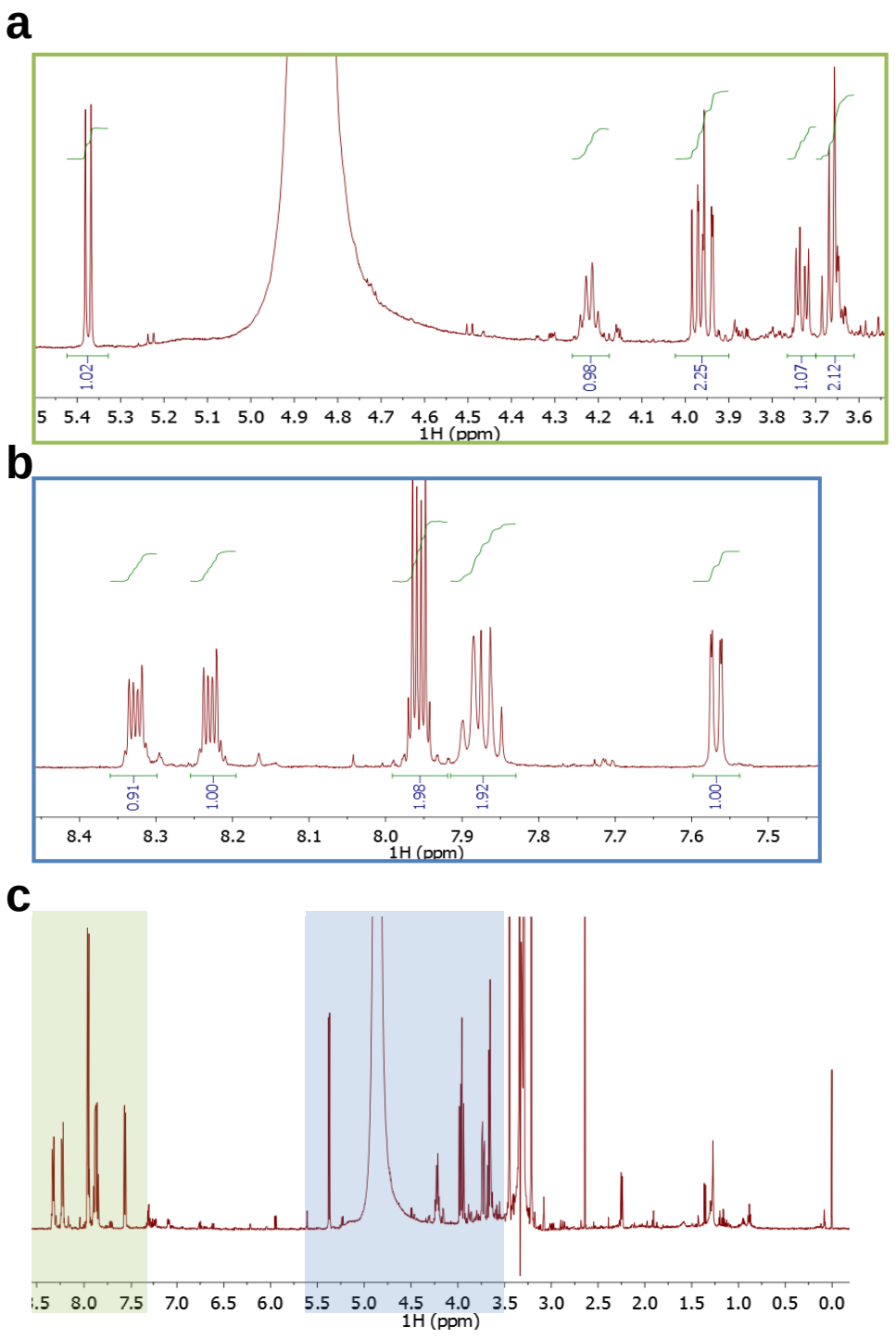

Figure D.5.3. ^{1}H NMR Spectrum (600 MHz, methanol-d_4) of purified 1-*O*-(3'-*O*-phospho-β-D-glucopyranosyl)-phenazine (*13*). Expansions showing the carbohydrate (a) and aromatic regions (b). (c) Full spectrum. Regions shown in (a) and (b) are highlighted in green and blue, respectively. *Data acquired by GS.*

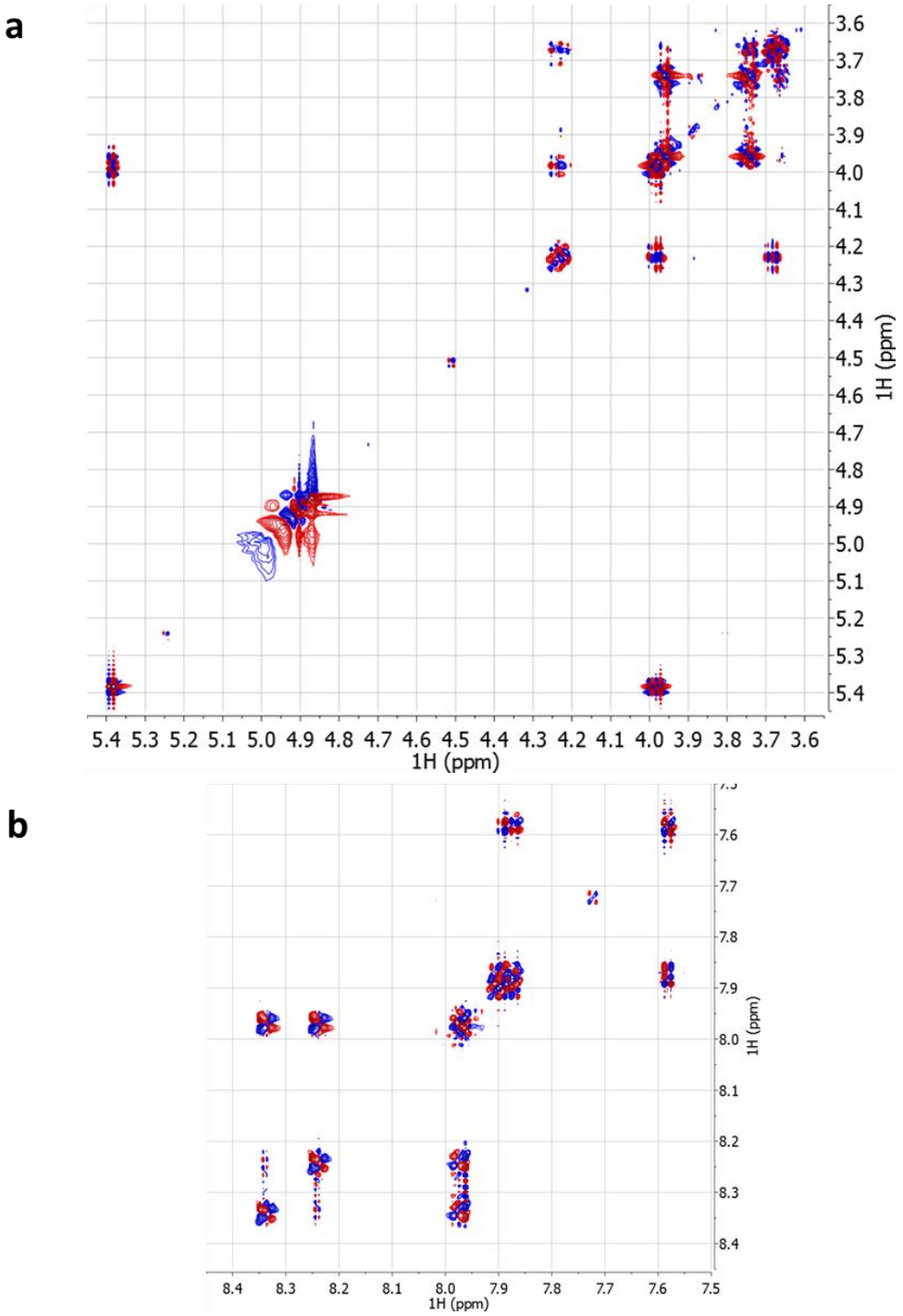

Figure D.5.4. dqfCOSY Spectrum (600 MHz, methanol-d_4) of purified 1-*O*-(3'-*O*-phospho-β-D-glucopyranosyl)-phenazine (*13*). (a) Expansions showing the carbohydrate and (b) aromatic regions. *Data acquired by GS.*

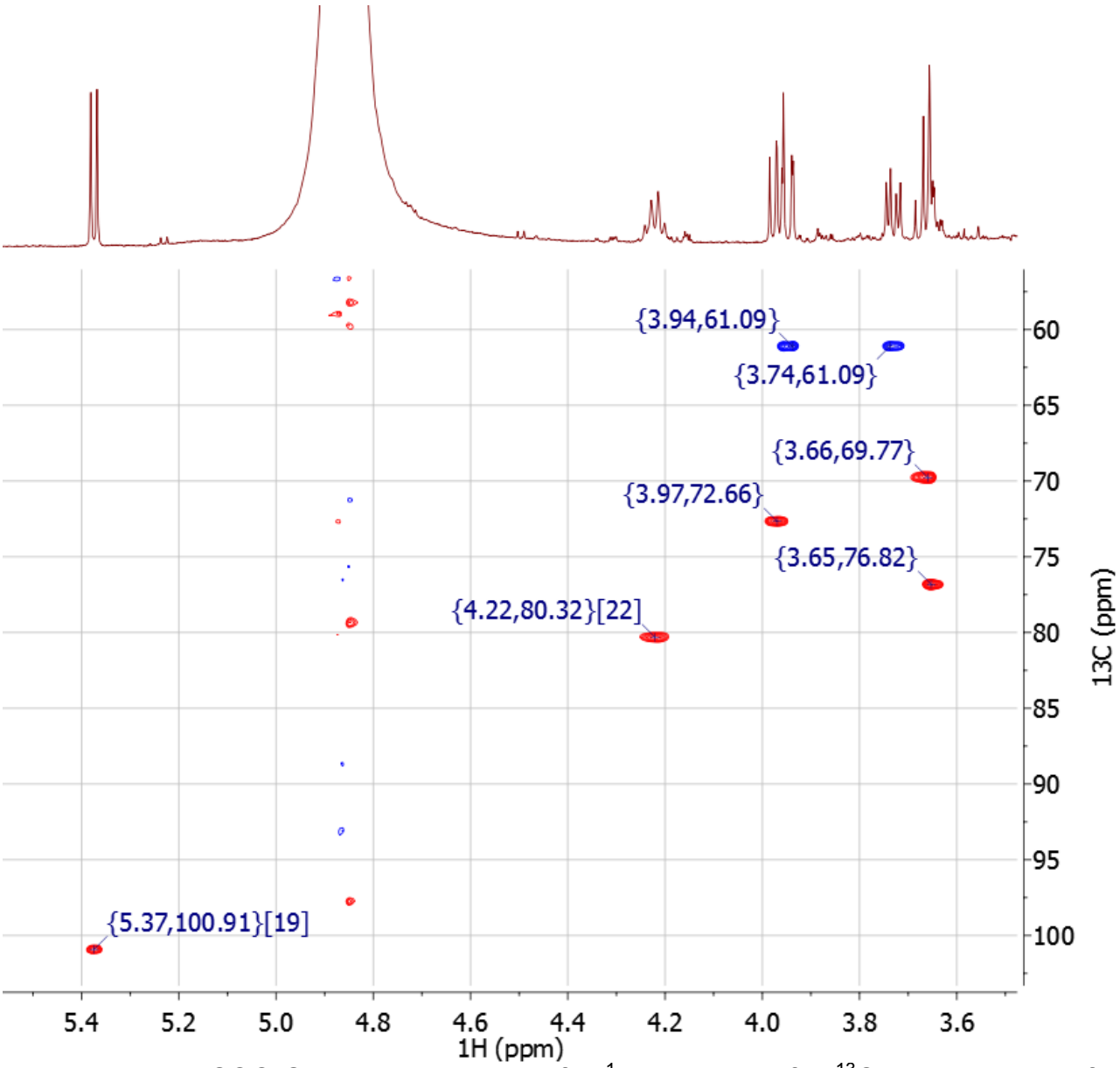

Figure D.5.5. HSQC Spectrum (600 MHz for ^{1}H, 150 MHz for ^{13}C, methanol-d_4) of purified 1-*O*-(3'-*O*-phospho-β-D-glucopyranosyl)-phenazine (*13*). Expansion showing the carbohydrate region. *Data acquired by GS.*

a

#	Type	δ_H [ppm]	J [Hz]	δ_C
1'	d	5.37	7.8	100.9
2'	dd	3.97	9.0, 7.8	72.7
3'	dd	4.24		80.3
4'	dd	3.68	9.7, 8.0	69.8
5'	ddd	3.65		76.8
6a'	dd	3.94	12, 1.7	61.1
6b'	dd	3.74	12, 5	61.1
2	dd	7.57	7.3, 1.5	112.1
3	dd	7.89		
4	dd	7.89		
6	ddd		6.7, 3.4	
7-8	ddd	7.96	6.6, 3.2	131.1
9	ddd		6.7, 3.4	

b

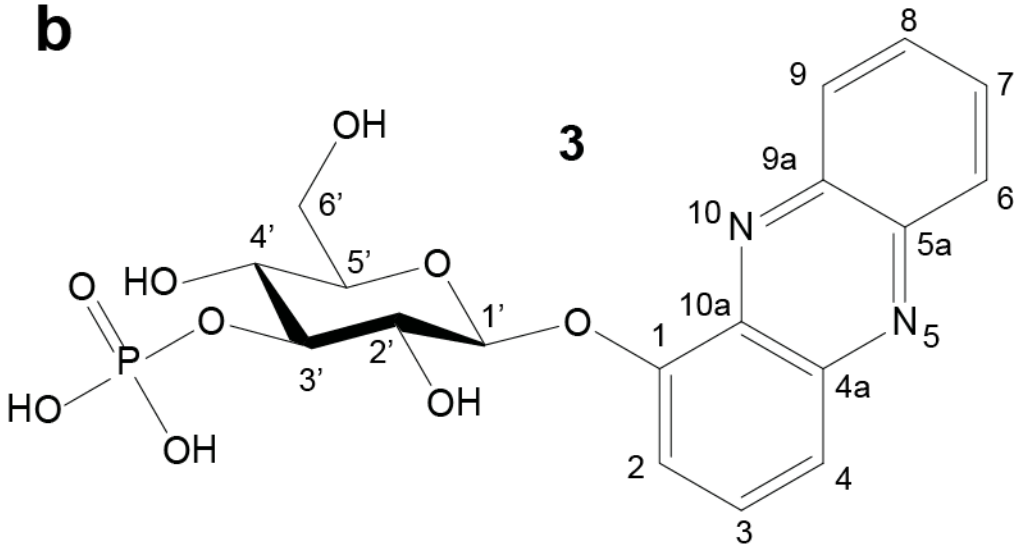

Figure D.5.6. NMR data of purified 1-*O*-(3'-*O*-phospho-β-D-glucopyranosyl)-phenazine (*13*) in methanol-d_4 . (a) Table showing assignments and (b) structure. *Data acquired by GS.*

a

Position	**(7)** δ ^{13}C [ppm]	**(7)** δ ^{1}H [ppm]	**(8)** δ ^{1}H [ppm]	**(7)** ^{1}H-^{1}H-coupling constants [Hz]	**(7)** HMBC correlations
2	126.2	7.40		$J_{2',3'}$ = 3.3	C-1 (weak), C-3', C-3a', C-7' (weak), C-7a'
3	103.2	6.49			C-2', C-3a', C-4' (weak), C-7a' (weak)
3a	130.3				
4	121.3	7.52		$J_{4',5'}$ = 8.0,	C-3', C-6', C-7a'
5	120.7	7.05		$J_{5',6'}$ = 7.4, $J_{3',5'}$ = 1.1,	C-3a', C-7'
6	122.4	7.15		$J_{6',7'}$ = 8.0, $J_{4',6'}$ = 1.0	C-4', C-7a'
7	111.2	7.54			C-3a', C-5'
7a	137.8				
1'	86.5	5.46	5.55	J1,2 = 9.0	C-2, C-3, C-5, C-2', C-7a'
2'	73.4	3.94	4.12	J2,3 = 9.0,	C-1, C-3
3'	78.9	3.60	4.24 (JH,P = 8 Hz)	J3,4 = 9.0	C-2, C-4
4'	71.2	3.50	3.68	J4,5 = 9.0	C-3, C-5, C-6
5'	80.4	3.58		J5,6a = 5.8	C-1, C-3, C-6
6'a	62.5	3.70		J6a,6b = 12.1	C-4, C-5
6'b		3.88		J5,6b = 2.2	C-4, C-5

[1]Characteristic ^{1}H NMR signals of (**8**).

b

7 (R = H)
8 (R = PO_3H_2)

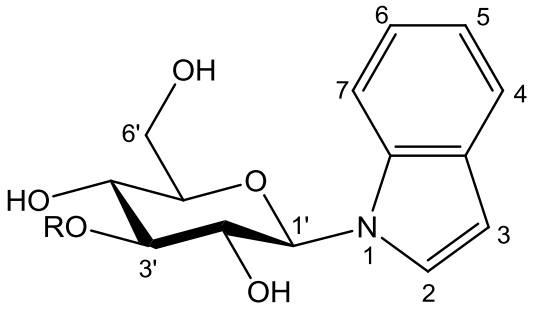

Figure D.6.1. NMR data of (purified or synthetic) *N*-(β-D-glucopyranosyl)-indole (7) and *N*-(3'-*O*-phospho-β-D-glucopyranosyl)-indole (8) (^{1}H (600 MHz), ^{13}C (151 MHz), and HMBC NMR spectroscopic data in methanol-d_4. Chemical shifts were referenced to ($CD_2\underline{H}OD$) = 3.31 ppm and ($\underline{C}D_2HOD$) = 49.05 ppm). (a) Table showing assignments (b) Structures. *Data acquired by SVH.*

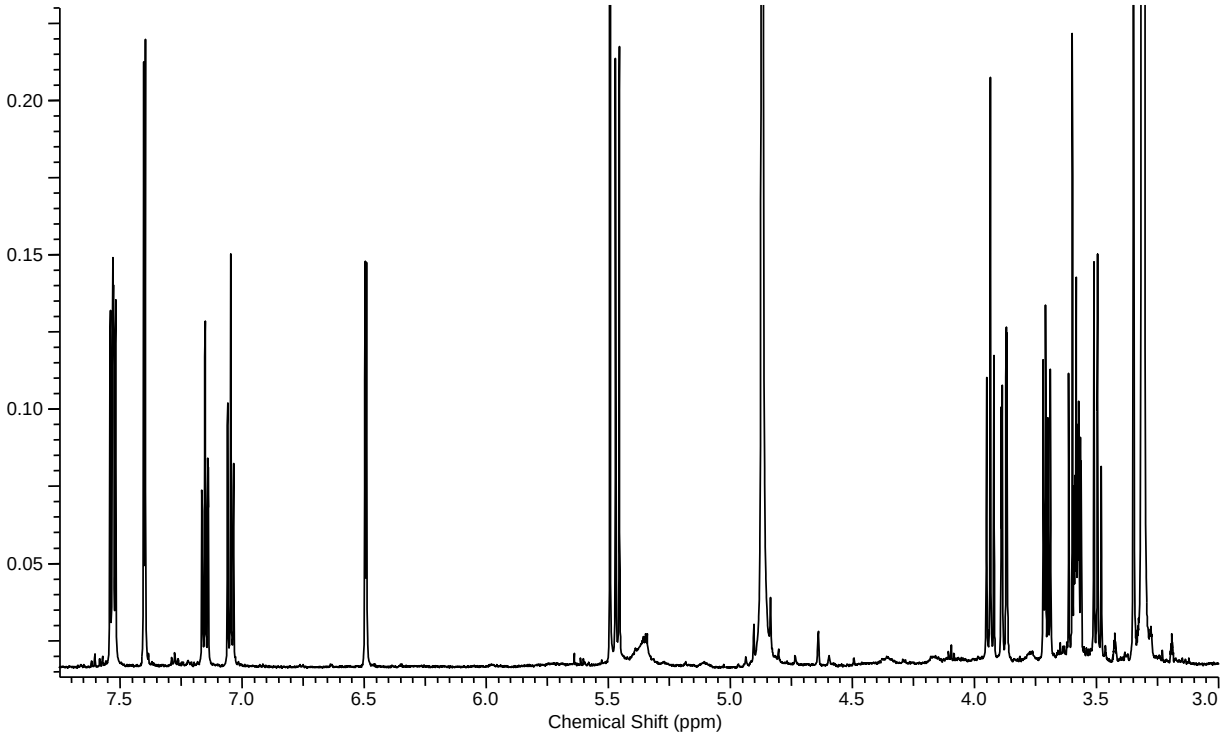

Figure D.6.2. ^{1}H NMR Spectrum (500 MHz, methanol-d_4) of purified *N*-(β-D-glucopyranosyl)-indole (7) from *C. elegans. Data acquired by SVH.*

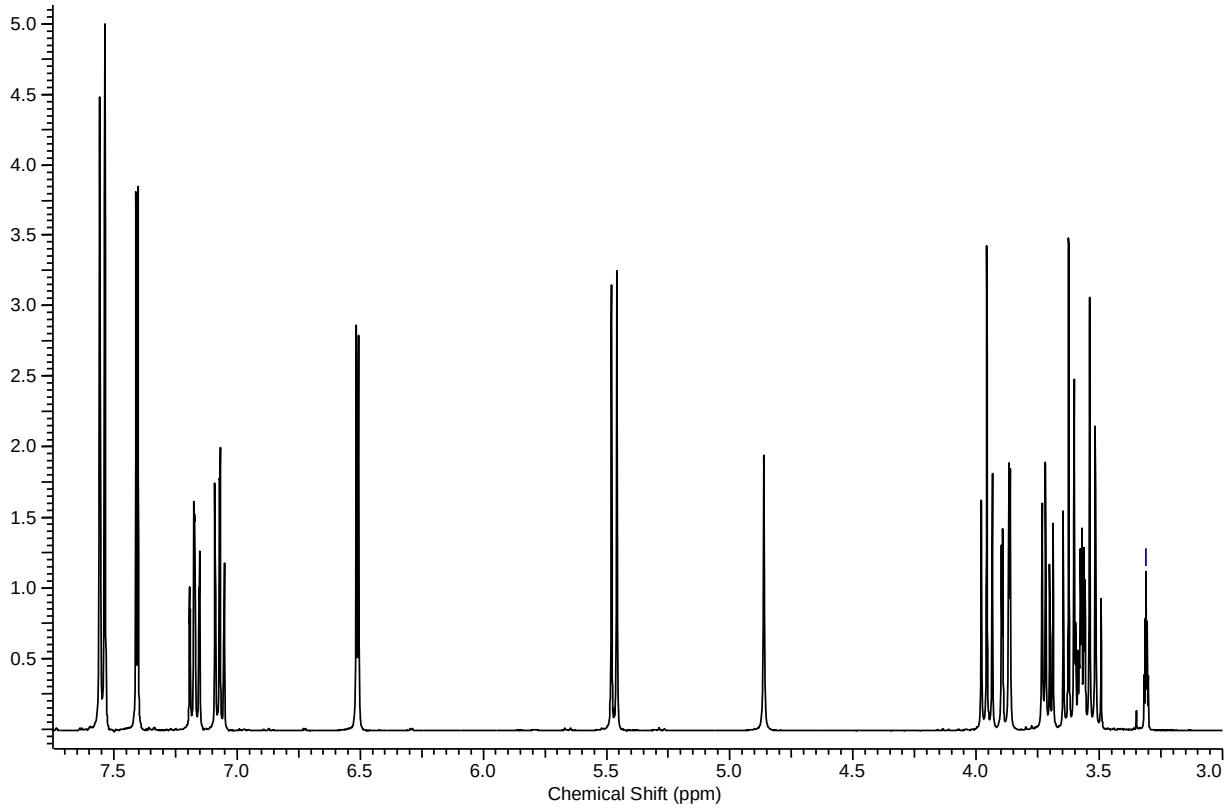

Figure D.6.3. ^{1}H NMR Spectrum (400 MHz, methanol-d_4) of synthetic *N*-(β-D-glucopyranosyl)-indole (7). *Data acquired by SVH.*

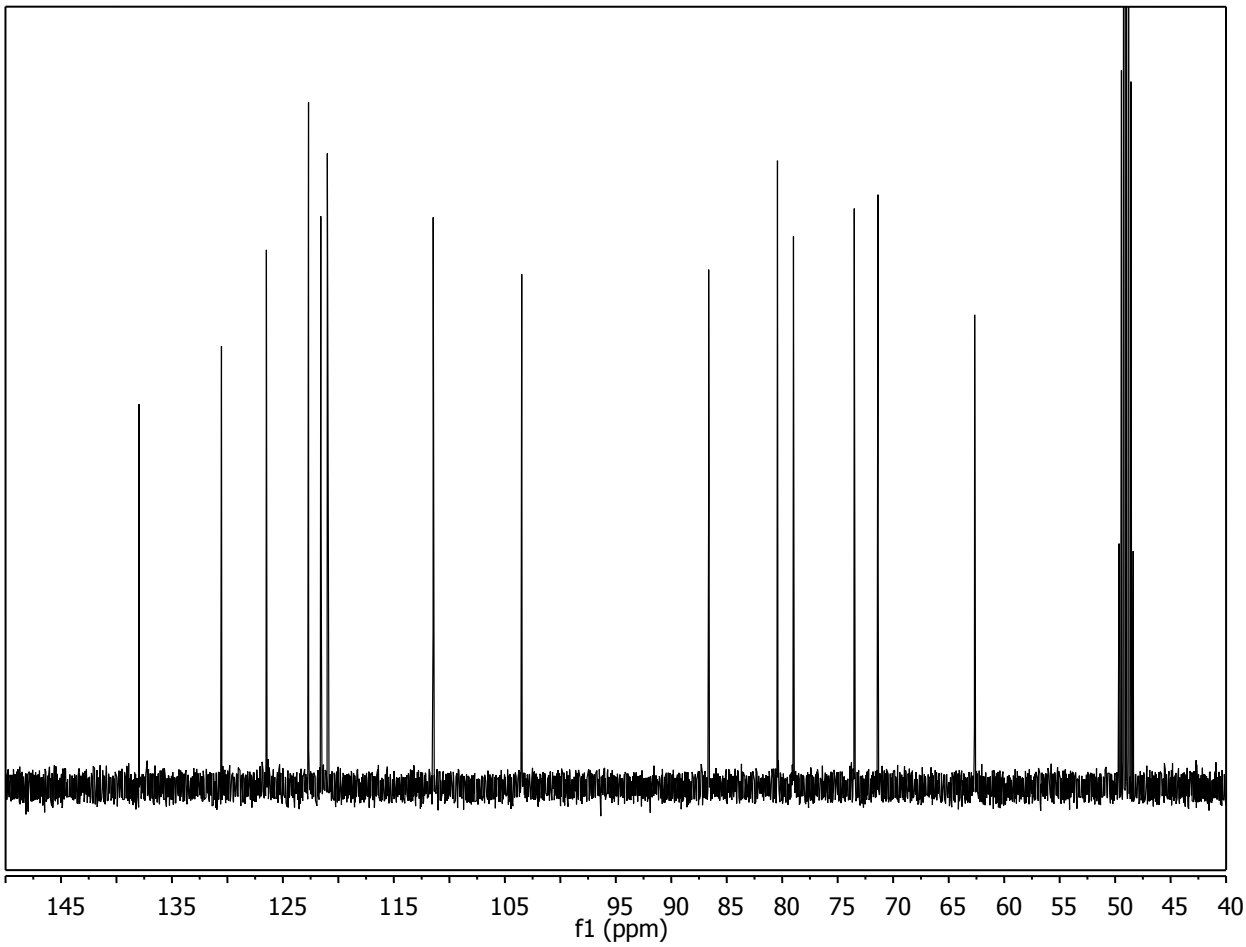

Figure D.6.4. ^{13}C NMR Spectrum (100 MHz, methanol-d_4) of synthetic *N*-(β-D-glucopyranosyl)-indole (7). *Data acquired by SVH.*

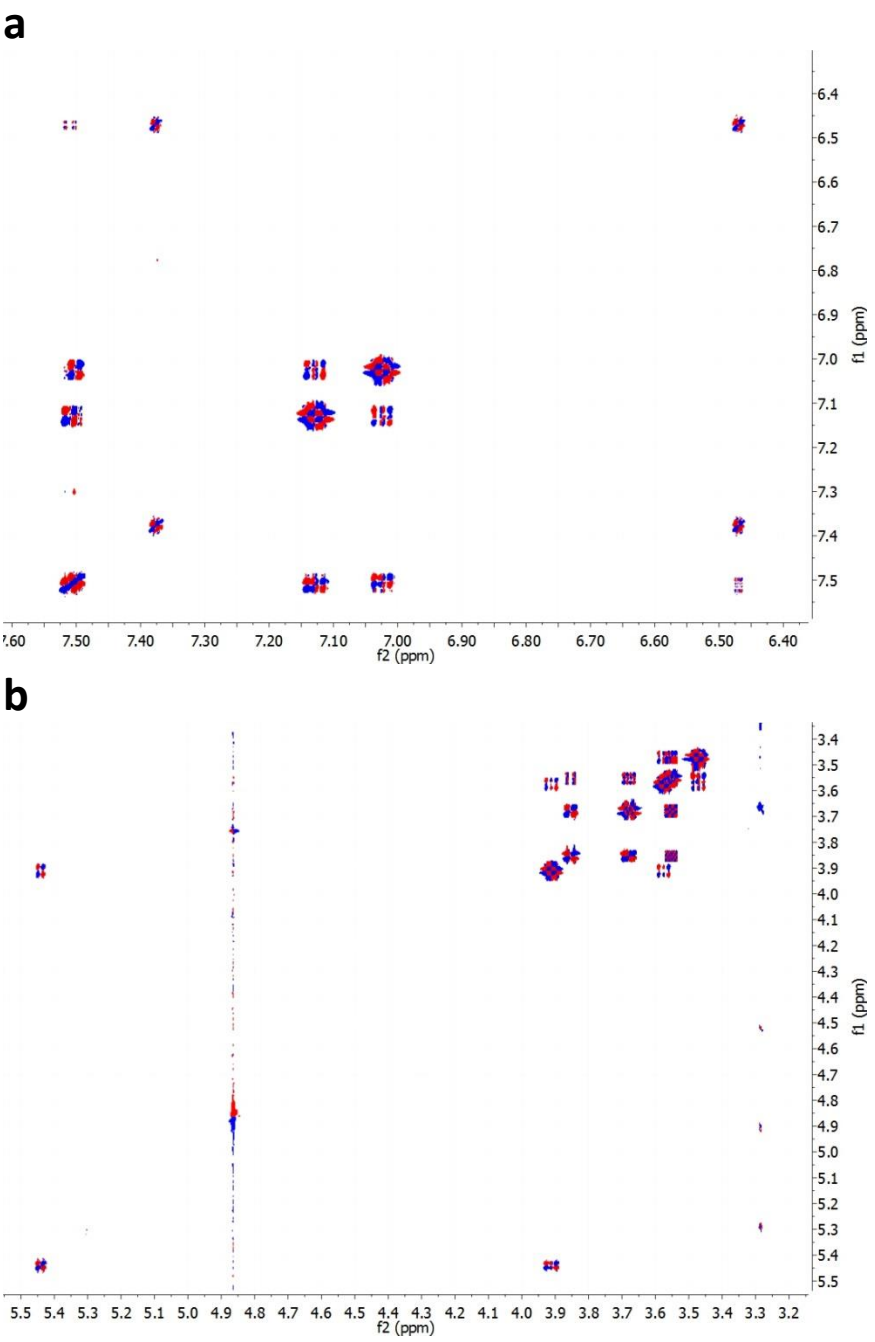

Figure D.6.5. dqfCOSY Spectrum (600 MHz, methanol-d_4) of synthetic *N*-(β-D-glucopyranosyl)-indole (7) Expansions showing the aromatic (a) and carbohydrate (b) regions. *Data acquired by SVH.*

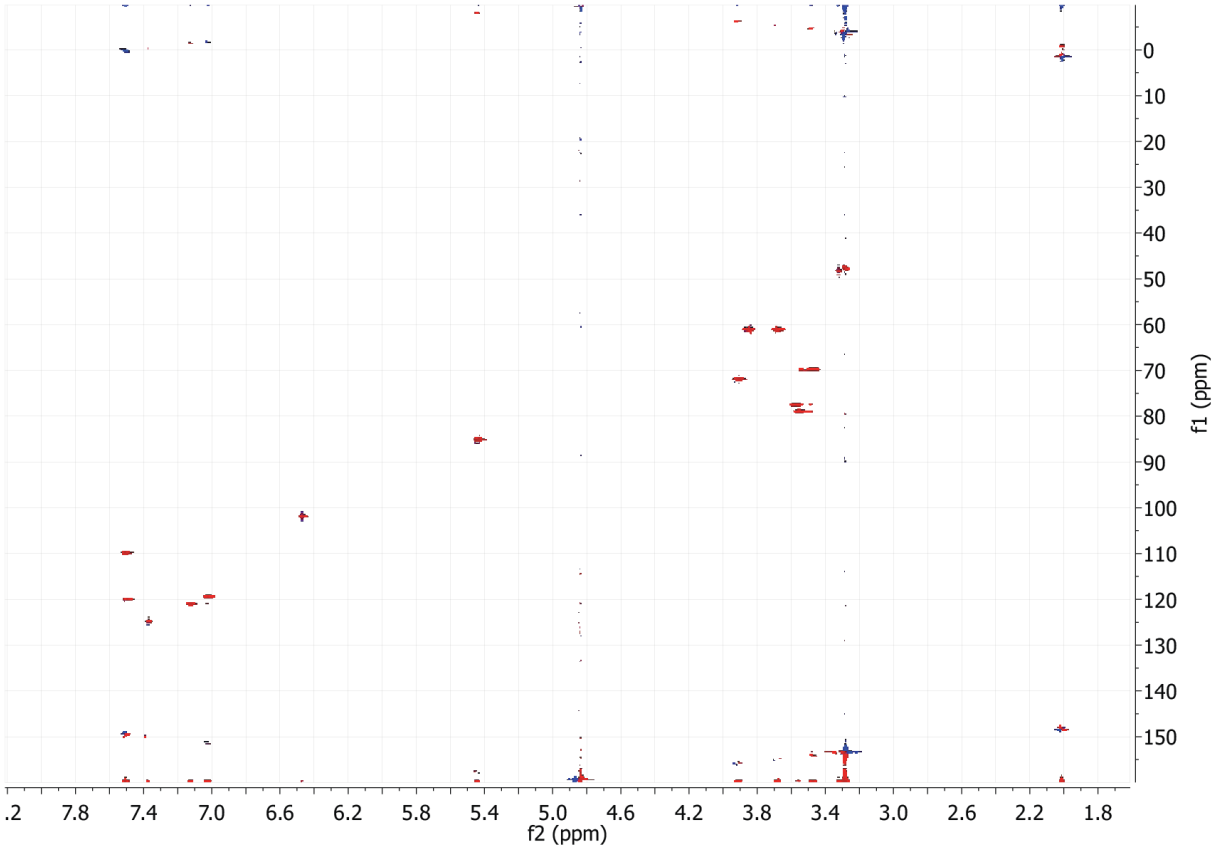

FigureD.6.6. HMQC Spectrum (600 MHz for ^{1}H 151 MHz for ^{13}C, methanol-d_4) of synthetic *N*-(β-D-glucopyranosyl)-indole (7). *Data acquired by SVH.*

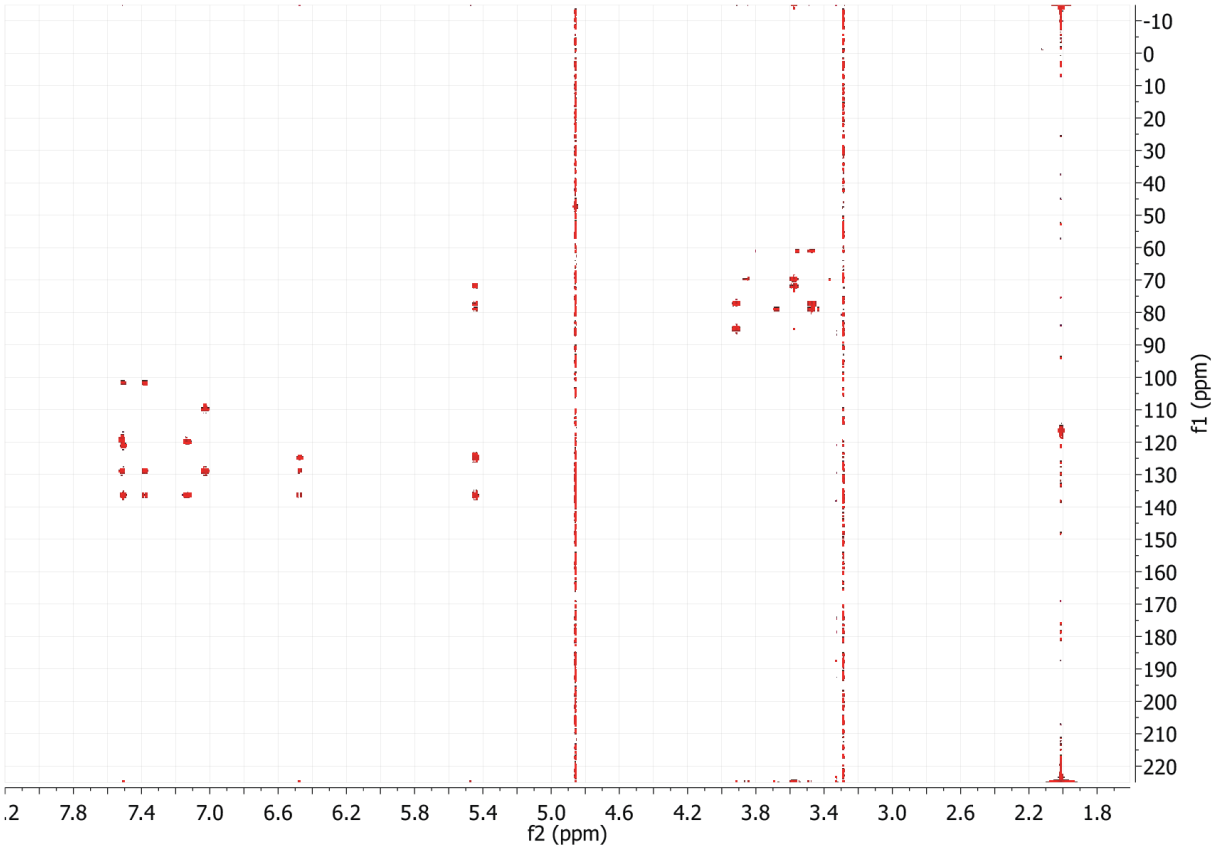

Figure D.6.7. HMBC Spectrum (600 MHz for ^{1}H 151 MHz for ^{13}C, methanol-d_4) of synthetic *N*-(β-D-glucopyranosyl)-indole (7). *Data acquired by SVH.*

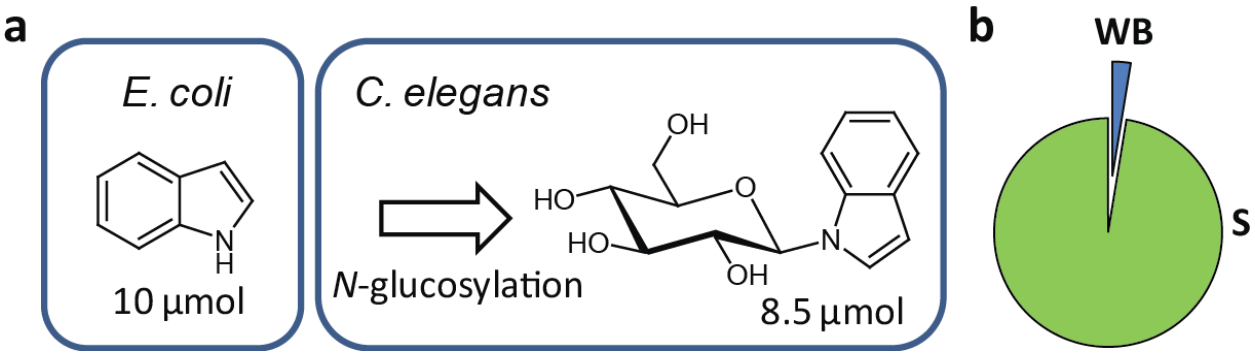

Figure 7. Detoxification of indole via *N*-glucosylation by *C. elegans*. (a) Using HPLC-UV-ESI-MS, we found that of the 10 µmol indole present in a bacterial *E. coli* pellet provided as food, ca. 85% can be recovered after conversion to *N*-(β-D-glucopyranosyl)indole via *N*-glucosylation by *C. elegans.* (b) Comparative analysis of *C. elegans* supernatant (S) and worm body (WB) extracts indicated that *N*-(β-D-glucopyranosyl)indole is predominantly released into the media supernatant. *Data acquired by SVH and YI.*

REFERENCES

1. Stupp, G. S., von Reuss, S. H., Izrayelit, Y., Ajredini, R., Schroeder, F. C., and Edison, A. S. (2013) Chemical detoxification of small molecules by *Caenorhabditis elegans*, *ACS Chem. Biol. 8*, 309-313.
2. Bommarius, B., Anyanful, A., Izrayelit, Y., Bhatt, S., Cartwright, E., Wang, W., Swimm, A. I., Benian, G. M., Schroeder, F. C., and Kalman, D. (2013) A family of indoles regulate virulence and Shiga toxin production in pathogenic *E. coli, PLoS One 8*, e54456.
3. Brenner, S. (1974) The genetics of *Caenorhabditis elegans*, *Genetics 77*, 71-94.
4. Anyanful, A., Easley, K. A., Benian, G. M., and Kalman, D. (2009) Conditioning protects *C. elegans* from lethal effects of enteropathogenic *E. coli* by activating genes that regulate lifespan and innate immunity, *Cell Host Microbe 5*, 450-462.
5. Feng, P., Weagant, S. D., and Monday, S. R. (2001) Genetic analysis for virulence factors in *Escherichia coli* O104 : H21 that was implicated in an outbreak of hemorrhagic colitis, *J. Clin. Microbiol. 39*, 24-28.
6. Anyanful, A., Dolan-Livengood, J. M., Lewis, T., Sheth, S., Dezalia, M. N., Sherman, M. A., Kalman, L. V., Benian, G. M., and Kalman, D. (2005) Paralysis and killing of *Caenorhabditis elegans* by enteropathogenic *Escherichia coli* requires the bacterial tryptophanase gene, *Mol. Microbiol. 57*, 988-1007.
7. McClay, K., Boss, C., Keresztes, I., and Steffan, R. J. (2005) Mutations of toluene-4-monooxygenase that alter regiospecificity of indole oxidation and lead to production of novel indigoid pigments, *Appl. Environ. Microb. 71*, 5476-5483.
8. Pungaliya, C., Srinivasan, J., Fox, B. W., Malik, R. U., Ludewig, A. H., Sternberg, P. W., and Schroeder, F. C. (2009) A shortcut to identifying small molecule signals that regulate behavior and development in *Caenorhabditis elegans*, *Proc. Natl Acad. Sci. USA 106*, 7708-7713.
9. Forseth, R. R., and Schroeder, F. C. (2011) NMR-spectroscopic analysis of mixtures: from structure to function, *Curr. Opin. Chem. Biol. 15*, 38-47.
10. Wei, O. L., Hilliard, A., Kalman, D., and Sherman, M. (2005) Mast cells limit systemic bacterial dissemination but not colitis in response to *Citrobacter rodentium*, *Infect. Immun. 73*, 1978-1985.
11. Lebeis, S. L., Bommarius, B., Parkos, C. A., Sherman, M. A., and Kalman, D. (2007) TLR signaling mediated by MyD88 is required for a protective innate immune response by neutrophils to *Citrobacter rodentium*, *J. Immunol. 179*, 566-577.
12. Hulme, S. E., and Whitesides, G. M. (2011) Chemistry and the worm: *Caenorhabditis elegans* as a platform for integrating chemical and biological research, *Angew. Chem. Int. Edit. 50*, 4774-4807.
13. Perna, N. T., Plunkett, G., 3rd, Burland, V., Mau, B., Glasner, J. D., Rose, D. J., Mayhew, G. F., Evans, P. S., Gregor, J., Kirkpatrick, H. A., Posfai, G., Hackett, J., Klink, S., Boutin, A., Shao, Y., Miller, L., Grotbeck, E. J., Davis, N. W., Lim, A., Dimalanta, E. T., Potamousis, K. D., Apodaca, J., Anantharaman, T. S., Lin, J., Yen, G., Schwartz, D. C., Welch, R. A., and Blattner, F. R. (2001) Genome

sequence of enterohaemorrhagic *Escherichia coli* O157:H7, *Nature 409*, 529-533.

Appendix E

2D NMR-BASED METABOLOMICS UNCOVERS INTERACTIONS BETWEEN CONSERVED BIOCHEMICAL PATHWAYS IN THE MODEL ORGANISM CAENORHABDITIS ELEGANS

***C. elegans* Strains and General Culture Methods.** Wild-type *C. elegans* (N2, Bristol), *daf-22*(*m130*), *daf-22*(*ok693*), *acox-1(ok2257)*, *maoc-1(hj13)*, and *dhs-28(hj8)* mutant strains were obtained from the *Caenorhabditis* Genetics Center (CGC). Strains were maintained at 20 °C on NGM plates with bacteria (*E. coli* OP50) as food.

Preparation of *C. elegans* Metabolite Extracts. Liquid cultures were grown as previously reported.(*3*) Briefly, wild-type or *daf-22* mutant worms were grown for two generations on NGM plates seeded with OP50. Three crowded 6 cm NGM plates were washed into 100 mL solution of S-medium in a 500 mL Erlenmeyer flask and grown at 22°C and 220 pm. Concentrated OP50 from 1 L bacterial cultures, grown over-night, were given on day 1 and day 3. On day 5 the liquid culture was split into two 500 mL Erlenmeyer flasks and the growth media volume was maintained at 100 mL. An additional 1 L OP50 pellet was given as food upon splitting. The cultures were harvested on day 7 by centrifugation at 4750 rpm. The supernatant was lyophilized and the residue extracted with 95% ethanol (300 mL) at room temperature for 12 h. The resulting suspension was filtered and evaporated *in vacuo* at room temperature to yield the crude extracts. In this manner four extracts each of wild-type (N2), *daf-22*(*m130*), and *daf-22*(*ok693*) cultures were prepared. For NAE quantification, mutant strains were grown as above in duplicate. Liquid cultures for ascaroside mixture experiments were

prepared as described above with addition of 2.5 µM of ascr#3 and 2.5 µM of ascr#9 at day 0.

In preparation for NMR-spectroscopic analysis, the crude extracts were suspended in 1:8 methanol (MeOH):dichloromethane (DCM), using 7.5 mL of this solvent mixture per 1 gram of crude extract. Following centrifugation, 2 mL aliquots of supernatant of each sample were filtered over 1 g of silica (EMD Chemicals Inc.) using 10 mL of 1:8 MeOH:DCM for elution. The filtrate was evaporated to dryness *in vacuo* prior to analysis. For NMR spectroscopic analysis, 10-20 mg of the resulting metabolite extracts was used.

Preparation of Bacterial Metabolite Extracts. *E. coli* OP50 was grown overnight at 37°C and 220 rpm to an OD of 1.2 in 2 L of Lysogeny broth (LB). The bacterial broth was spun for 20 min at 4750 rpm. The supernatant was then lyophilized, crushed with mortar and pestle and extracted with 150 mL 95% ethanol (2 times). The extract was filtered through a sintered crucible and concentrated *in vacuo* prior to analysis.

Mass Spectrometric Analysis. Metabolite extracts prepared as described above were resuspended in 1.5 mL methanol, centrifuged, and 30 µL of this sample was injected into HPLC-MS for analysis. HPLC-MS analysis was performed using the Agilent 1100 Series HPLC system with an Agilent Eclipse XDB-C18 column (9.4 x 250 mm, 5 µm particle diameter) connected to the Quattro II mass spectrometer using a 10:1 split. For short chain ascarosides, a 0.1% aqueous acetic acid–acetonitrile gradient was used. The gradient started with 5% acetonitrile for 5 minutes, then increased to 100% acetonitrile over 32 minutes. For long chain ascarosides, an acetonitrile-isopropanol

gradient was used, starting with 5% isopropanol in acetonitrile for 5 minutes; then isopropanol was increased to 75% over 32 minutes. Samples were analyzed by HPLC-ESI-MS in negative and positive ion modes using a capillary voltage of 3.5 kV and a cone voltage of -40 V and +20 V, respectively. The elemental composition of the long chain ascarosides was performed by high resolution MS and HPLC-MS using the Xevo G2 QTof.

EPEA and AEA (**14**) were quantified by HPLC-MS (using the Quattro II) using a water (0.1% acetic acid) – acetonitrile gradient as described above for short chain ascarosides. The retention time of EPEA and AEA were established by injection of an authentic standard (Enzo Life Sciences and Cayman Chemicals, respectively). Relative endocannabinoid content in wild type and mutant strains was quantified by integration of LC-MS signals from corresponding ion traces for $(M-H)^-$ or $(M+Cl)^-$. All integration values were normalized by the mass of the liquid culture pellet. All quantitative data reported in Figure 3 were from at least two independent biological repeats.

NMR Spectrometric Analysis. NMR samples sample were prepared by dissolving 10-20 mg portions of metabolite extract (see above) in 0.6 ml of CD_3OD. Samples were analyzed using a Varian INOVA 600 MHz NMR spectrometer. Non-gradient phase-cycled dqfCOSY spectra were acquired using the following parameters: 0.8 s acquisition time, 600 complex increments, 16 scans per increment. For processing with mvaDANS, spectra were zero-filled to 2048 × 1024 data points, a sine-square-shaped window function was applied in both dimensions prior to Fourier transformation, and spectra converted to magnitude mode prior to transfer to MATLAB.

For detailed analysis in phase-sensitive mode, dqfCOSY spectra were zero-filled to 8192 × 4096 data points and a cosine bell-shaped window function was applied in both dimensions before Fourier transformation. Gradient and non-gradient HSQCAD and HMBC spectra of purified fractions of *daf-22*-upregulated metabolites were acquired using 8-32 scans, 0.25 s acquisition time, and 256-500 complex increments. NMR spectra were processed using Bruker TopSpin, Varian VNMR, MestreLabs' MestReC, and MNova software packages.

Isolation of Major *daf-22*-Upregulated Metabolites. To 8 g of Celite (prewashed with ethyl acetate) was added a solution of *daf-22* metabolite extract from 16 100-ml liquid cultures. After evaporation of the solvent, the material was dry-loaded into an empty 25 g RediSep® *Rf* loading cartridge. Fractionation was performed using a Teledyne ISCO CombiFlash® system over a RediSep® *Rf* GOLD 40 g HP Silica Column using a normal phase dichloromethane-methanol solvent system, starting with 6 min of 100% dichloromethane, followed by a linear increase of methanol content up to 10% at 24 min, followed by another linear increase of methanol content up to 40% at 40 min, followed by another linear increase of methanol content up to 95% at 45 min which was then continued to 48 min. This yielded 70 fractions (~20 mL each) which were individually evaporated *in vacuo* and analyzed by NMR spectroscopy (^{1}H NMR, dqfCOSY) and HPLC-MS. ^{1}H NMR-spectroscopic signals identified via mvaDANS as representing *daf-22*-upregulated metabolites were detected in fractions 35-45. Isolation of major *daf-22*-upregulated metabolites was achieved by preparative HPLC using the same HPLC method described above for HPLC-MS analysis of long chain ascarosides.

Isolated fractions were characterized further by dqfCOSY, HSQC, and HMBC as well as high-resolution HPLC-MS using the Xevo G2 QTof.

Statistical Analysis. Figure 4d and Figure S6: we used unpaired student's *t*-tests with Welch's correction for comparing the relative abundance of EPEA and AEA in wild type and mutant strains. * P<0.05, ** P<0.01, *** P<0.001.

mvaDANS Analysis. For identification of *daf-22*-upregulated metabolites via mvaDANS, we acquired dqfCOSY spectra for metabolome extracts obtained from two different *daf-22* alleles (*m130*, *ok693*) and wild-type *C. elegans* (Figures 2, S1-S2). dqfCOSY spectra from four independent biological replicates were processed in magnitude mode using the mvaDANS algorithm in Matlab, which incorporated dynamic binning and multivariate pattern recognition analysis (Figure S3). Automatic cross peak identification and binning converted each of the dqfCOSY spectra into a set of crosspeak integrals which were corrected for dilution using Probabilistic Quotient Normalization,(*1*) mean-centered, and scaled to unit variance. This matrix of bin integrals was then subjected to statistical analysis including two-way hierarchical clustering, Principal Component Analysis (PCA) (Figure 2a),(*2*) and Partial Least Squares – Discriminant Analysis (PLS-DA) (Figure S7).(*3*) Coefficients from PCA loadings and PLS-DA predictors were back-projected onto the dqfCOSY spectra to enable the detection of NMR spectroscopic signals representing compounds differentially expressed in the three *C. elegans* strains (Figures S4, S8).

mvaDANS automation and spectral interpretation. Please see supporting information.

Supporting Methods

Automatic Cross Peak Identification and Integration for mvaDANS. Spectral segments are detected from a representative pseudo-spectrum- here, an average spectrum calculated from the mean along the third dimension of the spectral stack. To identify segments of the pseudo-spectrum corresponding to crosspeak regions, a local noise surface is calculated using the AUTOPSY(*4*) method (equations 1–4). AUTOPSY calculates a point-wise estimation of underlying noise as follows.

1) $$d_x = \min(\sqrt{\frac{1}{n}\sum_{i=1}^{n}\left(\delta_{xi} - \overline{\delta_x}\right)^2})$$

2) $$d_y = \min(\sqrt{\frac{1}{n}\sum_{i=1}^{n}\left(\delta_{iy} - \overline{\delta_y}\right)^2})$$

3) $$b = \min([d_x, d_y])$$

4) $$p_{xy} = \sqrt{(\sqrt{d_x^{\,2} - b^2})^2 + (\sqrt{d_y^{\,2} - b^2})^2 + b^2}$$

Here, d_x and d_y are noise values for each slice x and y in the direct and indirect dimensions of the 2D NMR spectrum, respectively. The noise value for a given slice δ_x or δ_y is calculated by splitting the slice up into 16 regions of size n=F1/16 for the direct dimension and n=F2/16 for the indirect dimension. The noise for that trace is then the standard deviation of the region with the minimum standard deviation as shown in equations 6 and 7. Each point p in the spectrum is intersected by two slices x and y whose noise values are d_x and d_y. The noise at point p_{xy} is combines the noise in slice *x* with the noise in slice *y* with a baseline noise value *b* as in equations 8 and 9. This method of calculating noise is very well suited to the noise structure of 2D NMR data, which is characterized by vertical noise such as T1 and water noise.

Once the noise surface p_{xy} has been calculated, peaks can be detected by identifying local maxima above a certain multiple of the noise surface. While the exact threshold can vary, values of 5-10 detect the large majority of cross-peaks. A threshold

of 10 was used for the high-concentration *C. elegans* samples used here. Segments are then defined as regions adjacent to detected peaks.

Initial spectral segments are identified as regions within 0.04 ppm of a peak in the ^{1}H dimension of homonuclear spectra. In the case of multiplicity, local maxima are grouped together into a single initial segment. Each segment is then labeled with a unique integer value and iterated minimum and maximum filtering expand these initial segments. Min/max filtering has the effect of growing the segments until they encounter another spectral segment or until they reach a maximum frequency range of approximately 0.2 ppm for ^{1}H. This procedure creates spectral segments with non-rectangular bounds that are bounded by nearby resonances yet avoid close cropping of cross-peak line shapes. These segments are then integrated using a trapezoidal numerical integration.

Pattern Recognition using Spectral Bins. Integration of detected spectral segments transforms the 2D NMR dataset from a three-dimensional stack of full resolution 2D spectra (ω_1, ω_2,N) to a two-dimensional matrix of features (N,P) where P is the number of detected segments. The resulting matrix of bin intensities is then normalized using Probabilistic Quotient Normalization(*1*) and variance stabilized using univariate scaling. These approaches, sometimes referred to as column-wise and row-wise normalization, are frequently applied in metabolomic data processing to account for dilution between samples or receiver gain differences between spectra and balance the variance of high and low intensity signals. Pattern recognition methods PCA and PLS-DA were then applied directly to the transformed bin matrix. The result of pattern recognition is, for each component in the model, a set of N scores showing the similarity of the samples to each other and a vector of P coefficients (referred to as loadings or predictors) that indicate the contribution of each bin to the separation between the samples.

The matrix of peak integrals was also represented as a log2-fold-change vs. median heatmap. The heatmap was clustered using the UPGMA hierarchical clustering algorithm.(*5*) Representing the bin matrix as a clustered heatmap allows rapid identification of groups of cross-peaks whose differential levels differentiate

experimental classes. Additionally, PLS-DA predictors and PCA loadings were ordered using the clustered indices of the cross peak regions. This representation displays the features of the data that are identified by pattern recognition.

To interpret the model and identify important metabolites, coefficients are back projected onto the full resolution spectra by using the spectral segments. For all segments in the full resolution matrix, the data points within the segment are replaced with the value of the coefficient from pattern recognition of the bin extracted from that segment to produce a full resolution loadings matrix. For stabilized data, loading coefficients are independent of signal intensity and thus peak shape is not visible. To produce full-resolution back-projected loadings that look like 2D NMR spectra, this matrix is then multiplied point-wise by the standard deviation along the third dimension of the 2D NMR stack. To visualize the loadings, contour lines are defined by the back-projected loadings, and the colors of these lines are defined by the coefficients themselves. While the mvaDANS algorithm was applied to dqfCOSY data processed in magnitude mode to reduce the number of local minima/maxima, regions of interest identified by mvaDANS were cross-referenced with the original phase-sensitive data for greater structural detail. mvaDANS is natively compatible with other ^{1}H-^{1}H NMR experiments, including TOCSY, COSY, and NOESY, and is compatible with only a few changes in parameters to heteronuclear experiments, including ^{1}H-^{13}C HSQC.

Validation and Spectral Interpretation. For analysis of *daf-22* specific crosspeaks, the back projection spectrum is overlaid with the original *daf-22* dqfCOSY spectra, processed in phase-sensitive mode. Spin systems including chemical shift and coupling constant values are obtained via manual interpretation of the original phase-sensitive spectra. Using available databases (Reaxys, Beilstein, Scifinder, HMDB, NMRshiftDB, BMRB), hypotheses about partial structures representing the identified spin systems are developed. Partial fractionation of *daf-22* exo-metabolome was used to generate enriched samples of the identified metabolites for further NMR-spectroscopic analysis via HMQC and HMBC (see Section 1.6 above).

Back projections from PCA analysis were used to identify *daf-22* specific crosspeaks. PLS-DA analysis was used to validate the statistically based separation of wild-type and *daf-22* metabolomes (Figures S7). Back projections from PLS-DA predictors (Figure S8) largely matched the back projection from PC 1 loadings (Figure S4). Peaks prominently present in dqfCOSY spectra of *E. coli OP*-50 metabolite extract (Figure S9) were excluded from further analysis.

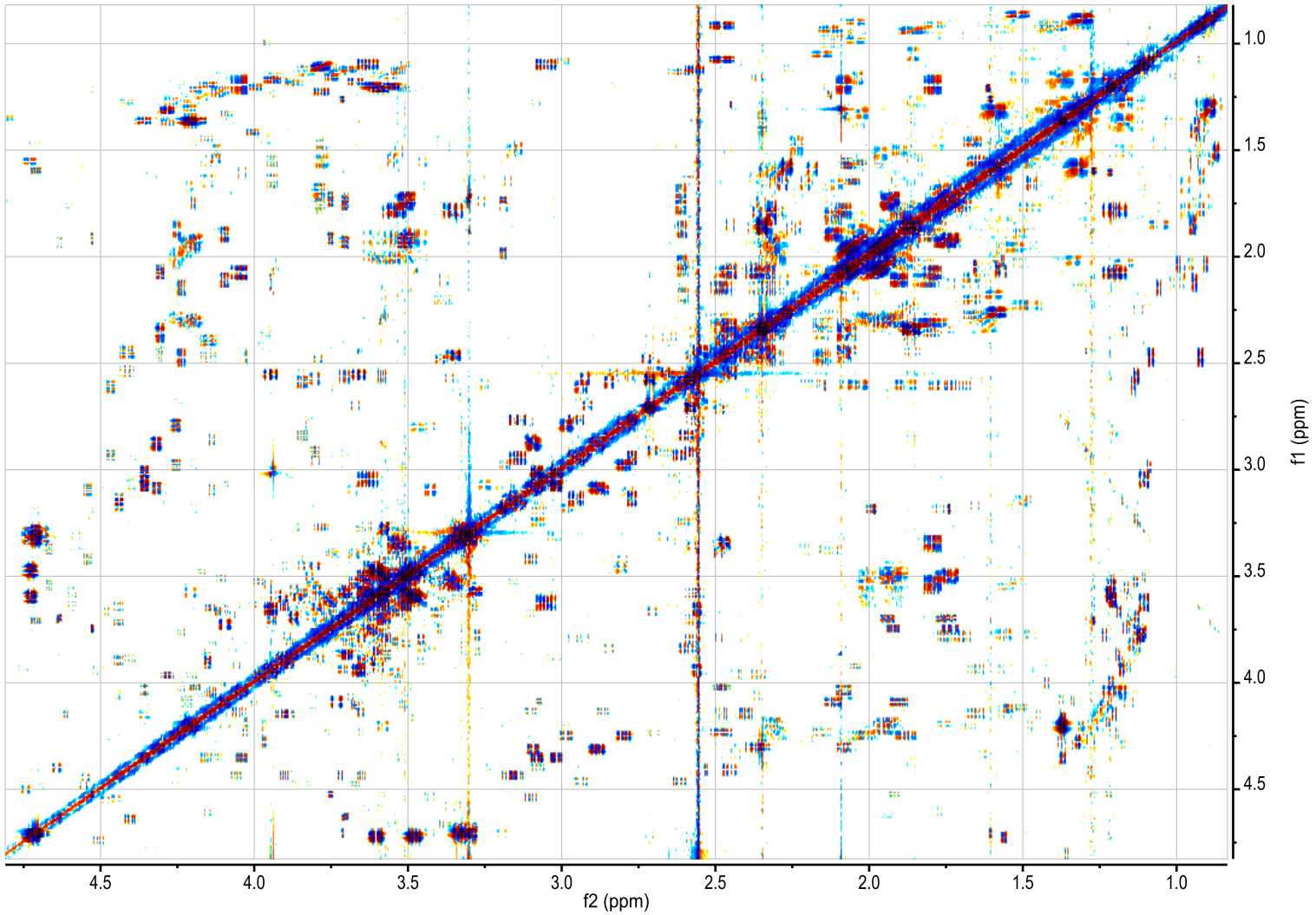

Figure E.1. Section (0.85-4.80 ppm) of dqfCOSY of one of four *C. elegans* wild-type exo-metabolome extracts. *Data acquired by YI.*

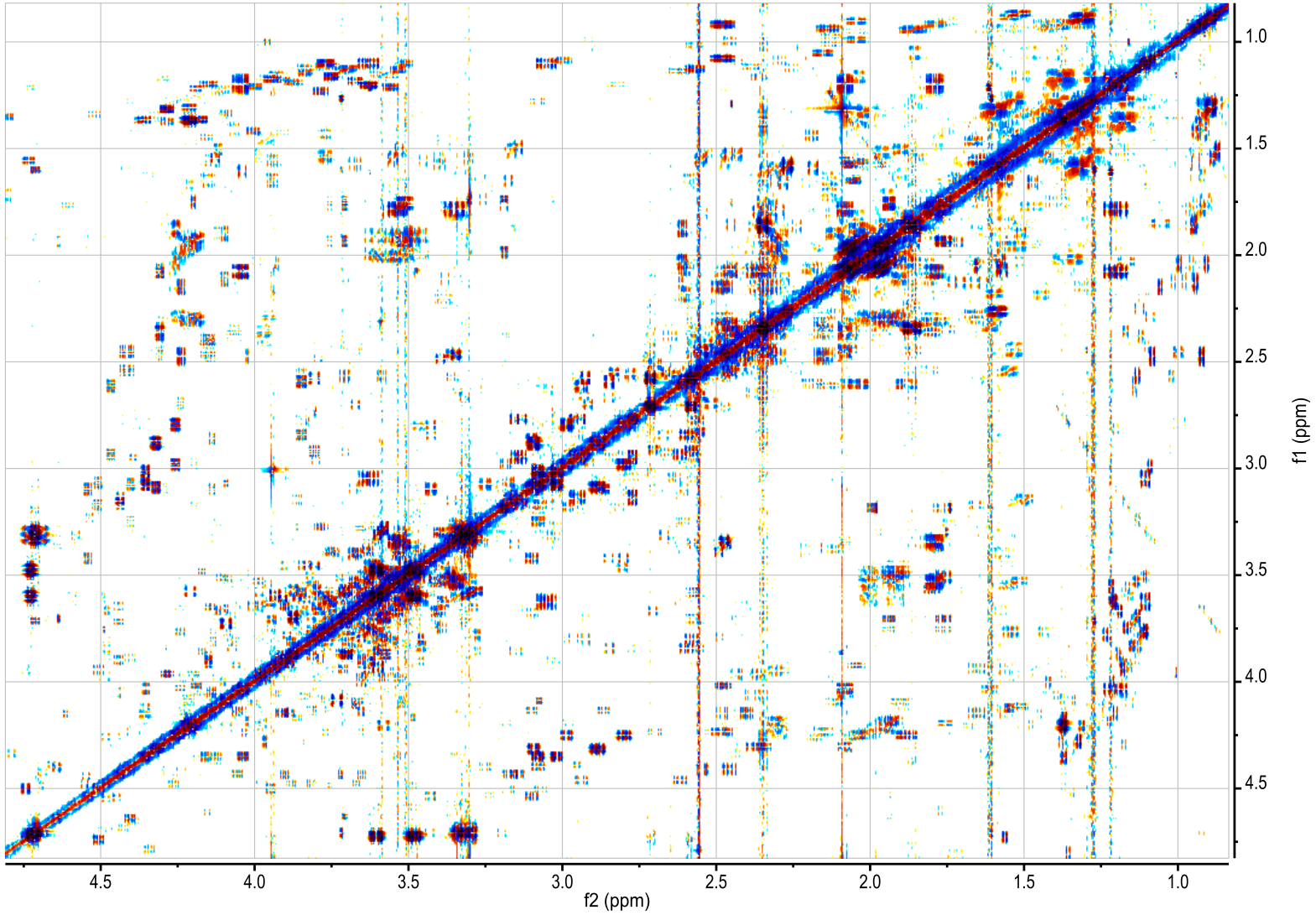

Figure E.2. Section (0.85-4.80 ppm) of dqfCOSY of one of four *daf-22(m130)* exo-metabolome extracts. *Data acquired by YI.*

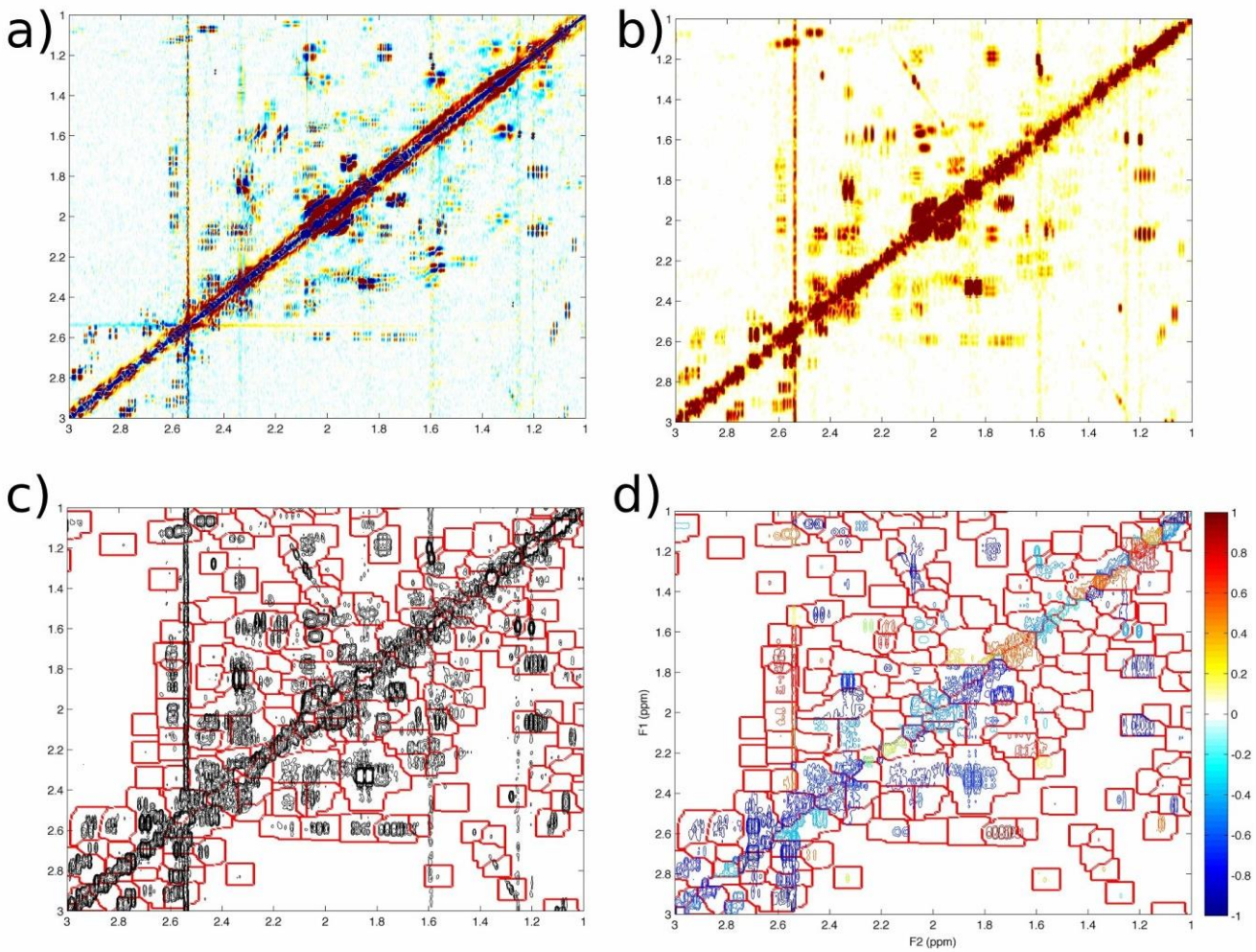

Figure E.3. mvaDANS automatically identifies spectral crosspeaks and creates statistically derived pseudo-spectra. a) 1-3 ppm region of phase-sensitive dqfCOSY spectrum of *C. elegans* wild-type metabolome. (b) Same NMR spectrum processed in magnitude mode prior to automatic binning. (c) Contour plot of NMR spectrum from (a) and (b) plotted with boundaries of bin regions identified by mvaDANS. (d) Back-projected pseudo-spectrum derived from Principal Component 1 of the *C. elegans* wild-type/*daf-22* comparison NMR dataset. Crosspeak colors indicate the normalized PC 1 loading coefficient of the region bin. *Data acquired by YI. Processed by YI and SVR.*

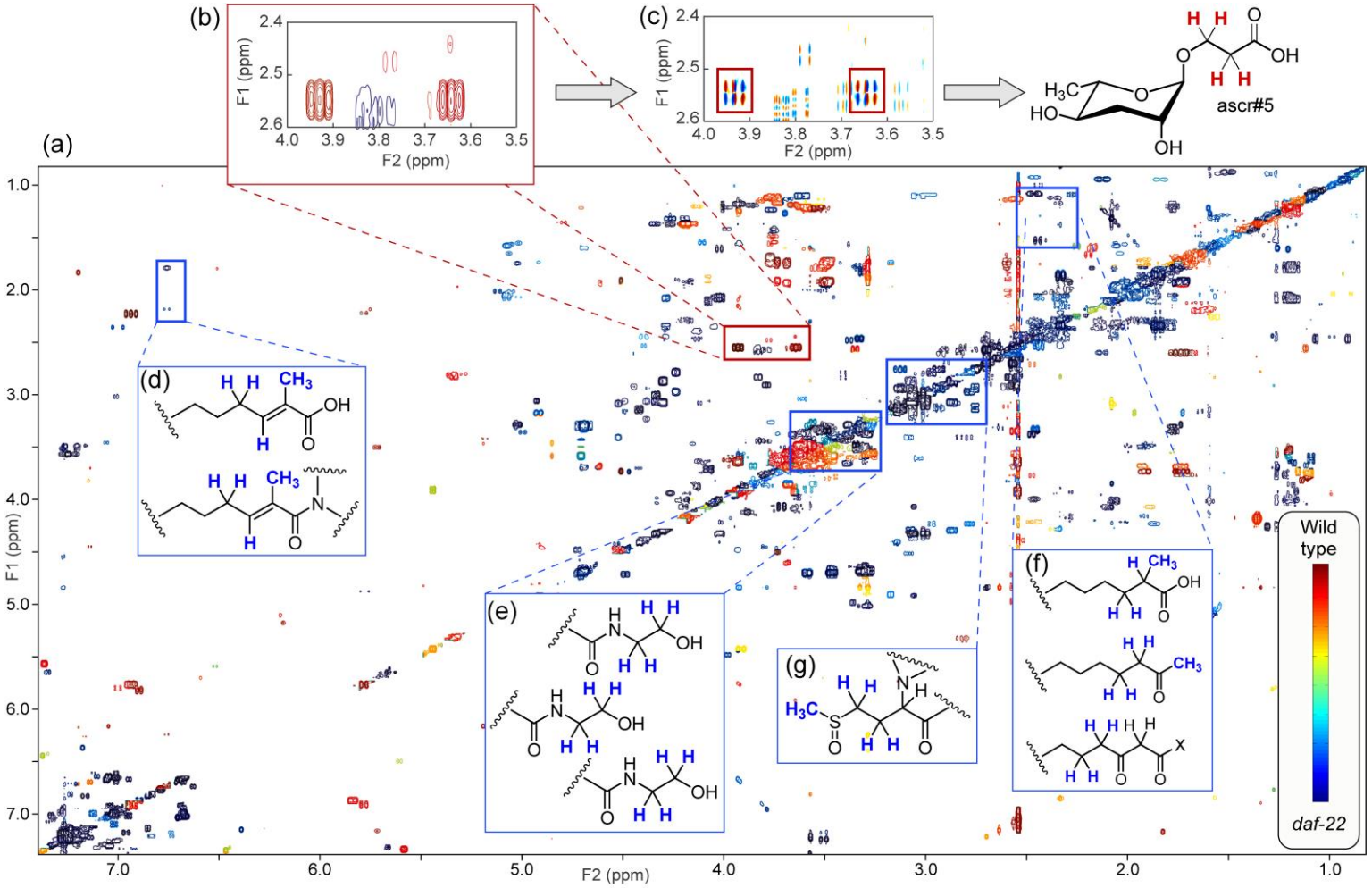

Figure E.4. PCA identifies crosspeaks distinguishing wild-type and two *daf-22* mutant alleles. (a) Back-projection of PC 1 loadings onto magnitude mode dqfCOSY spectrum identify crosspeaks increased (red) or decreased (blue) in wild-type spectra relative to mutant spectra. (b, c) Example for mvaDANS work flow and method validation via identification of a known compound. Analysis of crosspeaks in the phase sensitive dqfCOSY-spectrum shown in (c) corresponding to the wild-type specific red crosspeaks in (b) reveals the known ascaroside ascr#5, whose biosynthesis has previously been shown to be *daf-22* dependent. Similarly, most of the other wild-type specific (red) signals in (a) can be assigned to one of the known ascaroside pheromones. Also see Figure S7. (d-f) Partial structures inferred from analysis of *daf-22*-specific crosspeaks that suggest α-methyl branched fatty acids, methyl ketones,

and β-keto fatty acid derivatives. (g) Example for not strictly *daf-22* specific metabolite (a putative methionine derivative). This compound is upregulated in *daf-22* mutants but also present in wild-type. *Data acquired by YI. Processed by YI and SVR. Analyzed by YI and FS.*

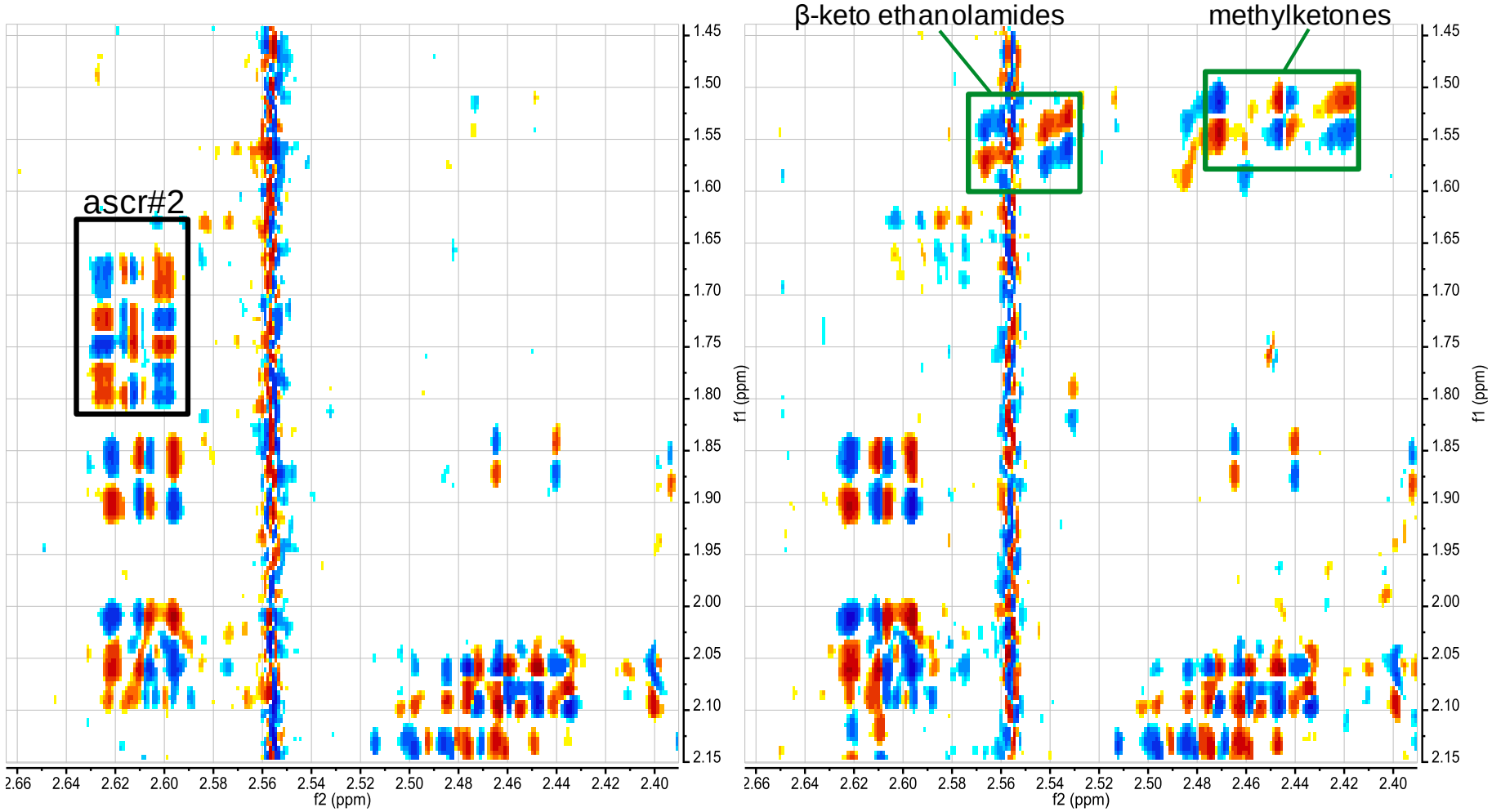

Figure E.5. Examples for differential crosspeaks identified by mvaDANS. Left: ascr#2-crosspeaks detected in wild-type spectrum from Figure E.5; right: β-keto ethanolamide and methylketone crosspeaks detected in the *daf-22(m130)* spectrum from Figure E.3. *Data acquired by YI. Processed by YI and SVR. Analyzed by YI and FS.*

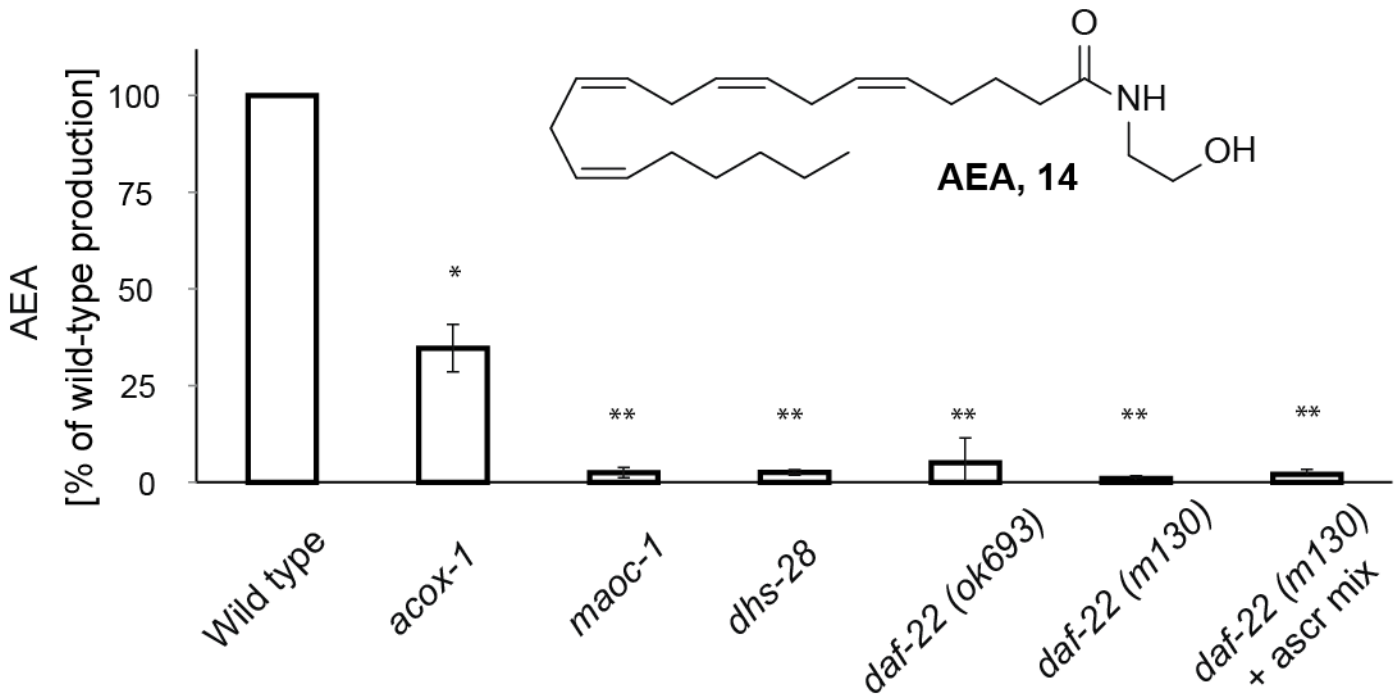

Figure E.6. Mutation of *maoc-1*, *dhs-28*, and *daf-22* greatly reduces AEA production, while mutation of *acox-1* slightly decreases AEA production. * P<0.05, ** P<0.01, *** P<0.001. *Data acquired by YI and NB.*

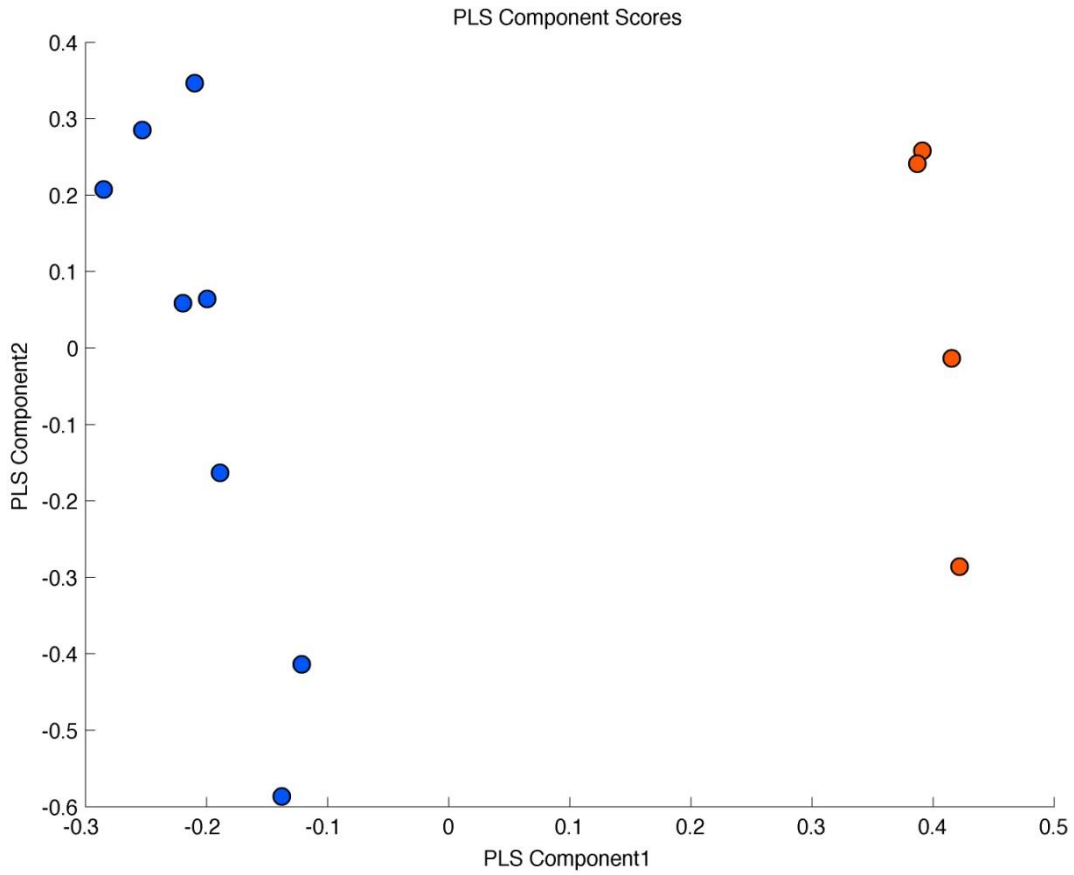

Figure E.7. PLS component scores separate 4 wildtype cultures (red dots) from 8 *daf-22* cultures (blue dots). *Data acquired by YI and NB.*

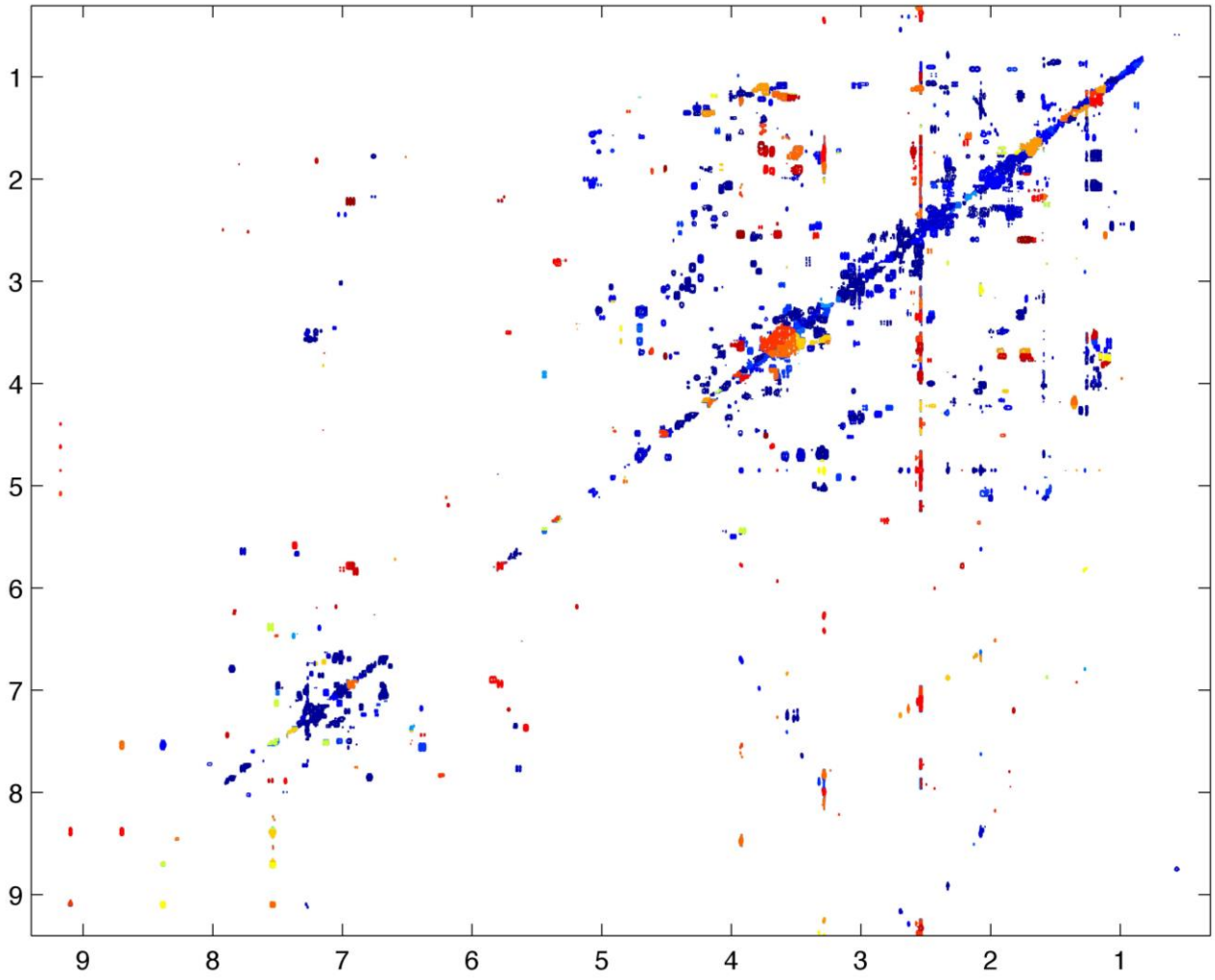

Figure E.8. Back projection of PLS-DA predictors from 1 component model with 4x cross validation, largely matching the result from PCA (Figure 3). More significant PLS-DA results would be achieved using a larger number of replicates for wild-type. *Data acquired by YI, processed by SVR.*

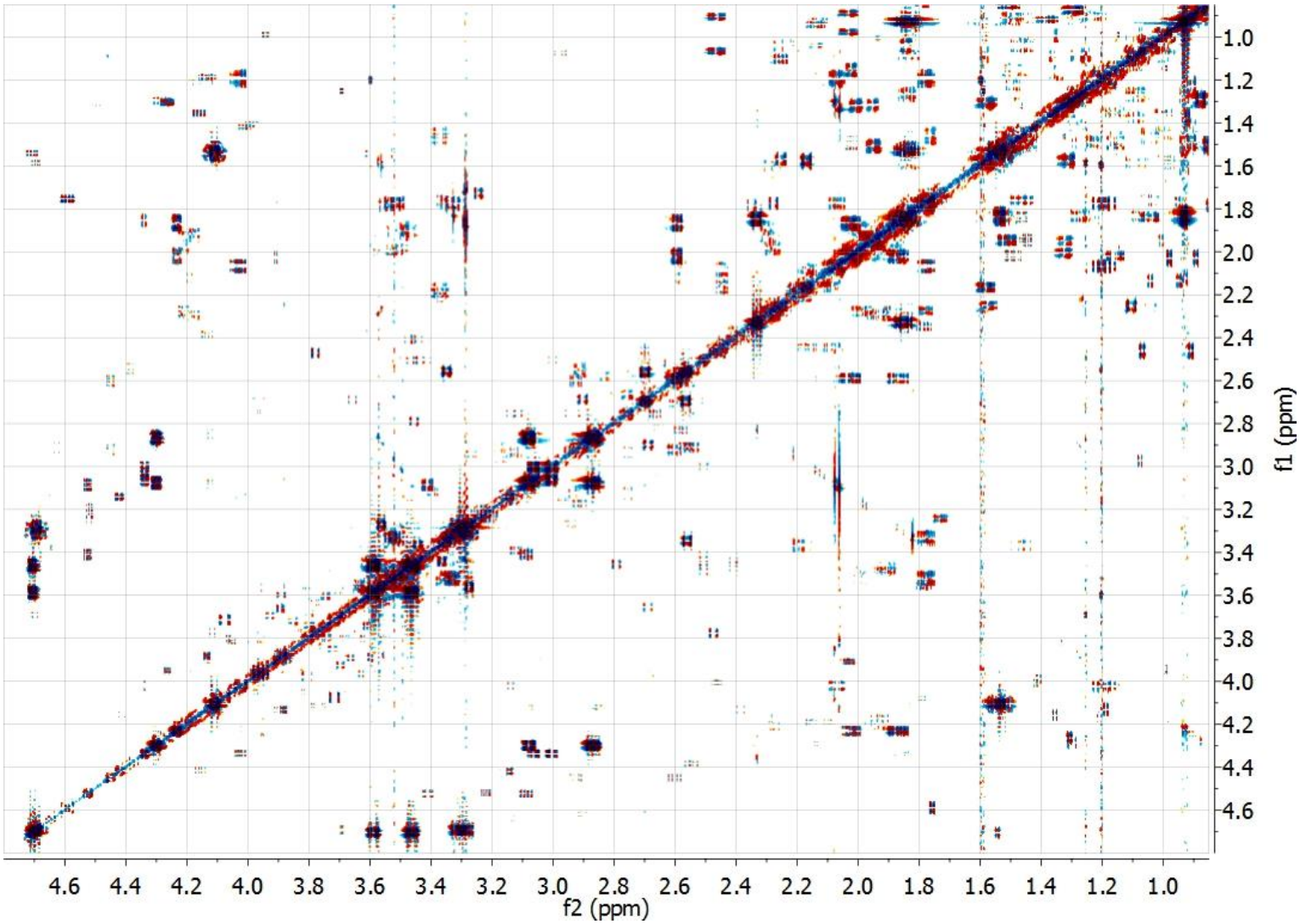

Figure E.9. Section (0.85-4.80 ppm) of dqfCOSY of *E. coli* OP50 for exo-metabolome extracts. *Data acquired by YI.*

Spectroscopic Data of *daf-22*-Upregulated Metabolites

(24*R*)-(3'*R*,5'*R*-Dihydroxy-6'*S*-methyl-(*2H*)-tetrahydropyran-2'-yloxy)-2-methyl-3-oxopentacosanoic acid ethanolamide (7).

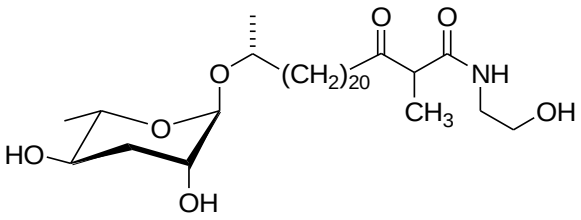

^{1}H NMR ($CDCl_3$, 600 MHz): δ 4.69 (m, 1H, 2'-H); 3.81 (m, 1H, 3'-H); 1.86 (ddd, *J* = 13.5, *J* = 11.0, *J* = 3.1, 1H, 4'-H_{ax}); 2.08 (ddd, *J* = 13.5, *J* = 4.5, *J* = 3.3, 1H, 4'-H_{eq}); 3.60 (ddd, *J* = 11.0, *J* = 9.2, *J* = 4.5, 1H, 5'-H); 3.70 (dq, *J* = 9.2, *J* = 6.3, 1H, 6'-H); 1.27 (d, *J* = 6.3, 3H, 6'-C$\underline{H}_3$); 1.12 (d, *J* = 6.2, 3H, 25-H); 3.79 (m, 1H, 24-H); 1.56 (m, 1H, 23-H); 1.43 (m, 1H, 23-H); 1.30-1.20 (m, 34H, 6-22H); 1.56 (m, 2H, 5-H); 2.55 (td, *J* = 7.3, *J* = 2.3, 2H, 4-H, 3.45 (qd, *J* = 6.5, *J* = 2.3, 1H, 2-H); 1.40 (d, *J* = 6.5, 3H, 2-C$\underline{H}_3$); 3.43 (q, *J* = 5.2, 2H, 1''-H); 3.72 (t, *J* = 5.0, 2H, 2''-H); 6.72 (t, *J* = 5.5, 1H, N-H).

^{13}C NMR ($CDCl_3$, 151 MHz): δ 96.0 (C-2'); 69.4 (C-3'); 35.1 (C-4'); 68.1 (C-5'); 69.7 (C-6'); 17.6 (6'-$\underline{C}H_3$); 18.9 (C-25); 71.7 (C-24); 37.2 (C-23); 28.9-30.5 (C-22 – C-6); 23.3 (C-5); 41.7 (C-4); 210.3 (C-3); 54.0 (C-2); 15.3 (2-$\underline{C}H_3$) 171.1 (C-1); 42.5 (C-1''); 62.3 (C-2'').

HR-MS (ESI$^+$) calculated for $C_{34}H_{65}NO_7Na$ $[M+Na]^+$ 622.4653, observed 622.4728.

(26*R*)-(3'*R*,5'*R*-Dihydroxy-6'*S*-methyl-(*2H*)-tetrahydropyran-2'-yloxy)-3-oxo-heptacosanoic acid ethanolamide (8).

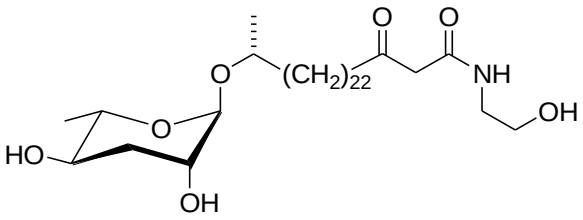

^{1}H NMR ($CDCl_3$, 600 MHz): δ 4.70 (m, 1H, 2'-H); 3.81 (m, 1H, 3'-H); 1.84 (ddd, *J* = 13.5, *J* = 11.0, *J* = 3.1, 1H, 4'-H_{ax}); 2.07 (ddd, *J* = 13.5, *J* = 4.5, *J* = 3.3, 1H, 4'-H_{eq}); 3.61 (ddd, *J* = 11.0, *J* = 9.3, *J* = 4.5, 1H, 5'-H); 3.69 (dq, *J* = 9.3, *J* = 6.2, 1H, 6'-H); 1.27 (d, *J* = 6.3, 3H, 6'-C$\underline{H}_3$); 1.12 (d, *J* = 6.2, 3H, 27-H); 3.79 (m, 1H, 26-H); 1.56 (m, 1H, 25-H); 1.42 (m, 1H, 25-H); 1.30-1.20 (m, 38H, 6-24H);1.57 (m, 2H, 5-H), 2.53 (t, *J* = 7.5, 2H, 4-H), (3.43, s, 2H, 2-H), 3.46 (q, *J* = 5.2, 2H, 1''-H); 3.74 (t, *J* = 5.0, 2H, 2''-H); 7.42 (t, *J* = 5.5, 1H, N-H).

^{13}C NMR ($CDCl_3$, 151 MHz): δ 96.1 (C-2'); 69.4 (C-3'); 35.1 (C-4'); 68.1 (C-5'); 69.7 (C-6'); 17.6 (6'-$\underline{C}H_3$); 18.9 (C-27); 71.7 (C-26); 37.2 (C-25); 28.9-30.5 (C-24 – C-6); 23.3 (C-5); 44.0 (C-4); 207.4 (C-3); 48.4 (C-2); 167.0 (C-1); 42.6 (C-1''); 62.3 (C-2'').

HR-MS (ESI$^+$) calculated for $C_{35}H_{67}NO_7Na$ $[M+Na]^+$ 636.4810, observed 636.4851.

(24*R*)-(3'*R*,5'*R*-Dihydroxy-6'*S*-methyl-(*2H*)-tetrahydropyran-2'-yloxy)-2-methyl-2*E*-pentacosenoic acid ethanolamide (9).

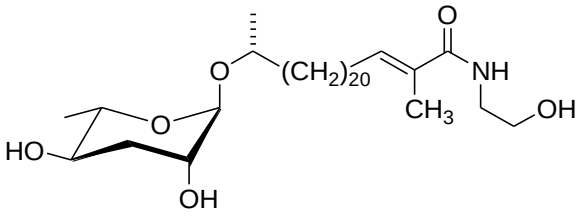

^{1}H NMR ($CDCl_3$, 600 MHz): δ 4.70 (m, 1H, 2'-H); 3.81 (m, 1H, 3'-H); 1.84 (ddd, *J* = 13.5, *J* = 11.0, *J* = 3.1, 1H, 4'-H_{ax}); 2.07 (ddd, *J* = 13.5, *J* = 4.5, *J* = 3.3, 1H, 4'-H_{eq}); 3.61 (ddd,

J = 11.0, *J* = 9.4, *J* = 4.5, 1H, 5'-H); 3.70 (dq, *J* = 9.4, *J* = 6.2, 1H, 6'-H); 1.28 (d, *J* = 6.2, 3H, 6'-C$\underline{H}_3$); 1.12 (d, *J* = 6.2, 3H, 25-H); 3.79 (m, 1H, 24-H); 1.56 (m, 1H, 23-H); 1.42 (m, 1H, 23-H); 1.34-1.20 (m, 34H, 6-22H); 1.41 (m, 2H, 5-H); 2.14 (q, *J* ≈ 7.2, 2H, 4-H); 6.41 (tq, *J* = 7.2, *J* = 1.2, 1H, 3-H); 1.86 (m, 3H, 2-C$\underline{H}_3$); 3.50 (q, *J* = 5.2, 2H, 1''-H); 3.77 (t, *J* = 5.0, 2H, 2''-H); 6.15 (t, *J* = 5.5, 1H, N-H).

^{13}C NMR ($CDCl_3$, 151 MHz): δ 96.1 (C-2'); 69.4 (C-3'); 35.1 (C-4'); 68.1 (C-5'); 69.7 (C-5'); 17.6 (6'-$\underline{C}H_3$); 18.9 (C-25); 71.7 (C-24); 37.2 (C-23); 28.9-30.5 (C-22 – C-5); 28.4 (C-4); 137.3 (C-3); 129.9 (C-2); 12.6 (2-$\underline{C}H_3$); 170.7 (C-1); 42.8 (C-1''); 62.9 (C-2'').

HR-MS (ESI$^+$) calculated for $C_{34}H_{65}NO_7Na$ $[M+Na]^+$ 622.4653, observed 622.4728.

(24*R*)-(3'*R*,5'*R*-Dihydroxy-6'*S*-methyl-(*2H*)-tetrahydropyran-2'-yloxy)-2-methyl-2*E*-pentacosenoic acid (10).

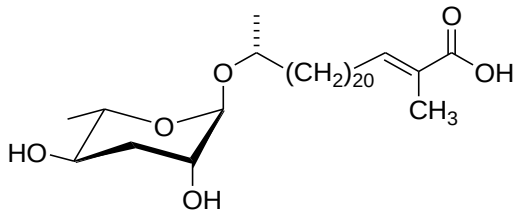

^{1}H NMR ($CDCl_3$, 600 MHz): δ 4.71 (m, 1H, 2'-H); 3.81 (m, 1H, 3'-H); 1.84 (ddd, *J* = 13.5, *J* = 11.0, *J* = 3.1, 1H, 4'-H_{ax}); 2.07 (ddd, *J* = 13.5, *J* = 4.5, *J* = 3.3, 1H, 4'-H_{eq}); 3.61 (ddd, *J* = 11.0, *J* = 9.4, *J* = 4.5, 1H, 5'-H); 3.70 (dq, *J* = 9.4, *J* = 6.2, 1H, 6'-H); 1.27 (d, *J* = 6.2, 3H, 6'-C$\underline{H}_3$); 1.12 (d, *J* = 6.2, 3H, 25-H); 3.79 (m, 1H, 24-H); 1.56 (m, 1H, 23-H); 1.42 (m, 1H, 23-H); 1.34-1.20 (m, 34H, 6-22H); 1.45 (m, 2H, 5-H); 2.18 (q, *J* ≈ 7, 2H, 4-H); 6.87 (tq, *J* = 7.2, *J* = 1.4, 1H, 3-H); 1.82 (m, 3H, 2-C$\underline{H}_3$).

^{13}C NMR ($CDCl_3$, 151 MHz): δ 96.2 (C-2'); 69.4 (C-3'); 35.1 (C-4'); 68.1 (C-5'); 69.7 (C-6'); 17.6 (6'-$\underline{C}H_3$); 18.9 (C-25); 71.7 (C-24); 37.2 (C-23); 29-30.5 (C-22 – C-5); 28.5 (C-4); 145.0 (C-3); 126.6 (C-2); 12.2 (CH_3-C2); 170.5 (C-1).

HR-MS (ESI$^+$): calculated for $C_{32}H_{60}NO_6Na$ $[M+Na]^+$ 563.4282, observed 563.4283.

(24*R*)-(3'*R*,5'*R*-Dihydroxy-6'*S*-methyl-(*2H*)-tetrahydropyran-2'-yloxy)-2-methyl-pentacosanoic acid (11).

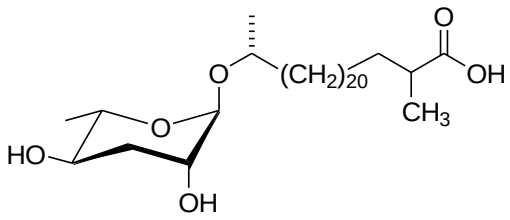

^{1}H NMR ($CDCl_3$, 600 MHz): δ 4.71 (m, 1H, 2'-H); 3.81 (m, 1H, 3'-H); 1.84 (ddd, *J* = 13.5, *J* = 11.0, *J* = 3.1, 1H, 4'-H_{ax}); 2.07 (ddd, *J* = 13.5, *J* = 4.5, *J* = 3.3, 1H, 4'-H_{eq}); 3.60 (ddd, *J* = 11.0, *J* = 9.4, *J* = 4.5, 1H, 5'-H); 3.70 (dq, *J* = 9.4, *J* = 6.3, 1H, 6'-H); 1.27 (d, *J* = 6.3, 3H, 6'-C$\underline{H}_3$); 1.12 (d, *J* = 6.2, 3H, 25-H); 3.79 (m, 1H, 24-H); 1.56 (m, 1H, 23-H); 1.42 (m, 1H, 23-H); 1.35-1.20 (m, 38H, 4-22H); 1.67 (m, 1H, 3-H); 1.42 (m, 1H, 3-H); 2.46 (sext., *J* ≈ 7, 1H, 2-H); 1.17 (d, *J* = 6.8, 3H, 2-CH_3).

^{13}C NMR ($CDCl_3$, 151 MHz): δ 96.2 (C-2'); 69.4 (C-3'); 35.1 (C-4'); 68.1 (C-5'); 69.7 (C-6'); 17.6 (6'-$\underline{C}H_3$); 18.9 (C-25); 71.7 (C-24); 37.2 (C-23); 29.0-30.5 (C-22 – C-4); 28.5 (C-4); 33.8 (C-3); 39.2 (C-2); 17.0 (2-$\underline{C}H_3$); 179.5 (C-1).

HR-MS (ESI$^+$): calculated for $C_{32}H_{60}NO_6Na$ $[M+Na]^+$ 563.4282, observed 563.4283.

(23*R*)-(3'*R*,5'*R*-Dihydroxy-6'*S*-methyl-(*2H*)-tetrahydropyran-2'-yloxy)-tetracosan-2-one (12).

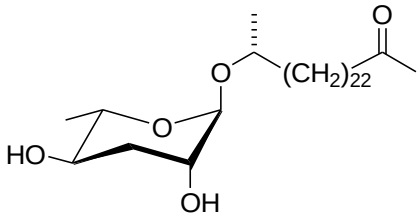

^{1}H NMR ($CDCl_3$, 600 MHz): δ 4.70 (m, 1H, 2'-H); 3.81 (m, 1H, 3'-H); 1.84 (ddd, *J* = 13.5, *J* = 11.0, *J* = 3.1, 1H, 4'-H_{ax}); 2.07 (ddd, *J* = 13.5, *J* = 4.5, *J* = 3.3, 1H, 4'-H_{eq}); 3.59 (ddd, *J* = 11.0, *J* = 9.2, *J* = 4.5, 1H, 5'-H); 3.69 (dq, *J* = 9.2, *J* = 6.2, 1H, 6'-H); 1.27 (d, *J* = 6.2, 3H, 6'-C$\underline{H}_3$); 1.12 (d, *J* = 6.2, 3H, 26-H); 3.79 (m, 1H, 25-H); 1.56 (m, 1H, 24-H); 1.42 (m, 1H, 24-H); 1.35-1.20 (m, 38H, 5-23H); 1.56 (m, 2H, 4-H); 2.41 (t, *J* = 7.5, 2H, 3-H); 2.13 (s, 3H, 1-H).

^{13}C NMR ($CDCl_3$, 151 MHz): δ 96.2 (C-2'); 69.4 (C-3'); 35.1 (C-4'); 68.1 (C-5'); 69.7 (C-6'); 17.6 (6'-$\underline{C}H_3$); 18.9 (C-24); 71.7 (C-23); 37.2 (C-22); 29.0-30.5 (C-21 – C-5); 23.9 (C-4); 43.8 (C-3); 209.6 (C-2); 29.9 (C-1).

HR-MS (ESI$^+$): calculated for $C_{32}H_{62}O_5Na$ $[M+Na]^+$ 549.4495, observed 549.4501.

Table E.1. HPLC/HR-MS (ESI^+) data of (ω-1)-ascarosyl-2-oxoalkanes in *daf-22* mutants.

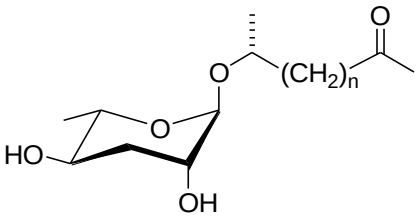

Side chain length (n)	Molecular formula	Molecular weight [amu]	*m/z* $[M+Na]^+$ calculated	*m/z* $[M-Na]^+$ observed	Retention time [min]
18	$C_{28}H_{54}O_5$	470.3971	493.3869	493.3869	6.55
19	$C_{29}H_{56}O_5$	484.4128	507.4025	507.4024	7.33
20	$C_{30}H_{58}O_5$	498.4284	521.4182	521.4178	8.39
21	$C_{31}H_{60}O_5$	512.4441	535.4338	535.4346	9.52
22	$C_{32}H_{62}O_5$	526.4597	549.4495	549.4501	11.14
23	$C_{33}H_{64}O_5$	540.4754	563.4651	563.4650	12.95
24	$C_{34}H_{66}O_5$	554.491	577.4808	577.4807	15.06
25	$C_{35}H_{68}O_5$	568.5067	591.4964	591.4967	17.50
26	$C_{36}H_{70}O_5$	582.5223	605.5121	605.5116	20.55

REFERENCES

1. Dieterle, F., Ross, A., Schlotterbeck, G., and Senn, H. (2006) Probabilistic quotient normalization as robust method to account for dilution of complex biological mixtures. Application in 1H NMR metabonomics, *Anal. Chem. 78*, 4281-4290.
2. Wold, S., Esbensen, K., and Geladi, P. (1987) Principal component analysis, *Chemometr. Intell. Lab. 2*, 37-52.
3. de Jong, S. (1993) SIMPLS: An alternative approach to partial least squares regression, *Chemometr. Intell. Lab. 18*, 251-263.
4. Koradi, R. (1998) Automated peak picking and peak integration in macromolecular NMR spectra using AUTOPSY, *J. Magn. Reson. 135,* 288-297.
5. Gordon, A. D. (1987) A review of hierarchical-classification, *J. Roy. Stat. Soc. A Sta. 150*, 119-137.

Appendix F

CONCLUSIONS AND OUTLOOK

Worm strains. The following *C. elegans* strains were obtained from the Caenorhabditis Genetics Center: wild type (N2), *sir-2.1(ok434)* and *him-5(e1490).* The Portman Laboratory (University of Rochester) kindly provided the following strains: Intestine feminization: UR933 - fsEx442 [Pnhx-2::tra-2(ic)::mcherry unc-54; Psulp-3::gfp]; him-5(e1490), intestine masculinization: UR937 - fsEx446 [Pnhx-2::fem-3(+)::mcherry unc-54; Psulp-3::gfp]; him-5(e1490), intestine feminization downstream of *tra-1*: CB3977 - mab-3(e1240); him-5(e1490). The Brunet Laboratory (Stanford University) kindly provided the following strains: *che-13(1e1805), ins-11(tm1053), and daf-2(e1370).* Nematode stocks were maintained on Nematode Growth Medium (*1*) plates with added bacteria (*E. coli* strain OP50) at 20 °C (http:// www.wormbook.org/).

Preparation of metabolite extracts. All strains were grown for at least two generations on NGM plates seeded with OP50. Since all strains had a *him-5* mutation incorporated in the genotype, mutant worms were synchronized by timed egg lay from mated parents. For exo-metabolome collection, 100 or 200 L4 male or hermaphrodite worms were picked with an aluminum wire pick and placed into 250 µL of water or S-media in a 96 well plate (BD Biosciences) and incubated for 17 hours at 22 °C and 220 pm. The solution was filtered over cotton to remove worms and evaporated *in vacuo* at room temperature. The extract was taken up in 100 µL methanol for subsequent HPLC-MS analysis.

Mass spectrometric analysis. HPLC-MS analysis was performed using an Agilent 1100 Series HPLC system equipped with an Agilent Eclipse XDB-C18 column (9.4 x 250 mm, 5 µm particle diameter) connected to a Quattro II spectrometer (Micromass/Waters) using a 10:1 split. Samples of 10-30 µL of metabolite extract dissolved in methanol was injected and run over a water (0.1% acetic acid) – acetonitrile gradient with a flow rate of 3.6 mL/min. The acetonitrile content was held at 5% for the first 5 minutes then increased to 100% over a period of 40 minutes. Samples were analyzed by HPLC-ESI-MS in negative and positive ion modes using a capillary voltage of 3.5 kV and a cone voltage of -40 V and +20 V, respectively. Single Ion Monitoring (SIM) in negative-ion ionization mode was used to detected the molecular ions of ascr#1, ascr#3, and ascr#10 at m/z 247.2, 301.2 and 303.2, respectively, for their corresponding $(M-H)^-$. Identification of ascarosides were confirmed by comparison with published retention times (*2*) and injection of authentic synthetic standards.

Quantification of ascarosides. Relative ascaroside content was quantified by integration of LC-MS signals from corresponding ion traces. Absolute quantification of ascarosides was achieved by injection of solutions of known concentration of synthetic ascr#1, ascr#3, and ascr#10.

Plate preparation. Ascarosides ascr#3 and ascr#10 were synthesized as described previously (*2, 3*). For preparation of ascaroside containing NGM plates, ~2mg of ascr#10 and ascr#3 were dissolved in 2 mL 100% ethanol producing stock solutions, which were further diluted with water to yield stock solutions of micromolar and nanomolar concentrations, as needed. Controls for mock treated had corresponding amounts of ethanol added. Plates were allowed to dry for 24 h.

Lifespan assays. For lifespan assays, worm strains were thawed from frozen stock and grown for two generations on well-fed conditions. 6-cm NGM plates containing 400 nM ascr#10, ascr#3, 1:1 mixtures of ascr#10 and ascr#3 and mock-treated control plates were used. Late L4-stage worms were picked from synchronized NGM plates and transferred (25-30 worms/plate) to experimental plates at 20°C. Survival was monitored by scoring for touch-provoked movement every other day, in some cases every day. Live worms were transferred every other day to remove progeny until day 10. Day 0 corresponds to the time of transfer of the worms at the L4 stage. SPSS V. 19 (IBM) statistical analysis package was used for all lifespan and thermotolerance statistics. *P*-values were calculated using the Log-rank (Mantel-Cox) method.

Preparation of male enriched liquid culture samples. Liquid cultures were grown with slight adaptation from (*3*). *him-5* mutant worms were grown for two generations on NGM plates seeded with OP50. Three crowded 6 cm NGM plates were washed into 100 mL solution of S-medium in a 500 mL Erlenmeyer flask and grown at 22°C and 220 pm. Concentrated HB101 from 1 L bacterial cultures, grown over-night, were given on day 1 and day 3. On day 5 liquid cultures were bleach synchronized and resupsended in S-medium in a 500 mL Erlenemyer flasks with HB101 from a 1L bacterial culture. On day 3, worms were filtered through a 35 micron filter (Small Parts) to filter out hermaphrodites. The worms that went through were then filtered through a 20-micron filter to let larval worms go through. This was repeated x 3 to achieve greater than 95% male rich cultures. Worms were allowed to settle in a 50 mL falcon tube and media was removed to clear off some additional larva. Enriched males were placed in fresh S-medium in a 500 mL Erlenmeyer flask with 1L HB101 and grown for 4 days before

harvest. Worms were allowed. Filtering protocol was established based on previously published work (Meyer, 1986 #1468). Wild type (N2) worms were grown similarly, without filtering.

Metabolome fractionation. Liquid cultures were allowed to settle in 50 mL falcon tubes, media was removed, and the pellets were frozen on dry ice acetone and stored at -20°C until use. Frozen pellets were blended with precooled methanol (200 mL/culture) in a Waring blender. Residue, after methanol was evaporated, was resuspended in water and lyophilized. The remaining residue was crushed with NaCL in a moretar and pesle and extracted twice with 9:1 ethyl acetate:ethanol (100 mL x 2) overnight. The filtrate was evaropated in vacuo at room temperature.

The extract dissolved In ethyl acteate:ethanol was loaded add to 2 g of Celite (prewashed with ethyl acetate over night). Evaporated celite was dry loaded into an empty 5 g RediSep *Rf* loading cartridge. Fractionation was performed using a Teledyne ISCO CombiFlash system and a RediSep*Rf* GOLD 4 g HP Silica Column using a dichloromethane-methanol solvent system, starting with 1.25 min of 100% dichloromethane, followed by a linear increase of methanol S32 content up to 10% at 3.2 min, followed by another linear increase of methanol content up to 40% at 9 min, followed by another linear increase of methanol content up to 95% at 10.2 min which was then continued to 10.7 min. 70 fractions (~3 mL each) generated in this manner were individually evaporated *in vacuo* and prepared for dauer rescue assays using *daf-9(dh6)* worms and subsequent analysis by SIM-GC/MS.

daf-9(dh6) **dauer rescue assay.** 96 well liquid based assay: metabolome fractions were resuspended in 20 uL ethanol. 0.5 uL was added to 40 uL 5× concentrated HB101

bacteria (from an overnight culture in lysogeny broth [LB] media) in S-complete media in one of the 96 plate wells. *daf-9(dh6)* worms from 4 overgrown 10 cm plates were bleach synchronized and starved as L1s. 10 uL of a 1mL solution of worms in S-comlete was added to the well. Rescue was scored by worm size four days after initiation. Positive control was 0.5 uL of 20 uM Δ4 dafachronic acid. Negative control was 0.5 uL of ethanol.

REFERENCES

1. Shivers, R. P., Youngman, M. J., and Kim, D. H. (2008) Transcriptional responses to pathogens in *Caenorhabditis elegans*, Curr. Opin. Microbiol. *11*, 251-256.
2. von Reuss, S. H., Bose, N., Srinivasan, J., Yim, J. J., Judkins, J. C., Sternberg, P. W., and Schroeder, F. C. (2012) Comparative metabolomics reveals biogenesis of ascarosides, a modular library of small molecule signals in *C. elegans*, J. Am. Chem. Soc. *134*, 1817–1824.
3. Pungaliya, C., Srinivasan, J., Fox, B. W., Malik, R. U., Ludewig, A. H., Sternberg, P. W., and Schroeder, F. C. (2009) A shortcut to identifying small molecule signals that regulate behavior and development in *Caenorhabditis elegans*, Proc. Natl Acad. Sci. USA *106*, 7708-7713.